

TURUN YLIOPISTON JULKAISUJA  
ANNALES UNIVERSITATIS TURKUENSIS

---

*SARJA - SER. D OSA - TOM. 998*

MEDICA - ODONTOLOGICA

# LIPOTOXICITY IN OBESITY AND CORONARY ARTERY DISEASE

Studies by PET, CT and MR

by

Marco Bucci

TURUN YLIOPISTO  
UNIVERSITY OF TURKU  
Turku 2011

From Turku PET Centre, Department of Clinical Physiology and Nuclear Medicine  
and Department of Medicine, University of Turku, Turku, Finland

### **Supervised by**

Docent Patricia Iozzo, MD, PhD  
Turku PET Centre  
University of Turku  
Turku, Finland

Institute of Clinical Physiology  
National Research Council (CNR)  
Pisa, Italy

and

Professor Pirjo Nuutila, MD, PhD  
Turku PET Centre and the Department of Medicine  
University of Turku  
Turku, Finland

### **Reviewed by**

Professor Fredrik Karpe, MD, PhD  
Oxford Centre for Diabetes, Endocrinology & Metabolism  
University of Oxford  
Oxford, United Kingdom

and

Professor Ulla Ruotsalainen, PhD  
Institute of Signal Processing  
Tampere University of Technology  
Tampere, Finland

### **Dissertation opponent**

Professor Gianluca Perseghin, MD, PhD  
Department of Sport, Nutrition and Health,  
Milan University and Internal Medicine,  
Scientific Institute H. San Raffaele,  
Milan, Italy

Department of Internal Medicine  
Monza Policlinic,  
Milan, Italy

ISBN 978-951-29-4839-0 (PRINT)  
ISBN 978-951-29-4840-6 (PDF)  
ISSN 0355-9483  
Painosalama Oy – Turku, Finland 2011

*To my parents  
and my family*

## ABSTRACT

**Marco Bucci**

### **LIPOTOXICITY IN OBESITY AND CORONARY ARTERY DISEASE**

Studies by PET, CT and MR.

Turku PET Centre, Department of Clinical Physiology and Nuclear Medicine and Department of Medicine, University of Turku, Turku  
Annales Universitatis Turkuensis

Lipotoxicity is a condition in which fatty acids (FAs) are not efficiently stored in adipose tissue and overflow to non-adipose tissue, causing organ damages. A defect of adipose tissue FA storage capability can be the primary culprit in the insulin resistance condition that characterizes many of the severe metabolic diseases that affect people nowadays. Obesity, in this regard, constitutes the gateway and risk factor of the major killers of modern society, such as cardiovascular disease and cancer. A deep understanding of the pathogenetic mechanisms that underlie obesity and the insulin resistance syndrome is a challenge for modern medicine. In the last twenty years of scientific research, FA metabolism and dysregulations have been the object of numerous studies. Development of more targeted and quantitative methodologies is required on one hand, to investigate and dissect organ metabolism, on the other hand to test the efficacy and mechanisms of action of novel drugs. The combination of functional and anatomical imaging is an answer to this need, since it provides more understanding and more information than we have ever had. The first purpose of this study was to investigate abnormalities of substrate organ metabolism, with special reference to the FA metabolism in obese drug-naïve subjects at an early stage of disease. Secondly, trimetazidine (TMZ), a metabolic drug supposed to inhibit FA oxidation (FAO), has been for the first time evaluated in obese subjects to test a whole body and organ metabolism improvement based on the hypothesis that FAO is increased at an early stage of the disease. A third objective was to investigate the relationship between ectopic fat accumulation surrounding heart and coronaries, and impaired myocardial perfusion in patients with risk of coronary artery disease (CAD). In the current study a new methodology has been developed with PET imaging with  $^{11}\text{C}$ -palmitate and compartmental modelling for the non-invasive *in vivo* study of liver FA metabolism, and a similar approach has been used to study FA metabolism in the skeletal muscle, the adipose tissue and the heart. The results of the different substudies point in the same direction. Obesity, at the an early stage, is associated with an impairment in the esterification of FAs in adipose tissue and skeletal muscle, which is accompanied by the upregulation in skeletal muscle, liver and heart FAO. The inability to store fat may initiate a cascade of events leading to FA oversupply to lean tissue, overload of the oxidative pathway, and accumulation of toxic lipid species and triglycerides, and it was paralleled by a proportional growth in insulin resistance. In subjects with CAD, the accumulation of ectopic fat inside the pericardium is associated with impaired myocardial perfusion, presumably via a paracrine/vasocrine effect. At the beginning of the disease, TMZ is not detrimental to health; on the contrary at the single organ level (heart, skeletal muscle and liver) it seems beneficial, while no relevant effects were found on adipose tissue function. Taken altogether these findings suggest that adipose tissue storage capability should be preserved, if it is not possible to prevent excessive fat intake in the first place.

**Keywords:** fatty acid metabolism, adipose tissue, liver, skeletal muscle, heart, obesity, CAD, functional imaging, anatomical imaging

## TIIVISTELMÄ

**Marco Bucci**

### **LIPOTOKSISUUS LIHAVUUDESSA JA SEPELVALTIMOTAUDISSA**

Tutkimuksia positroniemissiotomografialla, tietokonetomografialla ja magneettikuvauksella.

Valtakunnallinen PET-keskus, Kliininen fysiologia ja isotooppilääketiede sekä Sisätautioppi, Turun yliopisto, Turku  
Annales Universitatis Turkuensis

Lipotoksisuudella tarkoitetaan tilaa, jossa rasvahappoja ei kyetä varastoimaan rasvakudokseen tehokkaasti ja ylimääräiset varastoimattomat rasvahapot vaurioittavat kehon muita kudoksia. Rasvakudoksen kykenemättömyys varastoida rasvahappoja saattaa olla ensisijainen tekijä insuliiniresistenssissä. Insuliiniresistenssi liittyy aineenvaihduntasairauksiin ja erityisesti lihavuuteen. Lihavuus lisää riskiä sairastua moniin yhteiskunnallisesti merkittäviin sairauksiin, kuten sydän- ja verisuonisairauksiin sekä tiettyihin syöpiin. Rasvahappoaineenvaihduntaa ja sen toiminnan häiriöitä on tutkittu paljon viimeisten parinkymmenen vuoden aikana, mutta lihavuuden ja insuliiniresistenssin tarkkojen patogeneettisten mekanismien ymmärtäminen on edelleen haaste nykypäivän lääketieteelle. Kvantitatiivisten menetelmien kehittäminen tarkempaan kudostason aineenvaihdunnan tutkimiseen sekä uusien lääkkeiden tehon ja vaikutusmekanismien selvittämiseen on välttämätöntä. Toiminnallisen ja anatomisen kuvantamisen yhdistämisen etuna on tarkempi ja selkeämmin tulkittava tieto verrattuna aiempiin menetelmiin. Tutkimuksen ensimmäinen tavoite oli tutkia eri elinten aineenvaihdunnan häiriöitä, erityisesti rasvahappoaineenvaihdunnan häiriöitä lihavilla, muutoin terveillä henkilöillä. Toisena tavoitteena oli tutkia rasvahappojen oksidaatiota säätelevän trimetatsidiini-lääkeaineen vaikutuksia koko kehon ja eri elinten aineenvaihdunnan paranemiseen lihavilla henkilöillä, oletuksena, että lihavuuden alkuvaiheessa rasvahappojen oksidaatio on vilkkaampaa. Tutkimuksen kolmantena tavoitteena oli tutkia sydämeen ja sepelvaltimoiden ympärille kertyvän ektooppisen rasvan määrän ja heikentyneen sydämen verenvirtauksen välistä suhdetta potilailla, joilla on kohonnut sepelvaltimotautiriski. Tässä tutkimuksessa kehitettiin uusi PET-kuvantamista, <sup>11</sup>C-palmitaattia ja tilamallinnusta hyödyntävä menetelmä, jolla voidaan kehoon kajoamatta tutkia maksan rasvahappoaineenvaihduntaa. Tutkimustulokset osoittivat, että tämä kuvantamismenetelmä soveltuu myös luurankolihasen, rasvakudoksen ja sydämen rasvahappoaineenvaihdunnan tutkimiseen. Tulokset osoittivat myös, että lihavuus on alkuvaiheessa yhteydessä huonontuneeseen rasvahappojen esteröitymiseen rasvakudoksessa ja luurankolihasessa, ja samalla rasvahappojen oksidaatio on suurentunut niin rasvakudoksessa, luurankolihasessa kuin sydämessä. Rasvakudoksen kykenemättömyys varastoida rasvahappoja saattaa johtaa tapahtumaketjuun, jonka tuloksena rasvahappoja on liikaa tarjolla kehon rasvattomille kudoksille, jolloin oksidatiiviset aineenvaihduntareitit ylikuormittuvat, toksisia rasva-aineenvaihduntatuotteita ja varastorasvoja (triglyseridejä) kertyy elimistöön ja insuliiniresistenssi pahenee. Myös sepelvaltimotautipotilailla ektooppisen rasvan kertyminen perikardiumin sisään on yhteydessä sydämen huonontuneeseen toimintaan oletettavasti parakriinisten/vasokriinisten vaikutusten kautta. Näiden löydösten valossa on tärkeää pyrkiä ylläpitämään rasvakudoksen kykyä varastoida rasvaa, mikäli rasvan ylimääräisen saannin rajoittaminen ei ensisijaisesti ole mahdollista. Lihavuuden alkuvaiheessa, jolloin rasvahappojen oksidaatio on suurentunut kompensoimaan ylimääräistä rasvahappokuormaa, osittainen beetaoksideation esto ei ole haitallista terveydelle, päinvastoin yksittäisten elinten tasolla (sydän, luurankolihas ja maksa) vaikutukset ovat hyödyllisiä.

**Avainsanat:** rasvahappoaineenvaihdunta, rasvakudos, maksa, luurankolihas, sydän, lihavuus, sepelvaltimotauti, toiminnallinen kuvantaminen, anatominen kuvantaminen

**TABLE OF CONTENTS**

**ABSTRACT .....4**

**TIIVISTELMÄ .....5**

**TABLE OF CONTENTS .....6**

**ABBREVIATIONS.....9**

**LIST OF ORIGINAL PUBLICATIONS.....10**

**1 INTRODUCTION .....11**

**2 REVIEW OF THE LITERATURE .....14**

    2.1 FATTY ACID METABOLISM .....14

        2.1.1 Fatty acid systemic trafficking .....14

        2.1.2 Fatty acid turnover, lipolysis and regulation .....17

        2.1.3 Fatty acid disposal (utilization).....18

            2.1.3.1 Fatty acid uptake .....18

            2.1.3.2 Fatty acid esterification and body fat distribution .....18

            2.1.3.3 Fatty acid oxidation .....19

        2.1.4 Fatty acid metabolism regulation and interaction with glucose metabolism .....21

    2.2 ASSESSMENT OF FATTY ACID METABOLISM AND FAT STORAGE IN VIVO .....24

        2.2.1 Whole body fatty acid metabolism .....24

        2.2.2 Adipose Tissue.....24

        2.2.3 Liver.....25

        2.2.4 Skeletal Muscle.....26

        2.2.5 Heart .....27

        2.2.6 Positron Emission Tomography principles .....28

        2.2.7 Magnetic Resonance Spectroscopy principles .....31

        2.2.8 Fat distribution, assessment of whole body and regional fat depots .....31

    2.3 LIPOTOXICITY: A FATTY ACID METABOLISM DISORDER.....32

        2.3.1 Lipotoxicity in obesity: adipose tissue failure in storing fatty acids .....34

        2.3.2 Hepatic lipotoxicity.....35

        2.3.3 Skeletal muscle lipotoxicity .....36

        2.3.4 Myocardial lipotoxicity.....39

        2.3.5 CAD: links with lipotoxicity and the role of pericardial fat .....41

    2.4 FATTY ACID METABOLISM MODULATION DRUGS .....42

        2.4.1 Trimetazidine .....46

**3 OBJECTIVES OF THE STUDY .....48**

**4 SUBJECTS AND STUDY DESIGN.....49**

    4.1 STUDY SUBJECTS .....49

        4.1.1 Inclusion criteria and recruitment .....49

    4.2 STUDY DESIGN .....50

**5 METHODS.....54**

    5.1 POSITRON EMISSION TOMOGRAPHY (I-IV) .....54

        5.1.1 Production of positron emitting tracers.....54

        5.1.2 PET imaging study sessions (animals) (I).....54

            5.1.2.1 Assay of labelled <sup>11</sup>C-CO<sub>2</sub> .....55

            5.1.2.2 Assay of labelled lipid fractions .....55

        5.1.3 PET imaging study sessions (humans) (I-IV) .....55

            5.1.2.1 [<sup>11</sup>C]Palmitate – Fatty acid metabolism imaging (I-III).....56

            5.1.2.2 [<sup>18</sup>F]FDG –Glucose metabolism imaging (II,III) .....56

            5.1.2.3 [<sup>15</sup>O]H<sub>2</sub>O – Cardiac perfusion imaging (IV).....56

TABLE OF CONTENTS

---

5.1.4 Image preprocessing .....	56
5.1.5 Image analysis (animals).....	57
5.1.6 Image analysis (humans).....	57
5.1.6.1 [ <sup>15</sup> O]H <sub>2</sub> O – Cardiac perfusion imaging (IV).....	57
5.1.7 Kinetic modelling .....	60
5.1.7.1 Modelling of adipose tissue <sup>11</sup> C-palmitate kinetics (II).....	60
5.1.7.1 Modelling of skeletal muscle <sup>11</sup> C-palmitate kinetics (II).....	60
5.1.7.1 Modelling of myocardial <sup>11</sup> C-palmitate kinetics (III).....	63
5.1.7.4 Modelling of liver <sup>11</sup> C-palmitate kinetics (I).....	66
5.1.7.5 Modelling of <sup>18</sup> F-FDG kinetics (II,III).....	67
5.1.8 Calculation of glucose (II) and FA systemic disposal rates (I,II) .....	68
5.2 MAGNETIC RESONANCE IMAGING (I-III) .....	68
5.2.1 Abdominal fat masses assessment (I,II).....	68
5.2.2 Left ventricle (LV) function and dimensions (III).....	69
5.3 <sup>1</sup> H MAGNETIC RESONANCE SPECTROSCOPY (I – III).....	69
5.3.1 Skeletal muscle lipid and creatine content (II).....	69
5.3.2 Heart lipid and creatine content (III).....	70
5.3.3 Liver lipid content (I).....	70
5.4 COMPUTED TOMOGRAPHY (I-IV) .....	70
5.4.1 Coronary artery calcium score (IV).....	70
5.4.2 CT quantification of intra- and extra-pericardial fat volumes.....	71
5.4.3 CT Angiography .....	71
5.5 INVASIVE CORONARY ANGIOGRAPHY AND FRACTIONAL FLOW RESERVE (IV) .....	72
5.6 BIOCHEMICAL ANALYSES (I – III).....	72
5.7 OTHER MEASUREMENTS .....	73
5.7.1 Energy provision and LV work (III).....	73
5.8 STATISTICAL ANALYSIS .....	73
<b>6 RESULTS.....</b>	<b>75</b>
6.1 VALIDATION STUDY FOR LIVER FATTY ACID METABOLISM ASSESSMENT IN ANIMALS BY PET AND <sup>11</sup> C-PALMITATE (I).....	75
6.1.1 Image quality and model fit.....	75
6.1.2 PET-derived vs. measured fatty acid fluxes.....	75
6.1.2 Effects of insulin on liver fatty acid metabolism.....	77
6.2 VALIDATION STUDY FOR LIVER FATTY ACID METABOLISM ASSESSMENT IN HUMANS BY PET AND <sup>11</sup> C-PALMITATE (I).....	78
6.2.1 Image quality and model fit.....	78
6.2.2 PET-derived fluxes vs. measured indicators.....	78
6.2.3 Use of a single arterial input function and prediction of a dual input function.....	78
6.3 EFFECT OF OBESITY ON FATTY ACID ORGAN METABOLISM (I-III) .....	81
6.3.1 Anthropometric and metabolic characteristics of the study groups .....	81
6.3.2 Effects of obesity on hepatic fatty acid metabolism (I) .....	81
6.3.3 Effects of obesity on skeletal muscle and adipose tissue fatty acid metabolism (II).....	84
6.3.4 Effects of obesity on myocardial metabolism and function (III & unpublished data).....	86
6.4 EFFECTS OF TRIMETAZIDINE (II-III).....	87
6.4.1 Effects of trimetazidine on metabolic and whole body variables (II).....	87
6.4.2 Effects of trimetazidine on skeletal muscle and adipose tissue substrate metabolism (II).....	87
6.4.2 Effects of trimetazidine on myocardial metabolism and function efficiency (III).....	92
6.5 ASSOCIATION OF PERICARDIAL FAT AND HYPERAEMIC MYOCARDIAL BLOOD FLOW IN SUBJECTS WITH AND WITHOUT CAD (IV).....	95

---

TABLE OF CONTENTS

---

6.5.1 IPF and EPF volumes ..... 95

6.5.2 IPF and EPF in relation to CAD and CAC score ..... 95

6.5.3 IPF and EPF in relation with MBF ..... 98

6.5.4 Comparison of MBF predictors ..... 101

**7 DISCUSSION..... 103**

7.1 VALIDATION STUDY FOR LIVER FATTY ACID METABOLISM ASSESSMENT IN ANIMALS AND HUMANS (I)..... 103

7.1.1 Effect of insulin on healthy liver fatty acid metabolism (I) ..... 104

7.2 EFFECTS OF OBESITY ON FATTY ACID METABOLISM IN HUMANS (I-III) ..... 105

7.2.1 Effects of obesity on liver fatty acid metabolism (I)..... 105

7.2.2 Effects of obesity on skeletal muscle and adipose tissue fatty acid metabolism (II)107

7.2.3 Effects of obesity on myocardial fatty acid metabolism (III) ..... 108

7.3 EFFECTS OF TRIMETAZIDINE ON FATTY ACID AND GLUCOSE METABOLISM IN OBESE SUBJECTS (II-III) ..... 110

7.3.1 Effects of trimetazidine on whole body, skeletal muscle and adipose tissue substrate metabolism (II) ..... 110

7.3.2 Effects of trimetazidine on myocardial metabolism and function efficiency (III) ... 111

7.3.3 Effects of trimetazidine: reconciliation of other findings ..... 112

7.4 ASSOCIATION OF PERICARDIAL FAT AND HYPEREMIC MYOCARDIAL BLOOD FLOW IN SUBJECTS WITH AND WITHOUT CAD (IV)..... 113

7.5 LIMITATIONS OF THE STUDY AND FUTURE DIRECTIONS..... 115

**8 SUMMARY AND CONCLUSIONS ..... 118**

**9 ACKNOWLEDGEMENTS ..... 120**

**ORIGINAL PUBLICATIONS ..... 139**



## ABBREVIATIONS

[ <sup>15</sup> O]H <sub>2</sub> O	[ <sup>15</sup> O]-water
[ <sup>18</sup> F]FDG	[ <sup>18</sup> F]-2-fluoro-2-deoxyglucose
ATP	Adenosine triphosphate
BMI	Body mass index
CAC	Coronary artery calcium
CAD	Coronary artery disease
CFR (*)	Coronary flow reserve
CoA	Coenzyme A
CPT	Carnitine palmitoyltransferase
CT	Computed tomography
DAG	Diacylglycerol
FA (°)	Fatty acid
FFA (°)	Free fatty acid
FAO	Fatty acid oxidation
HDL	High-density lipoprotein
HR	Heart rate
IMTG	Intramyocellular triacylglycerol
LAD	Left anterior descendent coronary
LC-CoA	Long-chain acyl-CoA
LDL	Low-density lipoprotein
LPL	Lipoprotein lipase
LV	Left ventricle
LVEF	Left ventricular ejection fraction
MDCT	Multi-detector computed tomography
MBF (*)	Myocardial blood flow
MRI	Magnetic resonance imaging
MRS	Magnetic resonance spectroscopy
PET	Positron emission tomography
OGTT	Oral glucose tolerance test
Ra	Rate of appearance
ROI	Region of interest
ROS	Reactive oxygen species
RPP	Rate pressure product
SD	Standard deviation
SEM	Standard error of mean
SV	Stroke volume
TAC	Time activity curve
TAG	Triacylglyceride
VLDL	Very low-density lipoprotein

(°) The terms FA and FFA are often used indifferently, because their meaning is somewhat overlapping. In this thesis, the term FA is used to refer to the complexed fatty acids; FFA is used to refer to the unbound molecule, ready to be processed into intracellular/extracellular metabolic pathways.

(\*) Asterisks denote the lowest regional value of MBF and CFR (see section 5.1.6.1.)

## LIST OF ORIGINAL PUBLICATIONS

This dissertation is based on the following original publications, which are referred to in the text by the corresponding Roman numerals, I – IV.

- I. Iozzo P, **Bucci M**, Roivainen A, Någren, K, Järvisalo MJ, Kiss J, Guiducci L, Fielding B, Naum AG, Borra R, Virtanen K, Savunen T, Salvadori PA, Ferrannini E, Knuuti J, Nuutila P. Fatty Acid Metabolism in the Liver, Measured by Positron Emission Tomography, Is Increased in Obese Individuals. *Gastroenterology*, 2010; 139: 846-856.
- II. **Bucci M**, Borra R, Någren K, Maggio R, Tuunanen H, Oikonen V, Del Ry S, Takala T, Turpeinen AK, Giannessi D, Viljanen T, Taittonen M, Rigazio S, Knuuti J, Nuutila P, Iozzo P. Human obesity is characterized by defective fat storage and enhanced skeletal muscle fatty acid oxidation and trimetazidine gradually counteracts these abnormalities. *American Journal of Physiology – Endocrinology and Metabolism*, 2011; 301: E105-E112.
- III. **Bucci M**, Borra R, Någren K, Pärkkä JP, Del Ry S, Maggio R, Tuunanen H, Viljanen T, Cabiati M, Rigazio S, Taittonen M, Pagotto U, Parkkola R, Opie LH, Nuutila P, Knuuti J, Iozzo P. Trimetazidine Reduces Endogenous Free Fatty Acid Oxidation and Improves Myocardial Efficiency in Obese Humans. *Cardiovascular Therapeutics*, 2011; XX: 1-9. Epub 31 July 2011.
- IV. **Bucci M**, Joutsinemi E, Saraste A, Kajander S, Ukkonen H, Saraste M, Pietilä M, Sipilä HT, Teräs M, Mäki M, Airaksinen KEJ, Hartiala J, Knuuti J, Iozzo P. Intrapericardial, But Not Extrapericardial, Fat Is an Independent Predictor of Impaired Hyperemic Coronary Perfusion in Coronary Artery Disease. *Arteriosclerosis, Thrombosis and Vascular Biology*, 2011; 31: 211-218.

In addition some unpublished data are presented.

The original publications and the non-original figures presented in this thesis have been reprinted with the permission of the copyright holders.

## 1 INTRODUCTION

There has been increasing interest in lipid fuel metabolism over the past 20 years, partly because of the key role of lipids as mediators of insulin resistance in conditions such as obesity, dyslipidemia and type 2 diabetes (Boden, 1997; McGarry, 1992; Boden, 1998). While there is still debate on which is the organ that first fails or that is determinant in causing the insulin resistance syndrome (DeFronzo & Tripathy, 2009; Perseghin, 2009; Pagotto, 2009; Kahn *et al.*, 2006), there is consensus in identifying lipotoxicity as a condition in which fatty acids (FAs) are stored in non-adipose tissues, hence defined as ectopic fat. And there is agreement and evidence that the consequence of this ectopic accumulation is the impairment of the function of the interested organ, caused by lipid toxic metabolites and free radicals, leading ultimately to systemic diseases (Unger *et al.*, 2010; Gastaldelli & Basta, 2010; Cusi, 2010). One of the current mainstream hypotheses states that the adipose tissue might be the first organ affected by derangements that can directly cause lipotoxicity (Iozzo, 2009; Lelliott & Vidal-Puig, 2004). It is logical to think that if the adipose tissue fails to act as a sink for FAs, they can spread out and overflow into lean organs; herein FAs can damage organ functions, possibly via increased oxidative stress, promoted by increased oxidation, or providing substrates for peroxidation, but *in vivo* evidence in humans is needed to support this hypothesis. One of the organs that might be directly affected by an augmented circulation of FAs is the skeletal muscle. The reasoning that leads to this hypothesis might be too simplistic and a recent systematic review points out that circulating non esterified FA (NEFA) are not the key component of insulin resistance, and that augmented circulation of NEFAs are not necessarily associated with insulin resistance (Karpe *et al.*, 2011). Even if this is true, an increased flux of NEFA coming from adipose tissue towards lean tissues is augmented in overweight/insulin resistant states (Mittendorfer *et al.*, 2009). It is recognized that, in both animals and humans, elevated storage of intramuscular triglycerides (IMTG) is a common feature of obese and/or insulin resistance states (Hulver *et al.*, 2003; Goodpaster & Kelley, 2002). However the questions of whether it is a protective or a detrimental feature and whether the defect is primary or secondary (Karpe *et al.*, 2011), are controversial. It is also still in doubt whether skeletal muscle fatty acid oxidation (FAO) is increased or decreased during fasting in such altered metabolic states (Koonen *et al.*, 2010). A possible explanation can be that initially FAO increases, prompted by the augmented influx of lipid substrate trying to counteract IMTG accumulation. Once the pathway becomes saturated, the build-up of IMTG and free radicals may cause impairment of mitochondrial function (Turner *et al.*, 2007; Nair *et al.*, 2008). Augmented reliance on FAs can be deleterious also to the heart (Iozzo, 2010), especially because fatty acids are not the most efficient oxidable substrate oxygen-wise. Increased FA delivery to the myocardium leads to the subsequent increase in FAO that disrupts the metabolic plasticity of the heart (Iozzo, 2010), causing reduced glucose utilization and insulin resistance (Randle *et al.*, 1963), and because of the increased oxygen consumption (Peterson *et al.*, 2004) increases the risk of ischemia. The liver, being defined as the

“metabolic sensor of lipotoxicity” (Cusi, 2009), plays an important role in metabolic diseases. Liver steatosis, similarly to intramyocellular lipids, has been associated with direct mechanisms of lipotoxicity (McClain *et al.*, 2007; Jou *et al.*, 2008), whereas lipid depots are considered as “innocent bystanders” (Choi & Diehl, 2008; Jou *et al.*, 2008). An important role in the altered liver fatty acid metabolism is assumed by FAO, which produces ROS, that ultimately cause hepatic inflammation and fibrogenesis (Li *et al.*, 2008; Yang *et al.*, 2000; Fromenty *et al.*, 2004).

Obesity is an emerging pandemic health problem. It is defined as an increased body weight above a body mass index of 30 kg/m<sup>2</sup> (weight/height<sup>2</sup>); it affects 475 million people worldwide, and more than 20% of the Finnish population. This condition is particularly present in westernized countries where the abundance of food and technologization has led to an increased intake of calorie-rich food and decreased physical activity. Such environmental factors together with a susceptible genetic background are considered causes of the disease. Obesity is a chronic disease, associated with several co-morbidities and in general with a decreased life expectancy. It is one of the challenges of modern medicine to identify the primary culprit that at the early stages of the disease leads to the disruptive cascade of metabolic complications; then, we could tackle the problem aiming at the specific pathogenetic mechanisms through pharmacological interventions, when environmental and behavioural solutions fail in treating the disease. An additional challenge is to distinguish obese subjects with metabolic complications from the subjects that are “metabolically healthy”, in the sense that their body can compensate for the excess of body weight and fat by adjusting their metabolic rates to keep their organs fat free or at least to not incur metabolic complications. Nonetheless, obesity and diabetes are both risk factors for coronary artery disease (CAD). CAD is a disease characterized by the narrowing of the lumen (stenosis) of vessels that nourish the heart. Increased risk/presence of CAD has been associated with the accumulation of fat surrounding the heart (pericardial fat) (Rosito *et al.*, 2008; Sarin *et al.*, 2008; Gorter *et al.*, 2008; Greif *et al.*, 2009) but it is unclear whether fat can mediate anatomical damage to coronaries and even more importantly myocardial functional impairment. The fat surrounding vessels and heart may promote the progression of atherosclerosis via a paracrine/vasocrine effect, mediated by numerous hormones that have pro/anti-inflammatory effects and pro/anti-vasodilation effects (Iacobellis *et al.*, 2008). In this study the not fully explored association between ectopic fat accumulation and myocardial function was assessed in subjects with CAD.

The purpose of the present study was to provide evidence of the metabolic alterations hypothesized in lipotoxicity in humans *in vivo*. Therefore, obese subjects with no co-morbidities or diabetes, at the so-called “early stage” of the disease, were used as a valuable model to characterize fatty acid metabolism in different important organs:

- a) the adipose tissue, as the natural storage and supplier of lipid substrate, and

b) the skeletal muscle, as the most important lipid substrate consumer of the body were studied simultaneously to provide evidence of the hypothesized reciprocal inverse relation. According to the hypothesis, adipose tissue would be less prone to store fat and skeletal muscle would compensate the excess by burning more;

c) the liver fatty acid oxidation is a key process that for anatomical reasons has remained inaccessible to measurement for a long time: the aim was to validate a non-invasive measurement to characterize liver fatty acid metabolism in humans and compare obese and lean subjects;

d) the heart fatty acid oxidation route has been dissected for the first time so that both extracellular and intracellular lipid sources have been taken into account to quantify the process in obese subjects.

To pursue these aims the best choice was to adopt an integrated approach using non-invasive in vivo methods, which combine functional and anatomical imaging; thus obtaining a detailed picture of specific organ metabolisms and fat distribution and content. Functional imaging is represented by positron emission tomography (PET); this technique allows studying the short half-life isotope tracer distribution in tissues, and by signal modelling distinguishes the different metabolic pathways.  $^{11}\text{C}$ -palmitate, has been previously used for the study of myocardial and liver fatty acid metabolism, while [ $^{18}\text{F}$ ]-2-fluoro-2-deoxyglucose ([ $^{18}\text{F}$ ]FDG) remains the most common, widely used tracer for studying glucose metabolism. For this study it was necessary to develop/validate novel quantification approaches. Anatomical information was obtained by magnetic resonance and computed tomography (CT). Magnetic resonance imaging and spectroscopy provided fat masses and intra- and extracellular fat content, respectively. CT was used for both anatomical reference and to measure pericardial fat masses.

A metabolic modulator able to relieve the oxidative pressure caused by fatty acid overload can be an effective measure to prevent the long-term effects of lipotoxicity in the early stage of the disease. Trimetazidine is a partial inhibitor of fatty acid oxidation that has been used as an anti-angina drug and in vitro experiments have suggested that the mechanism of action is to shift myocardial metabolism towards glucose utilization (Kantor *et al.*, 2000). In this study trimetazidine has been tested for the first time in drug-naïve human obese subjects to evaluate a possible improvement in organ metabolism, such as heart, skeletal muscle and adipose tissue, using the same methods as described above.

## 2 REVIEW OF THE LITERATURE

In the present review of the literature, when possible, human investigations have been preferred to animal and in vitro studies. The review starts with a concise overview of FA metabolism and the assessment methods available for the characterization of the different processes involved in FA metabolism at systemic and organ level. It continues with a paragraph describing the mainstream theory behind the lipotoxicity concept, followed by references to obesity, organ lipotoxicity and CAD pathogenesis in relation to lipid metabolism. Finally, it briefly reports the metabolic modulators able to directly affect the fatty acid metabolism, with special reference to trimetazidine.

### 2.1 Fatty acid metabolism

#### 2.1.1 Fatty acid systemic trafficking

Most living organisms rely for their energy metabolism on essentially three main fuels: fatty acids, carbohydrates and proteins (Prout, 1827). FAs are the most efficiently storable source of energy. Thanks to their highly energetic molecular bonds, FAs can yield around twice as much ( $39.3 \text{ kJ}\cdot\text{g}^{-1}$ ) the amount of energy obtained by the same mass of carbohydrates ( $17.6 \text{ kJ}\cdot\text{g}^{-1}$ ) or proteins ( $23.7 \text{ kJ}\cdot\text{g}^{-1}$ ) (Jeukendrup & Gleeson, 2010). Furthermore, the relative hydrophobic nature of FAs makes it possible to store them in large quantities in the body, via esterification prompted by removal of space-occupying water molecules. Because of their special chemical properties FAs also constitute the building blocks of all biological membranes. Among their roles, FAs are precursors of essential bioactive organic molecules.

FAs are quite insoluble in plasma and are avidly and reversibly bound to albumin or esterified with glycerol to form triacylglycerides (TAGs) and packaged in lipoprotein particles for transport in the circulation (Spector, 1975). In the human body, FAs can be present as unbound (free fatty acids [FFAs] or non-esterified fatty acids [NEFAs]) or complexed to other molecules/substances (chylomicrons, TAG, low-density lipoproteins (LDLs), very low-density lipoproteins (VLDLs), high-density lipoproteins (HDLs), phospholipids, to cite the most important).

The network of trafficking of FAs is shown in Figure 2.1.1.1. (a) during fasting conditions and (b) during fed conditions (with insulin action). Most FAs constituting the human body are derived from dietary sources (gut); while an additional source is the De Novo Lipogenesis (DNL), that occurs in liver and adipocytes (Hellerstein, 1999). FAs digested in the gut are mobilized in complexes called chylomicrons. When lipid complexes arrive at the capillary beds, an enzyme called lipoprotein lipase (LPL) splits up proteins and glycerol from FFAs, freeing them. FFAs can enter the cells by either passive diffusion or by protein-mediated transport, although this is a matter of debate; recently the latter is the more accredited cellular uptake mechanism (Bonen *et al.*, 2007). After entering the cells, FFA fates are mainly three: oxidation for energy production, esterification for storage, generation of new biomolecules (membrane biosynthesis or lipid signalling molecules).

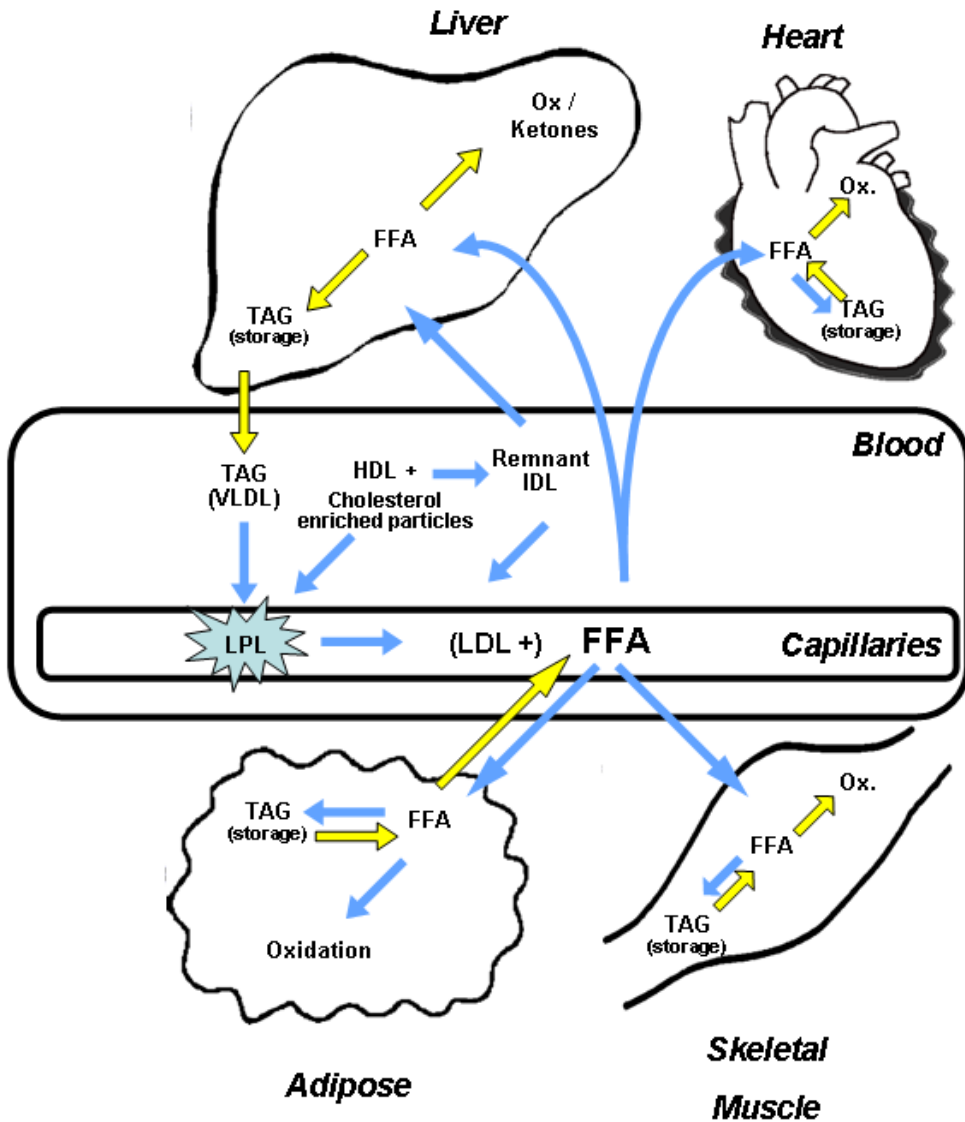


Figure 2.1.1.1. (a) The trafficking network of fatty acids (fasting state). Yellow arrows indicate processes that occur at higher rates during fasting than during the fed state. Blue arrows indicate processes not particularly activated or modulated by insulin. (Figure adapted from Nussey & Whitehead, 2001; Hodson & Frayn, 2011 and based on Frayn *et al.*, 2003).

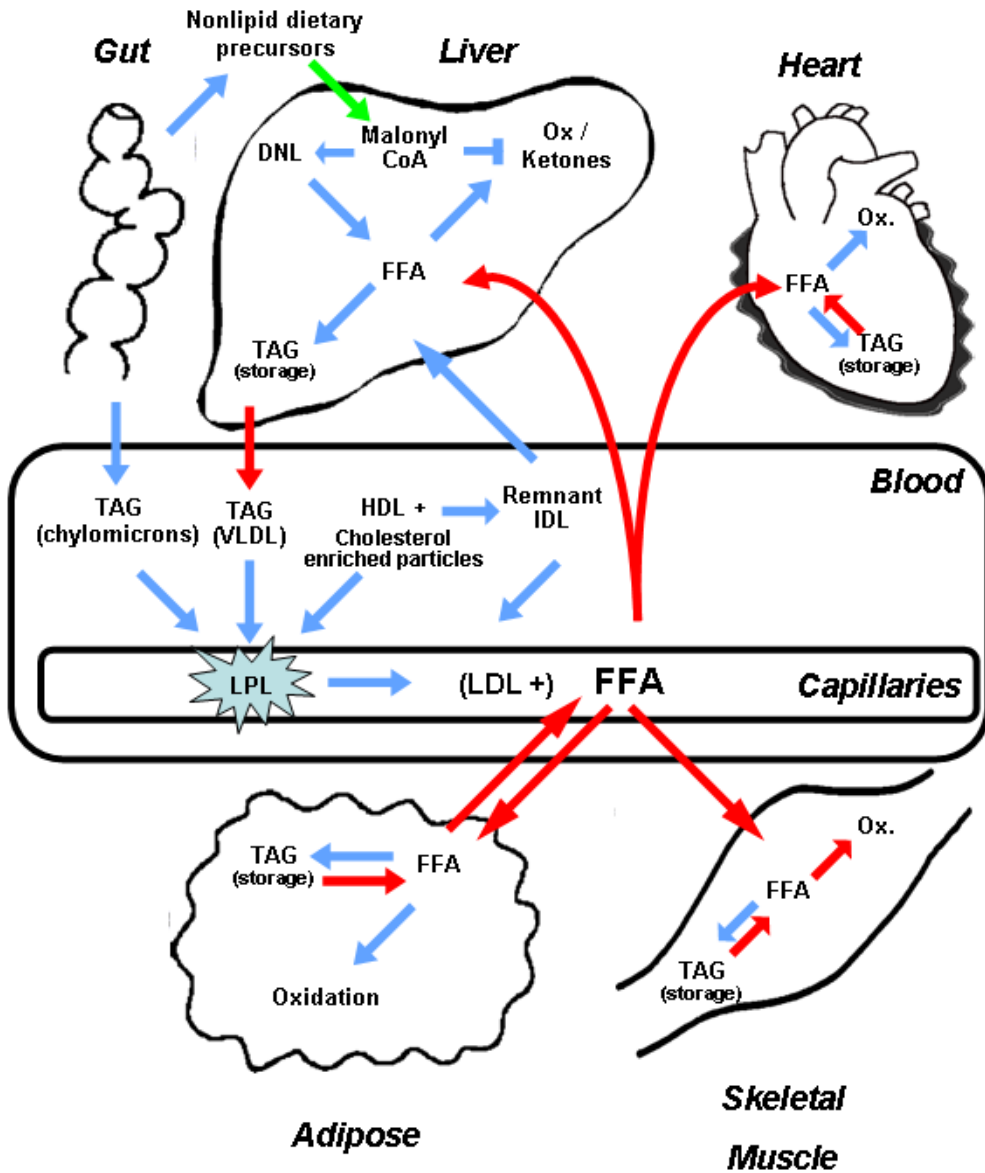


Figure 2.1.1.1. (b) The trafficking network of fatty acids (fed state). Red arrows indicate processes inhibited by insulin action and the green arrow the process promoted by insulin action. Blue arrows indicate processes not particularly activated or modulated by insulin. (Figure adapted from Nussey & Whitehead, 2001; Hodson & Frayn, 2011 and based on Vogelberg *et al.*, 1980; Campbell *et al.*, 1992).



### ***2.1.2 Fatty acid turnover, lipolysis and regulation***

White adipose tissue is the largest energy storage organ of the body (around 10-15 kg in a lean young adult) and more than 95% of the body's lipids are found stored as TAGs in adipose tissue, with small amounts in liver and muscle (both cardiac and skeletal) (Coppack *et al.*, 1994). In these tissues, mainly in the adipose, especially during the post-absorptive state, the TAG stores are mobilized through the lipolysis process, which refers to the hydrolysis of TAG into FFAs and glycerol. The main result of lipolysis, occurring both intracellularly and extracellularly, is to release FFAs into the circulation, while in other cells such as those of liver and muscle, lipolysis provides FFAs for local oxidation, and in the intravascular space lipolysis uses circulating lipids to allow the fatty acid tissue uptake. Whereas the TAG breakdown in the vascular space is operated by LPL, the rate-limiting enzyme involved in the lipolysis in the adipocytes is the hormone-sensitive lipase. As the name suggests, the action of this enzyme is promoted and inhibited by hormones, catecholamines (Galster *et al.*, 1981) and insulin (Coppack *et al.*, 1989) respectively. Thus, after a meal when insulin is present at high levels in the circulation, lipolysis is inhibited (Campbell *et al.*, 1992), while during fasting, catecholamines are high and insulin low, lipolysis is promoted and plasma FFA levels are consequently high, resulting in a high level of uptake and oxidation by tissues. This is because the rate of FA uptake is in turn dependent on the FFA concentration in plasma (Armstrong *et al.*, 1961). Adipose triglyceride lipase is equally important to the hormone sensitive lipase (HSL) (Zimmermann *et al.*, 2004). Along with monoacylglycerol lipase, they catabolize stored triglycerides in adipose tissue (Lafontan, 2008; Langin, 2006). Total plasma FFA concentration in humans varies from 90 to 1200  $\mu\text{mol/L}$  with basal values of 300-500  $\mu\text{mol/L}$ . The lowest concentrations occur with carbohydrate-rich diets, and the highest values appear, together with high lipolytic rates, or reduced FFA clearance, during fasting (Stern & Maickel, 1963), prolonged exercise (Havel *et al.*, 1963), diabetes (Taskinen *et al.*, 1985) and obesity (Nestel *et al.*, 1978). In these conditions, the major source of FA comes from adipose tissue TAG lipolysis, while after a meal the major sources of FA are the dietary and excesses of glucose stored as fat via the lipogenesis in liver and adipocytes. It must be considered that the plasma FFA pool is highly dynamic; in fact high clearance rates (the half-life of FFA is about 3-4 min at rest) accompany high rates of FFA uptake and release; this makes it possible that, even in micromolar quantities, FFAs are largely available, with release rates also being greater than utilization rates. On average, overnight post-absorptive FFA release rates are approximately 5-6  $\mu\text{mol/kg/min}$ , whereas whole body fatty acid oxidation rates account for only 3-4  $\mu\text{mol/kg/min}$  (Jensen, 2003). In healthy adults, the daily FFA flux rate is estimated to be 100g/day (Miles *et al.*, 2004).

### ***2.1.3 Fatty acid disposal (utilization)***

#### *2.1.3.1 Fatty acid uptake*

Fatty acid uptake by adipocytes of FFAs released from plasma TAGs by LPL represents an important buffering process among the normal adipose tissue functions (Frayn, 2002). The exact mechanism of transport of FFAs across membranes remains controversial (Kampf & Kleinfeld, 2007). The presence in the fat cell (Lafontan, 2008) and other tissue cell membranes of protein-mediated carrier systems, that operate at low substrate concentrations, is now more accepted, in light of new supporting evidence (Bonen *et al.*, 2007).

In the fasting state, approximately 30-40% of FFA uptake occurs in the splanchnic bed (Meek *et al.*, 1999), but there is no knowledge of the specific contributions of liver, gut or visceral adipose. Considering that most of the FFA uptake in the leg (15-20% of total (Meek *et al.*, 1999)) can be attributed to skeletal muscle, and that leg skeletal muscle constitutes about 40% of the total muscle, it can be stated that FFA uptake in whole body skeletal muscle is probably 40-50% of the total FFA disposal (Jensen, 2003). Myocardial FFA uptake accounts for roughly 5% of systemic FFA disposal, while kidney accounts for less than 4% (Jensen *et al.*, 2001).

Tissue FFA uptake is directly related to plasma FFA concentrations but increasing and lowering FFA concentrations affect FFA uptake differently. When plasma FFA concentration is increased, such as during fasting, there is no resulting shift in the relative proportions of FFA taken up by the different tissue beds, but an overall increase occurs in tissue FFA uptake (Jensen *et al.*, 2001). When FFA concentrations are lowered, such as after a meal (Jensen, 1995) or during insulin infusion (Meek *et al.*, 1999), the relative proportions of fatty acids that are taken up in different tissue beds change. In these conditions, a relative decrease (down to 20-25%) of splanchnic contribution to total FFA uptake and a relative increase (up to 20-30%) of leg tissue contribution are observed (Meek *et al.*, 1999).

Subcutaneous adipose tissue FFA uptake is lower than visceral adipose tissue per unit of fat mass (Hannukainen *et al.*, 2010), but although it is clear that subcutaneous fat plays a bigger role in the FFA removal due to its mass, their relative contribution to the total FFA uptake have not been quantified.

#### *2.1.3.2 Fatty acid esterification and body fat distribution*

The process of storing FAs in more complexed molecules is called esterification and results in the formation of triglycerides that are mainly stored in the adipose tissue. Adipose tissue can be distinguished topographically according to the fat depot location: subcutaneous, intra-abdominal (subdivided into visceral and retroperitoneal), epicardial (subdivided by the pericardial sac into intra-pericardial fat and extra-pericardial fat), extramyocellular, peri-vascular, lymphnodal, retro-orbital and facial, to cite the most important regions (Iozzo, 2009). Of particular importance are the paracervical and supraclavicular adipose tissue, which are examples of brown adipose tissue, and have been found to be functional in adult humans and histologically different from the

“typical” white adipose tissue (Virtanen *et al.*, 2009; Fruhbeck *et al.*, 2009). Besides these compartments, fatty acids can be stored intracellularly in lipid vesicles in other tissues; in this regard, the most studied organs are liver, skeletal muscle and heart. The intracellular lipid depots of these organs constitute an important dynamic pool providing fatty acids when there is a metabolic demand for substrate for oxidation (Kanaley *et al.*, 2009) or TG release (in liver only) (Diraison & Beylot, 1998). In post-absorptive conditions in skeletal muscle of healthy humans esterification was found to match lipolysis with a high rate of pool turnover (29 h pool<sup>-1</sup>) (Sacchetti *et al.*, 2004).

### 2.1.3.3 Fatty acid oxidation

To meet energy demands, once FFAs enter the cells, they can be activated and directed towards  $\beta$ -oxidation into the mitochondria for the production of adenosine triphosphate (ATP). ATP is the best known molecule that contains metabolic energy usable for the vast majority of chemical reactions within the cells and is produced in large quantities by the energy respiratory chain. One molecule of FA, for example, the palmitic acid (16 carbon atoms) is able to produce 129 molecules of ATP via its complete oxidation as compared with glucose (6 carbon atoms) that completely oxidized yields only 36 ATP molecules (Bailey & Ollis, 1986; Stipanuk, 2006).

Skeletal muscle especially in basal conditions is the major determinant of whole body energy expenditure (Zurlo *et al.*, 1990) and fatty acid oxidation is predominant in carbohydrate utilization (Andres *et al.*, 1956).

Fatty acid oxidation plays an important role also in liver metabolism, since 50% of fatty acid taken up undergoes oxidation (Sidossis *et al.*, 1999), while the other 50% is directed towards re-esterification to TAG (Diraison & Beylot, 1998) and subsequent VLDL secretion.

Convincing evidence demonstrates that white adipose tissue, even if capable of oxidizing FAs, oxidizes almost solely glucose (Frayn *et al.*, 2008). Compared to white adipose tissue, brown adipose tissue contains more mitochondria, therefore it is intrinsically capable to burn chemical energy (Fruhbeck *et al.*, 2009; Cannon & Nedergaard, 2004). In burning chemical energy, brown adipose tissue is characterized by the involvement of uncoupling proteins (UCPs) that dissipate energy and produce heat (Cannon & Nedergaard, 2004). Unlike white fat, brown adipose tissue has shown a selective uptake of fatty acids (especially under cold stimulation state) (Bartelt *et al.*, 2011) and it has been estimated that most of the substrate oxidation in brown adipose tissue derives from fatty acids (Virtanen *et al.*, 2009).

Figure 2.3.3.1.1 shows an overview of cardiac fatty acid metabolism, with special reference to the processes occurring inside the mitochondrion. Heart FFA oxidative metabolism under aerobic conditions represents 60-90% of the total substrate oxidation (Stanley *et al.*, 1997), while carbohydrates contribute only 10-40% of generated energy (Gertz *et al.*, 1988). It must be noted that glucose oxidation is more efficient in oxygen utilization than lipid oxidation (Ferrannini, 1988); for this reason fatty acid oxidation requires 10-15% more oxygen. These increased requirements and reliance on FFAs render the heart vulnerable in situations of low oxygen supply. A strategy to help the heart in critical situations will be described in section 2.4.1. Another important aspect

of heart FFA oxidative metabolism is the source of lipid fuel. It is known that skeletal muscle FFA oxidation rate during exercise exceeds the FFA availability and intracellular lipid depots assume an important role as substrate provider (van Loon, 2004). Taking into consideration that the heart is continuously working, it is reasonable to think that both sources (intracellular and circulating FA) are important. It is not known in a human what is the contribution of circulating FFA as compared to intracellular lipid depots to the myocardial fatty acid oxidation. This concept has already been studied in dogs (Kisrieva-Ware *et al.*, 2009).

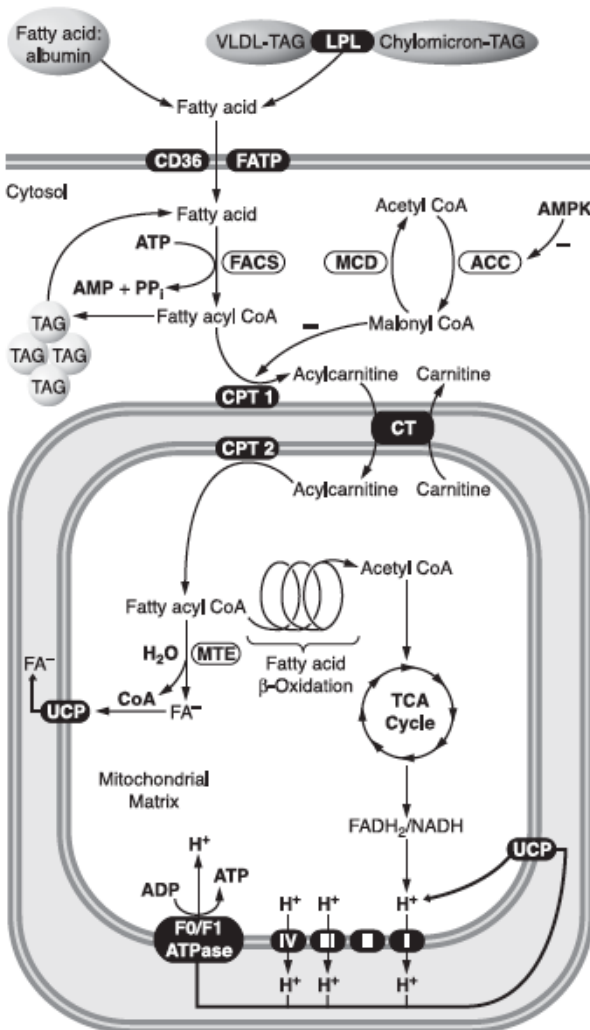


Figure 2.3.3.1.1. Overview of fatty acid  $\beta$ -oxidation in the heart. Fatty acids utilized for cardiac fatty acid  $\beta$ -oxidation primarily originate from either plasma fatty acids bound to albumin or from fatty acids contained within chylomicron or very-low-density lipoproteins (VLDL) triacylglycerol (TAG). Fatty acids are taken up by the heart either via diffusion or via CD36/FATP transporters. Once inside the cytosolic compartment of the cardiac myocyte, fatty acids (bound to fatty acid binding proteins) are esterified to fatty acyl coenzyme A (CoA) by fatty acyl CoA synthase (FACS). The fatty acyl CoA can then be esterified to complex lipids such as TAG, or the acyl group transferred to carnitine via carnitine palmitoyltransferase (CPT) 1. The acylcarnitine is then shuttled into the mitochondria, where it is converted back to fatty acyl CoA by CPT 2. The majority of this fatty acyl CoA then enters the fatty acid  $\beta$ -oxidation cycle, producing acetyl CoA, NADH, and FADH<sub>2</sub>. Under certain conditions, mitochondrial thioesterase (MTE) can cleave long-chain acyl CoA to fatty acid

anions (FA<sup>-</sup>), which may leave the mitochondrial matrix via uncoupling protein. (Figure and legend from Lopaschuk *et al.*, 2010).

### ***2.1.4 Fatty acid metabolism regulation and interaction with glucose metabolism***

It is not surprising that fatty acid metabolism is finely regulated, given the central role of FA in the body and cellular energy homeostasis. A gross acute regulation operated by insulin determines the switch between the predominant lipolysis/fatty acid oxidation during fasting and predominant lipid storage/glucose utilization following a meal. A long-term regulation is further operated by catecholamines. Finally, a fine regulation at cellular level is operated by the interaction of two main energy metabolisms (glucose and FA) through the well known substrates cycles (Frayn, 2003). Randle and colleagues were the first to describe how fatty acid oxidation fuelled by increased FA availability inhibits glucose uptake and oxidation (Randle *et al.*, 1963). The direct cellular mechanism of inhibition of glucose oxidation by fatty acids in the cardiac and skeletal muscle cell is shown in Figure 2.1.4.1. Fatty acids entry increases acetyl CoA and citrate content that inhibit pyruvate dehydrogenase (PDH) and phosphofructokinase (PFK), respectively. The subsequent excess of glucose-6-phosphate concentration inhibits hexokinase (HK) II activity, reducing cell glucose uptake. Nuutila and coworkers (Nuutila *et al.*, 1992) confirmed in vivo that elevation of FFA reduces whole body, skeletal and cardiac muscle glucose uptake. It is still matter of debate the intracellular mechanism originally proposed by Randle, which associates increased  $\beta$ -oxidation to insulin resistance. This mechanism has been questioned in skeletal muscle where increased FA concentrations reduced glucose uptake more than twice as much compared to the reduction in glucose oxidation and glycogen synthesis, probably mediated by inhibition of glucose transporter 4 (GLUT4) membrane translocation, rather than HK inhibition (Roden *et al.*, 1996). Later the insulin receptor signaling pathway has been suggested as mediator of increased cellular FA-CoA and inhibition of GLUT4 translocation (Roden, 2004; Perseghin *et al.*, 2003). However, in support of Randle cycle hypothesis, it has to be noted that the inhibitory effects of increased plasma FFA on whole body glucose storage and uptake is only apparent after 2-4 hours (Boden *et al.*, 1991), while glucose oxidation effects are evident during the first hour (Roden *et al.*, 1996; Roden, 2004). It was concluded that, during hyperinsulinemia, lipid rapidly replace glucose as oxidative substrate and inhibit glucose uptake. Studies from Hirabara and coworkers reconciled the two views, supporting both Randle cycle and the inhibition of insulin pathway in skeletal muscle in presence of FFA (Hirabara *et al.*, 2003; Hirabara *et al.*, 2007). They found increased intracellular glucose-6-phosphate in rat soleus muscle acutely exposed of to FAs in presence of insulin; they explained the findings, postulating that fatty acids acutely potentiate insulin-mediated glycogen synthesis via a mechanism that requires its metabolism (i.e. Randle cycle), thus reconciling both views. These studies and others reviewed elsewhere (Zhang *et al.*, 2010) and discussed in section 2.3.3 suggest caution in the approach aimed at increasing fatty acid oxidation for treating insulin resistance.

Randle's original article, proposing the so-called "glucose-fatty acid cycle", tried to describe the homeostatic mechanism that controls circulating concentrations of glucose and fatty acids between different organs, in a hormone-independent and a hormone-dependent fashion (Randle 1963). Figure 2.1.4.2 shows the original Randle cycle view.

The cycle permits the maintenance of a constant glucose plasma concentration in animals that feed intermittently with a hormone-independent mechanism. Insulin can interact, inhibiting adipose tissue lipolysis, reducing circulating concentrations of fatty acids, and thus affecting fuel selection in muscle and adipose tissue.

McGarry and Foster discovered that Randle's cycle can be reversed when the glucose excess inhibits the fatty acid oxidation (McGarry *et al.*, 1977). The mechanism of how increased glucose inhibits fatty acid oxidation is explained in Figure 2.1.4.2. When citrate escapes oxidation and is transferred to the cytosol it can regenerate acetyl-CoA, which in turn may be carboxylated to malonyl-CoA. Malonyl-CoA promotes through fatty acid synthase (FAS), fatty acid esterification and directly inhibits carnitine palmitoyltransferase (CPT) I, which regulates the LCFA entry and oxidation in mitochondria. This mechanism was discovered first in the liver (McGarry *et al.*, 1977).

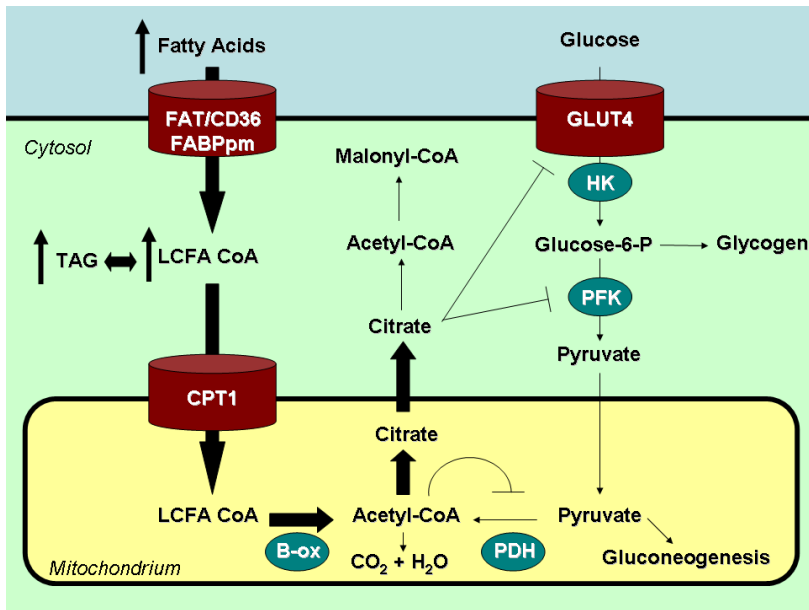


Figure 2.1.4.1. – Fatty acids inhibit glucose oxidation in cardiac muscle and partly in skeletal muscle (please refer to the text). In heart, the mechanism of inhibition is believed to be graded as more severe at the level of pyruvate dehydrogenase (PDH) and less severe at the level of 6-phosphofruct-1-kinase (PFK) or glucose uptake. (Figure adapted from Hue & Taegtmeier, 2009).

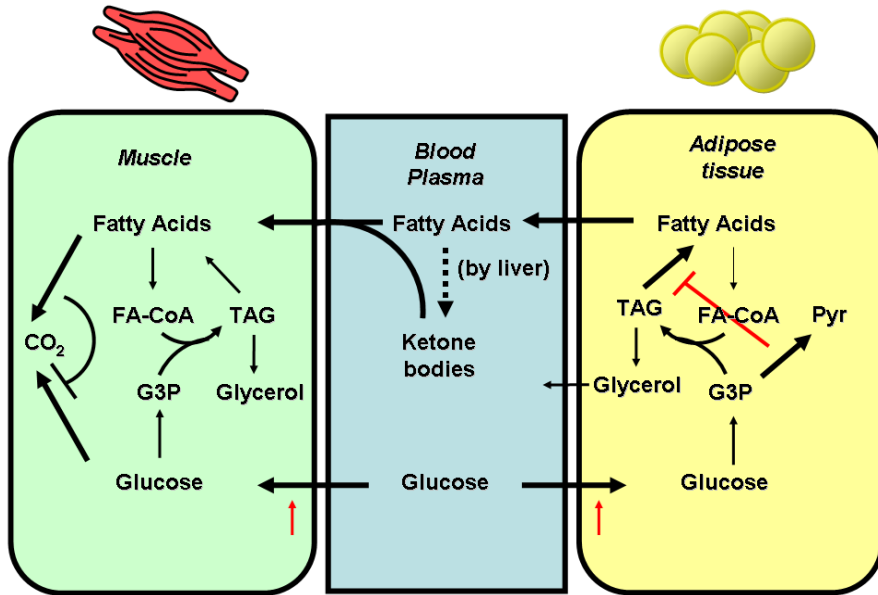


Figure 2.1.4.2. Randle's "glucose-fatty acid cycle": a reciprocal control (hormone independent) between glucose and fatty acid metabolism depicted by black arrows. Red arrows represent the control operated by insulin: glucose uptake stimulation and lipolysis inhibition. FA-CoA, Fatty acid acyl-CoA; G3P, L-glycerol-3-phosphate; TAG, triacylglycerol; Pyr, pyruvate. (Figure based on Randle *et al.*, 1963 and adapted from Hue & Taegtmeyer, 2009).

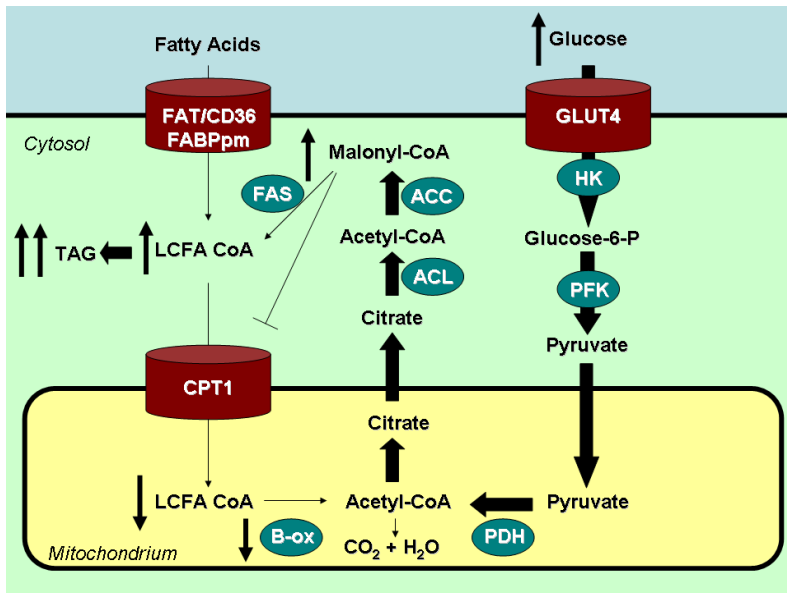


Figure 2.1.4.3. Glucose inhibits fatty acid oxidation in liver, cardiac and skeletal muscle. (Figure adapted from Hue & Taegtmeyer, 2009).

## 2.2 Assessment of fatty acid metabolism and fat storage in vivo

### 2.2.1 Whole body fatty acid metabolism

When considering the body in its entirety, pooling all tissues together, the two main processes ruling FA disappearance are: oxidation and esterification (storage). It is equally important to assess the FFA turnover, the balance between lipolysis and re-esterification, which regulates FFA plasma levels and is mainly determined by adipose tissue; the topic will be introduced in this section and expanded in the following dedicated to the specific tissue.

FA oxidation produces CO<sub>2</sub> that is carried to lungs and expelled by breathing; indirect calorimetry is a technique that measures the whole body gas exchange (VO<sub>2</sub> and VCO<sub>2</sub>) (Ferrannini, 1988). With this technique, total net lipid oxidation can be measured, but cannot differentiate and includes both oxidation of plasma FFA and oxidation of intracellular lipids, a concept revealed by the use of the following technique.

Radioactive isotope tracers, such as <sup>14</sup>C-palmitate, have been used to measure plasma FFA oxidation only (Frederickson & Gordon, 1958; Groop *et al.*, 1991). Comparing the results with indirect calorimetry, Groop and colleagues showed that oxidation of circulating FFA represents from 40% to 50% of total lipid oxidation, and the rest is released by intracellular depots (Groop *et al.*, 1991).

Palmitic acid accounts for ~ 30% of the total FFA pool regardless of the plasma FFA concentration (Hagenfeldt *et al.*, 1972). Because the fractional turnover of palmitate is very similar to that of total FFA, labelled palmitate can be used to trace total FFA turnover (Frederickson & Gordon, 1958; Hagenfeldt *et al.*, 1972; Groop *et al.*, 1989). Fatty acid turnover can also be measured using isotope dilution techniques involving the infusion of stable isotopomers of fatty acids (e.g. <sup>13</sup>C<sub>1</sub>-palmitate) (Wolfe & Peters 1987).

Nonoxidative FFA disposal, a measure of FFA re-esterification (or fat storage), is assumed to be measurable by the difference between FFA turnover rate (by radioactive isotope labelled tracer) and total net lipid oxidation (by indirect calorimetry) (Diraison & Beylot, 1998; Groop *et al.*, 1991; Waterhouse *et al.*, 1969).

The opposing process to FFA re-esterification is the FFA release (or lipolysis), and similarly as for FFA turnover, it has been demonstrated, via radioactive isotope tracers, that plasma palmitate Ra (Rate of appearance) is similar to total FFA Ra (or lipolysis) (within 15% of the real value). It must be noted that in fasting conditions, in the steady-state, FFA release equals FFA appearance and FFA turnover (Havel *et al.*, 1963). Whole body lipolysis can also be estimated using glycerol tracers to measure rates of appearance (Ra) (Wolfe & Peters 1987).

### 2.2.2 Adipose Tissue

*In vivo* assessments of systemic and regional adipose tissue FFA release have been carried out in humans under a variety of circumstances (feeding, fasting, exercise, obesity, diabetes, etc) (Frayn *et al.*, 1997). Similarly, measures of dietary and FFA storage in regional fat depots have been reported (Jensen, 2008).



The first two main techniques available to investigate regionally *in vivo* FA metabolism in adipose tissue were the arteriovenous technique (Frayn *et al.*, 1989) and microdialysis (Arner & Bulow, 1993; Arner & Bolinder, 1991). The evolution of the technology permitted the combination of the above-mentioned techniques with radioactive and isotopic tracers, usually used for systemic measurements (Coppack *et al.*, 1994).

The arteriovenous technique has some advantages compared to microdialysis. It can be used to estimate absolute substrate flux of hydrophobic molecules and lipoprotein particles, while this is not possible with microdialysis. On the other hand, both techniques require blood flow for the estimates, and microdialysis allows simultaneous blood flow assessment and is easier to perform than arteriovenous techniques, plus it can study more than one adipose depot. A limitation for both techniques is the inability to study the intra-abdominal adipose tissue (Frayn *et al.*, 1997), and a negative aspect can be their invasiveness.

Measurement of splanchnic FFA release by arteriovenous technique (hepatic vein catheterization) and isotope dilution gives only indirect estimates of visceral adipose tissue lipolysis (Nielsen *et al.*, 2004), since it is impractical to obtain direct measurements from the portal vein in humans. This limitation can be overcome by the use of non-invasive PET imaging of the abdominal area, by means of which the rate of lipolysis can be estimated in relation to the specific fat depot mass.

Dietary FA uptake in subcutaneous and visceral adipose tissue in normal weight humans has been compared by tissue biopsies, showing that VAT accumulates more dietary fat (milligram meal fat per gram of adipose tissue lipid) than either upper body subcutaneous or lower body subcutaneous fat (Jensen, 2008). Similar results, but related to circulating FFA, have been described in lean subjects with the use of PET and a long chain FA tracer ( $^{18}\text{F}$ -FTHA) (Hannukainen *et al.*, 2010), but before the present study there were no similar investigations in obese subjects.

### **2.2.3 Liver**

The liver plays an important role in the fatty acid trafficking, being active in utilizing and releasing FAs. Because of its anatomical location it is impractical to perform direct organ measurements; additional complications derive from the fact that the liver has a dual blood supply, from systemic circulation (hepatic artery) and from splanchnic circulation (portal vein). Indirect methods assessing liver FA metabolism, such as invasive procedures of splanchnic balance (DeFronzo, 1987; Sidossis *et al.*, 1999), have not been able to distinguish between the relative contributions to FA turnover of liver, visceral adipose and gut, except for two studies contextual to abdominal surgery (Hagenfeldt *et al.*, 1972; Vogelberg *et al.*, 1980).

Liver lipogenesis and FFA re-esterification contribute to about 50% of liver TG release. These results were obtained by indirect calorimetry and stable isotope-labelled tracers at whole body level (Diraison & Beylot, 1998), hence additional studies with direct regional measurements are warranted.

Before the current study, liver lipid oxidation has been extensively studied in animal models but in humans only indirectly via measurement of serum  $\beta$ -OH butyrate (Hodson & Frayn, 2011).

Using positron emission tomography it has been possible to non-invasively investigate liver metabolism as shown by the first study in humans that quantified hepatic FFA uptake by using the  $^{18}\text{F}$ -FTHA tracer (Iozzo *et al.*, 2004; Iozzo *et al.*, 2003) or  $^{11}\text{C}$ -Acetate and  $^{11}\text{C}$ -Palmitate (Rigazio *et al.*, 2008). It is now a challenge to go beyond the uptake measurement and assess individual pathways, such as FFA oxidation, esterification, or release of TG by the liver.

Another issue related to fatty acid metabolism is the amount of fat stored within specific tissue cells. For this purpose, magnetic resonance spectroscopy has been validated as a useful technique to measure non-invasively the hepatic intracellular fat content (Szczeplaniak *et al.*, 1999), and has been used in conjunction with other methodologies to investigate liver insulin sensitivity and systemic insulin resistance (Rigazio *et al.*, 2008; Kotronen *et al.*, 2008a).

#### **2.2.4 Skeletal Muscle**

Skeletal muscle is responsible for the majority of whole body lipid oxidation (Andres *et al.*, 1956; Zurlo *et al.*, 1990). Capaldo and coworkers first and Kelley and colleagues later were active in measuring RQ and fatty acid oxidation and uptake across the leg by indirect calorimetry with the organ balance method (Colberg *et al.*, 1995; Kelley & Simoneau, 1994; Capaldo *et al.*, 1988). Even if the measurements referred to skeletal muscle, it cannot be excluded that adipose tissue of the leg might have influenced the observations especially when comparing subjects with different degrees of adiposity. Particularly for FFA balance the problem arises that FAs are both taken up and released by the leg (Ahlborg *et al.*, 1974). FFA uptake occurs into muscle but possibly also into fat, and FFA release occurs from adipocytes (Guo *et al.*, 2000; Dyck *et al.*, 1997). Even if not convinced by this evidence, Jensen acknowledges that FFA net uptake across the leg does not reflect the total uptake (Jensen, 2003). Furthermore he underlines that change in local lipolysis can dramatically affect the measurements, thus requiring the use to be combined with isotopic tracers (Jensen, 2003).

By combining the use of tracers and A-V balance it has been possible to measure FFA oxidation, but it is still considered a rough estimation, because of labelling fixation issues (Jensen, 2003). The combined method has another limitation, it is, for example, extremely difficult to measure leg tissue RQ at rest, because of the small differences between arterial and venous concentrations of  $\text{CO}_2$ , even when specific analyzers are used (Jensen *et al.*, 1998).

PET imaging has a promising chance to provide non-invasive and quantitative measurement of skeletal muscle FFA metabolism. A first attempt has been carried out with the  $^{18}\text{F}$ -FTHA tracer, planned as an oxidation tracer via accumulation in the mitochondria, but that resulted in an FFA uptake tracer for skeletal muscle, since a study in pigs showed only 36% of the tracer uptake enters the mitochondria (Takala *et*

*al.*, 2002). Two studies in humans had been performed before the pig study (Maki *et al.*, 1998; Turpeinen *et al.*, 1999).  $^{11}\text{C}$ -Palmitate has been effectively used for tracing myocardial FAO (Bergmann *et al.*, 1996), but no studies have so far investigated the skeletal muscle with this tracer.

IMTG quantification has been the focus of extensive research in the past two decades. MR methodology has contributed considerably to the topic. In particular, proton ( $^1\text{H}$ ) MRS technique has been optimized to distinguish intramyocellular (IMCL) from extramyocellular lipid content (EMCL) *in vivo*, non-invasively (Boesch *et al.*, 1997; Szczepaniak *et al.*, 1999) and with a great reproducibility (Torriani *et al.*, 2005). MRI and CT quantification methods have also been effectively adopted, although both methods lack differentiation between IMCL and EMCL, and the second method does not provide absolute quantification (Dube & Goodpaster, 2006).  $^1\text{H}$ -MRS provides also additional information such as the creatine content (van der Meer *et al.*, 2007) that relates to skeletal muscle oxidative potential (Chansemaume *et al.*, 2008).

### 2.2.5 Heart

*In vitro* and *ex vivo* methodologies have been proven to be useful in many mechanistic studies, and they have been perfected over the years (Barr & Lopaschuk, 2000). PET methodology, which will be described in the following section, has high costs and may be technically demanding, but provides *in vivo* measurements that can be performed longitudinally.

PET studies in humans have shown that it is feasible to assess myocardial metabolism, as shown in Figure 2.2.5.1 (Iozzo, 2010).  $^{11}\text{C}$ -palmitate has been used to assess FA metabolism (including oxidation) (Schelbert *et al.*, 1986; Bergmann *et al.*, 1996). This technique measures the influx of FAs from the circulation and gives the relative fractions (rate constants) of substrate flowing to mitochondria for oxidation or moving in and out of triglyceride stores, but it cannot estimate the absolute amounts of intracellular lipid turnover. Estimation of the latter requires that the PET-derived rate constants are multiplied by the intracellular mass of FAs, as quantified by  $^1\text{H}$ -MRS. Figure 2.2.5.2 shows a simplification of the theory behind MRS (explained in detail in section 2.2.7) and its application in myocardial cardiac energy metabolism assessment, as recently reviewed (Iozzo, 2010). As measured by  $^1\text{H}$ -MRS, myocardial triglycerides in lean individuals are  $10\ \mu\text{mol/g}$  ( $= 30\ \mu\text{mol/g}$  of FAs) (Kankaanpaa *et al.*, 2006) which is more than twice as high as the hourly uptake of FAs from blood (about  $4\ \mu\text{mol/g/h}$  of triglycerides or  $12\ \mu\text{mol/g/h}$  of FAs, calculated from Peterson *et al.*) (Peterson *et al.*, 2004). This means that myocardial triglycerides might be an important source of oxidative energy. The first study that tackled this issue has been performed by Kisrieva-Ware and colleagues that have studied 26 dogs in different conditions with  $^{11}\text{C}$ -palmitate and lipid pool pre-labelling to measure fatty acid trafficking and oxidation derived from endogenous TG depots (Kisrieva-Ware *et al.*, 2009). However studies in humans are warranted.

### ***2.2.6 Positron Emission Tomography principles***

PET is a nuclear imaging technique that employs short-lived positron-emitting radioisotopes to label molecules of interest (e.g., substrate, perfusion indicator) and visualize their fate in individual organs. Emitted positrons annihilate when combined with an electron in the body tissue, generating two 511 KeV photons in quasi-opposite directions. Detectors are arranged all around the tissue of interest, and events interacting nearly simultaneously with opposite detectors are recorded and used to generate the image. After extracting from the image information pertaining to the time activity concentration of tracer in the blood and cardiac wall, mathematical modelling is used to quantify the rates of metabolic processes within the target tissue. The main advantages of PET imaging are that it is functional and quantitative, the short-lived nature of positron decay (<2 min to 110 min for the nuclides shown here) allows conduction of repeated studies, and most radionuclides ( $^{11}\text{C}$ ,  $^{13}\text{N}$ ,  $^{15}\text{O}$ ) are isotopes of naturally occurring elements in the organic matter and can be substituted in the target molecule without altering its structure; others ( $^{18}\text{F}$ ) are complexed to form analogues, which are meant to minimally or purposely affect the properties of the natural compounds (Iozzo, 2010).

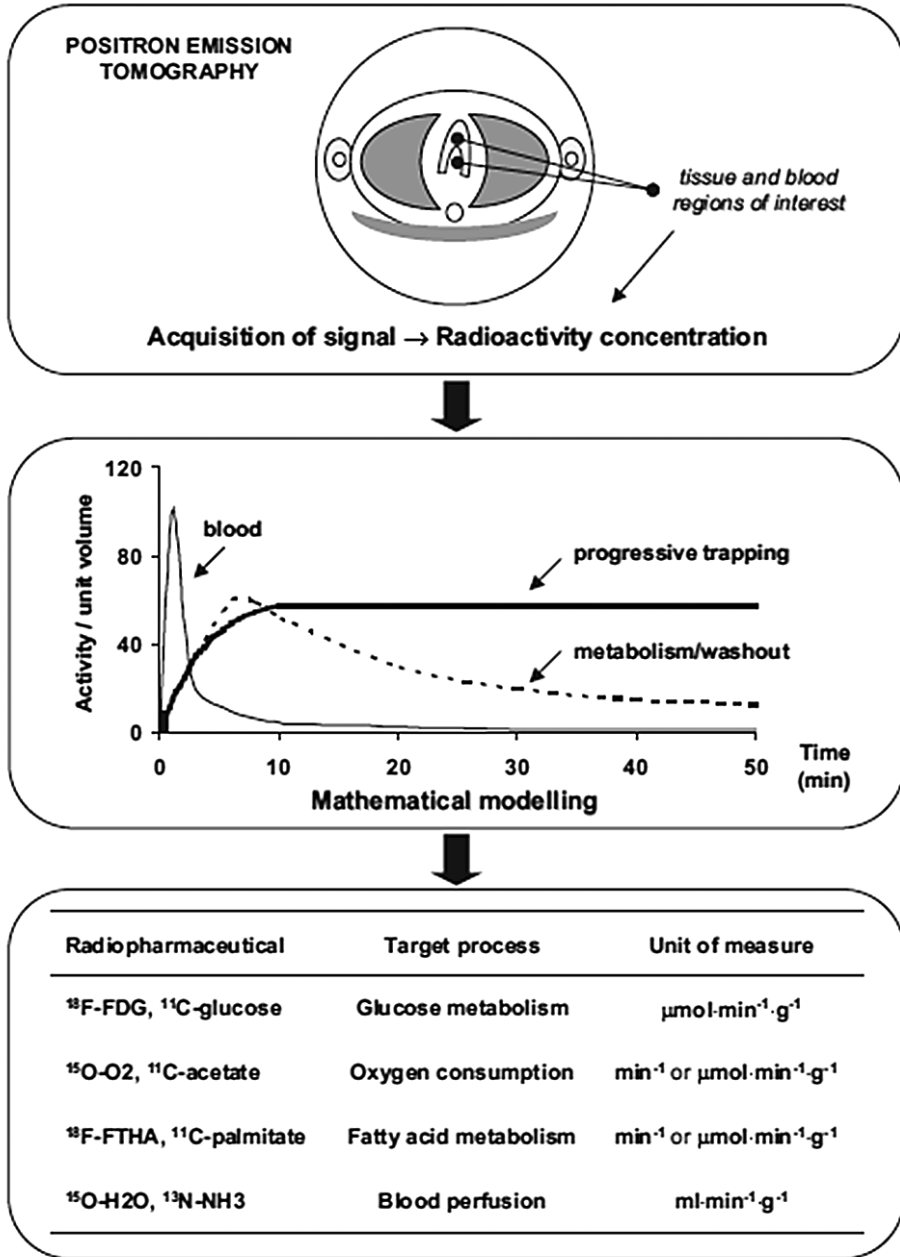


Figure 2.2.5.1. PET principles and the most commonly used PET tracers with the corresponding target myocardial metabolic processes are shown in the bottom table. (Figure from Iozzo, 2010).

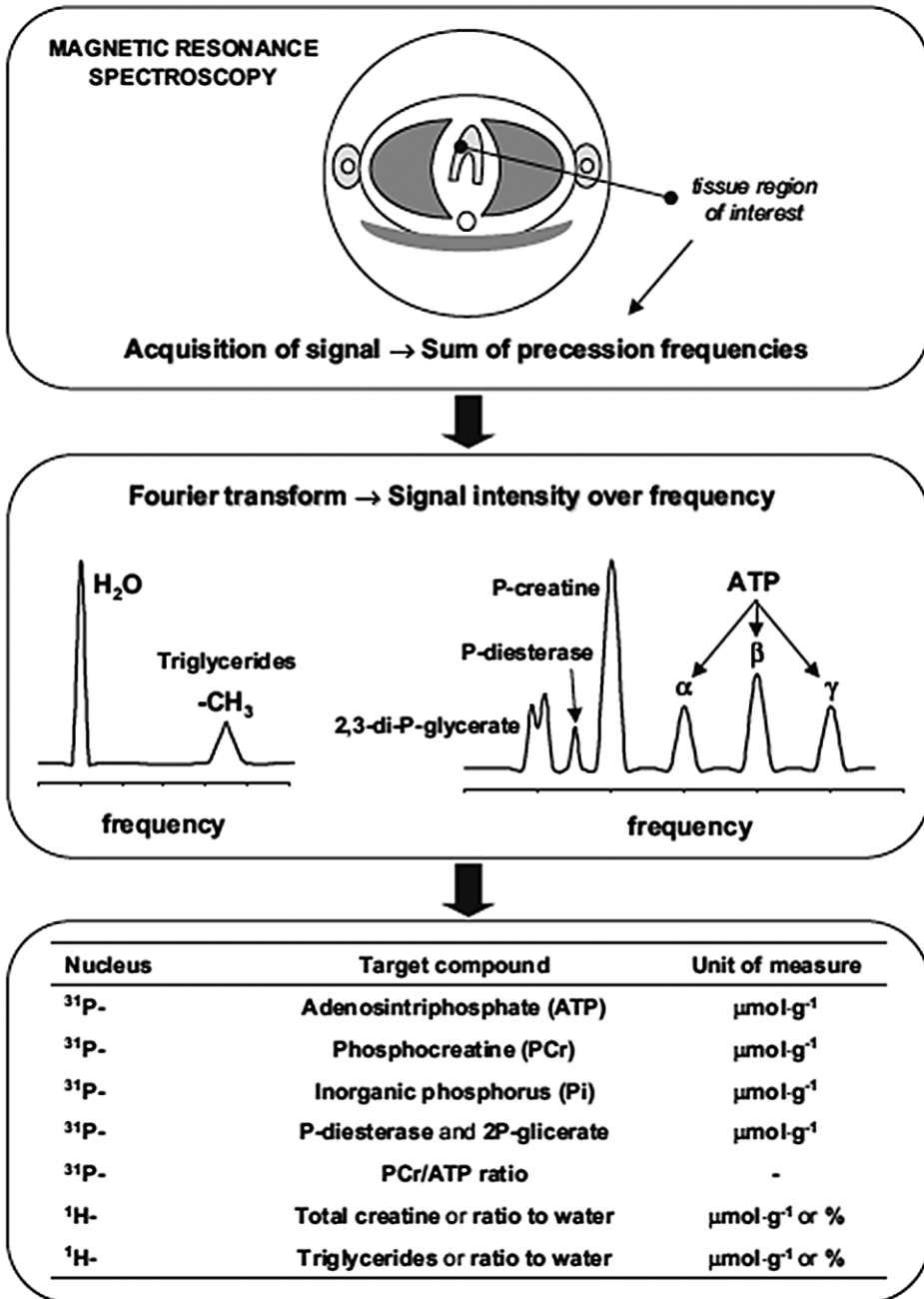


Figure 2.2.5.2. Principles of MRS and, as shown in the bottom table, its application in the study of cardiac high-energy phosphate metabolism and lipid toxicity by use of <sup>31</sup>P- and <sup>1</sup>H-MRS. (Figure from Iozzo, 2010).

### ***2.2.7 Magnetic Resonance Spectroscopy principles***

MRS provides quantitative information on the molecular composition of the different body tissues. The technique is based on the concept that, when nuclei with a net spin are subjected to a magnetic field they precess at highly specific frequencies. Besides, the electrons surrounding the nucleus of interest superimpose a unique magnetic force on the main field of the scanner, making nuclei of the same species in different metabolites resonate at slightly different frequencies. Such chemical shift properties enable distinction of molecules by MRS. The original signal, represented by a sum of frequencies recorded as a function of time is transformed into a spectrum of peak amplitudes as a function of frequency, in which peak-areas represent the relative abundance of corresponding metabolites (Iozzo, 2010).

### ***2.2.8 Fat distribution, assessment of whole body and regional fat depots***

Several methods have been validated to measure fat distribution in the human body, beyond the “classical BMI”. The simplest method to estimate fat composition is based on gender, height and weight (Hume, 1966). Direct measurement can be performed with dual energy X-ray absorptiometry (DEXA) (Haarbo *et al.*, 1991). Regarding abdominal fat distribution, waist circumference or waist/hip ratio have been adopted as practical ways to measure central adiposity, but the accurate measurement of visceral fat require the use of imaging techniques such as magnetic resonance imaging (MRI) or computed tomography (CT). Even if total volume quantification is the optimal method, it has been demonstrated that abdominal subcutaneous, intraperitoneal and retroperitoneal fat depots can be predicted and estimated from a single MRI axial slice at the level of the intervertebral disc L2-L3 (Abate *et al.*, 1997).

The fat accumulation surrounding the heart has been studied subsequently with more advanced techniques. One of the first imaging methods was echocardiography (Iacobellis & Willens, 2009) which allows the measurement of the epicardial and pericardial fat thickness. Recently, with imaging techniques such as magnetic resonance (Nelson *et al.*, 2009) and computer tomography (Mahabadi *et al.*, 2009) it has been possible to measure the volumes of intra- and extra-pericardial fat (see section 2.3.5 for explanation of nomenclature).

### 2.3 Lipotoxicity: a fatty acid metabolism disorder

One of the first appearances of the term “lipotoxicity”, in a scientific publication related to metabolic diseases, was in a research paper where Unger and coworkers described the toxic effects of excessive free fatty acids on pancreatic  $\beta$ -cell survival, suggesting that hyperlipidaemia has a role in the pathogenesis of the non-insulin-dependent diabetes mellitus or type 2 diabetes mellitus (T2DM) (Lee *et al.*, 1994). McGarry, one of the co-workers of this paper, already two years before, in a seminal paper, proposed a pioneering way of looking at T2DM; in his view, disordered fatty acid metabolism assumed a central role (McGarry, 1992). Afterwards, new evidence supported the concept of fatty acids as mediators of disease progression, with associations to the predisposing conditions: insulin resistance syndrome and obesity (Boden, 1997; Boden, 1998). By insulin resistance is meant a “pre-diabetic” condition where organs are less responsive to the insulin action, requiring an increased secretion of insulin from the pancreas, which in the long run burns-out its  $\beta$ -cells. It is important to mention that nowadays there is still an open debate on which is the first organ to fail and cause insulin resistance, whether it is the brain (Pagotto, 2009), the liver (Perseghin, 2009), the skeletal muscle (DeFronzo & Tripathy, 2009) or the pancreas (Kahn *et al.*, 2006). The review and the thesis are aimed to support a different hypothesis: adipose tissue is the first organ, the primary culprit that once hit causes the cascade of damaging events occurring in metabolic diseases. According to this hypothesis, lipotoxicity can be defined as a condition in which fatty acids are not properly stored in adipose tissue and they overflow to nonadipose tissues, accumulating in the so-called ectopic fat and causing a compensatory increase in fatty acid oxidation with formation of toxic lipid metabolites and free radicals. All this leads to organ insulin resistance and/or impairment of organ function (Iozzo, 2009; Lelliott & Vidal-Puig, 2004). Some evidence supporting the “lipotoxicity hypothesis” is reviewed in this section, but for more information, see recent more comprehensive reviews (Cusi, 2010; Iozzo, 2009; Mittendorfer, 2011).

Adipose tissue assumes a central role in the pathogenesis of metabolic diseases, especially of insulin resistance, being the organ that physiologically stores and releases fatty acids, and it has been substantiated by a great deal of evidence that elevated FFAs promote insulin resistance (Boden, 2011). Furthermore, the adipose tissue is the largest endocrine organ of the body and Figure 2.3.1 summarizes the main roles and effects of the principal fat-derived products that have been related to insulin resistance and metabolic risk. Based on the evidence reviewed, Iozzo proposed the cascade of events (reported in Figure 2.3.2) occurring when adipose tissue develops abnormally, causing a vicious circle of detrimental phenomena that lead to insulin resistance in nonadipose organs (Iozzo, 2009).



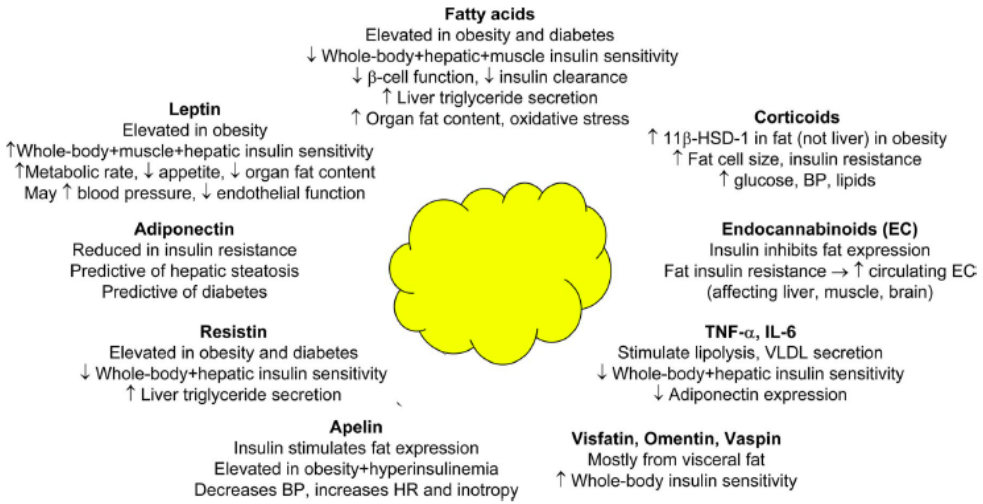


Figure 2.3.1. The adipose tissue as endocrine organ and the products involved in the metabolic risk. (Figure from Iozzo, 2009).

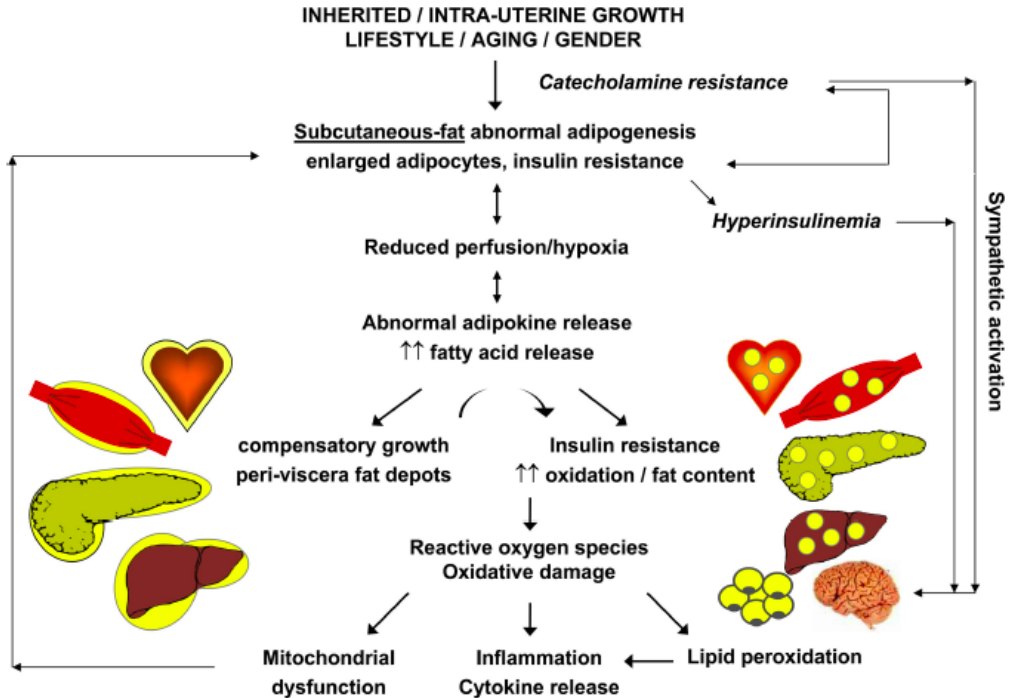


Figure 2.3.2. The cascade of events caused by abnormal subcutaneous adipose tissue adipogenesis. (Figure from Iozzo, 2009).

### 2.3.1 Lipotoxicity in obesity: adipose tissue failure in storing fatty acids

Obesity is nowadays considered a pandemic health problem. An obese subject is defined by the World Health Organization as a subject with a body mass index larger than 30 kg/m<sup>2</sup> (WHO Consultation, 1998). In 2010, it was estimated by the International Obesity Task Force that there were 475 million obese people worldwide, most of them in the developed countries where specific environmental conditions can trigger genetic backgrounds. The prevalence of the disease has steeply increased worldwide since World War II, partly due to culturally mediated changes like hypercaloric diets and the decreased level of physical activity associated with the modern industrialized society (Price et al., 1993). It has been proposed that several factors contribute to the development of the disease, the basic idea being that these factors, external or internal, act to disrupt the balance between food intake and energy expenditure, shifting the scale so that an increased food intake and/or a reduced energy expenditure lead the subject to accumulate fat mass in the body.

Obesity predisposes to a series of life-threatening comorbidities, strong relationships have been found by many studies between obesity and incidence of diabetes, cardiovascular disease and some types of cancers (Whitlock et al., 2009). Obesity is also closely associated with peripheral and hepatic insulin resistance (Boden, 1997) and with a low-grade inflammatory state characterized by elevated proinflammatory cytokines in blood and tissues (Tataranni & Ortega, 2005). These conditions contribute to the development of type 2 diabetes mellitus (T2DM), hypertension, atherogenic dyslipidemias, and disorders of blood coagulation and fibrinolysis (Boden, 2008). All of these disorders are also independent risk factors for atherosclerotic vascular disease such as heart attacks, strokes and peripheral vascular disease (Bray, 2004). Understanding the molecular mechanisms controlling the development of obesity is essential for designing effective therapies.

Obesity is characterised by an increase in the adipose deposits, resulting from an imbalance between food intake and energy expenditure. This adipose tissue expansion is a physiological and protective process (Ruge *et al.*, 2009). Not all obese subjects are metabolically “unhealthy”; it has reported that 20% of the obese population is metabolically healthy, *i.e.*, they have increased fat mass, but favorable cardiovascular risk profile (low TG, high HDL), high insulin sensitivity and low visceral fat (Karelis et al., 2004), but some report that the prevalence of this phenotype in the population might be lower than it was previously thought (Calori *et al.*, 2011), while others report higher values (Mittendorfer, 2011). In the Cremona Study, metabolically healthy obese subjects, defined by BMI and HOMA-IR cut-offs, had similar, if not better, survival than non-obese insulin-sensitive subjects (Calori *et al.*, 2011). Thus, what is dangerous is the wrong accumulation of fat (in ectopic sites) or the non-accumulation of fat, like in lipodystrophy (Frayn *et al.*, 2003). Hyperplastic obesity - in which newly differentiated adipocytes maintain the ability to store triglycerides - is typically more benign than fat hypertrophy (Iozzo, 2009). Insulin-sensitive individuals, in whom the anabolic effect of insulin is enhanced, gain more weight and have a fourfold more rapid decrease in insulin sensitivity than less insulin-sensitive subjects, as documented

by longitudinal studies in Pima Indians (Swinburn *et al.*, 1991). This means that even if BMI, as a rough measure of obesity, has worked quite well for several decades, the whole body fat accumulation is not the only factor to consider for identifying a subject at risk, and to progress, the aim should be the characterization of adipose tissue metabolism with non-invasive and reproducible methods and the association with insulin sensitivity measures. Nowadays a characterization of abdominal obesity is preferred to identify high risk individuals. The rationale behind this is that visceral adipose tissue is believed to be more prone to lipolysis in response to counter-regulatory hormones and more resistant to the antilipolytic effect of insulin (Ostman *et al.*, 1979; Despres, 2007). Moreover, it has been proposed that because visceral fat drains directly into the portal vein, FFA derived from it would have a more direct impact on liver metabolism than fat from peripheral (subcutaneous) lipolysis (Cusi, 2009). Even if the “portal hypothesis” seems reasonable to explain the development of hepatic insulin resistance by visceral adipose tissue, the finding that in healthy obese subjects the contribution of visceral fat to the peripheral plasma FFA pool increases only modestly (from 10% to only 25% compared to lean subjects) (Nielsen *et al.*, 2004), suggests that expansion of subcutaneous fat adipose tissue is important in the development of hepatic insulin resistance. Furthermore, since FFA from visceral fat contributes only 5% or less to the overall FFA pool (Nielsen *et al.*, 2004), it is unlikely to be primarily responsible for peripheral (muscle) insulin resistance, again highlighting the detrimental effect of overall adiposity (visceral and subcutaneous) as sources of FFA for subsequent ectopic (*i.e.*, muscle, liver,  $\beta$ -cells) fat deposition (Cusi, 2009).

Despite the dominant role played by adipose tissue in the regulation of systemic FA disposal, this tissue produces a variety of hormones and proinflammatory cytokines that affect insulin action, lipolysis, and oxidative stress (Wu *et al.*, 2009). And to further stress the increased importance of subcutaneous adipose tissue, leptin, the adipose tissue-derived peptide that has been clearly shown to have physiological relevance in man, is secreted in considerably greater amounts from subcutaneous than from visceral fat depots (Van, V *et al.*, 1998; Montague *et al.*, 1998).

In the following sections, the effects of lipotoxicity on different organs will be discussed with special reference to obese subjects.

### **2.3.2 Hepatic lipotoxicity**

The liver is considered the “metabolic sensor of lipotoxicity” (Cusi, 2009) and plays a central role as both a target and a cause in obesity-related disorders. Obesity increases the risk of developing non-alcoholic fatty liver disease (NAFLD), the most common chronic liver condition, characterized by insulin resistance and defined by a hepatic triglyceride content exceeding 5% of liver weight (Kleiner *et al.*, 2005). It has been estimated that one third of the adult population and two thirds of obese subjects in the United states are affected by fatty liver disease (Angulo, 2007; Wieckowska *et al.*, 2007). It is suggested that fatty liver, being the hepatic component of metabolic syndrome, is probably a better predictor of abnormal metabolism in insulin-resistant

states than visceral adipose tissue (Perseghin, 2011). NAFLD refers to a wide spectrum of liver diseases ranging from steatosis (accumulation of fat in the liver), to non-alcoholic steatohepatitis (NASH, fat in liver causing inflammation), to cirrhosis (irreversible damage with fibrotic scars resulting from chronic inflammation). Hepatic lipotoxicity is implicated in all these conditions, but it is important to identify the key process in the cascade of the alterations of the hepatic fatty acid metabolic pathways in order to predict the progression towards tissue damage. The accumulation of fatty acid has been advocated as the “first hit” in steatohepatitis (Day & James, 1998), and there is evidence suggesting that the amount of hepatic fat increases the exposure of hepatocytes to potentially toxic fatty acids (McClain *et al.*, 2007; Jou *et al.*, 2008) constituting a marker for metabolic disorders and insulin resistance independently from obesity (Kotronen *et al.*, 2008b). However, recent data indicate that intracellular triglycerides depots are just “innocent bystanders” in the processes leading to cellular injury and inflammation (Choi & Diehl, 2008; Jou *et al.*, 2008), an explanation presciently suggested by the eminent Austrian pathologist Heribert Thaler: “...the cause of steatosis, and not the fat accumulation by itself, produces cirrhosis” (Thaler, 1975) and might even have a protective role in sequestering FA, thus reducing their free intracellular levels (Yamaguchi *et al.*, 2007; Choi & Diehl, 2008). Instead, fat-laden hepatocytes are damaged by ROS, that, once released, cause hepatic inflammation and fibrogenesis (Li *et al.*, 2008; Yang *et al.*, 2000; Fromenty *et al.*, 2004).

Therefore, the assessment of FA oxidation is one key element in the characterization of the high-risk situation because this process is the source of reactive oxygen species in obesity-related hepatic lipotoxicity (Fromenty *et al.*, 2004; Nakamura *et al.*, 2009); at the moment, direct non-invasive measurement of hepatic FA oxidation in obese and humans in general is lacking.

The flux of FAs from white adipose tissue to the liver and its hormonal control are important determinants of hepatic FA exposure. The liver receives a dual FA supply, from the systemic circulation and from the portal vein; the latter drains the visceral compartment, which is expanded in obesity, and active in releasing FA (Nielsen *et al.*, 2004). Insulin promotes nutrient storage both in adipose tissue and in the liver; via its antilipolytic effect, it supports the FA buffering capacity of triglyceride depots. Loss of control of this process because of insulin resistance or deficiency may lead to enhanced FA oxidation and free radical formation. However this relation has not yet been tested in insulin-resistant humans.

### **2.3.3 Skeletal muscle lipotoxicity**

Skeletal muscle is one of the organs that are directly affected by lipotoxicity, and the consequences of its altered FA metabolism are reflected at the whole body level. A proof of this concept comes from studies where systemic FFA levels are acutely increased, for example, by infusing heparinized lipid emulsions; insulin-stimulated glucose uptake (that is known to occur for more than 80% in skeletal muscle) is reduced dose-dependently by lipid infusions in all individuals regardless of sex or age (Boden *et al.*, 1994; Boden & Chen, 1995). Under these conditions, insulin resistance

arises within 2-4 hours after plasma FFA levels increase, and disappears within 4 hours after normalization of FFA levels (Boden *et al.*, 1991).

If many agree that FFAs have a role in skeletal muscle insulin resistance, it must be noted that many other mediators have been proposed as opposers of glucose homeostasis by blocking insulin signal transduction in the context of obesity-related diseases, as reviewed in Figure 2.3.3.1 (Muoio & Newgard, 2006). Nonetheless, the main focus of this section is to illustrate the proposed mechanisms of action of FA in mediating the skeletal muscle alterations, including the mitochondrial dysfunctions.

Several lines of evidence support the hypothesis that the lipotoxic action of FFA on skeletal muscle insulin sensitivity is due to an increase in intramyocellular fat content (Abdul-Ghani & DeFronzo, 2010) and in both animals and humans it is recognized that elevated intramuscular triglyceride (IMTG) storage is a common feature of obese and/or insulin resistance states (Hulver *et al.*, 2003; Goodpaster & Kelley, 2002). Despite these correlations, there is increasing evidence that lipid metabolites such as 4-hydroxynonenal (4-HNE), diacylglycerols (DAGs), ceramides, and long chain acyl-CoAs (LC-CoAs) may play a more significant role than triglycerides in producing skeletal muscle insulin resistance (Chow *et al.*, 2010). The presence of increased IMTG might be just a marker of more direct events rather than being *per se* the causal element (Perseghin, 2005). For example, the theory does not fit when increased IMTG stores, in amounts similar or even higher than obesity, have been found in muscle of exercise-trained subjects with high insulin sensitivity (Goodpaster & Kelley, 2002). On the other hand, fatty acid oxidation has been thought to be a discriminant between athletes and obese subjects, with the latter having a higher IMTG/peroxidation ratio (Russell *et al.*, 2003). Skeletal muscle oxidative capacity (assessed by citrate synthase activity) has been shown to be a better predictor of insulin sensitivity than either IMTG or LC-CoA content (Bruce *et al.*, 2003).

As discussed above, the primary oxidative fuels supporting the skeletal muscle activity are fatty acids and glucose, and physiologically, skeletal muscle responds to supply and demand by shifting between substrates. Randle's and McGarry's substrate cycles (described in section 2.1.4) held a similar view in appointing to lipids a central role in mediating glucose resistance and both of them were related to fatty acid oxidation. However, while in Randle's view, the insulin resistance was provoked by an increase of fatty acid oxidation, in McGarry's view, it was mediated by a decreased fatty acid oxidation with accumulation of toxic fatty acid intermediates.

A considerable number of studies have investigated whether skeletal muscle fatty acid oxidation is increased or decreased in obesity and insulin resistance, and there has been consistently evidence supporting one or the other hypothesis, spreading confusion in the matter (Koonen *et al.*, 2010; Muoio & Newgard, 2006).

The concept of "metabolic inflexibility" has been an attempt to reconcile the opposing views, proposing that the muscle of obese and insulin resistant mammals loses the ability to switch between glucose and lipid substrates (Kelley & Mandarino, 2000). To support this idea, fat oxidation (measured by RQ across the leg) in type 2 diabetic and obese compared to lean subjects was found to be increased in the postprandial state and decreased in the fasting state (Kelley *et al.*, 1999). The root

cause of the inflexibility was ascribed again to IMCL accumulation and the Randle hypothesis was excluded (Kelley & Mandarino, 2000). Other studies have supported the theory of a diminished fatty acid oxidation in the post-absorptive state as a primary factor leading to an insulin-resistant state (Blaak, 2004). At variance with this view, a number of studies have reported how both obesity and insulin resistance are characterized by increased gene expression of lipid catabolic genes, related to trafficking and  $\beta$ -oxidation (Muoio & Newgard, 2006; Kelley *et al.*, 1999). Studies on fatty acylcarnitines further support the increased oxidation hypothesis; in fact accumulation of acylcarnitines in muscle of obese/insulin-resistant rats is the result of an increased incomplete fatty acid oxidation that does not match the demand, resulting in a backflux in the cytosol of fatty acid acylcarnitines (Muoio & Newgard, 2006). Therefore, recently it has been proposed and substantiated by evidence that increased fatty acid oxidation is the first step in the skeletal muscle insulin resistance cascade (Koves *et al.*, 2008; Nair *et al.*, 2008). This line of thought fits with another piece of the puzzle: the causative role of ROS in multiple forms of insulin resistance (Houstis *et al.*, 2006). Mitochondria are not only responsible for substrate oxidation and ATP generation, but are also the primary source of ROS (Turrens, 1997; Boveris *et al.*, 1972), and are actively involved in the antioxidant defence (Andreyev *et al.*, 2005). Given that mitochondrial integrity is crucial for cell survival, the adaptations favouring augmented IMTG and lowered fatty acid oxidation, seen in late or more severe obesity (Hulver *et al.*, 2005; Thyfault *et al.*, 2004; Hulver *et al.*, 2003), might be interpreted as protective measures to defend muscle mitochondria from lipid-induced insults (Muoio & Newgard, 2006). A possible sequence of events can be that adipose tissue lipotoxicity prompts an augmented influx of lipid substrate to the skeletal muscle that initially compensates with an increase in FAO trying to counteract IMTG accumulation, and in this regard, Randle's hypothesis is still valid. To support the "first stage" proposal, Perseghin and coworkers studied overweight subjects with normal IMCL and insulin sensitivity and found an increased post-absorptive lipid oxidation compared to leaner controls (Perseghin *et al.*, 2002). The "second stage" fostered by an overproduction of free radicals (Russell *et al.*, 2003) with concomitant or subsequent build-up of IMTG (Guo, 2007) (maybe via McGarry's theory), may lead to mitochondrial malfunction (Muoio & Newgard, 2006). Further research is needed to support the sequence of events, and more importantly it should be specified in the aims of the studies whether the early processes of the disease or the late ones are under evaluation, to avoid confusion in the literature.

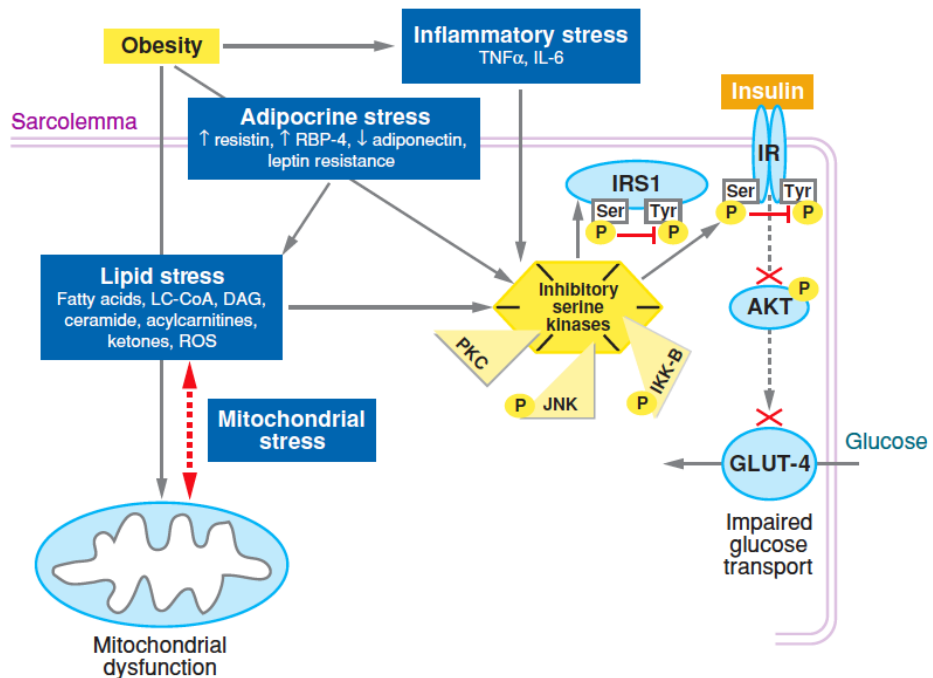


Figure 2.3.3.1. Obesity-related metabolic dysfunction in skeletal muscle. Obesity is associated with a host of metabolic, inflammatory, and adipocrine stresses that combine to mount a full-scale attack on both mitochondrial function and insulin signalling. These stresses converge to activate a network of inhibitory serine kinases that interfere with insulin signal transduction and hence glucose homeostasis. Abbreviations: AKT, protein kinase B; DAG, diacylglycerol; GLUT-4, insulin-regulated glucose transporter 4; IKK- $\beta$ , I $\kappa$ B kinase catalytic subunit  $\beta$ ; IL-6, interleukin-6; IRS1, insulin receptor substrate 1; JNK, c-jun amino-terminal kinases; LC-CoA, long-chain acyl-CoA; PKC, protein kinase C; RBP-4, retinol-binding protein 4; ROS, reactive oxygen species; Ser, serine; TNF $\alpha$ , tumor necrosis factor- $\alpha$ ; Tyr, tyrosine. (Figure and legend from Muoio & Newgard, 2006).

### 2.3.4 Myocardial lipotoxicity

The healthy myocardium is metabolically flexible, which means it is able to meet demands of adjusting energy and perfusion requirements according to the workload, and to switch substrate preference according to substrate availability and nutritional status. The loss of this plasticity is a common characteristic of different cardiac diseases, but also of lipotoxicity-related metabolic diseases such as obesity and diabetes (Iozzo, 2010). Therefore, extensive research has been carried out in the attempt to identify the precise mechanism(s) of action responsible for metabolic derangement-induced cardiac abnormalities in obese and diabetic models (Lopaschuk *et al.*, 2010); especially considering that such metabolic diseases predispose to cardiovascular diseases (Yusuf *et al.*, 2004); for example, obesity is an independent

risk factor for heart failure, as defined by the criteria of the Framingham heart study (Kenchiah *et al.*, 2002).

The earliest change that develops in response to an increase in caloric intake, as discussed above, is an increased FA supply to the organs, this alters myocardial substrate utilization and precedes mitochondrial and contractile dysfunction and cardiac steatosis (Wende & Abel, 2010).

Similarly to what has been described for skeletal muscle, the role of fatty acid  $\beta$ -oxidation in contributing to lipid-induced cardiac pathology seems controversial, because of apparently opposing findings, such as either increased or decreased fatty acid oxidation expression genes or metabolic rates in obese/diabetic/transgenic animal models (Lopaschuk *et al.*, 2010), but as discussed in some reviews, an altered myocardial FA supply is paralleled by an increase in fatty acid oxidation as observed in both animal models and in a few human studies (Lopaschuk *et al.*, 2010; Mittendorfer & Peterson, 2008; Iozzo, 2010). Characterization of alterations in FFA metabolism in obese humans has been carried out by using PET imaging in young women and it has been shown that myocardial FA uptake, utilization and oxidation are positively related to insulin resistance, and that myocardial FA uptake and oxygen consumption are positively related to BMI (Peterson *et al.*, 2004). An acknowledged limitation of previous studies that have failed to observe an increased fatty acid oxidation is the lack of direct measurement of endogenous (derived from intramyocardial lipid stores) fatty acid oxidation (Lopaschuk *et al.*, 2010; Young *et al.*, 2002). This process has never been measured in humans, and only one study has addressed the issue in dogs (Kisrieva-Ware *et al.*, 2009). Intramyocardial lipids should be an important source for oxidation, since with obesity the myocardial lipid pool almost trebles compared to the lean (Kankaanpaa *et al.*, 2006).

Cardiac steatosis is a *per se* hallmark of obesity and diabetes (Kankaanpaa *et al.*, 2006; Szczepaniak *et al.*, 2003; Rijzewijk *et al.*, 2008; McGavock *et al.*, 2007). Similarly to skeletal muscle steatosis, intramyocardial lipid stores have been suggested to be protective from heart dysfunction at an early stage of the disease by storing away (through esterification) the detrimental lipid intermediates (*i.e.* DAGs, LC-CoAs, ceramides, acylcarnitines), and be deleterious in the long run (Zhang & Ren, 2011; Brindley *et al.*, 2010). As for skeletal muscle, the reconciliation of findings supports the view of an increased FAO at the early stages of the disease prompted by an increased efflux of FA coming from the failing adipose tissue. According to this hypothesis, FAO should increase in compensation, but when the increase cannot match the abundant availability, cardiac steatosis can develop (Mittendorfer & Peterson, 2008) and act in turn to counteract the unused toxic lipids. After passing a certain “threshold” (Atkinson *et al.*, 2003) TG stores seem to stop being protective and become detrimental for the cell (Zhou *et al.*, 2000; Zhang & Ren, 2011; Brindley *et al.*, 2010; Lopaschuk *et al.*, 2010).

If, at first look, the compensatory increase of FA oxidation seems protective, it is unfortunately far from being beneficial since it is accompanied by mitochondrial uncoupling and reduced cardiac efficiency with oxygen wasting and an increase of ROS production that ultimately leads to cell apoptosis (Lopaschuk *et al.*, 2010; Iozzo,



2010). Mechanistic studies supporting this concept have been performed in both obese (Boudina *et al.*, 2005) and diabetic mouse models (Boudina *et al.*, 2007), as well as in diet-induced obese rats (Cole *et al.*, 2011). Furthermore, as already explained by the Randle hypothesis, not yet questioned in relation to cardiac metabolism, an increased FAO disrupts the insulin mediated signal for the promotion of glucose uptake and oxidation (Randle *et al.*, 1963); this lack of flexibility is negative in critical conditions such as ischemia and high workload when glucose oxidation is preferable for lower myocardium oxygen consumption.

### ***2.3.5 CAD: links with lipotoxicity and the role of pericardial fat***

CAD is a disease characterized by progressive development of atheromatous plaques within the intima of the vessels that nourish the heart; the plaques that constitute a significant obstruction are the ones that limit the blood flow to the myocardium. The pathological process of narrowing (or stenosis) of the lumen by the inward-growing plaques is also called atherosclerosis. Atherosclerosis is often defined as a chronic inflammatory disease (Ross, 1999); however, inflammation is only one of the driving forces of the disease, that is multi-factorial (Badimon *et al.*, 1993) and many of these factors, including inflammation, are linked with lipotoxicity. Among the causative risk factors for CAD, elevated serum cholesterol levels (Smith, Jr. *et al.*, 2000) are a characteristic of lipotoxic states; among the predisposing factors for CAD, are overweight and obesity (especially abdominal) and insulin resistance (Smith, Jr. *et al.*, 2000; DeFronzo, 2010). Among the conditional risk factors, C-reactive protein as inflammatory marker (Smith, Jr. *et al.*, 2000) is directly related to the altered hormone secretion profile of adipose tissue in the context of lipotoxicity (de Ferranti & Mozaffarian, 2008). C-reactive protein is not the only factor modulating the progression of CAD, many other inflammatory mediators can be secreted by adipose tissue, and in this regard the local fat depots surrounding the heart and vessels play a dual role as both protectors and promoters of atherosclerosis (Iacobellis *et al.*, 2008; Iozzo, 2011). Lipotoxicity promoting ectopic fat deposition might be one of the causes of the switch from the protective role to the aggravating role of the local fat depots in the context of CAD. The fat surrounding the heart can be differentiated into separate compartments: that inside the visceral portion of the pericardial sac, defined as intrapericardial fat (IPF) and elsewhere as epicardial adipose tissue (Sarin *et al.*, 2008; Greif *et al.*, 2009; Nelson *et al.*, 2009) or, in some cases, as pericardial fat (Mahabadi *et al.*, 2009), that overlying the parietal side of the sac, defined as extrapericardial fat (EPF), elsewhere as paracardial fat (Sarin *et al.*, 2008; Greif *et al.*, 2009; Nelson *et al.*, 2009) or pericardial fat (Iacobellis & Willens, 2009) and the fat depot in the mediastinic area still in continuity with the heart, defined as thoracic fat (Mahabadi *et al.*, 2009). Regardless of the nomenclature, IPF and EPF are not only anatomically distinct fat depots but they also have different embryological origins, and, more interestingly, different vascularization (Iacobellis & Willens, 2009). IPF is supplied by branches of coronary arteries and shares the same microcirculation of the myocardium,

while this is not true for EPF (Iacobellis & Willens, 2009). For these reasons and because there is no physical barrier between IPF and myocardium or the wall of the coronary vessels, IPF might have more direct effects on vascular remodelling and plaque complications than EPF, acting through vasocrine/paracrine signalling (Baker *et al.*, 2006; Zhou *et al.*, 2011; Barandier *et al.*, 2005; Mazurek *et al.*, 2003; Zhang & Zhang, 2009; Henrichot *et al.*, 2005; Payne *et al.*, 2009; Payne *et al.*, 2008); however, the mechanisms of the development/progression of CAD disease in relation to fat accumulation have not been fully elucidated. Increased risk/presence of CAD has recently been associated with the accumulation of fat surrounding the heart (Rosito *et al.*, 2008; Sarin *et al.*, 2008; Gorter *et al.*, 2008; Greif *et al.*, 2009). Nonetheless, the evidence of a continuous relationship between IPF and the severity of CAD remains controversial, especially if the evaluation endpoints are purely anatomical. Some studies have found an association between the number of vessels presenting stenosis and the amount of fat (Ueno *et al.*, 2009; Gorter *et al.*, 2008), whereas other studies have found no such association (Jeong *et al.*, 2007; Taguchi *et al.*, 2001). It must be noted that not all anatomical stenoses prevent blood flowing into the myocardium. It is therefore important to assess myocardial perfusion impairments together with the anatomical lesions to correctly define the severity of the disease and identify the significant obstructive stenosis (Gould, 2009; Tonino *et al.*, 2010). Thus, the relationship between impaired myocardial perfusion and pericardial fat becomes more interesting and has not been fully explored yet. One group has investigated and found a correlation between echocardiographically measured CFR and epicardial fat thickness in women with normal coronary arteries (Sade *et al.*, 2009), but the relationship in CAD subjects seems to be unaddressed.

## **2.4 Fatty acid metabolism modulation drugs**

As discussed in the previous sections, metabolic and cardiovascular diseases share common underlying pathological mechanisms related to alterations of fatty acid metabolism. Therefore, a potential treatment strategy to prevent or limit the progression of such diseases is to modulate fatty acid metabolism, and possibly to indirectly affect and improve glucose metabolism as well, these being extremely important in insulin resistance related diseases. Peroxisome proliferators-activated receptors (PPAR) became attractive therapeutic targets since the discovery that these transcription factors, belonging to the nuclear receptor superfamily, are involved in the transcription of genes related to lipid metabolism (Dreyer *et al.*, 1993). To date, 3 isoforms of PPAR have been identified, which includes PPAR $\alpha$ ,  $\beta/\delta$  and  $\gamma$ . All PPAR isoforms and therefore the modulation of PPAR activity has become an attractive treatment target for obesity and metabolic diseases (Zhang *et al.*, 2010). An alternative approach to the gene transcription modulation is to influence the specific enzyme activity; some examples of such metabolic modulators, with special reference to the fatty acid oxidation pathway, will be discussed.

The metabolic therapy can act at different levels: (1) targeting fatty acid supply and uptake; (2) modifying cytoplasmic lipid levels; (3) restoring fatty acid oxidation / glucose oxidation balance; (4) stimulating / inhibiting fatty acid oxidation.

- 1) A number of pharmacological approaches can be used to decrease the fatty acid supply to critical organs:
  - a. Fibrates are PPAR $\alpha$  receptor agonists. PPAR $\alpha$  receptors are expressed mostly in tissues that have a high capacity for fatty acid  $\beta$ -oxidation, such as the liver, heart and skeletal muscles. Activation of PPAR $\alpha$  leads to the increase in FA uptake as well as oxidation in these tissues. In human, fibrates decrease plasma levels of TG and FFA (Staels *et al.*, 1998) via increase of lipid uptake and oxidation in the liver, according to animal studies (Zhang *et al.*, 2010). Several clinical trials have confirmed the cardiovascular benefits of fibrates (Jun *et al.*, 2010) especially among diabetic subjects (Watts & Karpe, 2011). Overall, improvements in major cardiovascular events were related to coronary events rather than strokes and were largely confined to volunteers with dyslipidaemia (Watts & Karpe, 2011). However, if the PPAR $\alpha$  overactivation in liver is beneficial, this might be not the case for skeletal muscle and heart, as shown by specific transgenic mouse models (Zhang *et al.*, 2010). On the contrary, PPAR $\alpha$  null mouse models present lower fatty acid oxidation and improved glucose uptake and oxidation, and have a more efficient glucose disposal, being protected by insulin resistance resulting from high fat feeding (Zhang *et al.*, 2010).
  - b. Thiazolidinediones (TZDs) were widely used as insulin-sensitizers to treat diabetes and insulin resistance. They are agonists of PPAR $\gamma$  nuclear receptors, which are mainly located in the adipose tissue and their activation leads to increased fat storage (Zhang *et al.*, 2010). PPAR $\gamma$  receptors also increase expression of glucose transporters in adipose tissue and skeletal muscle ameliorating the glucose disposal. The first class of TZDs (troglitazone) was withdrawn from the market because of severe liver damage; the second class (rosiglitazone) has been reported in meta-analyses to be associated with possible increased risk of cardiovascular disease (CVD) events; the third TZD class (pioglitazone) reported side effects are weight gain, edema (DeFronzo *et al.*, 2011), bone loss and precipitation of congestive heart failure in at-risk individuals, but not increase in CVD/all cause mortality (Shah & Mudaliar, 2010). When pioglitazone treatment has been compared to rosiglitazone, the latter resulted in higher risk of congestive heart failure, myocardial infarction and death as compared to the former (Loke *et al.*, 2011). It might be that weight gain even if an undesirable effect of TZD, might be a mediating mechanism of action through expansion of subcutaneous adipose tissue, being positively correlated with the decline of HbA<sub>1c</sub> levels and a greater

- improvement in insulin sensitivity and beta-cell function (Miyazaki *et al.*, 2005).
- c. PPAR $\beta/\delta$  receptor agonists induce and increase oxidative metabolism in skeletal muscle as for PPAR $\alpha$  receptors, but the mice models overexpressing PPAR $\beta/\delta$  receptors in the heart also show an increased glucose metabolism (Zhang *et al.*, 2010). It is unsure whether the mechanism of action will be beneficial in humans.
  - d. Antilipolytic drugs, such as acipimox, the long-lasting form of nicotinic acid, are able to lower plasma FFA levels and enhance insulin action in obese subjects (Santomauro *et al.*, 1999). It has been reported that nicotinic acid increases HDL cholesterol levels, possibly due to increased cholesterol release from adipose tissue (Karpe & Chamas, 2010). The major complication of nicotinic acid is the cutaneous flushing, that can cause discontinuation of the therapy at rates as high as 25-40%, but several strategies have been proposed to prevent the side effect (Davidson, 2008).
- 2) Lowering lipid intermediate accumulation especially in skeletal muscle and heart has been suggested as a possible intervention. However, specific agents designed for this action are still lacking. Increasing DGAT, the enzyme that converts DAG to TG, could be a novel target since mice over-expressing it show improved insulin sensitivity and decreased DAG and ceramide (Zhang *et al.*, 2010). Acipimox, in this context, has been found useful, since total long chain CoA levels in the muscle were reduced by its action, in concomitance with improved whole body glucose disposal (Koves *et al.*, 2008).
- 3) Therapeutic interventions that aim to restore the balance between glucose and fatty acid metabolism should be beneficial for glucose disposal and reverse insulin resistance.
- a. PDH activators have been proposed as good candidates to re-establish the metabolic balance. After several attempts the most promising among this type of drugs is the PDK4 inhibition. PDK4 knockout mice show higher rates of glucose oxidation and lower rates of fatty acid oxidation in diaphragm muscle, and they seem more insulin sensitive than wild type mice when exposed to high fat diet (Zhang *et al.*, 2010).
- 4) Stimulating or inhibiting fatty acid oxidation is a dilemma and controversial as can be deduced from the previous section. Maybe the choice can be motivated by the status of the disease (early stages/inhibition, late stages/promotion); below are reported the different proposed approaches for fatty acid oxidation modulation:
- a. Malonyl CoA decarboxylase (MCD) inhibition, blocks conversion of malonyl CoA to acetyl CoA, thus increasing cytoplasmic levels of malonyl CoA, inhibiting FFA uptake into mitochondria and ultimately reducing fatty acid oxidation. Inhibition of MCD in skeletal muscle and heart has had beneficial results in animal studies (Zhang *et al.*, 2010), while increase of its activity in liver results in positive effects on insulin sensitivity as well (An *et al.*, 2004). Further studies are

- necessary to determine whether a specific organ should be targeted for the translation to human therapy.
- b. Etomoxir, an irreversible inhibitor of the activity of carnitine palmitoyltransferase I (CPT-I) to transfer FA from the cytosol into mitochondria. In a recent study, its use in living rats was not accompanied by any changes in FA uptake or oxidation, or in glucose uptake under basal or maximally stimulated metabolic states (Luiken *et al.*, 2009). A more recent investigation confirms that the effects produced by etomoxir in vitro are not reproduced in vivo (Schwarzer *et al.*, 2009). Furthermore, the use of etomoxir has been associated with the risk of cardiac hypertrophy (Cabrero *et al.*, 2003; Luiken *et al.*, 2009), increase in heart lipid content (Schmitz *et al.*, 1995), oxidative stress (Merrill *et al.*, 2002), and hepatotoxicity, leading to the interruption of a clinical trial (Holubarsch *et al.*, 2007).
  - c. Perhexiline is an alternative inhibitor of CPT-I. Initially developed as an antianginal drug, it has been recently employed in patients with heart failure. Perhexiline inhibits both CPT-I and CPT-II, causing an improvement in myocardial function and skeletal muscle energetics, but it has been associated with potential peripheral neuropathic (Meier *et al.*, 1986) and hepatotoxic effects, and for these reasons requires monitoring of plasma levels (Killalea & Krum, 2001).
  - d. ACC inhibitors block the enzyme that drives the opposite reaction that MCD catalyzes, thus they promote fatty acid oxidation. The rationale of the approach comes again from whole-body knockout mice (ACC2 *-/-*) that show improved insulin sensitivity when fed a high fat diet (Choi *et al.*, 2007). Like for the activation of MCD, the liver might be the organ primarily involved in the alleviation of the insulin resistance, thanks to decreased lipid metabolites (Atkinson *et al.*, 2002; Zhang & Zhang, 2009).
  - e. Activators of AMPK that both promote fatty acid oxidation via inhibition of ACC and translocation of GLUT4, have been shown to promote insulin sensitivity but it is not clear which of the two mechanisms is determinant in the improvement (Zhang *et al.*, 2010).
  - f. Trimetazidine (TMZ), being the object of the current thesis, will be dealt with in a separate section (2.4.1).
  - g. Ranolazine shares with TMZ the in vitro evidence of a shift in muscle substrate preference from FA to glucose (McCormack *et al.*, 1996). It was previously believed to be an activator of pyruvate dehydrogenase (Clarke *et al.*, 1996), but subsequently an in vivo study suggested that the drug might not inhibit FA oxidation (Wang *et al.*, 2007); nonetheless, the mechanism of action remains to be elucidated (Boden, 2010).

### 2.4.1 Trimetazidine

As confirmed by a recent meta-analysis, trimetazidine has a significant protective effect against all-cause mortality and cardiovascular events and hospitalisation in patients with heart failure (Gao *et al.*, 2011). However, more studies on humans are warranted to clarify the specific mechanisms of action of the drug. Table 2.4.1.1 summarizes the basic and clinical studies focussed on the investigation of trimetazidine mechanisms of action, with special reference to cardioprotection. Trimetazidine may improve myocardial energy metabolism by inhibiting FAO and promoting glucose metabolism. This speculation originates from *in vitro* and animal studies in which TMZ partially inhibits the beta-oxidation enzyme 3-keto-CoA-thiolase (Lopaschuk *et al.*, 2003; Kantor *et al.*, 2000). A recent PET study in patients with dilated cardiomyopathy is the only investigation in which FAO was measured during TMZ treatment, which improved cardiac efficiency and function, accompanied by a modest decline in plasma FAO rate constant (Tuunanen *et al.*, 2008). However, the role of intracellular lipids was not considered, glucose uptake was not measured, and patients had severe heart failure with metabolic and medication-related confounders. Based on current knowledge, there are no data about the reciprocal modulation of FA and glucose metabolism by TMZ on the heart, and the consequences on cardiac work efficiency in humans.

Regarding metabolic diseases, a metabolic modulator able to relieve the oxidative pressure caused by FA overload in the early phase of the disease might be an effective preventive measure. In cardiomyopathic patients with type 2 diabetes, trimetazidine has been shown to improve systemic glucose metabolism, as reflected by a reduction in fasting glycemia and an increase in forearm and whole body glucose uptake during hyperinsulinemic euglycemia (Fragasso *et al.*, 2003). The drug effects on forearm lipid metabolism were investigated only in the short term (15 days), demonstrating a downregulation in lipid oxidation during insulin stimulation (Monti *et al.*, 2006). It must be noted that the same study presented some unexpected results: a) even if the control group comprised the same T2DM cardiomyopathic patients with insulin resistance, one could expect a reduction in forearm lipid oxidation by insulin stimulation, and this was not observed; b) trimetazidine did not produce significant changes in forearm lipid oxidation in the fasting state, where lipid availability, hence oxidation, should be maximal (Monti *et al.*, 2006). However, the effects of trimetazidine on adipose tissue metabolism and adipokine secretion have not been investigated.

Table 2.4.1.1. Cardioprotective basic and clinical studies with TMZ.

Study type	TMZ effects & proposed mechanism(s)	Concentration or dose used	Reference
Isolated working rat hearts perfused with insulin, glucose and FFA	↑ glucose oxidation; ↓ FFA oxidation ↓ Activity of 3-ketoacyl CoA thiolase	Perfusions: TMZ 1 μmol/L; enzyme studies 75 μmol/L	(Kantor <i>et al.</i> , 2000)
Isolated rat heart perfusions; low flow ischemia	↓ tissue acidosis & Na gain during ischemia	TMZ 1 μmol/L	(El <i>et al.</i> , 2000)
Isolated rat heart perfusions	↓ ischemic contracture; no effect on glycolysis	TMZ 1 μmol/L	(Boucher <i>et al.</i> , 1994)
In situ rat fibrotic heart from pressure overload	↓ fibrosis via amelioration of NADPH oxidase-ROS-CTGF signalling pathway (all ↓)	TMZ 10mg/kg	(Liu <i>et al.</i> , 2010)
In situ/In vivo db/db mice heart	↑ hemodynamic parameters; ↓ ROS; ↑ antioxidant ability; ↓ PGC1α; ↓ serum TG / IMTG	TMZ 10mg/kg (low dose gr.) TMZ 30mg/kg (high dose gr.)	(Li <i>et al.</i> , 2010)
In situ rabbit heart	Less neutrophil infiltration after ischemia-reperfusion	TMZ 2.5mg/kg	(Williams <i>et al.</i> , 1993)
In situ rabbit heart	Inhibition of mitochondrial permeability transition pore (mPTP) opening; ischemic preconditioning-like effect on reperfusion injury	TMZ 5mg/kg	(Argaud <i>et al.</i> , 2005)
Human red blood cell (RBC) incubation	Erythrocytes incubated; subjected to oxidative stress; less potassium loss after TMZ	Prior TMZ 20 mg 3X daily (less for body wt <60 kg)	(Maridonneau-Parini & Harpey, 1985)
12 HF pts, 6 ischemic	↓ NYHA 3.04 to 2.45 (p=0.005); ↑ cardiac PCr/ATP ratio; ↑ effort stress test	TMZ 20 mg 3X daily for 2 cross-over periods of 90 days each	(Fragasso <i>et al.</i> , 2006a)
28 HF pts (17 ischemic) given TMZ, 27 controls	↓ NYHA; QoL better; ↓ LV ESV; ↑ EF	TMZ 20 mg 3X daily for mean of 13 months	(Fragasso <i>et al.</i> , 2006b)
30 ischemic HF patients given TMZ, 31 controls	↓ NYHA; ↑ LV EF; mortality ↓ by 58%; C-reactive protein (CRP less at 18 months)	TMZ 20 mg 3X daily for 48 months; open label	(Di Napoli <i>et al.</i> , 2005; Di Napoli <i>et al.</i> , 2007)
Human idiopathic cardiomyopathy; ischemia excluded; cardiac FAO directly measured	Improved forward work; modest 10% ↓ myocardial FFA oxidation; decreased whole body insulin resistance; synergism with β-blockade	TMZ 35 mg 2X daily for 3 months added to prior standard anti-HF drugs	(Tuunanen <i>et al.</i> , 2008)
Type 2 diabetes with HF; forearm AV levels of metabolites during euglycemic insulin clamp	↑ glucose oxidation & ↓ lipid oxidation; ↑ cyclic GMP release; ↓ endothelin release	Pre-treatment with oral TMZ 20 mg 3X daily for 15 days	(Monti <i>et al.</i> , 2006)
25 HF pts (16 ischemic) given TMZ, 19 controls	↓ whole body REE; ↓ NYHA; QoL better; ↓ LV ESV; ↑ EF	TMZ 20 mg 3X daily for 3 months	(Fragasso <i>et al.</i> , 2011)

FFA= free fatty acids; FAO = fatty acid oxidation; HF =heart failure; TMZ = trimetazidine; NYHA=New York Heart Association; QoL= quality of life; AV= arteriovenous; LV=left ventricle; EF=ejection fraction; ESV= endsystolic volume.

(Adapted from Opie & Knuuti, 2009).

### **3 OBJECTIVES OF THE STUDY**

The purposes of the present study were:

- 1) to develop and validate a new methodology (based on positron emission tomography) for the assessment of fatty acid metabolism in the liver (I);
- 2) to investigate the pathogenesis of obesity-related diseases in relation to the fatty acid metabolism and its deregulations (lipotoxicity) in organs such as liver (I), adipose tissue, skeletal muscle (II) and heart (II) in obese subjects;
- 3) to evaluate the mechanism and therapeutic effect of a metabolic drug called trimetazidine in modulating the fatty acid metabolism in adipose tissue, skeletal muscle (II), and heart (III) of obese drug-naïve subjects;
- 4) to evaluate the association between ectopic fat accumulation around heart (pericardial fat) and heart metabolism (myocardial perfusion) in CAD subjects (IV).



## 4 SUBJECTS AND STUDY DESIGN

### 4.1 Study subjects

In total six pigs and 123 human subjects were studied. Figure 4.1.1 shows how many study subjects, and with which characteristics (obese, controls, intermediate risk of CAD), were included in the studies (I-IV).

#### 4.1.1 Inclusion criteria and recruitment

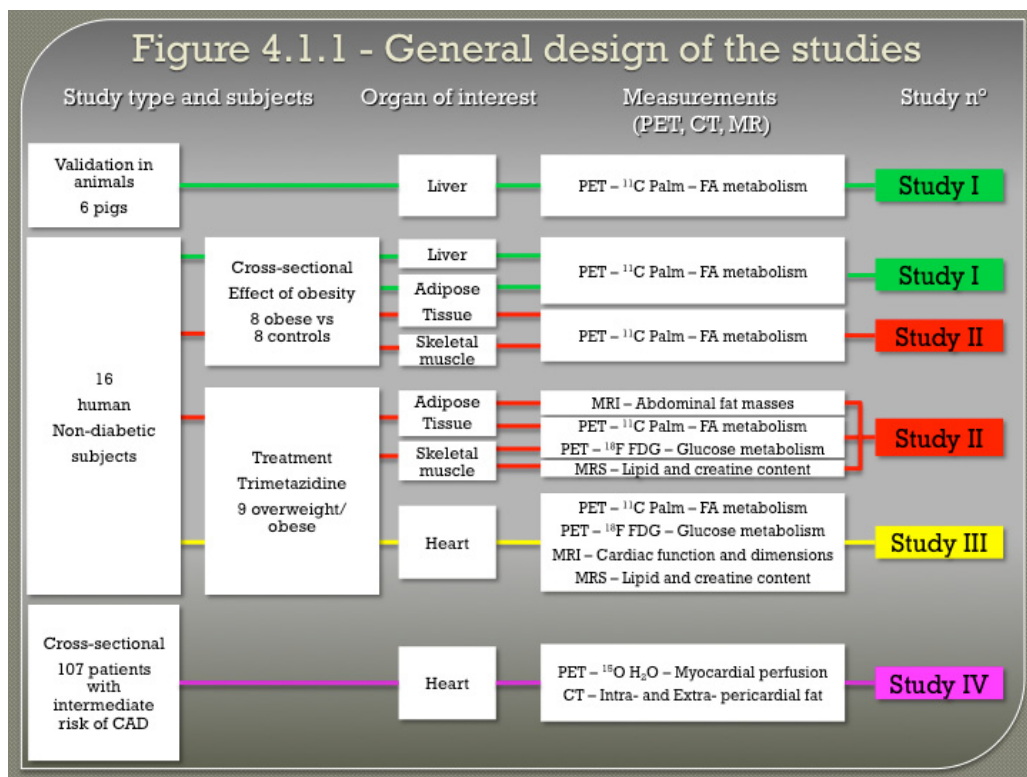
In studies I, II and III, subjects were recruited by local advertisement. Inclusion criteria were, age 20-75 years, no chronic diseases, no substance abuse, normal physical examination and a stable weight and diet for the previous three months. Routine blood testing was performed during the screening visit, together with a 75 g oral glucose tolerance test (OGTT) to exclude undiagnosed diabetes mellitus.

Studies I and II included a cross-sectional study where the effect of obesity was evaluated, comparing eight obese subjects with eight (seven in study I) healthy volunteers. A cutoff body mass index (BMI) of 30 kg/m<sup>2</sup> was used. One patient with full-blown metabolic syndrome but a BMI less than 30 kg/m<sup>2</sup> was included in the obese group.

Studies II and III included a substudy to evaluate the effects of trimetazidine including the eight obese and one control individuals (BMI  $\geq$  27 kg/m<sup>2</sup>) from the cross-sectional study who volunteered to undergo a one-month treatment with 35 mg daily of trimetazidine (Vastarel®, Servier).

Study IV included 107 consecutive out-patients (64 males and 43 females), prospectively enrolled, with a history of stable chest pain and 30-70% pre-test likelihood of CAD, as based on risk factors and symptom-limited exercise test (Diamond & Forrester, 1979; Diamond *et al.*, 1983). Exclusion criteria were atrial fibrillation (FA), iodine allergy, unstable angina, severe loss of kidney function, 2<sup>nd</sup> or 3<sup>rd</sup> degree AV-block, severe congestive heart failure (NYHA IV), symptomatic asthma and pregnancy. Patients with angiographically proven CAD or previous myocardial infarction were not eligible.

All patients and healthy subjects included in the studies (I-IV) gave written informed consent before their participation, after having obtained detailed information on the nature, purpose and potential risks of the study. The studies were conducted according to the guidelines of the Declaration of Helsinki and, furthermore, the study protocol was approved by the Ethics Committee of the Hospital District of Southwest Finland.



## 4.2 Study design

Figure 4.1.1 shows the general design of the studies, with the shared study protocols and the organs of interest in common. The measurements with PET, CT and MR are briefly reported. The colours help to distinguish the different substudy measurements in the different organs.

In study I, validation studies were conducted in six pigs, in which arterial, portal and hepatic vein catheterization simultaneously to a PET scan were performed to compare PET-derived with directly measured liver FA metabolism. The experiment protocol is described in Figure 4.2.1. The imaging methodology was transferred to humans, in which the effects of obesity were explored.

Studies I, II and III in humans included PET examinations that with one study session permitted the study of different organs at the same time point. The general study design for PET examinations is shown in Figure 4.2.2.

In particular, the second part of study I aimed to compare liver FA metabolism and visceral lipolysis between obese humans and healthy humans. The substudy included fifteen PET examinations, nine of which were performed *ad hoc* to carefully image the whole liver and visualize the portal vein, as part of the input function needed to

calculate FA metabolism from imaging data. These nine studies were first used to confirm relationships with circulating markers of liver metabolism, and to validate the extension of the current approach to studies lacking portal vein information, to be used in the remaining six human studies.

In study II, for the cross-sectional study, PET examinations were conducted to characterize FA metabolism in skeletal muscle and subcutaneous abdominal adipose tissue (SAT) in obese and healthy subjects.

Study II and study III share the treatment substudy evaluating the effect of trimetazidine on glucose and FA metabolism of different organs. The general outline of the treatment study is shown in Figure 4.2.3. After baseline examinations, a four-week treatment with TMZ (35 mg daily, Vastarel®, Servier) was started. Diet counselling was provided for the standardization of caloric intake, and patients were instructed to maintain their current lifestyle. After two weeks of treatment, an additional visit took place during which compliance was confirmed, a clinical examination was performed, and blood samples drawn. The PET and MR imaging examinations were repeated at the end of the treatment.

In study II, patients underwent PET imaging sessions using [ $^{18}\text{F}$ ]-fluorodeoxyglucose ( $^{18}\text{F}$ FDG) and [ $^{11}\text{C}$ ]-palmitate to determine glucose and FA metabolism of skeletal muscle, subcutaneous and visceral adipose. Systemic substrate metabolism was determined by both indirect calorimetry and plasma PET tracer kinetic, MRI/MRS were used to assess abdominal fat masses, skeletal muscle triglyceride and creatine content, and adipokines measurements were performed to comprehensively characterize the endocrine function of adipose tissue.

In study III, PET images were used to measure myocardial glucose and FA metabolism, MR imaging to assess left ventricular dimensions and function, and proton MRS to quantify the content of triglycerides and creatine in the left ventricular wall.

In study IV, all patients underwent CT calcium score and CTA assessment and myocardial PET perfusion imaging using a PET/CT hybrid scanner, followed by ICA within two weeks. The imaging protocol and study design are shown in Figure 4.2.4. No cardiac events took place during the interval. FFR measurements were performed for stenoses over 30% when feasible and appropriate. Some stenoses could not be evaluated because of technical limitations or because they were considered complicated lesions by the operator.

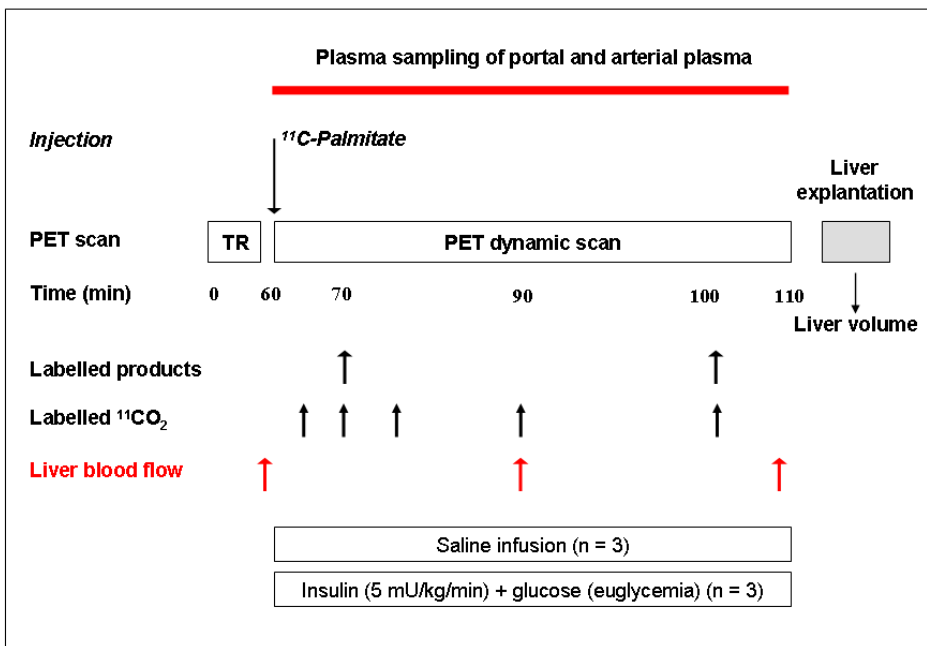


Figure 4.2.1. Study design I – Validation in pigs.

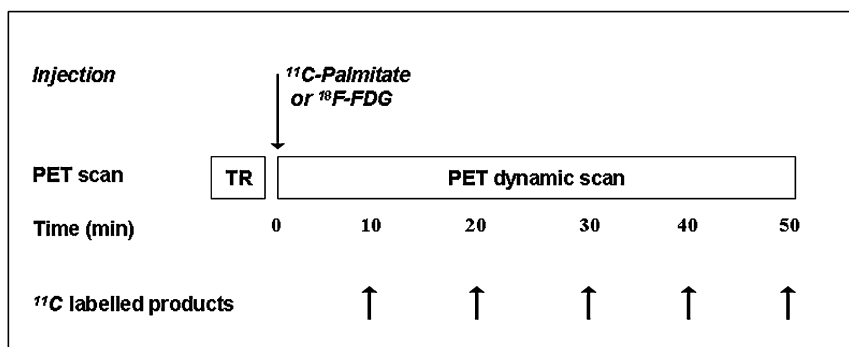


Figure 4.2.2. Study design I-III – PET in humans.

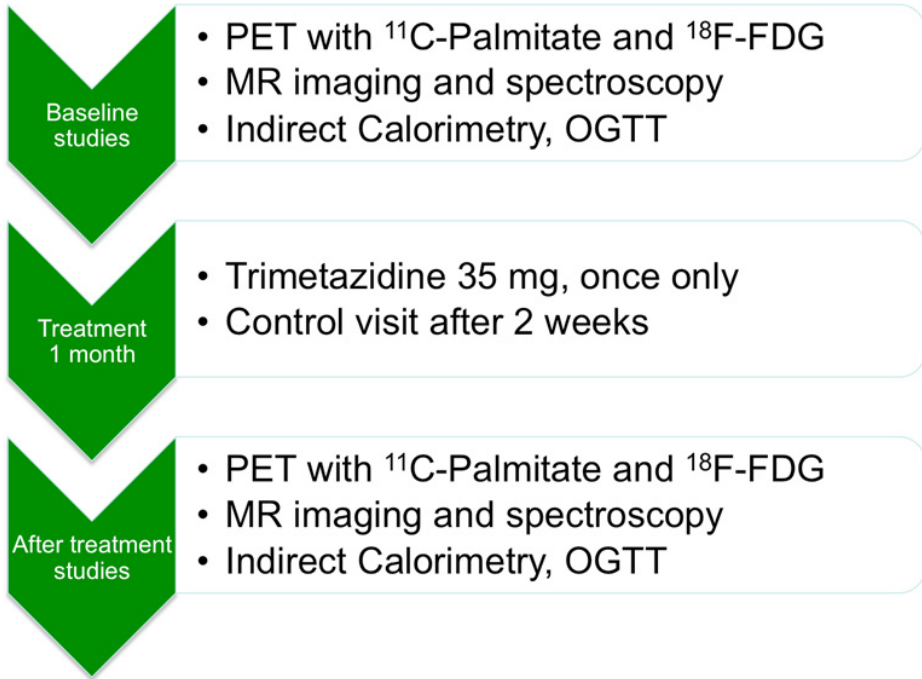


Figure 4.2.3. Study design I, II – Treatment study with trimetazidine.

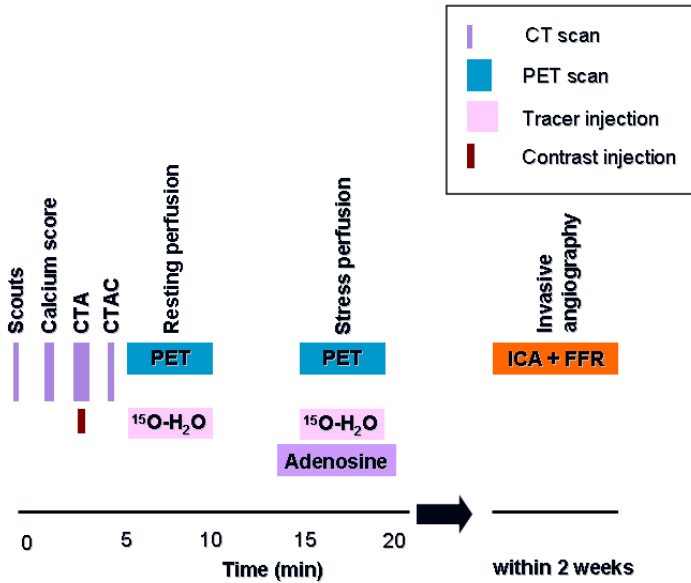


Figure 4.2.4. Study design IV.

## 5 METHODS

### 5.1 Positron emission tomography (I-IV)

#### 5.1.1 Production of positron emitting tracers

$[^{11}\text{C}]$ palmitate. (I-III)  $[^{11}\text{C}]$ palmitate ( $t_{1/2} = 20.4$  minutes) was synthesized via carbonation of n-pentadecylmagnesium bromide with  $[^{11}\text{C}]$ carbon dioxide (Padgett *et al.*, 1982). The radiochemical purity of the final product exceeded 98%.

$[^{18}\text{F}]$ FDG. (II,III)  $[^{18}\text{F}]$ FDG ( $t_{1/2} = 109$  minutes) was synthesized using a modified method of Hamacher *et al.* (Hamacher *et al.*, 1986). The radiochemical purity of the final product exceeded 98%.

$[^{15}\text{O}]$ H<sub>2</sub>O. (IV)  $[^{15}\text{O}]$  ( $t_{1/2} = 123$  seconds) was produced with a low-energy deuteron accelerator Cyclone 3 (Ion Beam Application Inc., Louvain-la-Neuve, Belgium).  $[^{15}\text{O}]$ -water ( $[^{15}\text{O}]\text{H}_2\text{O}$ ) was produced using the dialysis technique in a continuously working water module (Sipilä *et al.*, 2001). Sterility and pyrogenity tests were performed to verify the purity of the product. The radiochemical purity of the  $[^{15}\text{O}]$  was approximately 97%.

#### 5.1.2 PET imaging study sessions (animals) (I)

Anesthetized pigs (29-31 kg) were studied during fasting (n=3) or euglycemic hyperinsulinemia (n=3). Access to food was withdrawn at least 16 hours prior to the study. Animals were anesthetized with ketamine and pancuronium, and mechanically ventilated via tracheal intubation with normal room air (regulated ventilation, 16 breaths per minute). Catheters were placed in the jugular vein, carotid artery and femoral vein, for the administration of glucose, insulin, and  $^{11}\text{C}$ -palmitate, and for sampling of arterial blood. Splanchnic vessels were accessed by subcostal incision; after dissection of the hepatogastric ligament, purse string sutures were allocated to allow catheter insertion *via* a small incision in the hepatic and portal vein. Doppler flow-probes were placed around the portal vein, assumed to represent 83% of liver blood flow (Iozzo *et al.*, 2007). Surgical access was closed, and distal catheter extremities were secured to the abdominal surface to avoid tip displacement. Vital signs, blood pressure, and heart rate were monitored throughout the study (Figure 4.2.4). An ECAT 931-08/12 scanner (CTI Inc, Knoxville, TN, USA) was used. In the hyperinsulinemic experiments, insulin was infused in a primed-continuous fashion at a rate of  $5.0 \text{ mU}\cdot\text{kg}^{-1}\cdot\text{min}^{-1}$ , and euglycemia was maintained by a variable 10% glucose infusion; in fasting studies, saline was infused instead. A 20-min transmission scan was performed with a removable  $^{68}\text{Ge}$  ring source for attenuation correction. After 60 min had elapsed from the start of the insulin or saline infusion,  $^{11}\text{C}$ -palmitate ( $371\pm 67$

MBq) was injected and dynamic imaging was carried out for 50 min (20 frames, 8x15, 2x30, 2x120, 1x180, 6x300, 1x600 seconds). Blood was simultaneously drawn from a) the carotid artery and portal vein at each imaging time frame to measure total plasma radioactivity for computation of the input function, b) the carotid artery, and hepatic and portal veins at 10 and 40 min for the assessment of tracer partitioning between the FA, triglyceride, phospholipid, and water-soluble pool, as previously reported (Guiducci *et al.*, 2006), and at 3, 5, 10, 15, 30 and 50 min in the  $^{11}\text{C}$ -palmitate scan for the measurement of  $^{11}\text{C}$ -CO<sub>2</sub>. Unlabelled FA, glucose, and triglyceride levels were measured at baseline and during each scan, by previously described procedures (Iozzo *et al.*, 2004). At the end of each experiment, animals were sacrificed and the whole liver explanted. The volume of the organ was assessed by water displacement.

#### 5.1.2.1 Assay of labelled $^{11}\text{C}$ -CO<sub>2</sub>

Blood samples (2 mL) were collected into tubes without any additives from carotid artery, portal vein, and hepatic vein during  $^{11}\text{C}$ -palmitate PET imaging. Aliquots of blood (0.6 mL) were immediately transferred 1) to tubes containing 0.5 M NaOH (2.4 mL) in order to fix CO<sub>2</sub> as bicarbonate, capped quickly and briefly mixed; 2) to tubes containing isopropanol (1.8 mL) and 0.5 M HCl (0.6 mL) to prevent clotting and enabling evaporation of CO<sub>2</sub>, briefly mixed and then bubbled with argon or nitrogen for 10 min at 80°C. Radioactivity in both tubes was measured with an automatic gamma counter (1480 Wizard 3<sup>rd</sup> Gamma Counter; EG&G Wallac, Turku, Finland) cross-calibrated with a dose calibrator (VDC-202, Veenstra Instruments, Joure, Netherlands), and the amount of radioactivity associated with  $^{11}\text{C}$ -CO<sub>2</sub> was calculated accordingly.

#### 5.1.2.2 Assay of labelled lipid fractions

The procedure has been previously reported in detail, and metabolite analysis and image quality assessments in these animals have been previously reported (Guiducci *et al.*, 2006). Briefly, blood samples were collected in dry syringes, transferred to EDTA-coated tubes, mixed, and immediately stored in ice. After separation of plasma into organic and water components, as described (Guiducci *et al.*, 2006), the aqueous phase was counted, and the organic phase was passed through a solid-phase extraction (SPE-NH<sub>2</sub>) column, which had been previously activated by elution of 3 ml of heptane. Separation of triglycerides, FA, and phospholipids was obtained by subsequent column elution with 3 ml heptane:isopropanol (1:2 v/v), 4 ml 2% acetic acid in diethyl ether, and 3 ml MeOH, respectively. Radioactivity in each fraction was measured in a well counter.

#### 5.1.3 PET imaging study sessions (humans) (I-IV)

All subjects underwent a PET examination after an 8-10 hour overnight fast. Study subjects were positioned supine in one of the following PET scanners: the eight-ring ECAT 931/08-12 PET scanner (Siemens/CTI Inc., Knoxville, TN, USA) (I,III), the GE

PET-CT scanner (Discovery VCT, GE Medical systems, Milwaukee, WI, USA), and the Siemens HR+ PET scanner (Siemens Inc, Knoxville, TN, USA) (I-III).

In studies I-III, two catheters were inserted, one in an antecubital vein for injection of the radiolabelled tracer, another in the opposite antecubital vein for blood sampling. A heating pad was used to arterialize venous blood at the sampling site. Dynamic imaging of the thoracic area was performed after intravenous administration of the radiopharmaceutical.

#### 5.1.2.1 [ $^{11}\text{C}$ ]Palmitate – Fatty acid metabolism imaging (I-III)

[ $^{11}\text{C}$ ]Palmitate injected dose for patients who participated in the treatment study was  $295\pm 48$  MBq. The PET examinations lasted 50 min and the dynamic imaging acquisitions were subdivided into 20 frames (8x15, 2x30, 2x120, 1x180, 6x300, 1x600 seconds).

Blood samples were withdrawn at 10, 20, 30, 40, 50 min after the start of the scan to assess the fraction of unchanged versus metabolized radiopharmaceutical (Guiducci *et al.*, 2006).

Assay of  $^{11}\text{C}$  labelled metabolites was carried with the same procedure described for animals. Since the analysis in a subset of eight subjects showed an intra-individual coefficient of variation (CV) of 10% at 10 min and <5.5% afterwards, average percent values were applied to the individual plasma curves of the study subjects for whom metabolite measurements were not available. The fraction of parent compound was 90% at 10 min (CV 10%), 76% at 20 min (CV 5.5%), 48% at 30 min (CV 3.8%), 29% at 40 min (CV 4.4%), and 19% at 50 min (CV 3.9%).

#### 5.1.2.2 [ $^{18}\text{F}$ ]FDG – Glucose metabolism imaging (II,III)

[ $^{18}\text{F}$ ]FDG injected dose for patients who participated in the treatment study was  $156\pm 8$  MBq. The PET examinations lasted 50 min and the dynamic imaging acquisitions were subdivided into 20 frames (8x15, 2x30, 2x120, 1x180, 6x300, 1x600 seconds).

#### 5.1.2.3 [ $^{15}\text{O}$ ]H<sub>2</sub>O – Cardiac perfusion imaging (IV)

Rest-stress perfusion cardiac PET was performed immediately after CT.  $^{15}\text{O}$ -labelled water (900-1100 MBq) was injected (Radiowater Generator, Hidex Oy, Turku, Finland) at rest as an intravenous bolus over 15 s at an infusion rate of 10 ml/min. A dynamic acquisition of 4 min 40 s was performed (14x5, 3x10, 3x20 and 4x30 seconds). After allowing 10 min for the decay of  $^{15}\text{O}$  radioactivity, a stress scan was performed during adenosine-induced hyperaemia. Adenosine was started 2 minutes before the scan start and infused to the end of the scan at 140  $\mu\text{g}/\text{kg}$  body weight/min.

#### 5.1.4 Image preprocessing

In order to correct photon attenuation in the body, either a five-minute transmission scan with a removable ring source of  $^{68}\text{Ge}$  or a low radiation dose CT scan of the tissue in question was performed before emission scans. PET images were obtained from the



sinograms originated after the injection of the radioemitting tracers through the correction for tissue attenuation, dead time, and decay, during the image reconstruction with standard algorithms.

### **5.1.5 Image analysis (animals)**

Large circular regions of interest were placed on three to four consecutive image planes in the right lobe of the liver for hepatic radioactivity measurements. The model input function, representing the concentration of tracer available for liver extraction from arterial and portal venous plasma was directly measured in blood samples in animals. The intact fraction of  $^{11}\text{C}$ -palmitate was used as input function. Plasma radioactivity levels in the artery and portal vein were combined into one input function, resulting from the relative contributions of the two vessels to liver perfusion, which were set at 17% and 83%, respectively, based on previous determinations in similar studies (Iozzo *et al.*, 2007).

### **5.1.6 Image analysis (humans)**

Tissue and blood time activity curves (TACs) were obtained by drawing regions of interest (ROIs) on 3-4 consecutive transaxial planes corresponding to the abdominal SAT, paravertebral skeletal muscle, myocardium (horseshoe ROI) regions. CT images were used as reference to carefully place ROIs. Figure 5.1.6.1 shows an abdominal slice of a PET-CT fusion image.

$^{11}\text{C}$ -palmitate input TACs were obtained from PET images, by drawing a small ROI (10 mm of diameter) in the left ventricular heart cavity. Correction for partial volume and spillover from the myocardial wall into blood was considered by applying published calculations (Henze *et al.*, 1983). The errors due to spillover and partial volume effect calculated according to Henze *et al.* with the average wall thickness and resolution of the used scanner were negligible. For these reasons such correction was not considered necessary in this study.  $^{11}\text{C}$ -palmitate input functions were first converted in plasma activity curves by use of the hematocrit, then discounted for radioactivity in the metabolite fraction (see below for metabolite measurements) and used for FA metabolic rate calculations.

In study I, large circular regions of interest were placed on consecutive image planes in the right lobe of the liver for hepatic radioactivity measurements. An example of liver PET-CT image is presented in Figure 5.6.1.2. Plasma radioactivity levels in the artery and portal vein were combined into one (dual) input function (Iozzo *et al.*, 2007).

#### **5.1.6.1 [ $^{15}\text{O}$ ] $\text{H}_2\text{O}$ – Cardiac perfusion imaging (IV)**

Images were quantitatively analysed using Carimas<sup>TM</sup> software (Nesterov *et al.*, 2009) by an experienced reader, who was blinded to other results and clinical data. Standard polar plots of the heart were produced. Blood flow values were averaged according to the regions perfused by the three main coronary vessels: LAD (left anterior descending coronary artery), RCA (right coronary artery) and LCX (left

circumflex) artery. Coronary flow reserve (CFR) was computed as the ratio between stress and rest perfusion in corresponding regions. CFR\* and stress perfusion\* are used to indicate the lowest regional CFR or hyperemic flow values, among the three coronary regions.

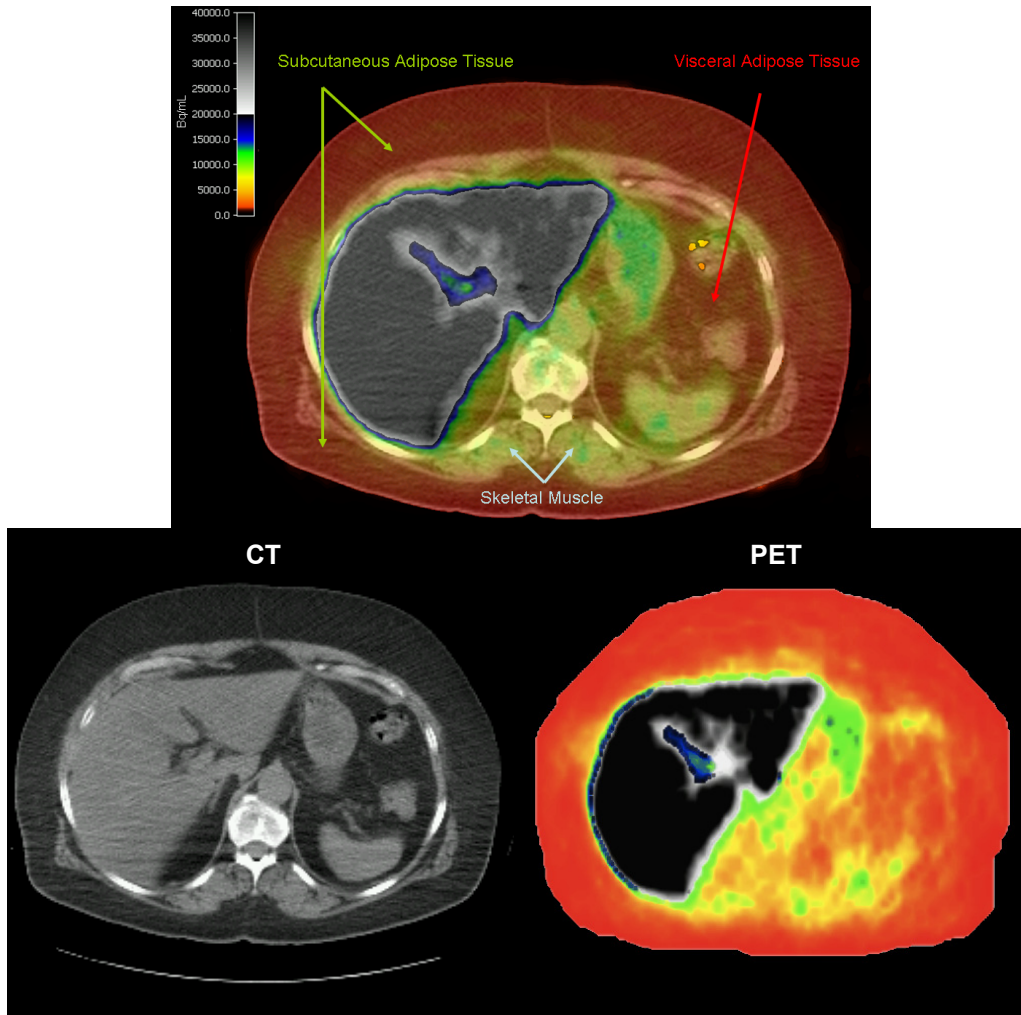


Figure 5.1.6.1. PET, CT and PET-CT fusion image of an abdominal slice. An image of  $^{11}\text{C}$ -palmitate distribution is displayed with an inverted intensity scale, to enhance the visualization of the tissues of interest, and superimposed onto a computerized tomography image for anatomical reference.

**Liver  $^{11}\text{C}$ -palmitate images in human subjects**

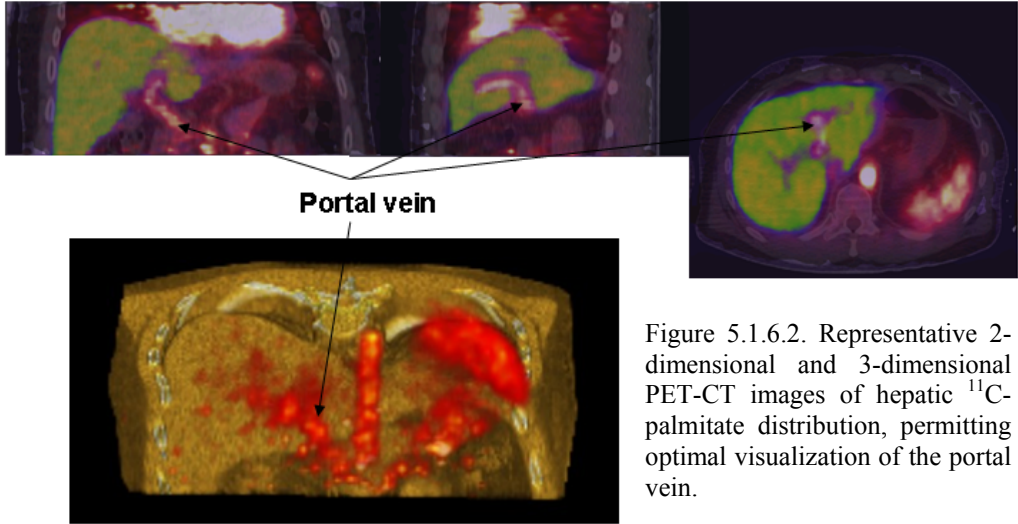


Figure 5.1.6.2. Representative 2-dimensional and 3-dimensional PET-CT images of hepatic  $^{11}\text{C}$ -palmitate distribution, permitting optimal visualization of the portal vein.

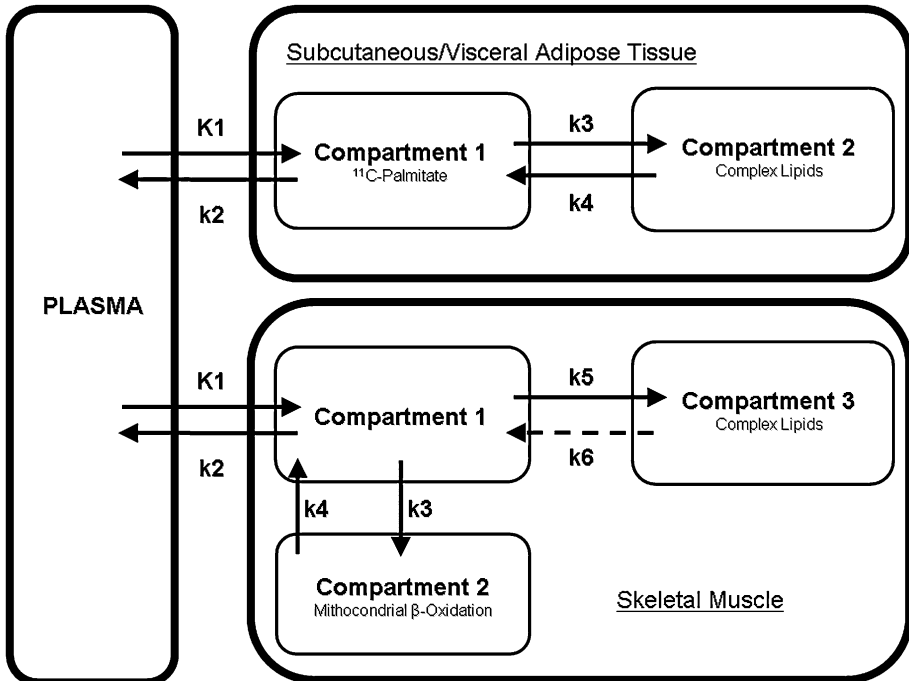


Figure 5.1.7.1. Compartmental models representing the flux of palmitate in the adipose tissue (top) and in skeletal muscle (bottom), and respective rate constants.

### 5.1.7 Kinetic modelling

#### 5.1.7.1 Modelling of adipose tissue <sup>11</sup>C-palmitate kinetics (II)

SAT and VAT were analyzed by the same compartmental model configuration represented in Figure 5.1.7.1. The model is composed of two tissue compartments, representing free [<sup>11</sup>C]-palmitate, [<sup>11</sup>C]-palmitate bound in complex lipids. The transfer of radioactivity between compartments is described by the four rate constant terms as given in figure.

The differential equations describing changing tracer concentrations in SAT and VAT compartments are:

$$\frac{dC_1}{dt} = C_a(t) \times K_1 - C_1(t) \times (k_2 + k_3) + C_2(t) \times k_4 \quad \text{Eq. 1}$$

$$\frac{dC_2}{dt} = C_1(t) \times k_3 - C_2(t) \times k_4 \quad \text{Eq. 2}$$

where  $C_a(t)$  is the plasma input function,  $C_{1-n}$  is the concentration of tracer in each tissue compartment; the total concentration of [<sup>11</sup>C]-palmitate in the tissue at a given time can be defined by the sum of the tracer in each compartment:

$$\text{Tissue}(t) = (1 - V_b) \times (C_1(t) + C_2(t)) + V_b \times C_b(t) \quad \text{Eq. 3}$$

where  $V_b$  is the volume fraction of arterial blood  $C_b(t)$  inside the tissue ROI.  $V_b$  for most of the organs does not exceed 5%, giving confidence that the blood component of the tissue signal does not constitute background noise (except during the peak phase at approximately 0-2 minutes). The biggest contribution to the  $K_1$  parameter comes from the signal during the peak phase, making  $K_1$  related to the flow.  $C_a(t)$  was used in place of  $C_b(t)$  to estimate the arterial plasma volume in the ROI. Kinetic parameters were constrained to positive values and multiple initial parameter estimates were used during the non-linear least squares fitting procedure using an iterative topographical global optimization algorithm (Törn & Viitanen, 1994; Sederholm, 2003). Examples of tissue TACs and model curve fit are shown in Figure 5.1.7.2.

The metabolic rates of FA in subcutaneous and visceral adipose tissue are described by the following equations:

$$\text{FA Esterification rate (FAE)} = [\text{FFA}] \times K_1 \times k_3 / k_2 \quad \text{Eq. 4}$$

$$\text{FA Uptake rate (FAU)} = [\text{FFA}] \times K_1 \times k_3 / (k_2 + k_3) \quad \text{Eq. 5}$$

Rates were expressed as  $\mu\text{mol}/\text{min}/100\text{g}$  of tissue or as  $\mu\text{mol}/\text{min}$  in the entire adipose tissue mass. In the study group, both visceral and retroperitoneal fat masses were quantified; the metabolic rates for the entire SAT were computed by discounting the whole body fat mass from the two intra-abdominal fat compartments.

#### 5.1.7.1 Modelling of skeletal muscle <sup>11</sup>C-palmitate kinetics (II)

The compartmental model used for fitting skeletal muscle [<sup>11</sup>C]-palmitate TACs consisted of 5k parameters and three compartments, namely, the cytosolic pool, the

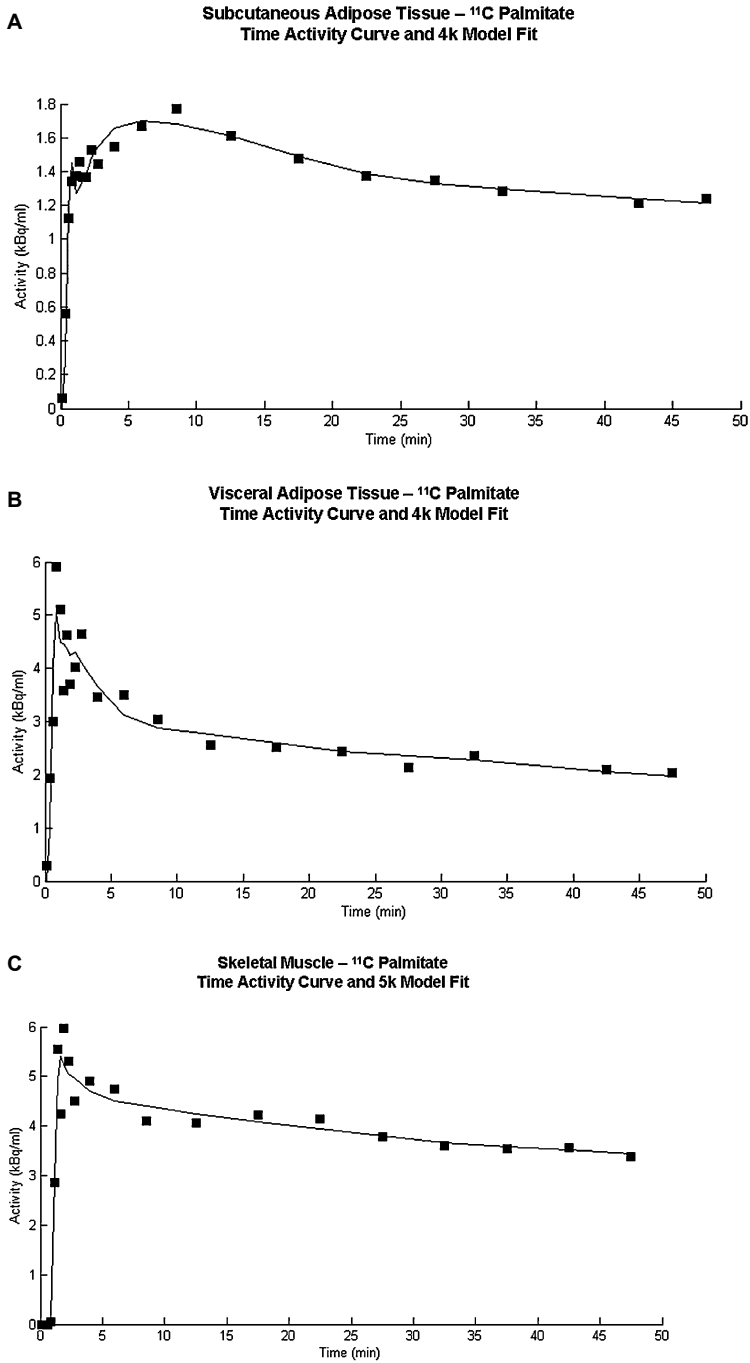


Figure 5.1.7.2.  $^{11}\text{C}$ -palmitate time activity curves (squares) in subcutaneous (A), visceral adipose tissue (B) and skeletal muscle (C), and their respective compartmental modelling fits (lines).

oxidative pool (mitochondria), and the complex lipid pool (fat stored intracellularly).  $K_1$  and  $k_2$  represent the transfer of tracer in and out of the cytosol,  $k_3$  is the fraction of fatty acids entering mitochondria, and  $k_4$  is the fraction of oxidative products returning to the cytosol and into blood,  $k_5$  represents the incorporation of labelled FA into complex lipids. The back transfer of  $^{11}\text{C}$ -palmitate from complex lipids to the cytosolic pool, *i.e.*, lipolysis, is shown as a dashed arrow ( $k_6$ ) in Figure 5.1.7.1. The possibility to estimate this process was examined, but in resolvable cases the  $k_5/k_6$  ratio was on average equal to 114, indicating that  $k_6$  was extremely small. In fact, the more complex model was not resolvable in all cases. This finding was taken as to indicate (in line with skeletal muscle physiology) that lipolysis is limited in magnitude and, more importantly, that it is a relatively slow process, therefore not quantitatively relevant in the 50 min of the current study. Furthermore, the comparison of the two models in terms of quality fitting criteria was in favour of the simpler 5k model, as both the Schwarz Criterion (30.2 vs. 28.2) and the Akaike Information Criterion (22.5 vs. 21.6) were smaller in the 5k model than in the 6k model. Finally, only the parameters derived from the 5k model ( $k_3$  and  $k_4$ ) were correlated with FA oxidation, as measured independently by indirect calorimetry ( $R=0.84$  and  $R=0.90$ , both  $p<0.005$ , respectively). Based on these results,  $k_6$  was defined as negligible, and a 5k model was adopted.

The equations describing changing tracer concentrations in skeletal muscle compartments are:

$$\frac{dC_1}{dt} = C_a(t) \times K_1 - C_1(t) \times (k_2 + k_3 + k_5) + C_2(t) \times k_4 \quad \text{Eq. 6}$$

$$\frac{dC_2}{dt} = C_1(t) \times k_3 - C_2(t) \times k_4 \quad \text{Eq. 7}$$

$$\frac{dC_3}{dt} = C_1(t) \times k_5 \quad \text{Eq. 8}$$

where  $C_a(t)$  is the plasma input function,  $C_{1-n}$  is the concentration of tracer in each tissue compartment; the total concentration of [ $^{11}\text{C}$ ]-palmitate in the tissue at a given time can be defined by the sum of the tracer in each compartment:

$$\text{Tissue}(t) = (1 - V_a) \times (C_1(t) + C_2(t) + C_3(t)) + V_a \times C_b(t) \quad \text{Eq. 9}$$

Kinetic parameters were fitted with the same methods as used for the SAT and VAT model. An Example of tissue TAC and model curve fit is shown in Figure 5.1.7.2.

Skeletal muscle FA metabolic rates equations were adapted from Bergmann et al. (Bergmann *et al.*, 1996):

$$C_1 (\text{FA pool}) = [\text{FFA}] \times K_1 / (k_2 + k_3 + k_5) \quad \text{Eq. 10}$$

$$\text{FA Oxidation rate (FAO)} = C_1 (\text{FA pool}) \times k_3 \quad \text{Eq. 11}$$

$$\text{FA Esterification rate (FAE)} = C_1 (\text{FA pool}) \times k_5 \quad \text{Eq. 12}$$

$$\text{FA Uptake rate (FAU)} = \text{FAO} + \text{FAE} \quad \text{Eq. 13}$$

Rates were expressed as  $\mu\text{mol}/\text{min}/100\text{g}$  of tissue or as  $\mu\text{mol}/\text{min}$  in the entire skeletal muscle mass.

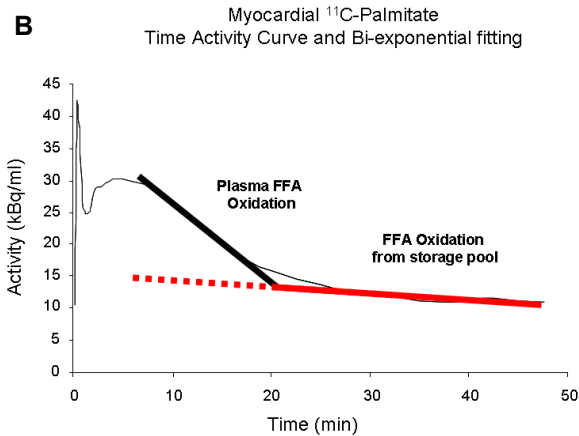
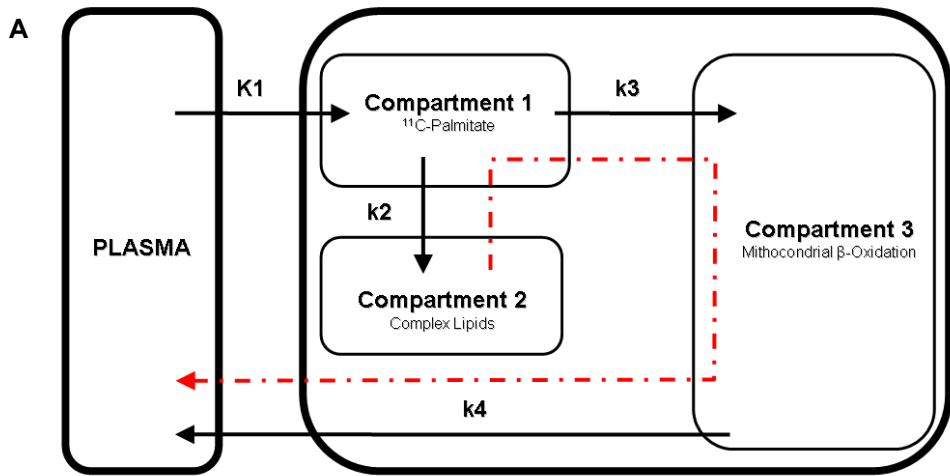


Figure 5.1.7.3. Kinetics of [ $^{11}\text{C}$ ]-palmitate in the heart as analyzed through (A) compartmental modelling, or (B) bi-exponential fitting. The tissue curve in “B” shows distinctly declining rates in the initial (fitted in black) and later phase of the myocardial washout phase (fitted in red). The dashed red arrow in “A” indicates slow fatty acid turnover and washout through oxidation.

### 5.1.7.1 Modelling of myocardial $^{11}\text{C}$ -palmitate kinetics (III)

$^{11}\text{C}$ -palmitate-TACs were analyzed with two recognized procedures to measure myocardial FFA uptake (MFU), FFA oxidation, FFA esterification, and oxidation of stored FAs:

- Compartmental model analysis** was implemented by using the model proposed by de Jong *et al* for the estimation of plasma free FA (FFA) oxidation, esterification and uptake rates (de Jong *et al.*, 2009). The model, which is shown in Figure 5.1.7.3 (A), is composed of three tissue

compartments, representing free [<sup>11</sup>C]-palmitate, [<sup>11</sup>C]-palmitate bound in complex lipids, and [<sup>11</sup>C]-breakdown products. The transfer of radioactivity between compartments is described by four rate constant terms, as given in Figure 5.1.7.3 (A). The differential equations describing changing tracer concentrations in the model compartments are:

$$dC_1/dt = Ca(t) \times K_1 - C_1(t) \times (k_2 + k_3) \quad \text{Eq. 14}$$

$$dC_2/dt = C_1(t) \times k_2 \quad \text{Eq. 15}$$

$$dC_3/dt = C_1(t) \times k_3 - C_3(t) \times k_4 \quad \text{Eq. 16}$$

and the total concentration of [<sup>11</sup>C]-palmitate in the myocardium at a given time can be defined by the sum of the tracer in each compartment and in the tissue blood fraction

$$\text{Myocardium}(t) = (1 - V_b) \times (C_1(t) + C_2(t) + C_3(t)) + C_b(t) \times V_b \quad \text{Eq. 17}$$

where  $C_b(t)$  is the blood tracer concentration, as derived from the left ventricle cavity ROI interpolated through a spline function,  $Ca(t)$  is the plasma concentration of unchanged [<sup>11</sup>C]-palmitate, *i.e.*, discounted for metabolites,  $V_b$  represents the fraction of arterial activity into the myocardial tissue, and  $C_n$  is the concentration of tracer in each tissue compartment. The rate constant  $k_4$  was fixed to be equal to  $k_3$ , as suggested (de Jong *et al.*, 2009).

The system of differential equations was solved numerically by using the commercial software SAAM II (Simulation Analysis and Modeling II, version 1.2.1, SAAM Institute). The rate constants obtained were used together with plasma (P) FFA concentration measurements ( $C_{FFA}$ ) to derive respective substrate flux rates, by assuming steady-state according to Bergmann and coworkers (Bergmann *et al.*, 1996):

$$\text{P-FFA esterification rate} = C_{FFA}(\mu\text{mol/mL}) \times (K_1 \times k_2) / (K_1 + k_2 + k_3) \text{ (1/min)} \quad \text{Eq. 18}$$

$$\text{P-FFA oxidation rate} = C_{FFA}(\mu\text{mol/mL}) \times (K_1 \times k_3) / (K_1 + k_2 + k_3) \text{ (1/min)} \quad \text{Eq. 19}$$

$$\text{P-FFA uptake rate} = \text{esterification} + \text{oxidation rates} \text{ (}\mu\text{mol/mL/min)} \quad \text{Eq. 20}$$

**b) Bi-exponential fitting** was applied to the myocardial [<sup>11</sup>C]-Palmitate TACs (Figure 5.1.7.3, B). The two wash-out rate coefficients have been used to represent FA oxidation rate constants. The initial and rapidly descending part of the curve is commonly interpreted as the immediate oxidation of plasma derived FFAs (Schon *et al.*, 1982), whereas the later and slower tissue activity decline represents the oxidation of FAs after they have been transferred in and out of the myocardial triglyceride pool (Kisrieva-Ware *et al.*, 2009). Since the triglyceride pool was measured by <sup>1</sup>H-MRS in the current study, it was possible to estimate the absolute oxidative flux of triglyceride-derived FAs (triglyceride:FA, 3:1) by using the following equation:

$$\text{Oxidation of stored FAs} = \text{Cardiac lipid} (\mu\text{mol/g}) \times 3 \times \text{rate constant} \text{ (1/min)} \quad \text{Eq.21}$$



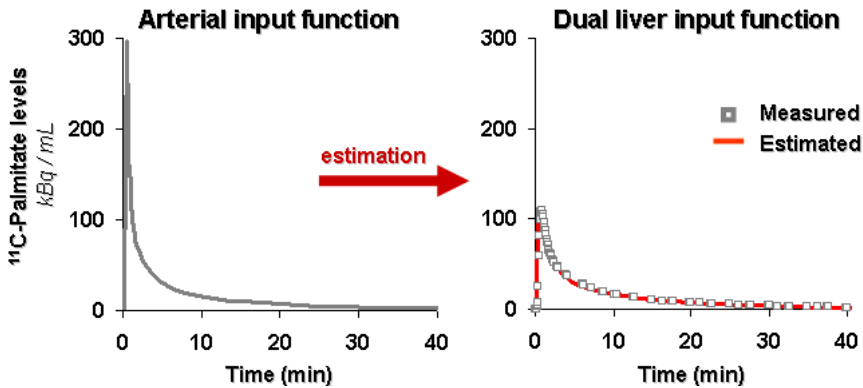
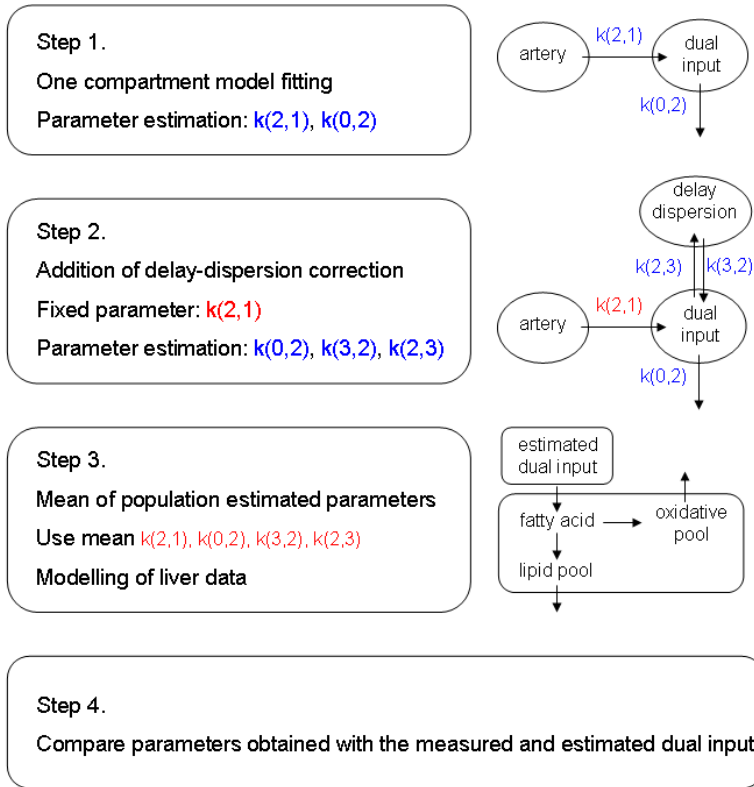


Figure 5.1.7.4. (Top) Flowchart representation of the sequence of operations and compartmental model used to estimate parameters that relate the dual to the arterial input function in human beings (steps 1 and 2). These parameters were subsequently used to create new dual-input functions from arterial ones and to estimate liver FA metabolism (step 3), the results of which were compared with those from the originally measured image-derived, dual-input function. (Bottom) The arterial input function (left) is used to estimate a dual-input function and the estimated is compared with the measured curve on the right.

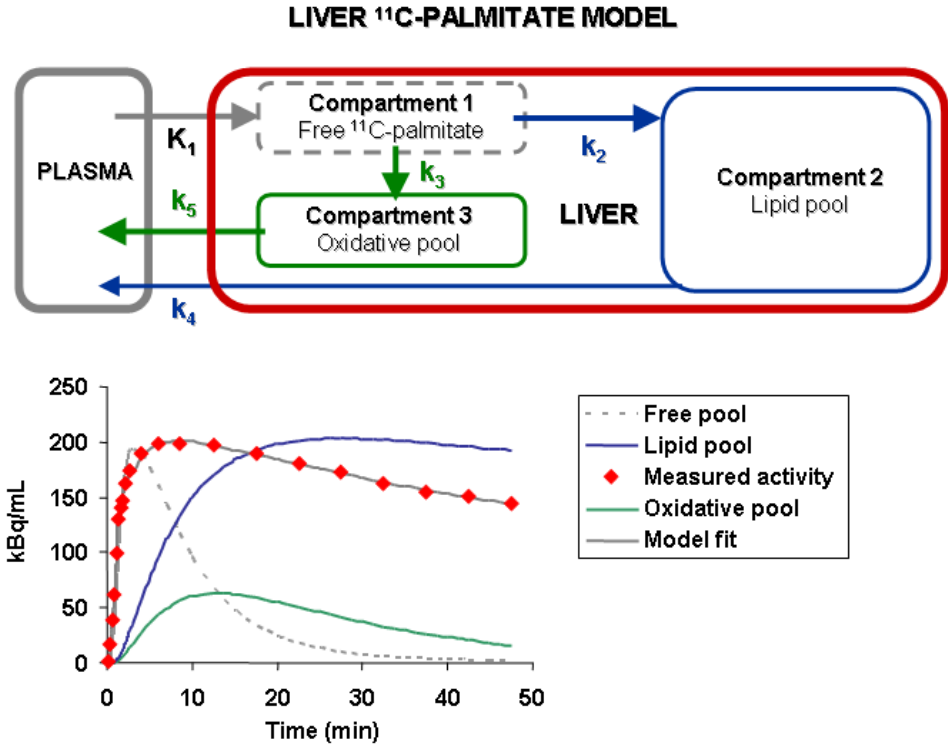


Figure 5.1.7.5. (Top) Configuration of the model used to derive the rate constants ( $K_1$ – $k_5$ ) describing the fractional inward/backward transfer of FA from plasma into the tissue and between the cytoplasm, and the lipid and oxidative pool compartments. (Bottom) The model fit to the measured tissue  $^{11}\text{C}$ -palmitate time-activity curve shows that the mathematical derivation predicts the measured tracer kinetics with excellent approximation; the tracer radioactivity in each model compartment is also shown, as derived from the estimated rate constants in one study animal.

#### 5.1.7.4 Modelling of liver $^{11}\text{C}$ -palmitate kinetics (I)

In nine studies, in which CT and image quality allowed identification of the portal vein, small regions of interest were drawn in this vessel and in the left ventricular cavity of the heart, to obtain radioactivity concentrations in portal and arterial blood, respectively, to be converted into plasma activity through the hematocrit. For the cases where dual input function was not resolvable from human images, a mathematical model was used to derive average kinetics parameters that would permit its estimation from the arterial input function, as shown in Figure 5.1.7.4. This input function was applied in six control individuals. Subsequent data analysis was done with either the dual (measured and estimated) or the single arterial input function for comparisons.

Compartmental modelling describes each process involved in FA handling by the liver, including inward transport, release of labelled  $^{11}\text{C}$ -products due to oxidation of palmitate, incorporation of  $^{11}\text{C}$ -palmitate into triglyceride, and the subsequent partial

release of labelled triglycerides ( $^{11}\text{C}$ -TG) into the circulation. The model, which is shown in Figure 5.1.7.5, consists of three tissue compartments, representing free  $^{11}\text{C}$ -palmitate,  $^{11}\text{C}$ -palmitate bound in complex lipids, and  $^{11}\text{C}$ -oxidative breakdown products. The exchange of radioactivity across compartments is described by five rate constant terms,  $K_1$ - $k_5$ . The differential equations describing changing tracer concentrations in the model compartments are:

$$dC_1/dt = C_a(t) \times K_1 - C_1 \times k_2 - C_1 \times k_3 \quad \text{Eq. 22}$$

$$dC_2/dt = C_1 \times k_2 - C_2 \times k_4 \quad \text{Eq. 23}$$

$$dC_3/dt = C_1 \times k_3 - C_3 \times k_5 \quad \text{Eq. 24}$$

and the total concentration of  $^{11}\text{C}$ -palmitate in the liver at a given time,  $C(t)$ , can be defined by the sum of the tracer in each compartment and in the tissue blood fraction

$$C(t) = (1 - V_b) \times [C_1(t) + C_2(t) + C_3(t)] + C_b(t) \times V_b \quad \text{Eq. 25}$$

where  $C_a$  is the metabolite corrected plasma tracer concentration,  $C_b(t)$  is the total blood radioactivity concentration,  $V_b$  represents the fraction of blood within the tissue region of interest, and  $C_{1-3}$  is the concentration of tracer in each tissue compartment. The rate constant  $k_5$  was fixed to be equal to  $k_3$ , as suggested (de Jong *et al.*, 2009).

The system of differential equations was solved numerically by using the commercial software SAAM II (Simulation Analysis and Modeling II, version 1.2.1, SAAM Institute). The rate constants obtained (1/min) were used together with plasma FA concentrations ( $C_{FA}$ ,  $\mu\text{mol/mL}$ ) to derive substrate steady-state flux rates ( $\mu\text{mol/mL/min}$ ), according to Bergmann and coworkers (Bergmann *et al.*, 1996), by using the following formulas:

$$\text{FA oxidation rate} = C_{FA} \times (K_1 \times k_3) / (k_2 + k_3) \quad \text{Eq. 26}$$

$$\text{FA esterification rate} = C_{FA} \times (K_1 \times k_2) / (k_2 + k_3) \quad \text{Eq. 27}$$

$$\text{Labelled TG release rate} = C_{FA} \times (K_1 \times k_2 \times k_4) / [3 \times (k_3 \times k_5 + k_2 \times k_4)] \quad \text{Eq. 28}$$

$$\text{FA uptake rate} = \text{esterification} + \text{oxidation rates} \quad \text{Eq. 29}$$

In which labelled TG release takes into account the 3:1 FA: TG molar ratio.

#### 5.1.7.5 Modelling of $^{18}\text{F}$ -FDG kinetics (II,III)

A three Ks, three-compartment model was used to describe [ $^{18}\text{F}$ ]FDG transport and phosphorylation rate constants (Sokoloff *et al.*, 1977; Nuutila *et al.*, 1992) in skeletal muscle, SAT and VAT. The fitting was performed with the same optimization algorithms as in the palmitate model. The organ-specific fractional extraction rate constant (1/min) was calculated by the following equation:

$$K_i = K_1 \times k_3 / (k_2 + k_3) \quad \text{Eq. 30}$$

Myocardial fractional extraction rate of [ $^{18}\text{F}$ ]FDG was calculated using graphical analysis (Patlak & Blasberg, 1985).

The glucose uptake rate (GU) was obtained by:

$$\text{GU} = [\text{plasma glucose}] \times \text{Ki} / \text{LC} \quad \text{Eq. 31}$$

where LC indicates the lumped constant. The lumped constant is a parameter used to account for the differences in transport and phosphorylation rates between glucose and [ $^{18}\text{F}$ ]FDG. An LC value of 1.2 for skeletal muscle (Peltoniemi *et al.*, 2000), 1.14 for adipose tissue (Virtanen *et al.*, 2001) and 1.0 for myocardium (Iozzo *et al.*, 2002; Ng *et al.*, 1991) was used.

### **5.1.8 Calculation of glucose (II) and FA systemic disposal rates (I,II)**

Circulating glucose and FFA plasma levels were determined three times during each PET scan to document steady concentrations. Plasma concentrations of [ $^{11}\text{C}$ ]-palmitate and [ $^{18}\text{F}$ ]FDG over time were used to calculate the whole body FFA and glucose clearances, as ratios of the injected doses to the areas under the tracer concentration curves ( $0 \rightarrow \infty$ ). The latter was calculated by the trapezoid rule. Clearance rates were multiplied by plasma FFA and glucose levels to obtain the rates of FA and glucose appearance (numerically equalling disappearance) in the circulation ( $\mu\text{mol}/\text{min}$ ) (Iozzo *et al.*, 2006). The clearance of palmitate was assumed to be representative of the overall FFA clearance, as supported by others (Mittendorfer *et al.*, 2003).

In study I, plasma curves of  $^{11}\text{C}$ -palmitate in arterial and portal venous plasma were used for the evaluation of the FA clearance rate in respective circulatory beds, and multiplied by arterial FFA levels to obtain corresponding rates of appearance, reflecting adipose tissue lipolysis. The difference between FA appearance in the two vessels was assumed to represent visceral fat lipolysis, draining directly into the liver; the use of arterial FFA values leads to a minimum estimate of visceral fat lipolysis.

## **5.2 Magnetic resonance imaging (I-III)**

A 1.5-T MR imager (Gyrosan Intera CV Nova Dual; Philips Medical Systems) with a flexible surface coil and body coil was used for MRI studies. To ensure identical voxel placement before and after trimetazidine treatment, voxel location was graphically recorded in each patient. All spectra were analyzed using LCModel (Provencher, 1993).

### **5.2.1 Abdominal fat masses assessment (I,II)**

A single T1W FFE image was obtained at the level of the intervertebral disc L2–L3 for analysis of abdominal adipose tissue masses, as previously described (Abate *et al.*, 1997). With this analysis, three compartments can be estimated in the abdomen:

subcutaneous, visceral and retroperitoneal adipose tissue volumes. Adipose tissue density of 0.9196 g/ml (Farvid *et al.*, 2005) was used for converting measured volumes into weight.

### **5.2.2 Left ventricle (LV) function and dimensions (III)**

Cardiac MR studies and relative calculations have already been published (Kankaanpaa *et al.*, 2006). In brief, LV mass, end diastolic volume (EDV), end systolic volume (ESV), and ejection fraction (EF) were measured from continuous short axis slices by using the balanced turbo field echo sequence. Imaging parameters were: repetition time (TR) of 3.8 msec, echo time (TE) of 1.9 msec, and matrix of 256 x 256. Slice thickness was 8 mm with no gap between slices. Image analysis was performed using Philips post-processing software (ViewForum R4.1; Philips Medical Systems). Cine loops were reviewed to identify end-diastolic and end-systolic frames. Epicardial and endocardial contours were outlined manually. Cardiac output and stroke volume (SV) were computed from ESV, EDV, and heart rate (Mohrman & Heller, 2006). LV work was calculated as the product of mean arterial blood pressure and CO, and then multiplied by 0.133 and divided by LV mass to obtain units of joules/min/g. The cardiac index was calculated as the ratio between cardiac output and body surface area. Peripheral vascular resistance was calculated as the ratio of mean blood pressure (mmHg) to cardiac output (ml/min).

## **5.3 <sup>1</sup>H Magnetic resonance spectroscopy (I – III)**

A 1.5-T MR imager (Gyrosan Intera CV Nova Dual; Philips Medical Systems) with a flexible surface coil and body coil was used for MRS studies. Patients were instructed to fast for 12 hours prior to the MR examinations. To ensure identical voxel placement before and after trimetazidine treatment (II, III), voxel location was graphically recorded in each patient. All spectra were analyzed using the user-independent software package LCModel (Provencher, 1993). The lipid and water amplitudes were corrected due to different T2 decay (Thomsen *et al.*, 1994) and molar concentrations of <sup>1</sup>H nuclei in fat and water for the different tissues (Schick *et al.*, 1993; Szczepaniak *et al.*, 1999; Nikolaidis *et al.*, 2006). <sup>1</sup>H-MRS findings of IMCL content have been validated in both animal and human studies (Szczepaniak *et al.*, 1999; Hannukainen *et al.*, 2011).

### **5.3.1 Skeletal muscle lipid and creatine content (II)**

A single voxel with a volume of 1.8 cm<sup>3</sup> was positioned in the tibialis anterior muscle to quantify the intramyocellular and extramyocellular lipid contents (IMCL, EMCL) and creatine-to-water ratios. A PRESS <sup>1</sup>H-MRS sequence was used with the following parameters: TR = 3000 ms, TE = 27 ms.

### **5.3.2 Heart lipid and creatine content (III)**

An extensive description of the methodology has been reported (Kankaanpaa *et al.*, 2006). In brief, a single volume of interest (VOI) (10 x 15 x 15 mm) was placed on LV short-axis images, and attention was paid to include only the myocardium. Single-voxel proton spectroscopy, with PRESS sequence, was used to determine the molecular contents of lipids and water. TE of 30 msec and TR of 3000 msec were used. Myocardial triglyceride content was defined as triglyceride in relation to the total weight of myocardial tissue (Thomsen *et al.*, 1994; Clarke & Mosher, 1952). Using the same MR spectra, creatine signals around 3.0 ppm were analyzed and myocardial creatine concentration was calculated as the creatine-to-water ratio (van der Meer *et al.*, 2007).

### **5.3.3 Liver lipid content (I)**

The methodology described below has been previously published (Rigazio *et al.*, 2008; Borra, 2009). A single voxel with a volume of 27 cm<sup>3</sup> was positioned in the liver outside the area of the great vessels. A PRESS <sup>1</sup>H-MRS sequence was used with the following parameters: TR = 3000 ms, TE = 25 ms with data acquired during breath-hold intervals. Measurements were performed during four consecutive breathhold series. During each single breathhold, four data frames (each containing the complete spectrum of water and triglyceride) were obtained. Therefore, the reported triglyceride values at each visit are the sum of 16 individual measurements of liver fat content, greatly contributing to the reliability and high signal-to-noise-ratio of the data. A manual quality check of the analysis of each individual spectrum (sums of 4 frames, 4 spectra per visit) was performed by an experienced MR spectroscopist before final (summed) analysis with the dedicated software.

## **5.4 Computed Tomography (I-IV)**

A 64-row PET/CT scanner (GE Discovery VCT, General Electric Medical Systems, WI, USA) was used to obtain low radiation dose scans to ensure the correct attenuation correction for PET scans and provide anatomical reference for ROI/VOI placement.

### **5.4.1 Coronary artery calcium score (IV)**

A dedicated CT acquisition protocol was used for calcium score assessment and has been described elsewhere (Schepis *et al.*, 2007). Coronary artery calcium (CAC) measured using standard GE ADW software was recorded for each patient. CAC score was entered in multiple regression models predicting perfusion since it has been found to be an independent predictor (Schenker *et al.*, 2008).

### 5.4.2 CT quantification of intra- and extra-pericardial fat volumes

Fat volume quantification was performed as previously published by Mahabadi and coworkers (Mahabadi *et al.*, 2009). Intra-pericardial (IPF) was defined as the fat inside the pericardial sac and extra-pericardial (EPF) the fat outside the sac, as shown in Figure 5.4.2.1. CT images were analyzed with an Advantage Workstation (ADW v.4.4, GE Healthcare). First, it was necessary to identify the volume of interest of the thoracic fat defined as any adipose tissue located within the thorax from the level of the right pulmonary artery to the diaphragm, and from the chest wall to the descending aorta; second, IPF was segmented by manual tracing of a region of interest delineating the pericardial sac on each axial slice; third, EPF was the result of the subtraction of IPF from the portion of thoracic fat defined above. Within the volumes of interest, fat was defined as voxels within a window of -195 to -45 Hounsfield units (HU) as previously published (Mahabadi *et al.*, 2009). Intra-observer reproducibility was excellent for both intra-epicardial (ICC 0.98) and extra-pericardial (ICC 0.99) fat depots, as tested in 25 random cases.

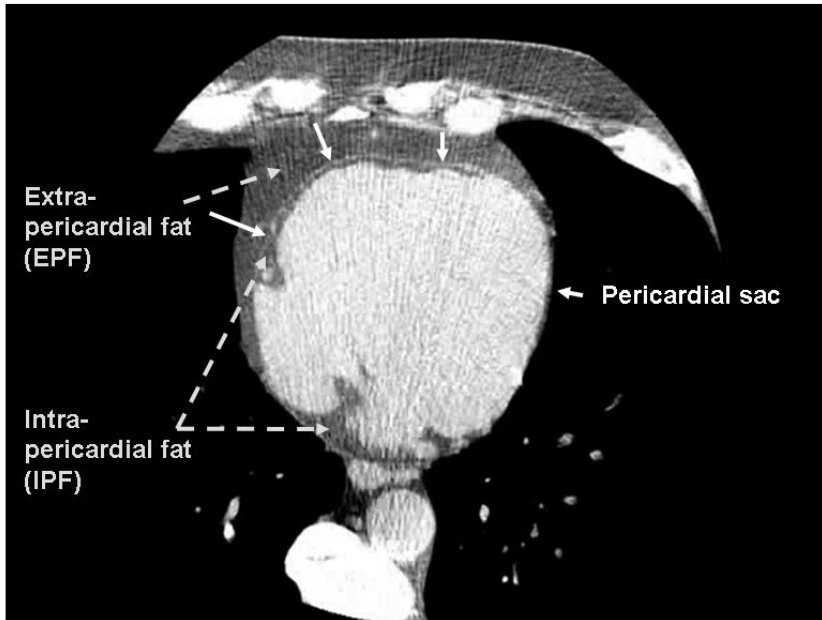


Figure 5.4.2.1. Computed tomography axial image of the heart where pericardial fat (shown by solid arrows) separates extra- from intra- pericardial fat (dashed arrows).

### 5.4.3 CT Angiography

If not contraindicated, 0-30 mg intravenous metoprolol was administered before the scan to reach the target heart rate (HR) of < 60/min, and 800 µg of sublingual nitrate was given prior to the scan. Iodinated contrast infusion (60-80 ml of 400 mg I/ml iomeprolol at 4-4.5 ml/s) was followed by a saline flush. The collimation was 64 x 0.625 mm, gantry rotation time 350 ms, tube current 600-750 mAs and voltage 100-

120 kV, depending on patient size. To reduce radiation dose, prospectively gated acquisition was applied whenever possible (86/107 patients). The technique has been described elsewhere in detail (Kajander *et al.*, 2009). When the retrospectively gated mode was used (21 patients), ECG-based tube current modulation was utilized.

An experienced cardiologist and radiologist analyzed the vessels separately and then in consensus on an ADW 4.4 Workstation (General Electric, Milwaukee, WI, USA) blinded to other results and clinical data, using a standard 17-vessel segment system adapted from the original AHA model (Austen *et al.*, 1975).

### 5.5 Invasive coronary angiography and fractional flow reserve (IV)

All coronary angiographies were performed with a Siemens Axiom Artis coronary angiography system (Siemens, Munich, Germany). In the presence of intermediate stenoses, a fractional flow reserve (FFR) measurement was performed using ComboMap<sup>®</sup> pressure/flow instrument and a 0.014-inch BrightWire<sup>®</sup> pressure guidewire (Volcano Corp., Rancho Cordova, CA, USA). The pressure was measured distally to the lesion during maximal hyperaemia induced by 18 µg intracoronary boluses of adenosine with simultaneous measurement of aortic pressure through the coronary catheter. FFR was calculated as the ratio between mean distal pressure and mean aortic pressure (Wilson *et al.*, 1990; Pijls *et al.*, 1996).

Quantitative analysis of coronary angiograms (QCA) was performed using software with automated edge detection system (Quantcore, Siemens, Munich, Germany) by an experienced reader blinded to the results of PET and FFR. Seventeen standard segments were analyzed.

A luminal diameter narrowing of  $\geq 50\%$  was considered significant. When FFR was available, stenoses with FFR  $> 0.8$  were classified as non-significant (Kern *et al.*, 2006), regardless of the degree of narrowing.

### 5.6 Biochemical analyses (I – III)

All laboratory specimens were drawn after a 12-h fasting period. Fasting plasma glucose was determined using the glucose oxidase method (Analox Glucose analyzer, GM9). Insulin was measured using electrochemiluminescence immunoassay (Roche Modular E170 analyzer; Roche Diagnostics GmbH, Mannheim, Germany). Serum FFAs were measured enzymatically (Wako Nefa C kit; Wako Chemicals GmbH, Germany). Total cholesterol, HDL-cholesterol, and triglyceride concentrations were measured in plasma by standard enzymatic methods using Roche Diagnostics reagents with an automated analyzer (Roche Modular P800). LDL-cholesterol concentrations were calculated using a modified Friedewald equation (Friedewald *et al.*, 1972).

Glycosylated hemoglobin (HbA<sub>1c</sub>) (II,III) was measured by the Variant II HbA<sub>1c</sub> analyzer based on chromatographic separation on a cation-exchange cartridge (Bio-Rad Laboratories, Hercules, CA).

In the trimetazidine study II, adipokine and cytokine levels [adiponectin, resistin, PAI-1, IL-6, IL-8, leptin (also in study III), tumour necrosis factor alpha (TNF $\alpha$ ),



macrophage chemoattractant protein-1 (MCP-1), and hepatocyte growth factor (HGF)] were determined by immunoassay using the LINCOp $lex$  kit (Luminex xMAP Technology).

Plasma concentrations of apelin-12 (II, III) were determined using a commercially available enzyme immunoassay without extraction (Phoenix Pharmaceuticals, Burlingame, CA, USA) according to the manufacturer's instructions. This assay employs an immunoaffinity purified rabbit antibody specific for apelin 1-12. The antibody has 100% cross-reactivity to apelin 1-12, 1-13 and 1-36. Each sample was assayed in duplicate. Plasma concentrations were obtained by the interpolation of the dose-response curves computed using a four-parameter logistic function (Pilo *et al.*, 1982).

## 5.7 Other measurements

Fat, fat-free and skeletal muscle masses were estimated according to published formulas (Hume, 1966; Abe *et al.*, 2003). Screening for diabetes was performed by a 75-g oral glucose tolerance test (OGTT). Insulin resistance was evaluated through the homeostasis model assessment (HOMA) index (Muniyappa *et al.*, 2008). The adipose tissue insulin resistance index (AIRI) was calculated as product of fasting FFA and plasma insulin concentrations (Chavez *et al.*, 2009). Indirect calorimetry was performed with standard procedures and previously published equations were used for calculations (Ferrannini, 1988).

### 5.7.1 Energy provision and LV work (III)

PET and MR data were used to estimate the amount of energy potentially provided by the substrates utilized in the heart. The rates of plasma FFA oxidation, triglyceride FA oxidation, and glucose uptake were multiplied by 129 or 36 (ATP net molecular yields for FAs and glucose, respectively) and then by 30.5 (joules/mol of ATP) in order to translate the respective energy production into the same units used for work estimations (watts/g of tissue) (Bailey & Ollis, 1986; Stipanuk, 2006). These measured energy production values were compared against the measured left ventricular forward work. This allowed estimation of the energy wasting due to an inefficient mechanical-metabolic coupling and the effect of TMZ on it.

## 5.8 Statistical analysis

Calculations were performed with the SPSS/Win statistical program (version 15.0 for Windows; SPSS, Chicago, IL). All data are presented as mean $\pm$ SEM. Cross-sectional differences were evaluated using ANOVA or the Mann-Whitney non-parametric test according to the distribution of the variables. Differences in paired data were tested with the non-parametric Wilcoxon signed rank test. Regression analyses were carried out according to standard techniques, by using Pearson or Spearman

correlation coefficients, as appropriate. A p-value  $< 0.05$  (I, II, IV) or  $\leq 0.05$  (III) was considered statistically significant.

In study I, comparisons between model-derived and measured variables were performed by Student's paired *t* test.

In study III, the *a priori* power analysis was based on a previous study carried out in the same institute (Tuunanen *et al.*, 2008), and showed that in a two-tailed paired test with alpha error of 0.05, a 15% significant change in plasma FAO could be detected with a power of 0.81 in a group of eight subjects.

In study IV, the nominal variables presented in tables were compared with Pearson's Chi-Square (2-sided) test, and Fisher's exact test for comparisons between groups. For three or more groups, post-hoc tests were computed when ANOVA was statistically significant. Dunnett's post-hoc test was utilized to compare fat depot differences among subjects with Obs-CAD with a different number of vessels involved, using the non-CAD as reference group. Bonferroni post-hoc test was used for comparisons of three groups. Multiple regression analysis examining IPF and EPF in relation to perfusion after adjusting for age, gender, BMI, and HDL were performed.

## 6 RESULTS

### 6.1 Validation study for liver fatty acid metabolism assessment in animals by PET and $^{11}\text{C}$ -Palmitate (I)

**6.1.1 Image quality and model fit.** Hepatic  $^{11}\text{C}$ -palmitate images were of excellent quality, showing progressive retention of radioactivity. Direct blood sampling in animals demonstrated that  $^{11}\text{C}$ -palmitate levels were higher in arterial than portal plasma only during the peak phase, *i.e.*, in the first min following tracer injection, converging to similar values after approximately three minutes (Fig. 6.1.1.1). Therefore, in the human studies, image-derived arterial and portal venous measurements of  $^{11}\text{C}$ -palmitate concentrations were combined over peak values, whereas arterial determinations were used for later time points. Representative examples of model-predicted vs. measured liver tissue time-activity curves have been given in Fig. 5.1.7.5, also showing the simulated time-activity concentrations in each tissue compartment. The goodness of fit was evaluated as the weighted sum of squares (Akaike, 1992), which averaged  $1.77 \pm 0.70$ . Model parameters did not show any significant autocorrelation (Table 6.1.1.1).

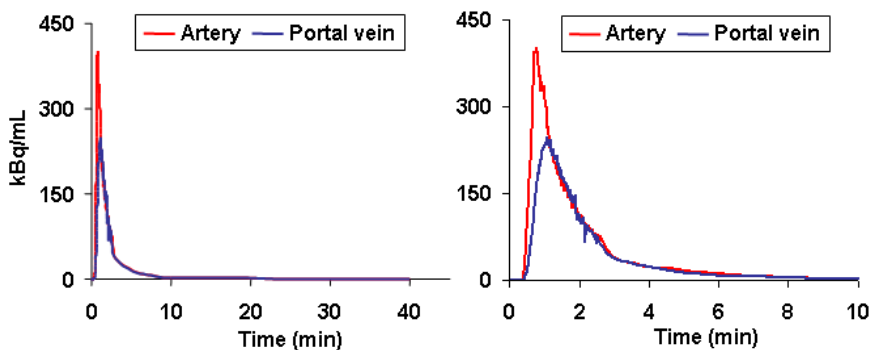


Figure 6.1.1.1. A representative example of arterial and portal venous concentrations of  $^{11}\text{C}$ -palmitate over time showing that the curves converge after the first sampling minutes (expanded time scale on the right).

**6.1.2 PET-derived vs. measured fatty acid fluxes.** As shown in Figure 6.1.2.1, the model-predicted outflow of FA oxidative products (kBq/min per mL of organ) and FA oxidative rate ( $\mu\text{mol}/\text{min}/\text{mL}$ ) indicated no significant difference as compared with the respectively measured values. The correlation of estimated and measured labelled water products was significant ( $R=0.91$ ,  $p=0.01$ ), and a strong tendency was shown between estimated and measured FA oxidative rates ( $R=0.63$ ,  $p=0.18$ ), which fell short of statistical significance, likely due to group size. In addition, the measured rate of release of  $^{11}\text{C}$ -oxidative products was significantly correlated with both the FA oxidation rate and the FA concentrations in the oxidative (mitochondrial) pool obtained

## RESULTS

from the model (Fig. 6.1.2.2). Similar correspondences were observed in relation to triglyceride (TG) metabolism and total hepatic FA uptake. The model predicted vs measured labelled-TG release and liver FA uptake were similar between the methods (Figure 6.1.2.1), and the estimated vs measured uptake rate showed a strong tendency towards a correlation ( $R=0.75$ ,  $p=0.15$ ) of borderline significance because of a limited sample size. Circulating triglyceride levels were significantly correlated with both model-predicted  $^{11}\text{C}$ -TG release rates and FA concentrations in the hepatic TG pool (Figure 6.1.2.2).

Table 6.1.1.1. Autocorrelation of kinetic parameters in the animal study <sup>o</sup>

	Absolute correlation coefficients (p values)			
	$k_4$	$K_1$	$k_3$	$k_2$
$k_4$	1	0.51 (0.30)	0.46 (0.35)	0.71 (0.11)
$K_1$	0.51 (0.30)	1	0.19 (0.72)	0.64 (0.17)
$k_3$	0.46 (0.35)	0.19 (0.72)	1	0.75 (0.08)
$k_2$	0.71 (0.11)	0.64 (0.17)	0.75 (0.08)	1

<sup>o</sup> Data are from six animal studies; absolute coefficients are shown without sign due to the absence of any correlation or tendency (p values are in parentheses).

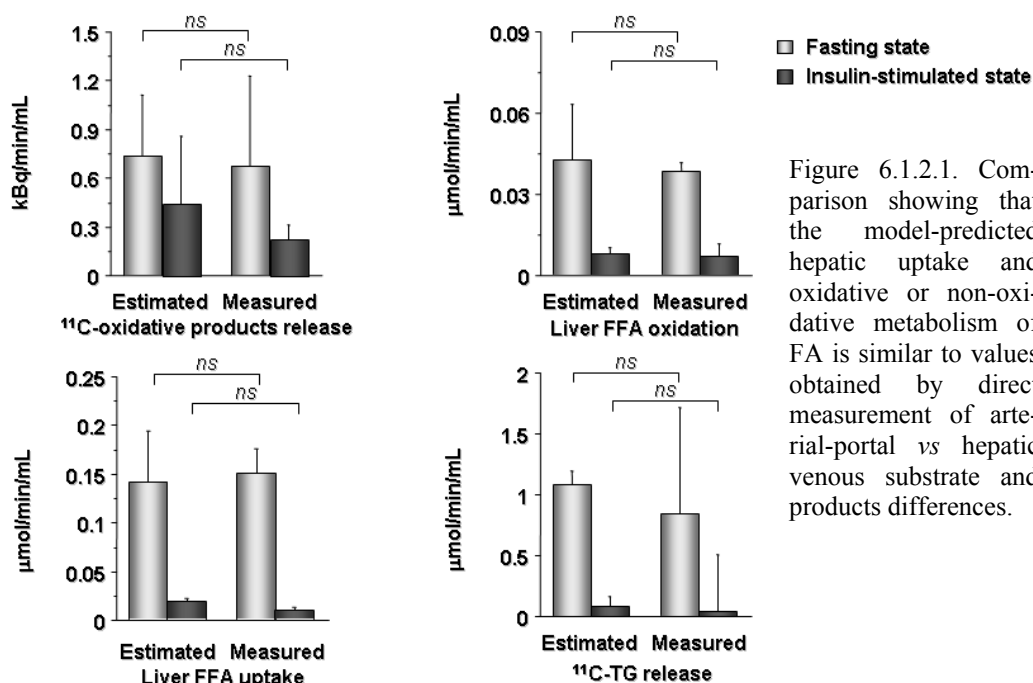


Figure 6.1.2.1. Comparison showing that the model-predicted hepatic uptake and oxidative or non-oxidative metabolism of FA is similar to values obtained by direct measurement of arterial-portal vs hepatic venous substrate and products differences.

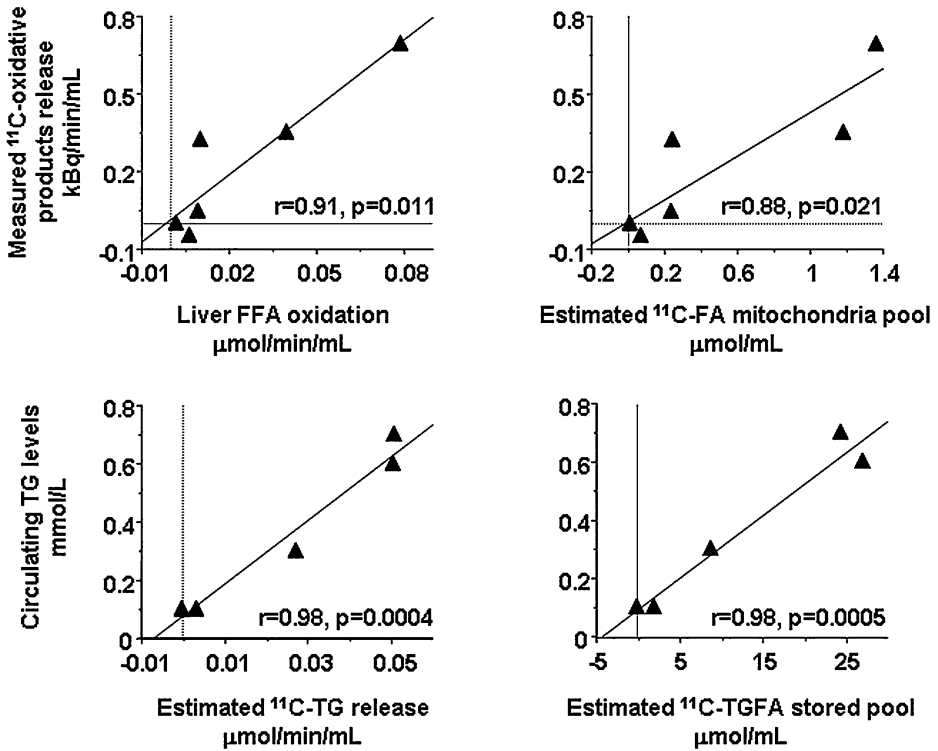


Figure 6.1.2.2. Regression analyses between the model-predicted hepatic oxidative or non-oxidative metabolism of FA and the related pools and processes.

**6.1.2 Effects of insulin on liver fatty acid metabolism.** The utilization of FA by the liver is a summation process, resulting from the combined contribution of FA delivery to the organ, *i.e.*, plasma FA levels, and the intrinsic tissue extraction and fractional partition of the substrate between oxidative and non-oxidative pathways. The model rate constants and the inward clearance rate represent the intrinsic tissue determinants, as they are independent of circulating FA concentrations. The animal experiments documented intrinsic effects of insulin (Figure 6.1.2.3) to suppress the efflux of labelled-TG from the liver, thereby likely promoting TGFA retention in the storage pool. The corresponding substrate fluxes, lumping together the intrinsic liver response and the extrinsic availability of circulating FA, documented a suppression of liver FA uptake, oxidation, esterification, and output.

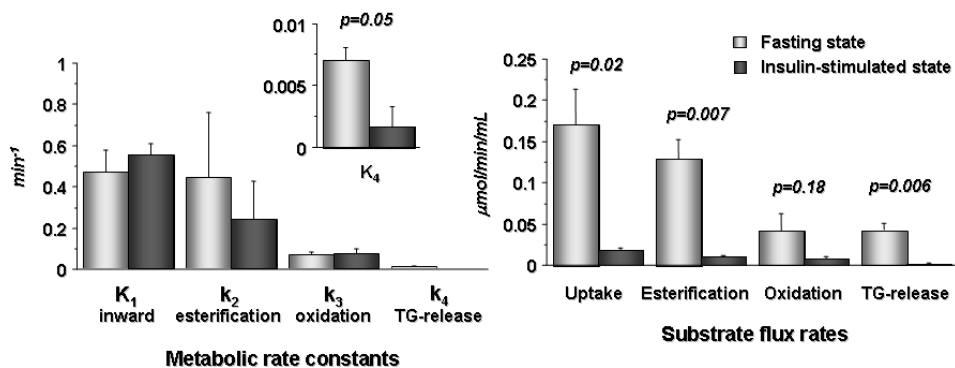


Figure 6.1.2.3. The effects of insulin on the hepatic FA model rate constants (top) document a direct suppression of the fractional release of labelled TG (magnified graph), whereas liver FA uptake and metabolic fluxes (right) are suppressed by indirect inhibition of circulating FA levels by insulin.

## 6.2 Validation study for liver fatty acid metabolism assessment in humans by PET and $^{11}\text{C}$ -Palmitate (I)

**6.2.1 Image quality and model fit.** Images obtained in human studies (Figure 5.1.6.2) allowed extraction of portal time activity curves. In the human studies, in which the dual input function was directly measured from the images, the goodness of fit, as weighted sum of squares (Akaike, 1992), was  $0.78 \pm 0.40$  (ns vs animal studies). The accuracy of estimation of each parameter, *i.e.*, the coefficient of variation, was  $6 \pm 1\%$ ,  $18 \pm 3\%$ ,  $16 \pm 4\%$ , and  $19 \pm 5\%$  for the inward, oxidative, esterification and output rate constants, respectively.

**6.2.2 PET-derived fluxes vs. measured indicators.** The nine human studies in which the dual input function was directly extracted from the PET-CT images were used as reference in the current validation. Circulating levels of  $\beta$ -hydroxybutyrate, which is an indirect, but organ-specific marker of liver FA oxidation, were positively associated with the model-predicted oxidative rate ( $R=0.76$ ,  $p=0.03$ ), after excluding one subject in whom  $\beta$ -hydroxybutyrate was below the detection level. Similar to findings in animals, circulating triglyceride levels in these subjects were correlated with  $^{11}\text{C}$ -palmitate esterification and  $^{11}\text{C}$ -TG release rates ( $R=0.80$ ,  $p=0.018$ ). Whole-body lipid oxidation derived from indirect calorimetry assessments was associated with the proportions of FA entering hepatic oxidation (positive) and esterification (negative).

**6.2.3 Use of a single arterial input function and prediction of a dual input function.** The use of a single arterial vs a dual arterial-portal input function to estimate liver FA metabolic fate was associated with a 46% underestimation of  $K_1$  ( $p=0.004$ ), similar oxidative and  $^{11}\text{C}$ -TG-output rate constants (ns), and an approximate 64% overestimation of the triglyceride synthetic rate constant ( $p=0.022$ ). Consequently, rates of FA uptake (-46%,  $p=0.003$ ), oxidative metabolism (-56%,  $p=0.008$ ),

esterification (-27%, p=0.004), and release (-28%, p=0.005) were all underestimated using the single vs dual input function model (Fig. 4c). In spite of absolute differences, the weighted sum of squares ( $0.70 \pm 0.28$ ) (Akaike, 1992), and coefficients of variation of individual parameters were not different, and proportional partition between pathways was preserved.

The use of the arterial input function to predict the dual input function by mathematical modelling provided parameters describing the dual input function with excellent approximation (Figure 5.1.7.4). The estimated parameters did not correlate with the amount of intra-abdominal fat (Table 6.3.2.1). These parameters were averaged and applied again to each arterial input function, demonstrating that the use of fixed-average parameters did not affect the model fit (Akaike criterion (Akaike, 1992)  $0.87 \pm 0.36$ ) or coefficients of variation of individual parameters (ns as compared with the individually measured dual input function), or the ultimate calculation of liver FA metabolic rate constants and fluxes, as shown in Figure 6.3.2.1. These parameters were used in the remaining six subjects, lacking access to portal vein images. The liver model parameters in the final analysis in humans did not show any significant autocorrelation (Table 6.3.2.2).

Table 6.3.2.1. Model-derived kinetic parameters for estimation of a dual from an arterial input function °

	Mean±sem (range) (kg)	Absolute correlation coefficients (p values)			
		k(0,2)	k(2,1)	k(2,3)	k(3,2)
Mean±sem (min <sup>-1</sup> )		2.26 ± 0.12	1.96 ± 0.12	0.40 ± 0.08	0.86 ± 0.17
Visc fat	1.70 ± 0.22 (0.65-2.62)	0.28 (0.47)	0.39 (0.31)	0.33 (0.39)	0.01 (0.98)
Retrop fat	0.95 ± 0.14 (0.50-1.75)	0.21 (0.58)	0.31 (0.43)	0.51 (0.17)	0.11 (0.78)
Visc+retrop fat	2.65 ± 1.05 (1.17-4.37)	0.26 (0.50)	0.36 (0.34)	0.41 (0.28)	0.04 (0.93)

° Mean values for fat masses (first column) and parameters (first row) are given. Data are from nine human subjects in whom fat masses were available, and the measured dual input function (obtained from arterial left ventricular cavity and portal vein blood, identified via co-registration of CT and PET images) could be compared with the estimated curves for validation purposes; absolute coefficients are shown without sign due to the absence of any correlation (p values are in parentheses)

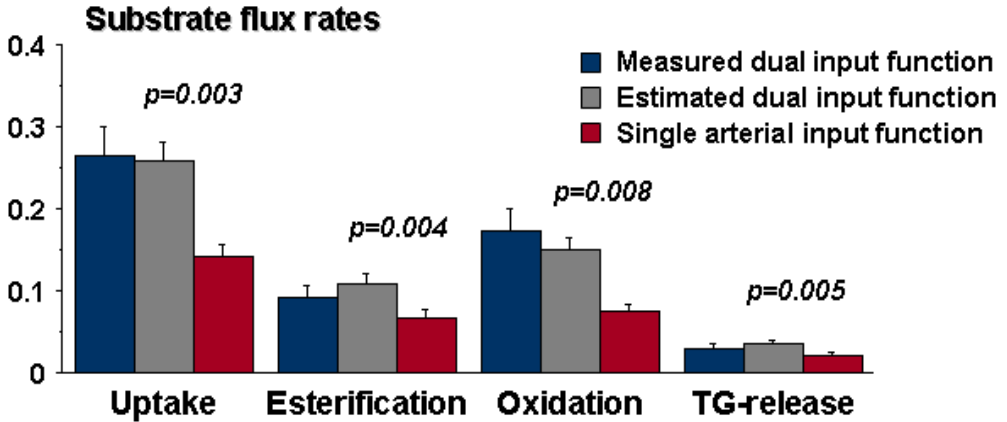


Figure 6.2.3.1. The comparison between FA flux rates (mean±sem) obtained with the original vs. estimated-dual vs. single-arterial input functions, showing good correspondence between the first two, and an underestimation in the parameters derived from the third approach.

Table 6.2.3.2. Autocorrelation of kinetic parameters in the human study °

	Absolute correlation coefficients (p values)			
	$k_4$	$K_1$	$k_3$	$k_2$
$k_4$	1	0.21 (0.45)	0.11 (0.69)	<0.01 (1.00)
$K_1$	0.21 (0.45)	1	0.30 (0.28)	0.04 (0.90)
$k_3$	0.11 (0.69)	0.30 (0.28)	1	0.19 (0.51)
$k_2$	<0.01 (1.00)	0.04 (0.90)	0.19 (0.51)	1

° Data are from fifteen human subjects; absolute coefficients are shown without sign due to the absence of any correlation or tendency (p values are in parentheses). The result did not change if obese and lean individuals were analyzed separately.



### 6.3 Effect of obesity on fatty acid organ metabolism (I-III)

#### 6.3.1 Anthropometric and metabolic characteristics of the study groups

Anthropometric and metabolic characteristics of study subjects are reported in Table 6.3.1.1. By definition, obese subjects had higher BMI and fat mass than the control group. Fasting FFA levels were not different between the two groups, while fasting insulin and triglycerides levels, and insulin resistance indexes (HOMA-IR and AIRI) were significantly greater in the obese group.

Table 6.3.1.1. Anthropometric and metabolic characteristics of the study groups °

	Control subjects	Obese subjects
N	8	8
Age (years)	50 ± 1	55 ± 3
BMI (kg m <sup>-2</sup> )	26 ± 1	32 ± 1 **
Fat mass (kg)	23 ± 2	34 ± 2 **
Fasting glucose (mmol L <sup>-1</sup> )	4.9 ± 0.1	5.3 ± 0.1
Fasting insulin (pmol L <sup>-1</sup> )	33 ± 4	61 ± 11 *
Fasting FFA (mmol L <sup>-1</sup> )	0.51 ± 0.03	0.63 ± 0.05
Glycosylated hemoglobin (HbA <sub>1c</sub> %)	5.4 ± 0.1	5.7 ± 0.1
Triglycerides (mmol L <sup>-1</sup> )	0.8 ± 0.2	1.7 ± 0.4 *
Cholesterol (mmol L <sup>-1</sup> )	4.8 ± 0.4	5.5 ± 0.3
HDL (mmol L <sup>-1</sup> )	1.4 ± 0.1	1.5 ± 0.2
LDL (mmol L <sup>-1</sup> )	3.1 ± 0.3	3.2 ± 0.2
HOMA-IR index	1.0 ± 0.1	2.0 ± 0.4 *
Adipose tissue IR index (AIRI)	17 ± 2	41 ± 10 *

° IR = insulin resistance, HOMA = homeostasis model assessment. \* P < 0.05, \*\* P < 0.01

#### 6.3.2 Effects of obesity on hepatic fatty acid metabolism (I)

In control subjects, FA oxidation and esterification rates accounted for 40% and 60% of liver FA uptake, respectively (Figure 6.3.2.1, on the left of the bottom panel). Hepatic FA oxidation rates were on average 100% greater in obese than control individuals (Figure 6.3.2.1, top panel); thus, the intracellular partition between oxidation and esterification was significantly shifted in favour of the former. No

## RESULTS

differences were noted between men and women. The rate of systemic FA appearance, *i.e.*, lipolysis, was not different between lean and obese individuals. However, the difference between FA appearing in the portal *vs* the systemic circulation was significant in obese, and less pronounced in control subjects, resulting in a tendency (just short of statistical significance) towards a higher visceral fat FA contribution in the former group (Figure 6.3.2.2, top panels). Systemic and portal FA appearance (lipolytic) rates were the strongest predictors of hepatic esterification (Figure 6.3.2.2, bottom panels) and release rate of FA in triglycerides.

Hepatic FA oxidation was associated with circulating insulin levels ( $R=0.61$ ,  $p=0.016$ ), HOMA index, and adipose tissue insulin resistance (Figure 6.3.2.3, top panels). The estimated visceral fat FA contribution to the liver was correlated with the intra-abdominal, but not total body fat mass (Figure 6.3.2.3, bottom panels), supporting the current interpretation of this variable. Liver FA uptake, *i.e.*, the sum of oxidative and non-oxidative components, was correlated with HOMA and fat insulin resistance indexes ( $p<0.05$ ), as well as with systemic and portal FA appearance rates ( $p\leq 0.02$ ).

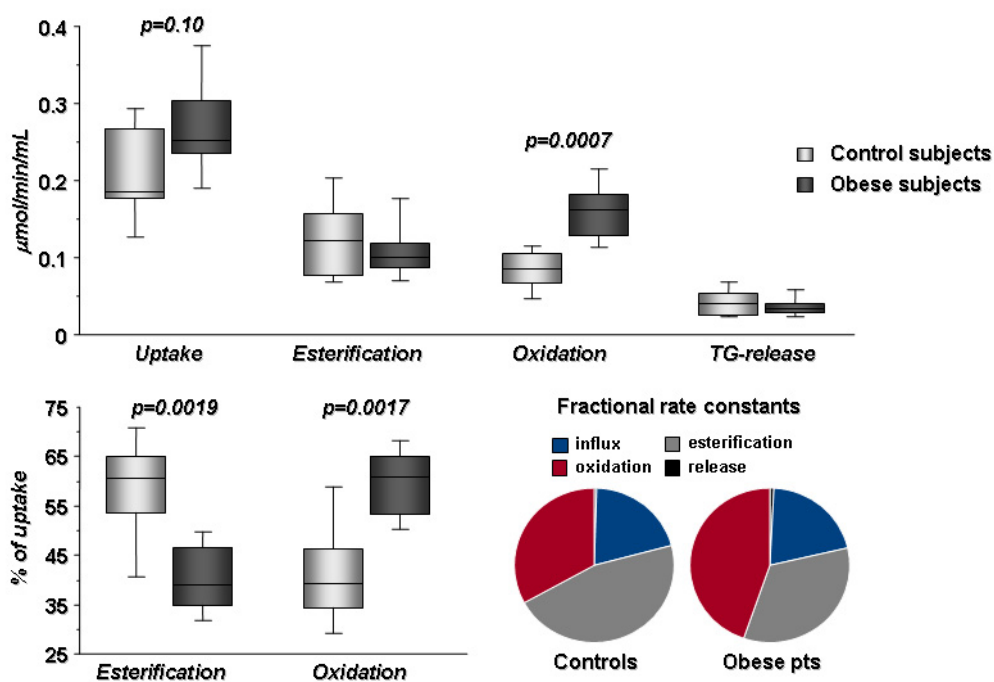


Figure 6.3.2.1. (Top panel) Metabolic flux rates of FA in the liver in obese and control subjects (mean  $\pm$  standard error of the mean), showing a 2-fold increase in hepatic FA oxidation in the former group, leading to the relative shift in favour of the oxidative *vs.* esterification pathway, as shown in bottom panel, given as percentages of uptake on the left and rate constants on the right.

RESULTS

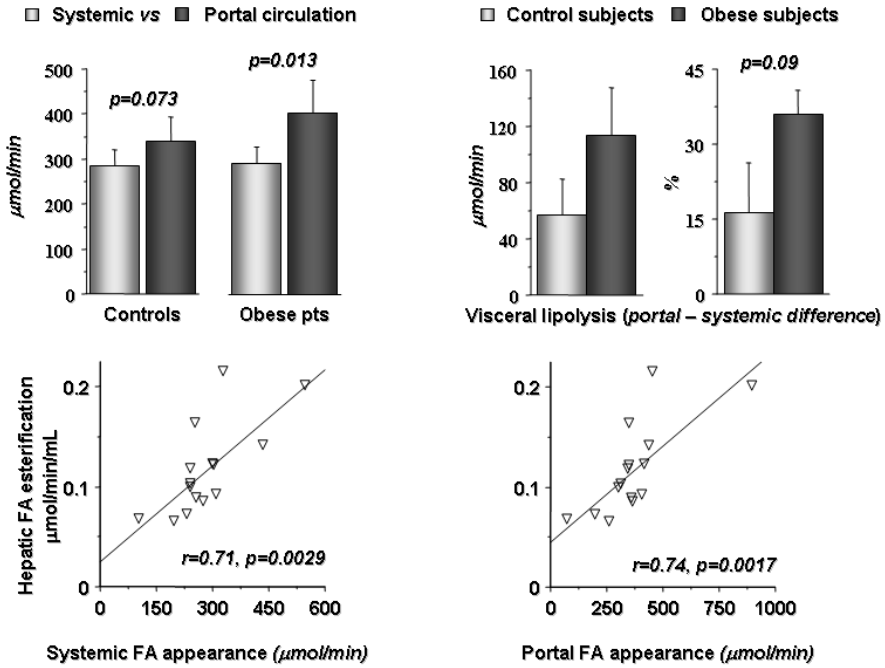


Figure 6.3.2.2. (Top panels) Lipolytic rates, as determined from  $^{11}\text{C}$ -palmitate arterial and portal venous plasma levels (left); the difference between the 2 measurements (right) represents the visceral contribution. (Bottom panels) Regression analyses in 15 human subjects show significant positive relationships between hepatic FA esterification and extrahepatic lipolysis.

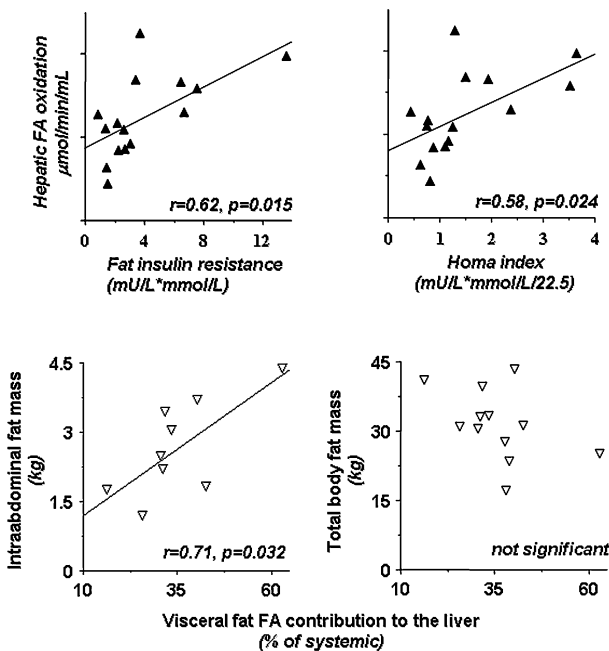


Figure 6.3.2.3. (Top panels) Regression analyses in 15 human subjects show significant positive relationships between hepatic FA oxidative metabolism and indexes of insulin resistance. (Bottom panels) The visceral FA contribution to the liver appears dependent on the mass of the corresponding fat depot, and not on that of total body fat.

### 6.3.3 Effects of obesity on skeletal muscle and adipose tissue fatty acid metabolism (II)

Results from PET modelling showed that obese subjects were characterized by a decreased skeletal muscle FA esterification rate constant ( $k_5$ ) ( $p=0.002$ , Table 6.3.3.1) and an increased FAO (Figure 6.3.3.1 A,C), as compared to the control group. The esterification rate in SAT was markedly lower at the unit-of-tissue level, *i.e.*, nearly halved in obese subjects with respect to that of leaner controls (Figure 6.3.3.1 B), although the difference was compensated by an increased whole body fat mass (Figure 6.3.3.1 D). Systemic lipolysis did not differ significantly between the groups (control vs obese group,  $352\pm34$  vs  $291\pm39$   $\mu\text{mol}/\text{min}$ ), though if expressed per kg of fat mass, it was lower in obese than control subjects ( $9\pm2$  vs  $16\pm2$   $\mu\text{mol}/\text{min}/\text{kg}$  of fat mass,  $p<0.03$ ). In the whole study population, skeletal muscle esterification rate constant, FAO and SAT esterification rate were not only different by groups but also individually correlated with the degree of obesity, as a higher BMI was related to lower esterification parameters in both tissues ( $R=-0.79$ ,  $R=-0.66$ ) and higher skeletal muscle FAO ( $R=0.53$ ). The SAT esterification rate was associated with the fractional contribution of FA esterification and oxidation to the FA uptake in skeletal muscle ( $R=0.50$ ,  $R=-0.50$ ,  $p<0.05$ ); thus the higher the SAT esterification capacity, the lower was the FAO contribution to skeletal muscle FA uptake. Insulin and HOMA-IR were both negatively associated with the skeletal muscle FA esterification rate constant ( $R=-0.50$ ,  $p<0.05$ ) and positively with FAO ( $R=0.50$ ,  $p<0.03$ ). AIRI was positively associated with skeletal muscle FA uptake and FAO ( $R=0.60$ ,  $p<0.02$ ).

Table 6.3.3.1. [ $^{11}\text{C}$ ]-palmitate kinetics rate constants in the study groups  $^{\circ}$

	Control subjects	Obese subjects
<b>Skeletal Muscle</b>		
$K_1$ ( $\text{mL min}^{-1} \text{mL}^{-1}$ )	$0.051 \pm 0.010$	$0.085 \pm 0.014^*$
$k_2$ ( $\text{min}^{-1}$ )	$1.198 \pm 0.305$	$1.556 \pm 0.192$
$k_3$ ( $\text{min}^{-1}$ )	$0.204 \pm 0.045$	$0.230 \pm 0.033$
$k_4$ ( $\text{min}^{-1}$ )	$0.246 \pm 0.041$	$0.199 \pm 0.026$
$k_5$ ( $\text{min}^{-1}$ )	$0.292 \pm 0.019$	$0.164 \pm 0.016^{**}$
<b>Abdominal SAT</b>		
$K_1$ ( $\text{mL min}^{-1} \text{mL}^{-1}$ )	$0.014 \pm 0.003$	$0.016 \pm 0.002$
$k_2$ ( $\text{min}^{-1}$ )	$0.418 \pm 0.162$	$0.749 \pm 0.256$
$k_3$ ( $\text{min}^{-1}$ )	$0.221 \pm 0.050$	$0.167 \pm 0.034$
$k_4$ ( $\text{min}^{-1}$ )	$0.026 \pm 0.004$	$0.026 \pm 0.002$
<b>Abdominal VAT</b>		
$K_1$ ( $\text{mL min}^{-1} \text{mL}^{-1}$ )		$0.055 \pm 0.020$
$k_2$ ( $\text{min}^{-1}$ )		$1.000 \pm 0.363$
$k_3$ ( $\text{min}^{-1}$ )		$0.221 \pm 0.070$
$k_4$ ( $\text{min}^{-1}$ )		$0.039 \pm 0.008$

$^{\circ}$  SAT, Subcutaneous Adipose Tissue; VAT, Visceral Adipose Tissue. \*  $P < 0.05$ , \*\*  $P < 0.01$ .

## RESULTS

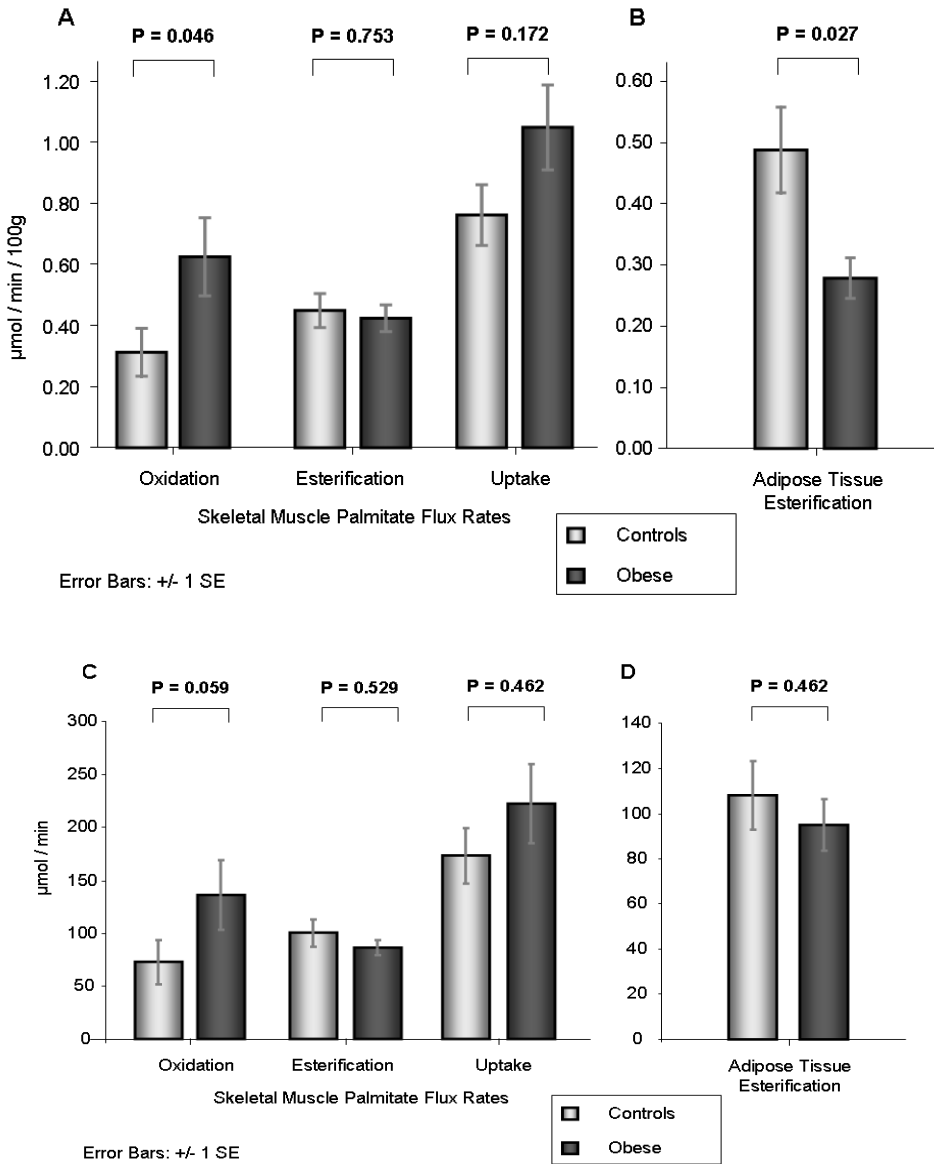


Figure 6.3.3.1. Comparison of skeletal muscle (A and C) and adipose tissue fatty acid (FA) flux rates (B and D) expressed as  $\mu\text{mol} \cdot \text{min}^{-1} \cdot 100 \text{ g tissue}^{-1}$  or accounting for the whole organ mass between obese and control groups. Figure shows elevated skeletal muscle FA oxidation at both tissue level (A) and whole body level (C), and defective adipose tissue esterification rates at tissue level in obese individuals (B).

**6.3.4 Effects of obesity on myocardial metabolism and function (III & unpublished data)**

In the nine subjects included in study III, the BMI correlated positively with the cardiac oxidation rate of plasma FFA ( $R=0.80$ ,  $p=0.01$ , Figure 6.3.4.1, A) and with LV work ( $R=0.95$ ,  $p=0.001$ , Figure 6.3.4.1, B). LV work was also positively associated with the plasma FFA oxidation rate ( $R=0.87$ ,  $p=0.002$ , Figure 6.3.4.2, A) but not with the oxidation rate from intracellular triglyceride stores (Figure 6.3.4.2, B).

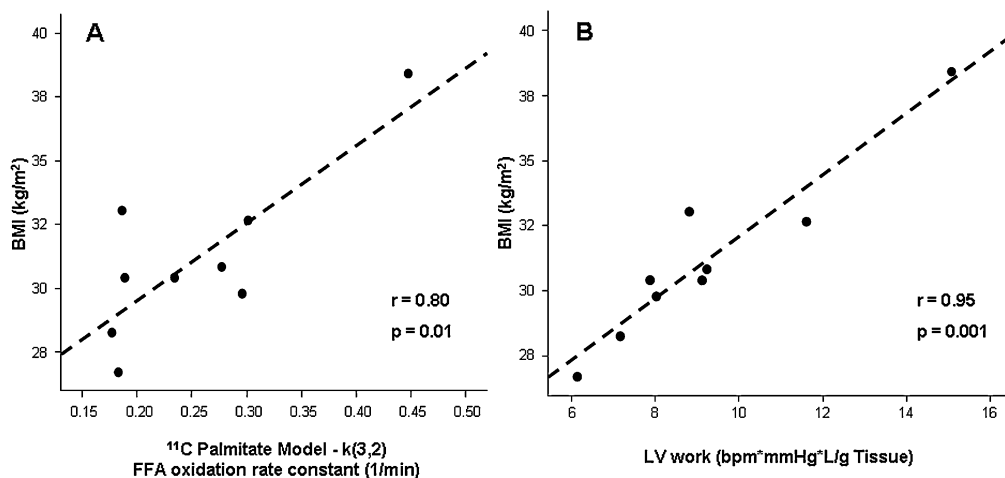


Figure 6.3.4.1. Positive relationships between BMI and (A) plasma fatty acid oxidation or (B) LV work.

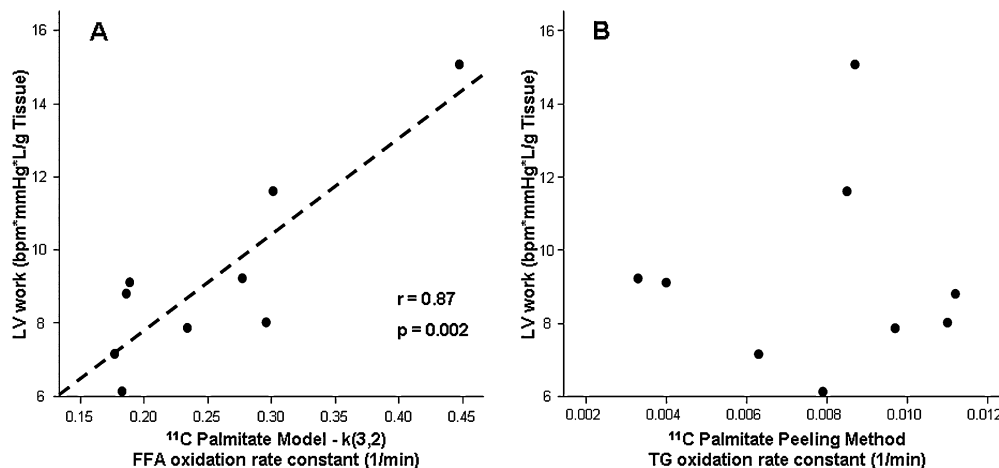


Figure 6.3.4.2. Relationships between LV work and (A) plasma fatty acid oxidation (positive) or (B) intracellular triglycerides oxidation (absent).

Plasma FFA oxidation rate constant was different between obese and lean subjects (the same group of study I,  $P < 0.01$ ) as shown in Figure 6.3.4.3.

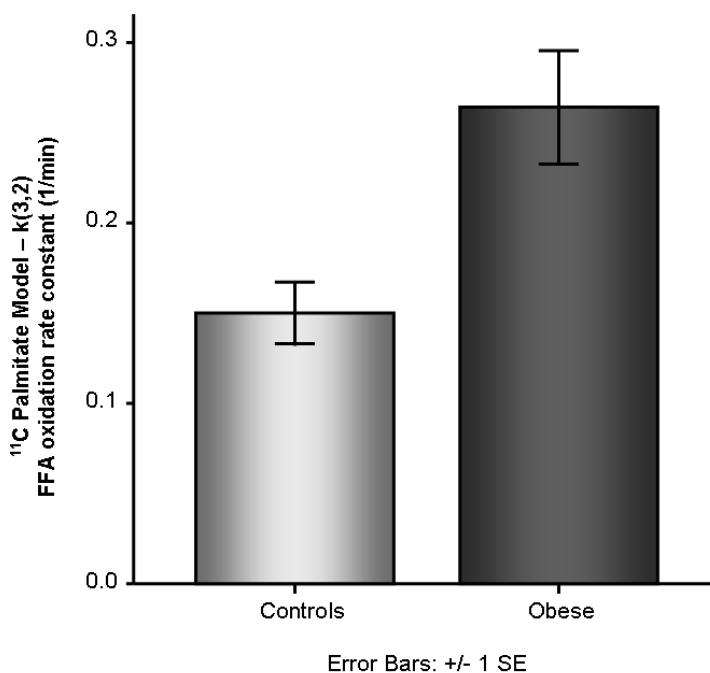


Figure 6.3.4.3. Plasma fatty acid oxidation rate constant is increased in obesity.

## 6.4 Effects of trimetazidine (II-III)

### 6.4.1 Effects of trimetazidine on metabolic and whole body variables (II)

All patients completed the study and their general characteristics before and after treatment are reported in Table 6.4.1.1. The fat mass distribution, insulin resistance indexes, blood metabolic profile, and adipokines were not affected by the treatment. There was a tendency to a decrease in  $\text{HbA}_{1c}$  and LDL cholesterol. Whole body substrate oxidation assessed by indirect calorimetry or by PET kinetics did not change after treatment as reported in Table 6.4.1.2.

### 6.4.2 Effects of trimetazidine on skeletal muscle and adipose tissue substrate metabolism (II)

Whole body and regional utilization rates of glucose and FA in skeletal muscle, subcutaneous and visceral adipose tissue, assessed by PET, are reported in Table 6.4.1.2 and in Figure 6.4.2.1 (A,B), and they did not change. The baseline comparison between visceral and subcutaneous adipose tissue FA uptake showed significantly greater values in the former (Figure 6.4.2.1 B). FA oxidation from indirect calorimetry

## RESULTS

Table 6.4.1.1. Effects of trimetazidine on anthropometric and metabolic variables <sup>o</sup>

	Baseline	After one month
Weight (kg)	89 ± 4	87 ± 3 <sup>^</sup>
BMI (kg m <sup>-2</sup> )	31 ± 1	31 ± 1 <sup>^</sup>
Fat mass (kg)	34 ± 2	33 ± 1 <sup>^</sup>
Fat-free mass (kg)	55 ± 3	54 ± 3 <sup>^</sup>
Visceral fat mass (kg)	1.7 ± 0.2	1.7 ± 0.2
Retroperitoneal fat mass (kg)	1.0 ± 0.1	0.9 ± 0.1
IMCL (% of water resonance)	0.5 ± 0.2	0.5 ± 0.2
EMCL (% of water resonance)	1.5 ± 0.7	2.2 ± 0.9 <sup>*</sup>
IMCL+EMCL (% of water resonance)	2.0 ± 0.8	2.8 ± 1.0 <sup>*</sup>
IMCL/EMCL (Ratio)	0.9 ± 0.7	0.4 ± 0.2
Adipose tissue IR index (AIRI)	39 ± 9	40 ± 8
HOMA-IR index	1.9 ± 0.4	2.0 ± 0.4
Fasting glucose (mmol L <sup>-1</sup> )	5.2 ± 0.1	5.4 ± 0.2
Fasting insulin (pmol L <sup>-1</sup> )	58 ± 10	57 ± 10
Fasting FFA (mmol L <sup>-1</sup> )	0.62 ± 0.05	0.68 ± 0.04
Glycosylated hemoglobin (HbA <sub>1c</sub> %)	5.6 ± 0.1	5.5 ± 0.1 <sup>^</sup>
Triglycerides (mmol L <sup>-1</sup> )	1.8 ± 0.3	2.0 ± 0.6
Cholesterol (mmol L <sup>-1</sup> )	5.6 ± 0.3	5.3 ± 0.3
HDL (mmol L <sup>-1</sup> )	1.5 ± 0.2	1.5 ± 0.2
LDL (mmol L <sup>-1</sup> )	3.3 ± 0.2	2.9 ± 0.2
Apelin-12 (pg mL <sup>-1</sup> )	340 ± 42	271 ± 26
Adiponectin (µg mL <sup>-1</sup> )	22 ± 3	21 ± 4
Resistin (ng mL <sup>-1</sup> )	13 ± 1	13 ± 1
PAI-1 total (ng mL <sup>-1</sup> )	55 ± 4	47 ± 3
IL-6 (pg mL <sup>-1</sup> )	5.8 ± 3.1	6.4 ± 3.1
IL-8 (pg mL <sup>-1</sup> )	5.9 ± 1.0	6.1 ± 1.0
Leptin (ng mL <sup>-1</sup> )	27 ± 9	32 ± 11
TNFα (pg mL <sup>-1</sup> )	5.8 ± 0.6	5.7 ± 0.7
MCP-1 (pg mL <sup>-1</sup> )	329 ± 31	365 ± 42
HGF (pg mL <sup>-1</sup> )	543 ± 98	535 ± 96

<sup>o</sup> IR = insulin resistance, HOMA = homeostasis model assessment. \* P<0.05, <sup>^</sup> P<0.08



## RESULTS

Table 6.4.1.2. Effects of trimetazidine on substrate utilization at the whole body level

<b>Indirect calorimetry</b>	<b>Baseline</b>	<b>After one month</b>
VCO <sub>2</sub> (ml min <sup>-1</sup> )	187 ± 9	176 ± 9
VO <sub>2</sub> (ml min <sup>-1</sup> )	223 ± 9	217 ± 10
RQ mean	0.84 ± 0.01	0.81 ± 0.02
Glucose oxidative disposal rate (g min <sup>-1</sup> )	0.109 ± 0.016	0.082 ± 0.017
Lipid oxidative disposal rate (g min <sup>-1</sup> )	0.043 ± 0.006	0.050 ± 0.007
Glucose non-oxidative disposal rate (g min <sup>-1</sup> )	0.063 ± 0.013	0.095 ± 0.026
Energy production rate (kcal min <sup>-1</sup> )	1.078 ± 0.046	1.042 ± 0.048
<b>PET tracer kinetics</b>		
<i>Whole body</i>		
Glucose disposal rate (μmol min <sup>-1</sup> )	958 ± 75	983 ± 85
FA disposal rate (μmol min <sup>-1</sup> )	293 ± 34	335 ± 44
<i>Whole body skeletal muscle</i>		
Glucose uptake rate (μmol min <sup>-1</sup> )	236 ± 36	266 ± 48
FA oxidation rate (μmol min <sup>-1</sup> )	144 ± 30	151 ± 28
FA esterification rate (μmol min <sup>-1</sup> )	88 ± 7	97 ± 12
FA uptake rate (μmol min <sup>-1</sup> )	232 ± 34	248 ± 36
<i>Whole body SAT</i>		
Glucose uptake rate (μmol min <sup>-1</sup> )	224 ± 22	260 ± 66
FA uptake rate (μmol min <sup>-1</sup> )	64 ± 10	66 ± 14
<i>Whole body VAT</i>		
Glucose uptake rate (μmol min <sup>-1</sup> )	18 ± 4	24 ± 4
FA uptake rate (μmol min <sup>-1</sup> )	15 ± 4	16 ± 4

measurements was positively correlated with skeletal muscle FAO as derived by PET, supporting the validity of the current methodology (R=0.8, p<0.05).

The only changes observed after treatment included an elevation in the esterification rate constant of FA (p=0.008) and a tendency toward an increment in the glucose phosphorylation rate constant (p=0.066) in skeletal muscle (Table 6.4.2.1). No significant changes were observed in the rate constants of SAT. Skeletal muscle EMCL-to-water and IMCL+EMCL-to-water ratios were significantly increased (Table 6.4.1.1), in the six patients with available measurements before and after treatment. Trimetazidine did not change significantly IMCL-to-water and IMCL-to-EMCL ratios, but positive correlations were found between changes in these variables and those in

RESULTS

plasma triglycerides ( $R=0.8$ ,  $p=0.035$ ;  $R=0.9$ ,  $p=0.011$ , respectively). The Cr/water ratio was associated with the PET-derived skeletal muscle oxidative pool (positively,  $R=0.8$ ,  $p<0.05$ ) and with the esterification rate constant (negatively,  $R=-0.8$ ,  $p<0.05$ ).

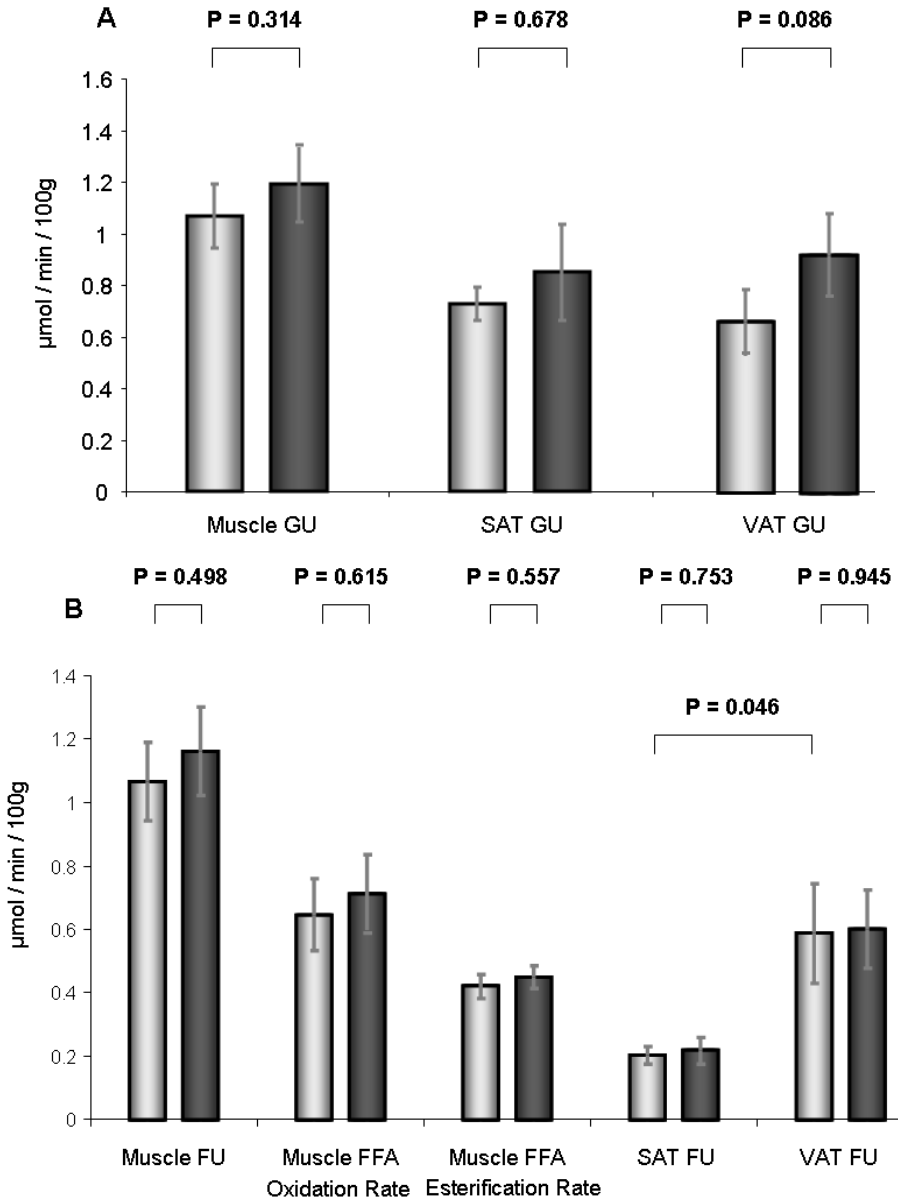


Figure 6.4.2.1. (A) Glucose uptake (GU) rates expressed as  $\mu\text{mol}\cdot\text{min}^{-1}\cdot 100\text{ g}^{-1}$  in the skeletal muscle, subcutaneous adipose tissue (SAT), and visceral adipose tissue (VAT) at baseline (light bars) and after treatment (dark bars). (B) FA metabolic rates expressed as  $\mu\text{mol}\cdot\text{min}^{-1}\cdot 100\text{ g}^{-1}$  in skeletal muscle, SAT, and VAT at baseline (light bars) and after treatment (dark bars). Notably, VAT FA uptake (FU) is significantly higher than SAT FU.

RESULTS

Table 6.4.2.1. [<sup>11</sup>C]-palmitate and [<sup>18</sup>F]-FDG kinetics rate constants before and after treatment °

	Baseline	After one month
<b>Skeletal Muscle - [<sup>11</sup>C]-palmitate</b>		
K <sub>1</sub> (mL min <sup>-1</sup> mL <sup>-1</sup> )	0.083 ± 0.012	0.094 ± 0.017
k <sub>2</sub> (min <sup>-1</sup> )	1.547 ± 0.170	2.460 ± 0.365
k <sub>3</sub> (min <sup>-1</sup> )	0.261 ± 0.042	0.371 ± 0.083
k <sub>4</sub> (min <sup>-1</sup> )	0.218 ± 0.030	0.280 ± 0.066
k <sub>5</sub> (min <sup>-1</sup> )	0.172 ± 0.017	0.230 ± 0.024 **
<b>Skeletal Muscle - [<sup>18</sup>F]-FDG</b>		
K <sub>1</sub> (mL min <sup>-1</sup> mL <sup>-1</sup> )	0.074 ± 0.011	0.074 ± 0.014
k <sub>2</sub> (min <sup>-1</sup> )	0.446 ± 0.064	0.484 ± 0.058
k <sub>3</sub> (min <sup>-1</sup> )	0.017 ± 0.002	0.02 ± 0.002 ^
<b>Abdominal SAT - [<sup>11</sup>C]-palmitate</b>		
K <sub>1</sub> (mL min <sup>-1</sup> mL <sup>-1</sup> )	0.015 ± 0.002	0.017 ± 0.004
k <sub>2</sub> (min <sup>-1</sup> )	0.683 ± 0.235	1.126 ± 0.393
k <sub>3</sub> (min <sup>-1</sup> )	0.112 ± 0.040	0.191 ± 0.029
k <sub>4</sub> (min <sup>-1</sup> )	0.024 ± 0.004	0.034 ± 0.007
<b>Abdominal SAT - [<sup>18</sup>F]-FDG</b>		
K <sub>1</sub> (mL min <sup>-1</sup> mL <sup>-1</sup> )	0.026 ± 0.005	0.062 ± 0.041
k <sub>2</sub> (min <sup>-1</sup> )	0.287 ± 0.041	0.403 ± 0.114
k <sub>3</sub> (min <sup>-1</sup> )	0.017 ± 0.002	0.018 ± 0.002
<b>Abdominal VAT - [<sup>11</sup>C]-palmitate</b>		
K <sub>1</sub> (mL min <sup>-1</sup> mL <sup>-1</sup> )	0.055 ± 0.020	0.075 ± 0.023
k <sub>2</sub> (min <sup>-1</sup> )	1.003 ± 0.363	1.304 ± 0.423
k <sub>3</sub> (min <sup>-1</sup> )	0.221 ± 0.070	0.152 ± 0.017
k <sub>4</sub> (min <sup>-1</sup> )	0.039 ± 0.008	0.029 ± 0.004
<b>Abdominal VAT - [<sup>18</sup>F]-FDG</b>		
K <sub>1</sub> (mL min <sup>-1</sup> mL <sup>-1</sup> )	0.071 ± 0.009	0.076 ± 0.016
k <sub>2</sub> (min <sup>-1</sup> )	0.485 ± 0.040	0.546 ± 0.059
k <sub>3</sub> (min <sup>-1</sup> )	0.009 ± 0.001	0.013 ± 0.002 ^

° SAT, Subcutaneous Adipose Tissue; VAT, Visceral Adipose Tissue; \*\* P < 0.01, ^ 0.06.

### **6.4.2 Effects of trimetazidine on myocardial metabolism and function efficiency (III)**

Ejection fraction and stroke volume increased slightly, though significantly, after the treatment ( $p=0.01$ ) (Table 6.4.2.1), and the end systolic, but not end diastolic volume was decreased ( $p=0.028$ ,  $p=0.123$ , respectively). The other MR parameters did not change. Proton MRS data showed that the cardiac creatine-to-water ratio was significantly decreased after the treatment period ( $p<0.03$ ), whereas myocardial triglyceride content was unchanged (Table 6.4.2.1).

The measured parameters of myocardial substrate metabolism are summarized in Table 6.4.2.1. MGU and MFU did not differ from baseline to end of treatment. The rate of oxidation of plasma-derived FAs and the esterification of FAs into triglycerides were not affected by TMZ. However, the oxidation of FAs derived from intracellular stores and, subsequently, the total myocardial FA oxidation were decreased by 40% and 57%, respectively. The relative contribution of plasma and intracellular FAs to myocardial oxidation was shifted in favour of the former, from 41% to 54% and from 59% to 46%, respectively ( $p<0.04$ ) (Figure 6.4.2.1). Total FFA oxidation was measured by two different methods (bi-exponential fitting and compartmental modelling); the values were significantly correlated ( $R=0.71$ ,  $p=0.03$ ).

The comparison between LV forward work and the energy production from substrate oxidation at baseline and after treatment is shown in Figure 6.4.2.2. After one month of treatment, the two variables levelled off, *i.e.*, the LV work did not change significantly, but the overall work potentially deriving from substrate use was decreased, mostly due to the reduced oxidation of lipid stores.

## RESULTS

Table 6.4.2.1. Left Ventricle Structure, Function and Metabolism before and after treatment °

	Baseline	After Treatment	p
<b>MRI Measurements and Indexes</b>			
Ejection Fraction, %	66.0 ± 2.0	69.7 ± 1.7	<b>0.012</b>
Stroke Volume, ml	98.1 ± 4.2	106.5 ± 3.7	<b>0.012</b>
Cardiac Output, L/min	6.46 ± 0.30	6.60 ± 0.31	0.310
End Diastolic Volume, mL	150 ± 9	154 ± 8	0.123
End Systolic Volume, mL	52 ± 6	47 ± 5	<b>0.028</b>
Left Ventricle Mass, g	95 ± 9	95 ± 9	0.575
Peripheral Vascular Resistance, mmHg*min/L	18.26 ± 1.10	17.30 ± 1.22	0.401
Left Ventricle Work, bpm*mmHg*L	655 ± 48	685 ± 47	0.401
<b><sup>1</sup>H-MRS Measurements</b>			
Heart Lipid Content, %	0.80 ± 0.24	0.70 ± 0.18	0.889
Creatine/water ratio *10 <sup>3</sup>	1.27 ± 0.26	0.82 ± 0.24	<b>0.025</b>
<b>PET Metabolism</b>			
MGU, μmol/(min*g)	0.035 ± 0.015	0.046 ± 0.037	0.401
MFU, μmol/(min*g)	0.11 ± 0.01	0.11 ± 0.01	0.327
Plasma FAO Rate, μmol/(min*g)	0.095 ± 0.009	0.096 ± 0.009	0.575
Plasma FFA Esterification Rate, μmol/(min*g)	0.011 ± 0.002	0.012 ± 0.002	0.779
Intracellular FAO Rate, μmol/(min*g)	0.24 ± 0.08	0.10 ± 0.02	<b>0.036</b>
Intracellular FAO Rate Coefficient (1/min)	0.008 ± 0.001	0.005 ± 0.001	<b>0.025</b>
LV Total FAO Rate, μmol/min	32.7 ± 8.1	19.7 ± 4.0	<b>0.05</b>

° MGU, indicates Myocardial Glucose Uptake Rate; MFU, Myocardial FFA Uptake Rate; FFA, Free Fatty Acids; FAO, Fatty Acid Oxidation; n=8, Values are mean ± SEM. p value (Wilcoxon Paired T test)

## RESULTS

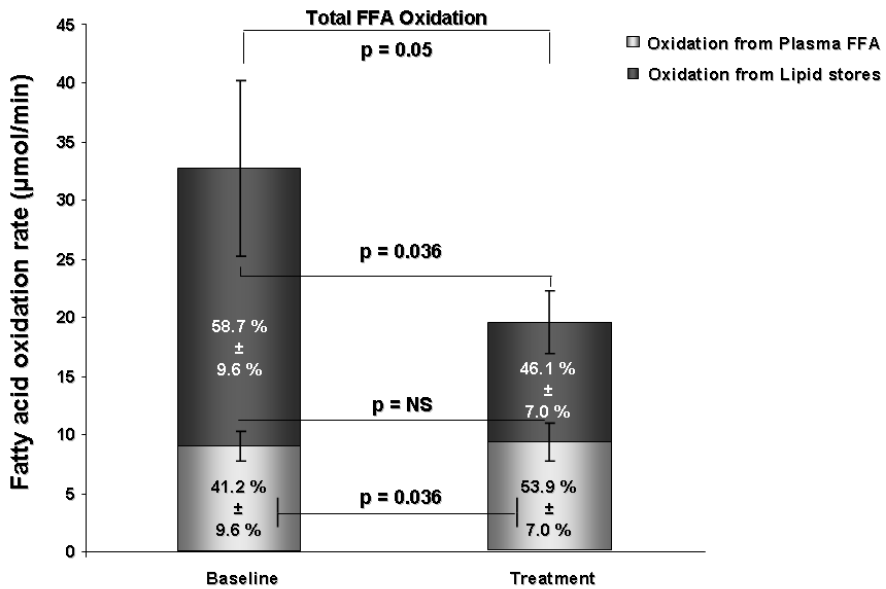


Figure 6.4.2.1. Myocardial plasma FFA oxidation (light bars) and intra-cardiac lipid oxidation (dark bars), at baseline and after treatment, showing significant changes in total and triglyceride-derived fatty acid oxidation.

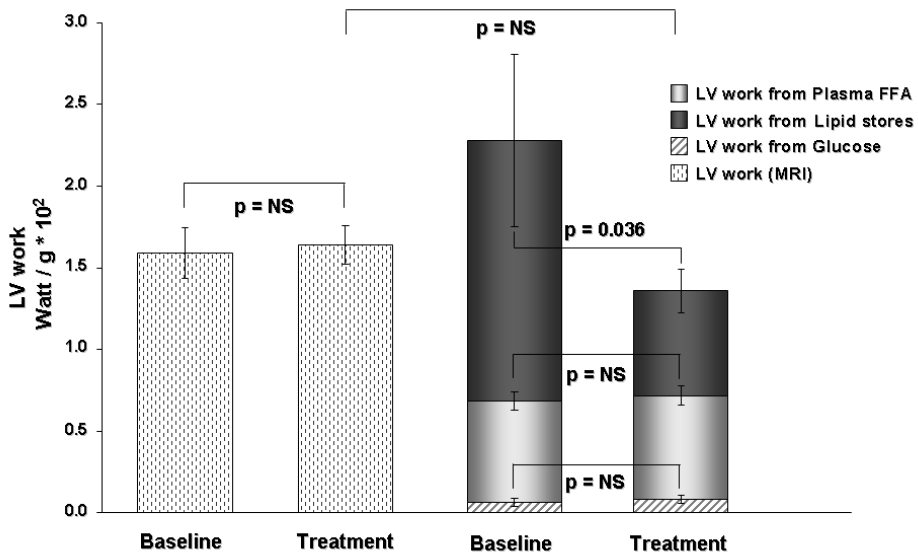


Figure 6.4.2.2. Left ventricular work as assessed by MRI, and maximum work attainable from the measured substrate utilization rates, namely, glucose uptake, plasma FFA oxidation and triglyceride FA oxidation rates. The graph demonstrates that baseline substrate uptake tended to exceed the work performed by the organ, whereas the two processes achieved tighter coupling after treatment.

## 6.5 Association of pericardial fat and hyperaemic myocardial blood flow in subjects with and without CAD (IV)

Subject characteristics of the whole cohort and of the subgroups are reported in Table 6.5.1.

Table 6.5.1. Subject characteristics (IV) °

Characteristics†	All subjects (30%-70% Pretest Likelihood of CAD)	Those Without CAD (n=22)	Those With Nonobstructive CAD (n=45)	Those With Obstructive CAD (n=40) ‡
Male:female ratio	64:43	6:16	24:21	34:6§¶
Age, mean ±SEM, y	63±1	62±2	62±1	65±1
BMI, mean ±SEM, Kg/m <sup>2</sup>	26.8±0.4	25.6±0.8	26.5±0.6	27.9±0.6
<b>Risk factors for CAD</b>				
Family history (n=103, 21 vs. 43 vs. 39)	45.6	57.1	41.9	43.6
Diabetes mellitus (n=106, 22 vs. 44 vs. 40)	14.2	0	11.4	25.0¶
IGT (n=103, 22 vs. 42 vs. 39)	8.7	9.1	4.8	12.8
Hypertension	41.1	31.8	35.6	52.5
Hypercholesterolemia (n=101, 20 vs. 43 vs. 38)	52.5	40.0	53.5	57.9
Smoker/ex-smoker (n=106, 22 vs. 45 vs. 39)	25.5/1.9	18.2/0	22.2/4.4	33.3/0
<b>Medications</b>				
β-blockers	59.8	63.6	44.4	75.0§
Aspirin	72.9	63.6	64.4	87.5§¶
ACE inhibitors (n=106, 22 vs. 44 vs. 40)	25.5	18.2	20.5	35.0
Statins	51.4	27.3	40.0	77.5§¶

° ACE indicates angiotensin-converting enzyme; IGT, impaired glucose tolerance.

\*Data are given as percentage of positive of each group unless otherwise indicated.

†Missing values and number of subjects are specified between parentheses.

‡The statistical tests for group comparison of nominal variables were the  $\chi^2$  and the Fisher exact tests; and for continuous variables, ANOVA.

§P<0.05 for nonobstructive CAD vs obstructive CAD.

¶P<0.05 for no CAD vs obstructive CAD

### 6.5.1 IPF and EPF volumes

Measurements of IPF and EPF volumes were performed in all patients (n=107), resulting in 110±4 cm<sup>3</sup> (95%CI 101-119) and 175±9 cm<sup>3</sup> (95%CI 158-192), respectively. IPF and EPF were correlated with each other (R=0.71, P<0.0001) and they were smaller in women than men (P=0.005 and P<0.0001, respectively).

### 6.5.2 IPF and EPF in relation to CAD and CAC score

IPF and EPF were higher in patients with CAD (n=85) than in subjects without CAD (n = 22), as assessed by CT (p<0.001). When CAD subjects were subdivided into a non-obstructive CAD (n=45) and an obstructive CAD group (n=40), EPF was

increased regardless of the degree of stenoses, while IPF was specifically increased in subjects with obstructive stenoses as compared with subjects without or with non-obstructive stenoses, as shown in Figure 6.5.2.1 (A,B). Figure 6.5.2.2 shows IPF and EPF volumes separately for CAD disease and sex. When obstructive CAD patients were subgrouped for the number of vessels presenting critical stenoses, both EPF and IPF showed no significant differences among groups as shown in Figure 6.5.2.1 (C,D).

Both IPF and EPF positively correlated with the Agatston CAC scores ( $R=0.25$ ,  $R=0.26$ ,  $P<0.02$ ); however, when accounting for age and sex, these associations lost then significance ( $R=0.17$ ,  $P=0.8$ , and  $R=0.11$ ,  $P=0.27$ , respectively).

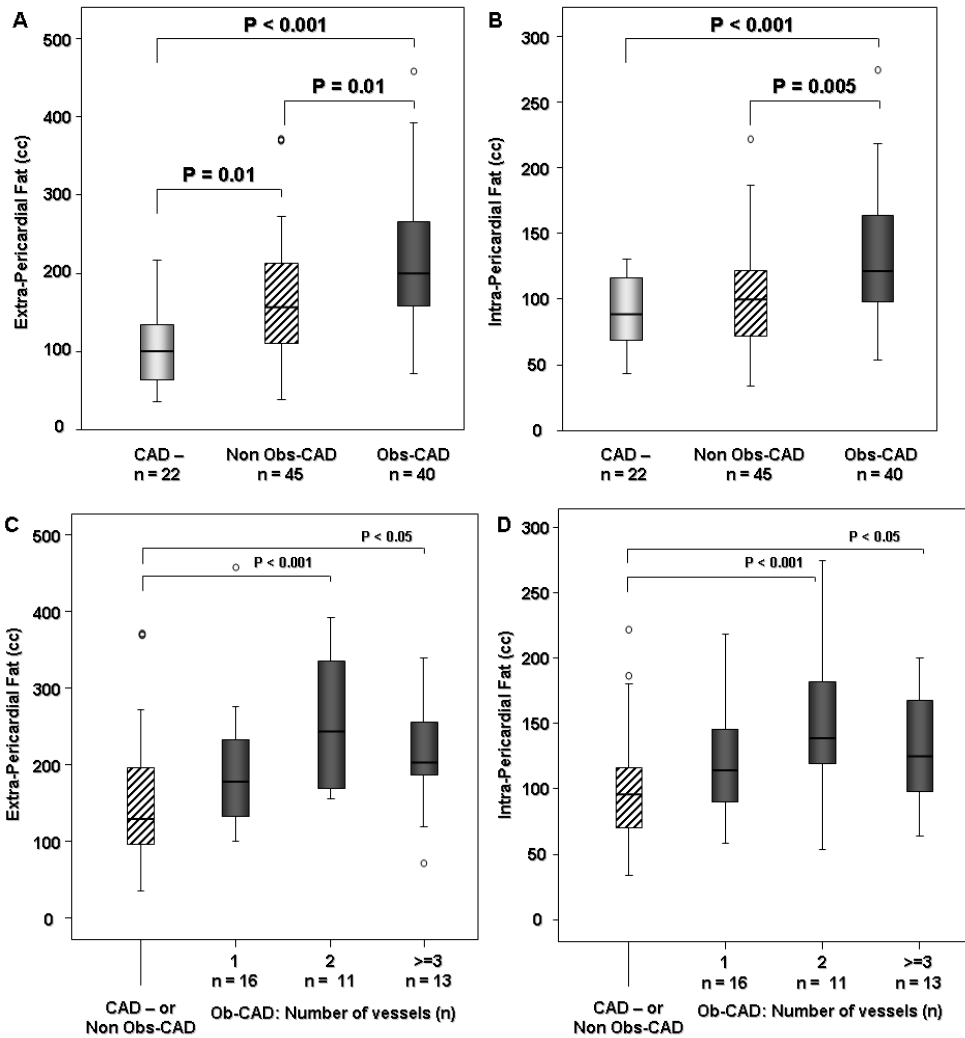


Figure 6.5.2.1. (A and B) EPF and IPF levels are both increased with CAD; IPF is specifically increased in obstructive CAD, whereas EPF is increased regardless of the functional impairment of stenoses. (C and D) There is no significant trend between fat depots and the increasing number of diseased vessels.



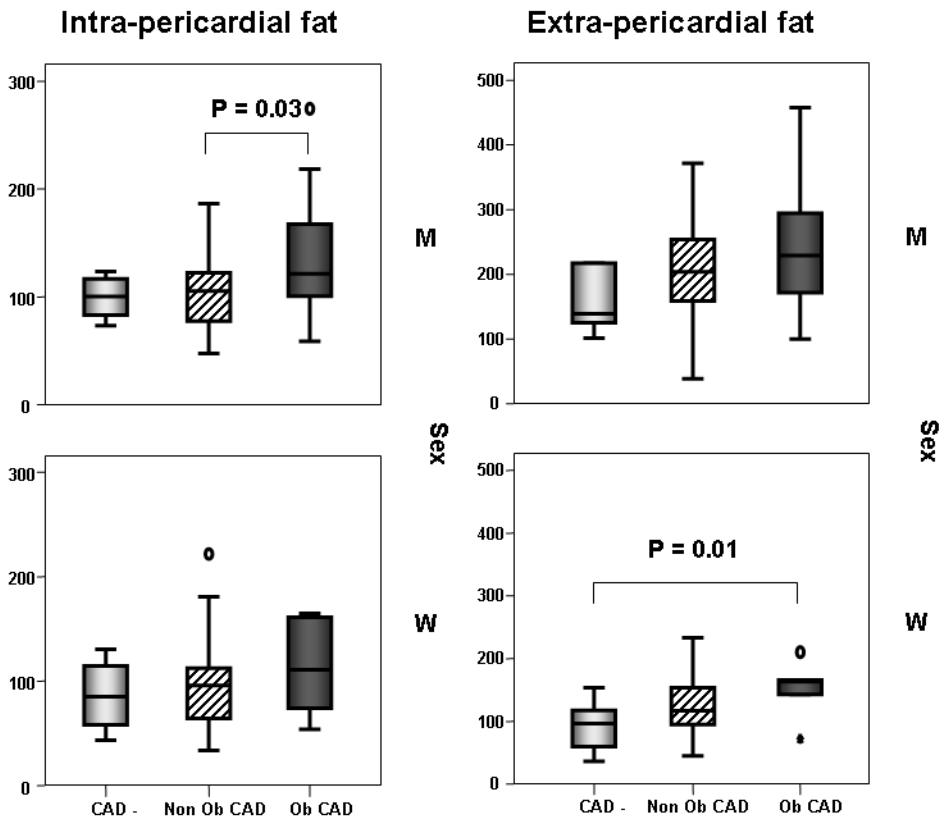


Figure 6.5.2.2. EPF and IPF levels divided according to sex. In men, IPF is specifically increased in obstructive CAD compared to subjects with non obstructive CAD, whereas in women, EPF is increased compared to subjects without CAD.

### 6.5.3 IPF and EPF in relation with MBF

Both IPF and EPF were negatively associated with CFR\* ( $R=-0.40$ ,  $R=-0.39$   $P<0.0005$ ), stress MBF\* (Figure 6.5.3.1, vs IPF) ( $R=-0.44$ ,  $P<0.0005$ , vs EPF), and with regional CFR and stress MBF (LAD, LCX, RCA, all  $P<0.0005$ ).

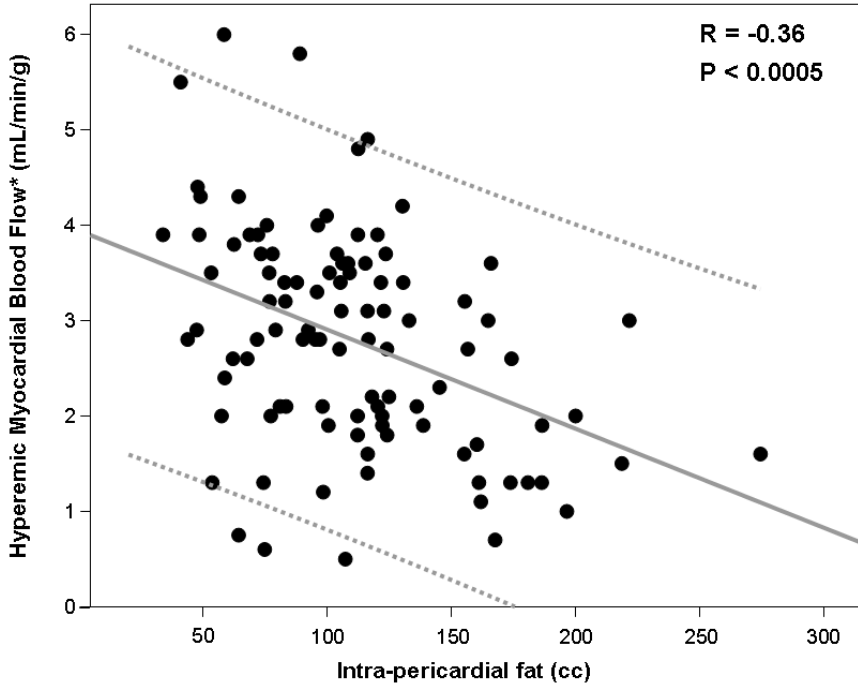


Figure 6.5.3.1. Negative linear association between the lowest (\*) myocardial blood flow and intra-pericardial fat volume.

The relationship between CAD and myocardial perfusion and the role of the fat depots were further explored by stratifying obstructive CAD patients according to a hyperemic MBF\*  $>$  or  $\leq$  1.75 mL/min/g, according to the median of the group. Four patients with microvascular disease (no CAD but abnormally reduced perfusion) were excluded from the comparison. IPF was significantly increased in patients with obstructive CAD and stress MBF  $\leq$  1.75 mL/min/g as compared to patients with obstructive CAD but less severe perfusion deficit, or without significant CAD. In addition, no significant difference was found between the latter two groups with similarly normal MBF (Figure 6.5.3.2 A). Instead, EPF was not significantly different between the above-mentioned obstructive CAD sub-groups (Figure 6.5.3.2 B).

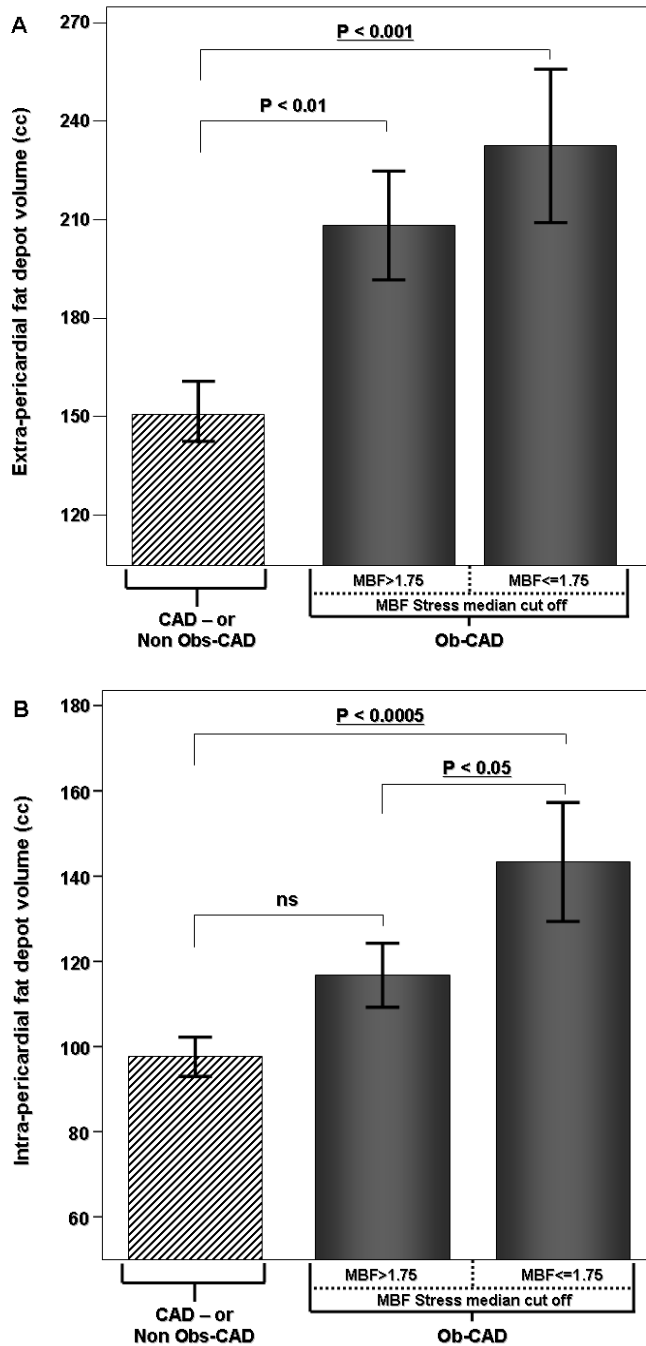


Figure 6.5.3.2. A, intra-pericardial fat is significantly increased in patients with obstructive CAD and reduced perfusion, but there is no significant difference in patients with or without CAD and preserved perfusion. B, extra-pericardial fat was significantly increased in obstructive

## RESULTS

CAD regardless of the impaired perfusion. Four patients with microvascular disease (no CAD but abnormally reduced perfusion) were excluded from this comparison.

Multiple regression analyses are summarized in Table 6.5.3.1, showing that hyperemic perfusion was predicted independently by IPF volume, but less or not significantly by EPF volume, and that male gender was a strong negative predictor of stress MBF and CFR.

Regression models accounting for age, BMI and HDL were evaluated. HDL levels were included in the model because of their correlation with stress MBF\* (R=0.34, P=0.001), stress LAD MBF (R=0.32, P=0.001) and CFR\* (R=0.20, P=0.05). However, none of these three factors (age, BMI and HDL) was significant in the prediction of the dependent variables, when evaluated together with sex and fat depots. Notably, only gender and IPF remained significant in predicting hyperemic perfusion. Multiple regression models of regional hyperemic blood perfusion values showed a tendency of IPF to explain better the LAD variability, maybe reflecting the larger proportion of the population with the lowest hyperemic MBF in this region (51%) as compared to LCX (29%) and RCA (20%).

Table 6.5.3.1. Stress perfusion and coronary reserve flow (CFR) predicted by sex and fat depots <sup>o</sup>

Independent Variables (Multiple Regression Models)	Dependent Variables									
	Stress Perfusion*		CFR*		Stress Perfusion (LAD)		Stress Perfusion (LCX)		Stress Perfusion (RCA)	
	B	P	B	P	B	P	B	P	B	P
Sex (Male =1, Female = 2)	0.48	<0.001	0.21	<0.001	0.51	<0.001	0.4	<0.001	0.49	<0.001
Intra-pericardial fat volume, cm <sup>3</sup>	-0.23	0.008	-0.33	0.019	-0.21	0.019	-0.22	0.015	-0.18	0.037
R <sup>2</sup> value	0.34		0.19		0.37		0.26		0.32	
Sex (Male =1, Female = 2)	0.43	<0.001	0.11	<0.001	0.48	<0.001	0.33	0.002	0.45	<0.001
Extra-pericardial fat volume, cm <sup>3</sup>	-0.20	0.052	-0.34	0.1	-0.16	0.1	-0.24	0.022	-0.16	0.1
R <sup>2</sup> value	0.32		0.17		0.35		0.26		0.30	
Sex (Male =1, Female = 2)	0.47	<0.001	0.15	<0.001	0.52	<0.001	0.354	0.001	0.48	<0.001
Extra-pericardial fat volume, cm <sup>3</sup>	-0.02	0.9	-0.14	0.8	0.03	0.8	-0.12	0.4	-0.02	0.9
Intra-pericardial fat volume, cm <sup>3</sup>	-0.21	0.076	-0.25	0.049	-0.23	0.049	-0.15	0.2	-0.17	0.2
R <sup>2</sup> value	0.34		0.19		0.37		0.27		0.32	

<sup>o</sup> LCX indicates left circumflex artery; RCA indicates right coronary artery.

\*Lowest regional value

### 6.5.4 Comparison of MBF predictors

Progressive linear regression models were used to compare the contribution of CAC score, IPF and EPF in explaining the variability in the hyperemic MBF values. Gender was always taken into account, given its consistent relationship with MBF and fat volumes. The strongest predictors were (in order of importance) gender, CAC score and IPF (Table 6.5.4.1). The models including all three variables explained more variability ( $R^2$ ) than each independent variable alone (Table 6.5.4.1). Since diabetes, dyslipidemia, and cardiovascular or metabolic medications may affect coronary vasodilation and endothelial function, the predictive effect of the main co-morbidities (hypercholesterolemia, diabetes) and medications was evaluated, together with age, BMI, sex, IPF (or EPF) on MBF (Table 6.5.4.2), showing that IPF, but not EPF was still significantly associated with LAD hyperemic flow and CRF regardless of all confounders.

Table 6.5.4.1. Multiple linear regression predicting LAD stress myocardial blood flow and lowest regional stress myocardial blood flow <sup>o</sup>

No.	Model	Unstandardized β Coefficient	Standardized β Coefficient	P Value	95% CI for β	
					Lower Bound	Upper Bound
<b>LAD stress MBF value</b>						
1	Sex (male=1 and female=2)	1.196	0.497	<0.001	0.808	1.584
	CAC score (Agatston)	-0.001	-0.272	0.001	-0.001	0.000
2	Sex (male=1 and female=2)	1.097	0.456	<0.001	0.705	1.489
	CAC score (Agatston)	0.000	-0.244	0.003	-0.001	0.000
	IPF, cm <sup>3</sup>	-0.005	-0.174	0.034	-0.009	0.000
<b>Lowest regional stress MBF value</b>						
1	Sex (male=1 and female=2)	1.065	0.455	<0.001	0.687	1.443
	CAC score (Agatston)	-0.001	-0.326	<0.001	-0.001	0.000
2	Sex (male=1 and female=2)	0.967	0.413	<0.001	0.585	1.348
	CAC score (Agatston)	-0.001	-0.297	<0.001	-0.001	0.000
	IPF, cm <sup>3</sup>	-0.005	-0.177	0.031	-0.009	0.000

<sup>o</sup> MBF, Myocardial Blood Flow. Model summary for LAD stress MBF and lowest regional stress MBF value: 1,  $R^2=0.40$ ; and 2,  $R^2=0.43$ , for both.

RESULTS

Table 6.5.4.2. Multiple regression models accounting for co-morbidities and medications. Intra-pericardial fat is an independent predictor of stress MBF (top). Extra-pericardial fat is not an independent predictor of stress MBF (bottom) °

Model predicting Stress Perfusion (LAD)	Unstandardized Coefficients	Standardized Coefficients	Sig.
	(B)	(β)	
Age	0.001	0.006	0.946
<b>Sex</b>	<b>1.215</b>	<b>0.530</b>	<b>&lt;0.0001</b>
BMI	0.030	0.110	0.287
Diabetes	-0.058	-0.018	0.841
<b>Hypercholesterolemia</b>	<b>-0.447</b>	<b>-0.198</b>	<b>0.021</b>
<b>ACE inhibitors</b>	<b>-0.463</b>	<b>-0.180</b>	<b>&lt;0.05</b>
Beta-blockers	-0.390	-0.168	0.065
Ca-antagonists	-0.361	-0.102	0.215
Anticoagulants	-0.129	-0.012	0.887
Aspirin	-0.118	-0.045	0.619
NSAID	-0.624	-0.112	0.181
Lipid lowering drugs	0.019	0.008	0.928
<b>Intra-pericardial fat</b>	<b>-0.006</b>	<b>-0.225</b>	<b>0.026</b>

R<sup>2</sup>=0.51

Model predicting Stress Perfusion (LAD)	Unstandardized Coefficients	Standardized Coefficients	Sig.
	(B)	(β)	
Age	-0.002	-0.013	0.866
<b>Sex</b>	<b>1.170</b>	<b>0.510</b>	<b>&lt;0.001</b>
BMI	0.015	-0.053	0.636
Diabetes	-0.073	-0.022	0.809
<b>Hypercholesterolemia</b>	<b>-0.472</b>	<b>-0.209</b>	<b>0.017</b>
<b>ACE inhibitors</b>	<b>-0.494</b>	<b>-0.192</b>	<b>0.041</b>
Beta-blockers	-0.366	-0.158	0.090
Ca-antagonists	-0.357	-0.101	0.232
Anticoagulants	-0.098	-0.009	0.917
Aspirin	-0.133	-0.051	0.585
NSAID	-0.655	-0.118	0.180
Lipid lowering drugs	0.019	0.008	0.928
Extra-pericardial fat	-0.002	-0.122	0.354

R<sup>2</sup>=0.48

° n = 104 (both).

## 7 DISCUSSION

### 7.1 Validation study for liver fatty acid metabolism assessment in animals and humans (I)

To the best of this author's knowledge, there are no previous studies addressing in a systematic manner the fatty acids metabolic pathways of the liver, by using a non-invasive method;  $^{11}\text{C}$ -palmitate PET imaging in combination with compartmental kinetic modelling has been used to quantify the fate of fatty acids in the liver, distinguishing processes such as FAO, FA esterification and TG release. In humans, liver metabolism is generally extrapolated from splanchnic balance studies, which are invasive, and cannot distinguish between the relative contributions of gut, visceral adipose tissue, and liver. This limitation is especially important in the metabolism of FA relative to other substrates, since simultaneous FA uptake and release occur continuously and to variable extents in these organs. The present methodology offers the important advantages of estimating the intracellular fate of fatty acids between the oxidative and non-oxidative pathways, and the contribution of visceral fat to FA flowing to the liver.

In the validation study, it has been chosen to use a limited number of animals, which were studied in depth by parallel PET-imaging and gold standard methodology, and parameter estimation by compartmental modeling of liver  $^{11}\text{C}$ -palmitate kinetics was compared with conventional flux assessments obtained during fasting and insulin stimulation. The swine model was chosen for its organ size, permitting a) the use of a human scanner, thus allowing test image quality and analysis tools for immediate exportation into humans, and b) easier access to the significant blood sampling required in this study. FA esterification was significant in the pigs, despite the notion that these animals are not prone to develop steatosis. An extensive protocol was used to attain simultaneous measurements from the two perfusing and one draining liver vessels, together with organ blood flow and volume, in order to compute steady-state influx-efflux differences. The total uptake of free and bound fatty acids and the release of labelled  $^{11}\text{C}$ -TG or  $^{11}\text{C}$ -oxidative products were compared with the corresponding estimates by PET. Because liver oxidative metabolism includes generation of ketones by partial FA oxidation, and recycling of  $\text{CO}_2$  *via* production and release of urea and glucose, it was assumed that the organ arterial-portal *vs* venous difference of  $^{11}\text{C}$ -water-soluble compounds and of  $^{11}\text{CO}_2$  encompasses all the above products and represents total hepatic fatty acid oxidation, as previously done by others (Sanyal *et al.*, 2001). Furthermore, the exchange of oxygen and  $\text{CO}_2$  across the liver was measured to calculate lipid oxidation rates by use of indirect calorimetry equations. The quality of PET images indicated that the liver is fatty-acid avid, as confirmed by the numerical results, showing that approximately 40% of FA flowing to the liver is extracted by the organ. Modelling parameters were robustly identifiable, as reflected by their coefficients of variation and lack of autocorrelation. The directly measured and the PET-derived variables showed similar and correlated results, and the imaging

methodology showed an elevated sensitivity in discriminating group differences with sufficient statistical power despite the limited sample size.

The liver receives a dual blood supply from the hepatic artery and portal vein, and the latter is not directly accessible in humans. It was possible to extract the portal time activity curve from the images in the subjects who were studied with PET/CT. However, this approach may be impractical if anatomical CT images are lacking in human PET scanners, or if the lower portion of the liver is not within the imaging field of view, and it remains far from the resolution capabilities of small animal tomographs, which are increasingly used in metabolic studies. The bias associated with the alternative use of the single arterial input function in the modelling of liver  $^{11}\text{C}$ -palmitate data was first explored, and showed that this method leads to an underestimation of hepatic substrate rates, affecting more severely the earlier (uptake, oxidation) than the later (esterification, release) intracellular processes. The metabolic pathways maintained some degree of reciprocal proportionality, suggesting that the method may still be acceptable for group comparisons. To obtain more accurate absolute estimates, the possibility to derive kinetic parameters describing the dual from the arterial input function was evaluated, by using a compartment model that accounts for the delay and dispersion of arterial tracer concentrations in the passage of blood through the visceral compartments upstream to the portal vein. The results obtained in this study demonstrate an optimal correspondence of the measured and the estimated (either with individual or group-averaged rate constants) dual input functions. Within the range of intra-abdominal fat mass values available in this study, covering four-fold differences, the estimated parameters did not correlate with the amount of fat. However, it cannot be ruled out that the accuracy of the model for estimating the dual input may be affected by the amount of visceral fat in more severely obese individuals, who may have higher uptake and release of  $^{11}\text{C}$ -palmitate by visceral adipose tissue.

### ***7.1.1 Effect of insulin on healthy liver fatty acid metabolism (I)***

The current dataset documents that insulin exerts a direct (intrinsic) effect on TGFA output from the liver, thus promoting lipid storage. This finding identifies the pathway of insulin action hypothesized in previous human studies, in which the acute inhibition of triglyceride-rich lipoprotein production by insulin implicated an FA-independent hepatic mechanism (Malmstrom *et al.*, 1998; Lewis *et al.*, 1995). An *in vitro* study showed that the addition of insulin to rat-cultured hepatocytes reduced the rate of triglyceride secretion; this was the only process in triglyceride metabolism that was affected by the hormone in a direct fashion (Durrington *et al.*, 1982). An *in vivo* catheterization study, contextual to invasive surgery (cholecystectomy), evaluated the acute effect of insulin injection into the portal vein on hepatic production of VLDL-TG. The authors found that the investigated process, as well as the hepatic FFA uptake rate, was inhibited in their stimulation conditions in healthy humans (Vogelberg *et al.*, 1980). The present study extends the previous findings in several aspects. The modulation of insulin has been evaluated *in vivo*, in a more controlled physiological insulin-stimulated steady-state condition, by euglycemic hyperinsulinemic clamp. The



present study allowed the evaluation of insulin effects at both intrinsic (liver metabolic rate constants, independent of FFA levels) and extrinsic (liver metabolic FA flux rates, dependent on FFA levels) response. In addition to the previous *in vivo* study, both arterial and vein liver inputs were considered and FFA oxidation and esterification processes were evaluated together with the previously investigated uptake and TG release rates. At the extrinsic level (modelling rate constants), this study extends *in vivo* the notion that insulin exerts a direct inhibitory effect on hepatic TGFA release and excludes the other pathways. Since in this study it was possible to evaluate the insulin systemic effects on FFA levels, the observed pronounced reduction in hepatic FA uptake, oxidation and esterification rates, in response to insulin stimulation, can be entirely attributed to the hormonal suppression of adipose tissue lipolysis. This dual action of insulin appears to rule out a role for this hormone in the direct enzymatic control of liver FA esterification and oxidation. These findings need to be confirmed in humans, and imply that liver metabolism may not be studied in isolation from the concomitant control of the hepatic-adipose axis.

## **7.2 Effects of obesity on fatty acid metabolism in humans (I-III)**

### ***7.2.1 Effects of obesity on liver fatty acid metabolism (I)***

The obese group included in this study presented prodromal features of the metabolic syndrome, including overweight, hyperinsulinemia and mild insulin resistance, slight increases in plasma glucose and triglyceride levels, and a mild elevation in blood pressure. Circulating FFAs were not significantly elevated compared to the control group, presumably because of the hyperinsulinemia, thus minimizing any interference of substrate mass action on measured hepatic FA metabolism.

The main finding was a 100% elevation in hepatic FA oxidation in obese individuals, in the face of a preserved FA uptake and esterification rate. It has been previously shown that impaired glucose tolerance is associated with a defect in hepatic FA uptake, and it has been hypothesized that the occurrence of substrate competition, *i.e.*, elevated glucose oxidation is due to hyperglycemia (Iozzo *et al.*, 2004). The current study groups had normal glucose tolerance, and fasting plasma glucose levels, though marginally higher in the obese subjects, were below the threshold of impaired fasting glucose. The effect of obesity could not be investigated in the previous study (Iozzo *et al.*, 2004) as those patients had been purposely matched for BMI. The current dataset showed that, in the absence of hyperglycemia, obesity is characterized by preserved hepatic FA uptake and increased FA oxidation. Circulating insulin levels and adipose tissue insulin resistance were the main correlates of hepatic FA oxidation, and the hepatic exposure to FA due to the contribution of visceral fat was more pronounced in obese than control individuals, by  $\sim 40 \mu\text{mol}/\text{min}$  corresponding to  $\sim 20\%$  of systemic lipolysis, in line with the estimates reported by others (Nielsen *et al.*, 2004). The findings of the present study are the first to demonstrate by direct measurement that the primary hepatic response to obesity is the activation of FA oxidation as a consequence of systemic and adipose tissue insulin resistance and visceral adiposity (Fromenty *et*

*al.*, 2004). This observation corroborates previous evidence in animals, showing elevated capacity for mitochondrial oxidation and greater activities of citrate synthase and total carnitine palmitoyltransferase in genetically obese vs lean rodents (Brady *et al.*, 1985), and supports the concept that a deficient insulin action may reduce the affinity of carnitine palmitoyltransferase for malonyl-CoA, thus limiting the inhibitory effect of the latter on the former (Cook & Gamble, 1987). This study corroborates the recent evidence that obesity upregulates genes involved in oxidative phosphorylation in the liver of diabetic patients (Takamura *et al.*, 2008).

Beyond its protective action to remove FFA from the intracellular space (Hodson *et al.*, 2010), FA oxidation is also a prerequisite of oxidative stress in obesity-related inflammatory liver disease (Day & James, 1998; Fromenty *et al.*, 2004). In fact, recent *in vitro* experiments demonstrate that the accelerated oxidation of palmitate causes excess electron flux in the mitochondrial respiratory chain, resulting in increased free radical generation and hepatic insulin resistance, and that the production of reactive oxygen species (ROS) can be reduced by pharmacological inhibition of FA oxidation (Nakamura *et al.*, 2009). In high-fat-fed animals, the upregulation of FA oxidation and ROS formation precedes the development of insulin resistance (Matsuzawa-Nagata *et al.*, 2008). In humans,  $\beta$ -hydroxybutyrate is more elevated in progressive than in benign obesity-related liver disease, and is accompanied by mitochondrial structural defects (Sanyal *et al.*, 2001). Unfortunately, specific measurements of oxidative stress were not addressed.

The hepatic flux of FA into the esterification pathway appeared to be related to the rate of FA appearance in the circulation, consistent with previous findings in patients with type 2 diabetes and high liver fat content (Kotronen *et al.*, 2008a). Because lipolysis was effectively restrained by hyperinsulinemia in the obese subjects participating in this study, as previously shown in subjects with similar BMI and normal plasma FA levels (Bickerton *et al.*, 2008), the hepatic FA esterification and labelled TG release rates were preserved. Notably, the possibility of the liver to compensate for adipose tissue insulin resistance *via* the upregulation of FA oxidation is limited, since this process is already very active in the healthy organ (Havel *et al.*, 1970; Muller, 1998). Thus, the increase in hepatic FA oxidation in the obese individuals studied here suggests a progressive exhaustion of its buffering capability, to be eventually followed by the diversion of FA into the esterification pathway. Fostered by a worsening of FA release from fat, this mechanism may contribute to the accumulation of lipids in the organ and to the pathogenesis of liver steatosis in more severe obesity. Measurements of liver fat content in nine subjects showed a non-significant tendency for higher hepatic uptake and esterification rates in a subgroup of four with liver fat content >6.5% (data not shown). Esterification may have been best evaluated during a meal challenge, but fasting studies were done to obtain the best picture of the oxidative pathway and because of the steady-state requirements of the current and traditional PET kinetic modelling approach.

### ***7.2.2 Effects of obesity on skeletal muscle and adipose tissue fatty acid metabolism (II)***

To the best of the author's knowledge, this is the first study to address the relationship between FA metabolism in adipose tissue and skeletal muscle non-invasively in obese and non-obese humans. It is acknowledged that the study includes a limited number of subjects, and that the novel methodologies used require further validation. Nonetheless, the PET methodology allows to calculate both rate constants (intrinsic system response) and substrate flux rates. The rate constants are the fraction (or percentage) of tracer that enters a pathway, representing the intrinsic system response discounted from the mass action or systemic contribution of the tracee. Conversely, the flux rate incorporates the combined effect of intrinsic tissue response and extra-tissue substrate delivery. In synthesis, the rate constant identifies tissue-related defects, whereas the flux includes the changes in tissue metabolism due to extrinsic, in addition to intrinsic causes. The main finding of the study is the evidence of an impairment in FA esterification capability in obese subjects in both adipose tissue (esterification rate per unit mass) and skeletal muscle (rate constant), and a possibly compensatory increase of FAO in skeletal muscle during the fasting state. The fasting state was chosen as the target condition, in which FAs are the main fuel for skeletal muscle, and adipose tissue lipolysis is not inhibited by post-prandial insulin levels. The results of this study support the findings of another study, in which adipose tissue dietary fatty acid trafficking and relative gene expression resulted depressed in abdominally obese subjects as compared to lean controls (McQuaid *et al.*, 2011). Similarly to McQuaid and coworkers' work, the obese subjects included in the study had systemic lipolytic rates and FFA levels similar to those of controls. This is likely explained by fasting hyperinsulinemia, compensating for adipose tissue insulin resistance, as found in these subjects. This is in agreement with previous evidence of an inverse relation between lipolysis and insulin levels in uncomplicated obesity (Groop *et al.*, 1992; Bickerton *et al.*, 2008), and with larger population studies, showing that obesity is accompanied by a reduction in lipolysis relative to the increase in adiposity (Mittendorfer *et al.*, 2009), though the release of FA with respect to the fat free mass remains greater, indicating an overload of FAs to lean tissues. The findings of the present study corroborate and extend these observations, although in a small cohort of subjects, by suggesting that the FA overload translates in a hyper-activation of skeletal muscle FAO in obese individuals, an effect that was evident at both tissue (per unit mass) and whole body levels (per whole organ). This observation is in line with some, but not all previous evidence. By use of indirect calorimetry, Perseghin *et al.* reported an elevation in fasting lipid oxidation in individuals with a greater, as compared with those with a smaller fat mass. In line with this author's interpretation, they suggested a compensatory role of muscle FAO against the increasing flux of FA to lean tissues (Perseghin *et al.*, 2002). Others have used in vitro gas exchange measurements to show that only extremely obese subjects have a defective FAO in skeletal muscle, again confirming that overweight/obese individuals show a trend towards higher FAO rates as compared to lean subjects (Hulver *et al.*, 2003). The

findings of the current study are also compatible with the lack of suppression in leg FAO during insulin infusion shown by Kelley and coworkers (Kelley *et al.*, 1999), but these authors observed a defect in oxidation during fasting conditions, which is at variance with the data presented in this work. Different methodologies may explain the discrepancy, since these authors used the organ balance technique, which cannot discount the contribution of adipose tissue to the resulting FAO; since the amount of fat in the leg differs between subjects, it variably affects the results in terms of both blood flow and gas exchange, *i.e.*, the variables used in FAO calculations. The use of PET is more specifically targeted to the individual contribution of skeletal muscle and adipose tissue to the process of interest. In support of the current interpretation of the compartmental configuration of skeletal muscle FA metabolism, a significant association between the Cr/water ratio and the intracellular oxidative pool can be observed in the data presented in this study, in accordance with the notion that the creatine content relates to the oxidative potential of skeletal muscle (Chanseau *et al.*, 2008), and FA oxidation, as measured independently with indirect calorimetry, was positively related to the PET-derived FA oxidative rate and with the rate constants regulating the transfer of activity in and out of the oxidative compartment.

There is a growing belief that the progression of lipotoxicity relies on the balance between adipose tissue function and FAO; that this relationship changes dynamically across different severities of obesity and its complications, and that changes in FAO represent an adaptive or maladaptive response rather than a primary event (Muoio & Newgard, 2006; Lelliott & Vidal-Puig, 2004; de Ferranti & Mozaffarian, 2008). In this study, a severe impairment was observed in the capability of adipose tissue to incorporate FA in triglyceride depots at the level of the unit mass (*i.e.*, per 100 g of tissue). This defect was compensated by an increased adipose tissue mass in obese individuals. This may lead to speculation that the defect in storage fosters the development of “compensatory” obesity. In turn, the growth of adipose tissue in obese individuals may limit (or delay) the propagation of the intrinsic tissue defect (and the consequent release of substrates) to the rest of the body. It is of note that the ability for re-esterification was also impaired in skeletal muscle, in spite of the FA overload. The correlations found in this study show that, as insulin resistance grows, the esterification rate declines and FAO increases, and that these two metabolic processes occur in a reciprocally related fashion. Though associations do not establish cause-effect relationships, these observations rule in favour of the primacy of an FA storing defect leading to the activation of FAO.

### ***7.2.3 Effects of obesity on myocardial fatty acid metabolism (III)***

This study aimed to distinguish the contributions of plasma and intracellularly stored FA to myocardial FAO in obese individuals. Subjects with obesity release more FA from peripheral adipose tissue into the circulation (Groop *et al.*, 1992), associated with an expanded myocardial intracellular triglyceride pool (Kankaanpaa *et al.*, 2006). Enhanced FA oxidation is associated with mitochondrial respiratory chain uncoupling, free radical formation, oxygen wasting, and impaired LV efficiency, *i.e.*, inability to

match the amount of substrate consumed to the work output (Boudina & Abel, 2006). In this study, obesity was not severe and circulating FA and intracellular lipid levels were quite normal. However, the observed correlation between BMI and FA oxidation or cardiac work is compatible with previous findings (Peterson *et al.*, 2004).

One important finding of the current study was that, in the obese individuals studied here, myocardial triglycerides represented a major source of FAs that underwent oxidation. To the best of this author's knowledge, this is the first human study with quantification of cardiac metabolism to include the turnover of intracellular triglycerides obtained by exploiting information derived from two complementary imaging techniques. Two methods have been commonly adopted in the literature to quantify FA metabolism from [<sup>11</sup>C]-palmitate PET data. The compartmental model suggested by de Jong *et al.* has been implemented to calculate fluxes of plasma derived FFA oxidation, esterification and uptake (de Jong *et al.*, 2009). In this study, the FFA oxidation rate was strongly correlated with that obtained with the alternative bi-exponential fitting method (Schon *et al.*, 1982). Thus, from the latter, the second exponential of the myocardial [<sup>11</sup>C]-palmitate washout curve has been used to represent the rate constant for the mobilization and oxidation of cardiac lipids. This rate constant was multiplied by the cardiac triglyceride concentration, as obtained with proton MRS, to give the absolute flux of triglyceride oxidation in the heart. The washout values obtained in this study are consistent with those of Kisrieva-Ware and colleagues (Kisrieva-Ware *et al.*, 2009), and they are in the order of  $10^{-3}$ , *i.e.*, approximately thirty times smaller than the corresponding rate constant of plasma FA oxidation (de Jong *et al.*, 2009). These figures may suggest that triglyceride metabolism is negligible under normal fasting and resting conditions (Kisrieva-Ware *et al.*, 2009). However, it should be kept in mind that rate constants represent only the fraction of substance moving between compartments, whereas the absolute flux depends on the size of the source pool. Concentrations of plasma FFA and cardiac triglyceride FAs are typically around 0.4-0.7  $\mu\text{mol/g}$  in blood *versus*  $>20 \mu\text{mol/g}$  of tissue, a ratio of approximately thirty or more in favour of the latter, thus balancing out the above difference in rate constants.

Therefore, the most salient finding of the current study was that the oxidation of endogenous lipids was quantitatively relevant as compared to the plasma FAs in the overweight individuals included in the study, representing almost 60% of the total myocardial oxidation of FAs. This finding is consistent with the recent evidence that the myocardial triglyceride pool is dynamic (Taegtmeyer & Harmancey, 2008; Hammer *et al.*, 2008). In support of this figure, in this study, the amounts of substrates that would be required to fulfill the left ventricular work measured with MRI were estimated. The current data indicate that the full oxidation of substrates extracted from plasma would not provide sufficient energy, unless the contribution of intracellular stores is taken into account.

Unpublished data presented in this thesis provide a direct comparison between obese and control subjects, showing that myocardial plasma-derived FAO is increased in obesity, and supporting the already discussed correlation with BMI. In the future, it will be interesting to evaluate whether there are any differences in the myocardial intracellular lipid-derived FAO between obese and lean subjects.

### **7.3 Effects of trimetazidine on fatty acid and glucose metabolism in obese subjects (II-III)**

#### ***7.3.1 Effects of trimetazidine on whole body, skeletal muscle and adipose tissue substrate metabolism (II)***

The treatment of obese subjects (with the metabolic abnormalities evidenced in paragraph 7.2) with a partial inhibitor of mitochondrial beta-oxidation resulted in a diversion of FA from the oxidative towards the non-oxidative pathway in skeletal muscle, reverting these processes towards the values observed in the control group. The hypothesized shift towards glucose metabolism produced by the drug was observed as a tendency of the glucose phosphorylation pathway to increase after treatment.

The long-term metabolic effects of the partial inhibitor of beta-oxidation trimetazidine were studied in a drug-naïve human model of moderately obese subjects in whom the still flexible stage of the disease is characterized by an increased FAO, and all measurements were performed during fasting to avoid the confounding suppressive effects of insulin on FA metabolism. One previous study in which the modulation of FA and glucose metabolism by trimetazidine was simultaneously investigated in humans in an organ different from the myocardium (Monti *et al.*, 2006) in diabetic patients with cardiomyopathy, showed that forearm lipid and glucose oxidation were reciprocally modulated during the insulin-stimulated state, but no changes occurred during the fasting state, in spite of the higher FA turnover typical of fasting *vs* insulin-stimulated conditions. The current study extends the previous findings in several regards, since a) the chosen human model discounts for the confounding actions of disease and multiple medications, b) the treatment period was prolonged to one month (*vs* 15 days), c) imaging techniques for the assessment of regional metabolism were adopted, thus targeting skeletal muscle and adipose tissue separately, and d) by combining plasma tracer kinetics and indirect calorimetry, endogenous glucose production, hepatic insulin sensitivity and whole body FA release and oxidation were estimated.

In agreement with previous findings in idiopathic-dilated cardiomyopathic patients, in whom an improvement in glycemic and cholesterol profiles was reported following three months of treatment (Tuunanen *et al.*, 2008), the data presented here indicate an immediate tendency towards a decline in HbA<sub>1c</sub> and LDL cholesterol, in spite of a shorter study duration. Neither endogenous glucose production, nor systemic FA release were changed, thus the modifications in glucose control and insulin sensitivity observed here and/or in previous investigations seem to be mediated by substrate consuming, rather than producing organs.

Trimetazidine did not affect skeletal muscle FAO, in line with results from indirect calorimetry at the whole body level. In a recent study, Fragasso *et al.* did not find a change in whole body lipid oxidation and RQ after three months of trimetazidine treatment of patients with heart failure, confirming the results of this study (Fragasso *et al.*, 2011). However, they found a decrease in whole body resting energy expenditure, which, as they discuss, is related to sympathetic activity, and appears to be higher in

patients with heart failure than in healthy controls (Fragasso *et al.*, 2011). Thus, their subjects might have been more prone to a decrease in a generally higher baseline value. However, in this study, the whole body resting energy expenditure decreased in most but not all subjects, and due to the limited number and probably to the smaller treatment dose, and the shorter study duration, no significant decrease was observed. Nonetheless, in the skeletal muscle, trimetazidine significantly accelerated the movement rate of FA towards the non-oxidative, *i.e.*, esterification pathway. This change was accompanied by a borderline increase in the glucose phosphorylation rate constant in this target tissue. Early changes in the rate constants confirm the reciprocal substrate regulation by trimetazidine, and are likely to precede a net diversion of FA from oxidation towards esterification in complex lipids, in line with the reported observation that trimetazidine stimulates phospholipid synthesis (Sentex *et al.*, 1997), with potential protective effects on cellular membranes (Sentex *et al.*, 1997; Sentex *et al.*, 2001).

It was interesting to observe a higher baseline visceral as compared to subcutaneous FA uptake. Previous studies have used tissue biopsies to compare dietary FA uptake in subcutaneous and visceral adipose tissue in normal weight humans, showing that VAT accumulates more dietary fat (milligram meal fat per gram of adipose tissue lipid) than either upper body subcutaneous or lower body subcutaneous fat (Jensen, 2008). Similar results have been previously described with PET and a different long-chain FA tracer in lean subjects (Hannukainen *et al.*, 2010); this investigation extends the finding to obese humans. The current results show that fasting FA uptake was approximately tripled in visceral compared to subcutaneous fat. Notably, glucose uptake was 12 times greater in the whole body SAT-organ than in the entire VAT mass, as opposed to FA uptake which was only four times greater in SAT than in VAT. Thus, VAT is proportionally more FA avid and much less glucose-avid than SAT. *Ad hoc* studies are required to explain the mechanisms underlying this finding, and to clarify whether SAT is relatively more effective in preventing fasting hyperglycemia, by serving as a glucose sink.

Adipokines did not seem to play a role as mediators of trimetazidine action within the time frame of the present study. Similarly, adipose tissue topography and absolute masses of either visceral, or subcutaneous fat, or IMCL content were not changed. The only exception was the expansion in the extramyocellular lipid content, suggesting that a preferential diversion of fat stores in adipose tissue adjacent to skeletal muscle may prevent IMCL accumulation.

### ***7.2.2 Effects of trimetazidine on myocardial metabolism and function efficiency (III)***

This study is the first to evaluate whether TMZ provokes inverse changes in FA and glucose metabolism in a drug-naive human model, and whether there is any difference in inhibition of myocardial FA oxidation derived from plasma or intracellular stores' FA sources. Concordant with previous studies, TMZ led to an improvement in cardiac

efficiency. The proposed action of TMZ is that it lessens FA metabolism in skeletal (Tuunanen *et al.*, 2008) and cardiac muscle (Fragasso *et al.*, 2003) by partial inhibition of mitochondrial  $\beta$ -oxidation, resulting in decreased insulin resistance with a shift in substrate utilization from FA to glucose. The data presented in this study show a remarkable suppression of total and endogenous myocardial FA oxidation by the drug in obese individuals. The reduction in triglyceride oxidation without a change in the cardiac lipid content suggests the diversion of FAs into a different cellular pool, in line with increased phospholipid synthesis in the myocardium (Sentex *et al.*, 1997). *Via* this route, and other mechanisms mediated by the decline in FA oxidative metabolism, TMZ may consolidate mitochondrial stability and function (Tabbi-Anneni *et al.*, 2003; Sentex *et al.*, 2001). The inhibition of FA oxidation induced by TMZ was accompanied by a compensatory enhancement in myocardial glucose uptake, though this increment did not achieve statistical significance. Stronger inhibitors of FA metabolism have been previously used, as reported in section 2.4. Overall, the recent literature suggests that *in vitro* studies do not prove the *in vivo* actions, supporting the rationale of the current study. The data presented are in line with the other reports, in showing that TMZ is similar to other FA oxidation inhibitors in causing limited or no changes in the oxidation of plasma FA and uptake of glucose. However, the novelty of this study is the disclosure of an important effect of TMZ in reducing FA oxidation from endogenous sources. This process was not determined in previous studies and this may justify the controversial or negative findings.

Notably, the pre-treatment rate of substrate utilization exceeded, though not significantly, the strict mechanical work requirements, suggesting oxygen wasting. The metabolism of FAs was reduced for the same amount of work, suggesting a tighter metabolic-mechanical coupling and greater left ventricular efficiency. Taken together, the findings of a reduction in FAO and a small compensatory change in glucose utilization by the heart indicate a decrease in the global amount of substrate-derivable energy, in accordance with the evidence of creatine depletion. This energy-sparing effect may result from the multiple TMZ effects on mitochondria (Tabbi-Anneni *et al.*, 2003; Sentex *et al.*, 2001).

### ***7.2.3 Effects of trimetazidine: reconciliation of other findings***

Taking into consideration the tendency that TMZ showed in shifting fatty acid oxidative processes towards esterification, one might think that this drug would promote lipid storage with deleterious effects. But as discussed above, whole body fat masses, cardiac or skeletal muscle lipid storage were not increased. It must be noted that other results from this study published elsewhere support the notion that TMZ does not promote ectopic fat accumulation, but rather the opposite, as shown by a decrease of 44% of the liver lipid content of these subjects measured with  $^1\text{H}$ -MRS (Borra, 2009).



#### **7.4 Association of pericardial fat and hyperemic myocardial blood flow in subjects with and without CAD (IV)**

In the past few years, several groups have documented the association between fat inside the pericardial sac and CAD, or vascular calcification (Alexopoulos *et al.*, 2009; Eroglu *et al.*, 2009; Gorter *et al.*, 2008; Greif *et al.*, 2009; Rosito *et al.*, 2008; Sarin *et al.*, 2008). Myocardial perfusion characterizes the functional consequences of atherosclerosis and may be affected by the vasocrine action of adipose tissue. In spite of this dual importance, its relationship with pericardial fat in CAD patients has not been investigated.

The main novelty of the study was to address the relationship of absolute MBF and cardiac adiposity in subjects of both genders, with and without CAD. There is growing recognition that the measurement of hyperemic MBF plays an important role in the management of patients with coronary stenoses. Revascularization trials have demonstrated that, once the invasive treatment is guided by FFR rather than percent stenosis, the number of coronary events during follow-up is significantly reduced (Gould, 2009). As expected, the distribution of male sex was skewed in favour of CAD, and especially in favour of the obstructive CAD groups, compared with that of women; also, male sex was a strong positive predictor of fat volumes and a negative predictor of hyperemic MBF.

The present measurements confirm previous studies that associate increased fat surrounding the heart with the presence of CAD (Djaberi *et al.*, 2008; Alexopoulos *et al.*, 2009; Eroglu *et al.*, 2009; Greif *et al.*, 2009; Gorter *et al.*, 2008; Sarin *et al.*, 2008; Rosito *et al.*, 2008). Nonetheless, uncertainties about the relation remain, since current results and previous studies have found no relationship between IPF and severity of CAD, expressed as the number of vessels with critical stenoses, or atherosclerosis scores based on the number of significant obstruction (Chaowalit *et al.*, 2006; Djaberi *et al.*, 2008; Ueno *et al.*, 2009; Gorter *et al.*, 2008) and the composition of plaques (Gorter *et al.*, 2008). Helping to explain this controversy, one of the key findings of the current study was that, among patients with CAD, only those with Obs-CAD had a greater IPF volume, while EPF was increased regardless of whether the stenosis was obstructive or not. This observation supports the potential vasocrine influence previously described. More important, it may be taken as an explanation for the discrepancy between CAD severity and adipose tissue mass, by suggesting that in patients with CAD and fat enlargement, the latter promotes coronary endothelial dysfunction, whereas in patients with CAD and normal IPF, no impairment in MBF occurs. In addition, IPF is nourished by coronary vessels, and it cannot be excluded that hypoperfusion and ischemia might accentuate the inflammation of neighbouring adipose tissue (Iacobellis & Willens, 2009; Trayhurn & Wood, 2004), especially once adipose tissue is expanded, and therefore requires an increment in perfusion. In this scenario, a defective MBF would exacerbate adipose tissue hypoxia, and adipose tissue damage would in turn worsen the coronary dysfunction. The assessment of pericardial adipose tissue perfusion in concomitance with MBF by PET is theoretically possible but requires specific protocols accounting for the contamination of the nearby

myocardium, which is a high-flow and moving organ. Overall, the present data suggest that cardiac adiposity may have a role in aggravating ischemia in CAD patients.

The CAC score in concomitance of CAD has also been extensively investigated in its relationship to fat depots surrounding the heart (Alexopoulos *et al.*, 2009; de Vos *et al.*, 2008; Djaberi *et al.*, 2008; Gorter *et al.*, 2008; Greif *et al.*, 2009; Rosito *et al.*, 2008; Sarin *et al.*, 2008). The current results regarding the relation between EPF and IPF with CAC scores are also in line with previous investigations. The present data show that augmented fat surrounding the heart is associated with higher CAC scores, similar to the evidence by other groups measuring peri-coronary fat thickness (de Vos *et al.*, 2008) or epicardial adipose tissue volume (de Vos *et al.*, 2008; Djaberi *et al.*, 2008; Rosito *et al.*, 2008). However, the amount of IPF did not increase linearly with the degree of calcification in an independent manner, when accounting for sex and age in the current dataset, and in previous studies (Djaberi *et al.*, 2008; Gorter *et al.*, 2008). To support the notion that the CAC score is not so closely related to fat accumulation, Greif *et al.* found no differences in pericardial fat depots between patients with different plaque composition (calcified, mixed, or non-calcified only), and reported that fat accumulation was already present without plaque calcification (Greif *et al.*, 2009). Alexopoulos *et al.* found no difference between epicardial fat volumes in subjects without plaques as compared with those with calcified plaques, whereas they found greater fat accumulation in subjects with mixed and non-calcified plaques (Alexopoulos *et al.*, 2009).

In women with normal coronary arteries, Sade *et al.* reported a negative association between CFR and epicardial fat thickness assessed by 2D and colour Doppler echocardiography (Sade *et al.*, 2009), reflecting potential microvascular disease. The current study extends this observation in several regards, and it covers different clinical questions. This study included a larger cohort of patients of both genders and with CAD, and measured MBF in an absolutely quantitative and regional fashion (Kaufmann & Camici, 2005; Knuuti & Bengel, 2008; Kaufmann & Di Carli, 2009; Gould, 2009). By using MDCT, the opportunity has been taken to evaluate the independent effects of IPF and EPF. The present study showed an inverse association between both IPF and EPF and (hyperemic) MBF, but multiple regression analysis, discounting for factors known to cross-correlate with either MBF or cardiac fat masses established that IPF, but not EPF, is negatively related to the MBF parameters considered here. There are two potential explanations for this association. The MBF parameters and IPF, but not EPF, are linked to a common risk factor. The other possibility is the direct influence of an enlarged perivascular fat mass on vessel wall dysfunction, as has been suggested in obesity and type 2 diabetes (Zhang & Zhang, 2009), in heart disease animal models (Galvez *et al.*, 2006), and more specifically in the modulation of coronary endothelial function (Payne *et al.*, 2008; Payne *et al.*, 2009). Inflammation, vasoactive adipokines and mediators secreted locally by IPF could explain the present findings. In fact, enlarged adipocytes increase the proportion of macrophages, T lymphocytes (Henrichot *et al.*, 2005), and detrimental adipocytokines, such as leptin, resistin, interleukin 6, and tumour necrosis factor alpha. Inflammation may alter the balance between vascular NO, endothelin-1, and

superoxide production, promoting vasoconstriction (Zhang & Zhang, 2009). Samples of pericardial fat from patients with CAD showed increased mRNA, protein levels of inflammatory cytokines relative to subcutaneous fat (Mazurek *et al.*, 2003), and lower expression of adiponectin relative to that in patients without CAD. Perivascular fat can also stimulate smooth muscle cell proliferation, contributing to the progression of atherosclerosis (Barandier *et al.*, 2005). In fact, adiponectin levels in the coronary lumen are associated with corresponding mRNA expression in epicardial fat (Iacobellis *et al.*, 2005).

Since the CAC score has been reported to be a risk factor for low myocardial blood flow (Schenker *et al.*, 2008), the relative powers of IPF and CAC score in predicting stress myocardial blood perfusion have been compared. Even after taking into account common confounders, including hypertension, as suggested by others (Sade *et al.*, 2009), IPF remained an independent predictor of MBF, and more significantly so than EPF, BMI, and hypertension. It is worth noting that, IPF and CAC score together explained around one fifth of myocardial perfusion variability, though among single risk factors, male sex was the strongest negative predictor of myocardial perfusion.

## 7.5 Limitations of the study and future directions

The limitation of the evaluation of the effect of obesity on the measured processes was in the small sample size that did not allow the evaluation of gender differences, which are known to play a role in fatty acid metabolism (Mittendorfer *et al.*, 2009; Jensen, 1995). Thus, this study, considered to be a pilot, can be used as a background for a larger study where gender will be taken into consideration as well as the different body fat distribution, another aspect not fully addressed in this study. Another future perspective is to associate the PET metabolic measurements with stress oxidative markers and compare different stages of the metabolic disease (hence early vs late stages) to further support the supposed cascade of events.

<sup>11</sup>C-Palmitate PET methodology (I-III) had some limitations. The studies used acquisition protocols of only 50 minutes and some concern may arise regarding whether all processes can be detected in such a short time. It is acknowledged that a different technique and longer study protocols might have reached a better steady state. However, during the present studies, TG fractions and other metabolites were measured along with the input function (FFA). A remarkable increase of the TG fraction could be seen from the 10<sup>th</sup> minute onwards. The study of Guiducci *et al* also concluded that TG splanchnic release is detectable in most PET studies, starting after 10 minutes (Guiducci *et al.*, 2006). In the present results, the lack of difference in hepatic TG release between overweight/insulin resistant subject group and controls could be explained by the observation that insulin levels of the former are increased compared to the latter and this suppresses TG release. Further evidence for this explanation comes from the same observation made for the insulin stimulated state, in the animal study presented here and in other studies (Malmstrom *et al.*, 1998; Lewis *et al.*, 1995).

A significant technical limitation in this study is the use of a free fatty acid to study fat deposition of fat in adipose tissue. The direct uptake of free fatty acids by adipose tissue in the fasting state constitutes a very minor pathway – almost all fatty acids stored in adipose tissue arise from plasma triglycerides (Bickerton *et al.*, 2007), and the uptake is primarily taking place in the postprandial state. However, the investigation was designed to evaluate the intervention of trimetazidine on fatty acid oxidation, which is known to be maximal in the fasting state. It must be also noted that the postprandial state condition would have imposed more inconvenience to the patients in what was already a demanding study protocol involving PET/CT, MRI and MRS imaging sessions (twice). Furthermore the increased radiation dose would need to be justified ethically.

The limitation of the treatment substudies (II, III) was in the lack of a placebo control group, a decision that was guided by the demanding nature of the studies and the radiation exposure, which (though limited, *i.e.*, within the clinical diagnostic routine range) could not be justified in a pilot phase. Though the few changes observed may have benefited from the comparison with a placebo group, they seem sufficient to clarify that trimetazidine actions in moderate obesity are relatively mild and may require a long time before translating into systemic effects. The most conclusive value of this investigation was in the large number of measured variables that did not change, thus allowing the confident conclusion of a series of potential mechanisms from being mediators of trimetazidine action. In the future, a longer treatment study with the association of oxidative stress markers will add valuable knowledge to the mechanisms of action of the drug.

Especially in study III, though the same author's group has previously shown that placebo treatment for three months did not alter cardiac function and metabolism in heart failure patients (Tuunanen *et al.*, 2008), this finding may not be directly extrapolated to the subjects of the current study. Thus, this study only assessed the association between treatment with TMZ and subsequent effects, especially with reference to the previously surmised metabolic shift in myocardial metabolism. The current data support this action, primarily on the reduction of FA oxidation. Obese individuals were selected to guarantee sufficient magnitude of FA oxidation and lipid content to maximize the likelihood of detecting a reduction in cardiac FA metabolism. The current findings show that changes in myocardial metabolism have effects on cardiac efficiency. The limited number of subjects, the inter-subject variability, and the low rates of fasting glucose uptake may have weakened the significance of changes in glucose metabolism. In addition, the TMZ dose used was half of the therapeutic dose utilized in the previous study in heart failure patients. This was because some caution was preferred in healthy subjects; however, the dose of TMZ may have been suboptimal to delineate all the relevant metabolic effects of the drug, especially with reference to the change in glucose uptake. Despite the instructions not to change their lifestyle and diet, patients experienced a slight decline (borderline of significance) in average body weight. It cannot be established whether this was a drug or placebo effect. However, changes in body weight did not correlate with, and are unlikely to account for the changes in metabolic variables. Finally, though a slight change in

cardiac function was observed, these subjects had normal baseline function and the study design was not targeted towards this process.

In study IV, the cross-sectional design of the study allows only speculation on the causal relationship of the associations found. The study included subjects of both genders with a moderate to intermediate risk of CAD and stable angina; only 40 of 107 patients had CAD. The limited study sample was balanced by the use of reliable and reproducible quantification techniques, as reflected by high ICC coefficients ( $\geq 0.98$ ), furthermore the use of a blind design, and the power achieved with the sample appeared sufficient to verify the hypothesized relationships. Follow-up data in these patients are not yet available; thus, the study cannot verify prognostic implications, which can be a future aim. A recent report on outcome suggested that pericardial fat is a better predictor of incident CAD than are more general measures of adiposity, but cardiac adiposity was determined at follow-up and not at baseline (Ding *et al.*, 2009). Estimation of the 10-year likelihood of myocardial infarction and coronary death based on a published score (Wilson *et al.*, 1998) developed in patients without overt CAD, showed an independent association with stress MBF or CRF (known predictors of cardiac mortality) and IPF or EPF ( $p < 0.02$ ) in the population of this study (data not shown).

## 8 SUMMARY AND CONCLUSIONS

**The results of the present study can be summarized as follows:**

**(I)** the methodology developed and validated is able to non-invasively describe the fate of FA in the liver with satisfactory accuracy and in adequate detail. The current study strongly implies that a higher FA oxidation is the first metabolic change in the liver of obese individuals, occurring in the context of adipose tissue insulin resistance and increased FA flux from visceral adipose depots. This hepatic response is maladaptive to the extent that a greater FA oxidation presumably results in the overproduction of reactive oxygen species already at this prodromal stage of obesity-related metabolic syndrome.

**(II)** Overall, the current data suggest that uncomplicated obesity is characterized by adipose tissue and whole body insulin resistance, which are accompanied (or may be preceded) by a proportional inability to store FA in adipose tissue and skeletal muscle fat depots. Accordingly, hyperinsulinemia and FAO may act against the overflow of FA into the circulation, the former by inhibiting the breakdown of existing tissue fat depots, and the latter by augmenting the washout of FA from the circulation *via* oxidation.

Trimetazidine increased the FA esterification and glucose phosphorylation rate constants in skeletal muscle, and the EMCL in one month, supporting the hypothesis of an indirect, though very gradual diversion of FA from the oxidative to the non-oxidative pathway. A longer time may be required before the known systemic benefits of this compound become appreciable in moderately obese, otherwise healthy individuals.

**(III)** The current work introduces for the first time the complementary use of molecular imaging modalities, namely, MRS and PET, thereby making the absolute flux of triglyceride-derived FAs accessible for direct measurement. In the heart of obese subjects, the myocardial triglyceride pool provided a major contribution to the total substrate oxidation. The inhibition of this process by TMZ was accompanied by an increase in left ventricular work efficiency in obese individuals.

**(IV)** CAD is accompanied by augmented fat depots surrounding the heart. The findings reported in this work demonstrate a negative relationship between IPF or EPF and hyperemic blood perfusion or CFR. Intra-pericardial fat was an independent predictor of myocardial perfusion, together with CAC score, and both risk factors explained 20% of hyperemic coronary blood perfusion variability. These results support the hypothesis of a direct paracrine/vasocrine effect of perivascular fat on coronary vessels, and suggest that an enlarged IPF is a more specific index of CAD complicated by myocardial ischemia, than of CAD alone.

**Conclusions.** The results of the different substudies point in the same direction. Obesity is associated with an impairment in the esterification of FA in adipose tissue and skeletal muscle, which is accompanied by the upregulation in skeletal muscle, liver and heart FAO. The inability to store fat may initiate a cascade of events leading to FA oversupply to lean tissue, overload of the oxidative pathway, and accumulation of toxic lipid species and triglycerides, and it was paralleled by a proportional growth in insulin resistance. Even in subjects with CAD, the accumulation of ectopic fat inside the pericardium is associated with impaired myocardial perfusion, presumably via a paracrine/vasocrine effect. Taken altogether these findings suggest that adipose tissue storage capability should be preserved, if it is not possible to prevent excessive fat intake in the first place. At the beginning of the disease, when FAO is increased to compensate the FA overload, partial inhibition of beta-oxidation is not detrimental to health; on the contrary at the single organ level (heart, skeletal muscle and liver) it seems beneficial.

## 9 ACKNOWLEDGEMENTS

This study was carried out in the Turku PET Centre, the Department of Clinical Physiology and Nuclear Medicine and the Department of Medicine, University of Turku. The analyses and the scientific articles presented in this book have been produced during the years 2007-2010.

I express sincere thanks to Professor Juhani Knuuti, Director of the Turku PET Centre, to Professor Jaakko Hartiala, the head of the Department of Clinical Physiology and Nuclear Medicine, and to Professor Jorma Viikari, the head of the Department of Medicine, for providing such excellent research facilities and for finding interest in the topics dealt with in this book.

A special acknowledgement goes to Professor Juhani Knuuti for having trusted me and shared his patient dataset so that I could perform the analyses of study IV. It is admirable how you have been able to hold the office of director of such a prestigious PET Centre for so many years and at the same time you have still been able to be a clinician and follow scientific projects in detail, among all the other tasks. It has been an honour to work with you, Juhani: "Grazie!"

I owe my greatest gratitude to my supervisors Docent Patricia Iozzo and Professor Pirjo Nuutila (in alphabetical order). I thank you both, for having taken good care of me. You have both been more than just supervisors. I could not have asked for better mentors. You have both always been available in teaching me, and have always let me make the decisions that concerned my career and research.

Patricia, thank you for your endless patience and enthusiasm in following my education. Your passion, devotion to the research world and multifaceted expertise have been an example for me.

Pirjo, I have admired from the beginning your ability to handle different aspects of clinical, political and scientific (besides personal) life. You can be serious and determined and positive and energetic and at the same time show an unrivalled sense of humour.

You both gave me strength when I needed it and I reached this point thanks to you and to your trust in me. I thank you both for having had meetings until late when it was necessary, even sacrificing your free time. There are not enough pages to fully express my gratitude to you, so I will summarize everything with one word: "Grazie!"

Professor Fredrik Karpe and Ulla Ruotsalainen are warmly acknowledged for their review and constructive criticism of this manuscript. Thank you, for your careful reading of the papers included in this thesis, for providing valuable suggestions, and motivating opinion. Your comments and discussions have improved this thesis.



These studies could not have been performed without the hard work of several co-authors. I especially thank (mainly in alphabetical order): Ronald Borra, for his valuable help and expertise in MRI/MRS techniques. Esa Joutsiniemi, Sami Kajander and Antti Saraste, for their assistance and availability for the preparation of study IV. Jan Kiss and Alexandru Naum are thanked for carrying out the pig experiments, together with Ronald and many others. Romina Maggio: without you the trimetazidine study would not exist, thanks for doing the PET/MR examinations! Maja Mäki for her kindness and expertise in the analysis of PET flow images. Kjell Någren for having performed dangerous palmitate radiosyntheses: I hope we can still collaborate in the future to proceed with the palmitate studies. Riitta Parkkola and Jussi Pärkkä: for your guidance and unselfish sharing of knowledge of the MRI analysis world. Anne Roivanen: for your patience and willingness to collaborate on different projects. I would like to express my warm thanks to Mika Teräs for his guidance in the PET/CT world, especially at the beginning of my path. To all of you: “Grazie!”

I feel indebted to Vesa Oikonen, for his generosity in sharing with me his expert knowledge of modelling, mathematics, and informatics, and for being such a constructive and reassuring co-author. “If I agreed with you, then we would both be *right*”. “Grazie!”

I would like to express my warm thanks to the CardMetab research group and Turku PET Centre colleagues, especially: Jarna Hannukainen, for the precious advice work-wise and in the personal sphere. Iina Laitinen, for being a colleague, friend and kind of sister in her attitude to giving me advice, we had fun and we were serious, thanks for all of that. Kirsi Virtanen: thanks for the good scientific discussions. Kari Kalliokoski and Ilkka Heinonen: even if with different backgrounds and interests, we have found a way to collaborate, thanks for letting me in your “circle”. Virva Lepomäki: for your assistance with MRI/MRS techniques. Anna Karmi: for your kindness and very useful exchange of opinions. Hanna-Riikka Lehto: for your assistance in pericardial fat quantification. Helena Tuunanen and Saira Kauhanen: you helped me in a way that you can't imagine. Antti Viljanen, for being such a good friend when I had just arrived. Even if my brain research is not present in this study, I still wish to thank Jussi Hirvonen and Jere Virta for the generous assistance I got in this regard. Kaisa Sederholm and Nobuyuki Kudomi: for your help with modelling. Irina Lisinen, for the valuable help in statistical analysis. Thanks also to Riikka, Miikka, Erika, Heidi, Janne and Tam for being friends to me. You have all enriched my background, and made me a better researcher. “Grazie!”

I am grateful to the personnel of the Turku PET Centre who have helped me through my research career, especially to the radiochemists: Olof Solin and Tapio Viljanen. To the modeling team: Chunlei, Sauli and Jouni. Jouni: we had fun playing board games and we were serious about mathematical modelling, I enjoyed both. IT team: Markko Tattalainen and Rami Mikkola for their endless patience and availability in providing assistance in computer related issues. Nurses: thanks to Heli for her help for D-Day (dissertation-day) arrangements. Sanna: thanks for your help with patient data retrieval. Hannele, thanks for your MRI console assistance. Thanks to Anne-Mari, Minna and all the other nurses that work hard every day. I express very special appreciation to Mirja Jyrkinen for her

## ACKNOWLEDGEMENTS

---

generous assistance, patience and kind attitude. I also thank secretaries Sinikka Lehtola and Laura Jaakkola. Special thanks go to secretaries Outi Irjala and Riitta Paju: without your help I would not have made it. “Grazie!”

Some of the colleagues were also friends, I warmly thank all my fellow researchers: Anu, Pauliina, Tommi, Henkka, Nikke and Tiina for their friendship and fun. You made me understand that life is not only work. “Grazie!”

I owe my deepest gratitude to my fellows and friends Gaber, Jarkko, Harri, Markus and don. Serge (in alphabetical order). I thank you all for the many nice scientific discussions between a kebab and a beer. “Grazie!”

Thank you Kirsi Virtanen, Jarna Hannukainen and Anna Karmi for the Abstract to Abstrakti translation; I thank Jacqueline Välimäki for the official language review of this thesis and Sir. Tony Shepherd for the last minute language revision checks, you made it, we made it! Very much obliged. “Grazie”!

I thank all the patients and healthy subjects who were involved in this study. Without your voluntary participation and patience, this work would have been impossible. “Grazie”!

I do not want to forget my background in nuclear medicine and endocrinology in Bologna University and I want to thank all colleagues that I have worked with during my formation years. Thank you, Stefano Fanti, Cristina Nanni, Valentina Ambrosini, Stefano Boschi, and my fellow Carmelo Quarta. Thank you Carmelo, for the prolific scientific discussions we have had and the nice mice work together. “Grazie”!

I am especially grateful to my mentor, Professor Uberto Pagotto, of whom I have been co-worker during the last 5 years, for being proud of my scientific independence and always being within reach for constructive suggestions and some financial support on my projects. “Grazie”!

I thank all of those, who believe themselves to have been important to me and yet have not been properly acknowledged (sorry for that). I thank all the readers of this book; because you give it a meaning, even if you are reading only this section ... I know some of you are reading only the acknowledgments! To all: “Grazie!”

I wish to thank once again those of you who took care of me during these years, this is what I mean by “family”, and this book is dedicated to you too.

Among all my friends, Salsa friends are warmly thanked for the moments shared outside the scientific world. Your friendship has been very important to me. You are too many to all be mentioned. Among my Italian friends I wish to especially thank Antonio, Luca, Sara, Mara and Giacomo. Among the friends met in Finland, Mesfin and Elina with whom I have shared the happiest and saddest moments of my life in Finland. Thanks for being there for me, when I needed you most. I would also like to thank Dodo, Terhi, Stefania and Filipe. To all: “Grazie!”

## ACKNOWLEDGEMENTS

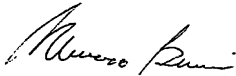
---

I thank collectively all my friends not named here and all the friends of my family for supporting me during these years. From the latter I wish to thank Gigi, Nora and Antonella P. You are really important in my life. To all: “Grazie!”

Last but not least, I owe my deepest gratitude to my parents. My dear mum and dad, thanks for your unconditional love and constant support throughout my life. Thank you for being there in the good and the bad times. Thank you for having believed in me and for letting me go when I chose to do so, it must have been hard for you. “Grazie!”

This work has been conducted and financed within the Centre of Excellence in Molecular Imaging in Cardiovascular and Metabolic Research, which is supported by the Academy of Finland, the University of Turku, Turku University Hospital, and Åbo Akademi, Turku, Finland. Financial support has been provided by the Finnish Cultural Foundation, the Finnish Diabetes Foundation and the University of Turku Foundation. Some of this work was part of the project “Hepatic and Adipose Tissue and Functions in the Metabolic Syndrome” (HEPADIP) which is supported by the European Commission as an Integrated Project under the 6th Framework Programme (contract LSHMCT-2005-018734). This work is also partially supported by the European Foundation for the Study of Diabetes, the Finnish Heart Foundation, the Hospital District of Southwest Finland and the Turku Collegium for Science and Medicine of the University of Turku.

Turku, November 2011



Marco Bucci

## 10 REFERENCES

- Abate N, Garg A, Coleman R, Grundy SM, & Peshock RM (1997). Prediction of total subcutaneous abdominal, intraperitoneal, and retroperitoneal adipose tissue masses in men by a single axial magnetic resonance imaging slice. *Am J Clin Nutr* **65**, 403-408.
- Abdul-Ghani MA & DeFronzo RA (2010). Pathogenesis of insulin resistance in skeletal muscle. *J Biomed Biotechnol* **2010**, 476279.
- Abe T, Kearns CF, & Fukunaga T (2003). Sex differences in whole body skeletal muscle mass measured by magnetic resonance imaging and its distribution in young Japanese adults. *Br J Sports Med* **37**, 436-440.
- Ahlborg G, Felig P, Hagenfeldt L, Hendler R, & Wahren J (1974). Substrate turnover during prolonged exercise in man. Splanchnic and leg metabolism of glucose, free fatty acids, and amino acids. *J Clin Invest* **53**, 1080-1090.
- Akaike H (1992). [Data analysis by statistical models]. *No To Hattatsu* **24**, 127-133.
- Alexopoulos N, McLean DS, Janik M, Arepalli CD, Stillman AE, & Raggi P (2009). Epicardial adipose tissue and coronary artery plaque characteristics. *Atherosclerosis*.
- An J, Muoio DM, Shiota M, Fujimoto Y, Cline GW, Shulman GI, Koves TR, Stevens R, Millington D, & Newgard CB (2004). Hepatic expression of malonyl-CoA decarboxylase reverses muscle, liver and whole-animal insulin resistance. *Nat Med* **10**, 268-274.
- Andres R, Cader G, & Zierler KL (1956). The quantitatively minor role of carbohydrate in oxidative metabolism by skeletal muscle in intact man in the basal state; measurements of oxygen and glucose uptake and carbon dioxide and lactate production in the forearm. *J Clin Invest* **35**, 671-682.
- Andreyev AY, Kushnareva YE, & Starkov AA (2005). Mitochondrial metabolism of reactive oxygen species. *Biochemistry (Mosc)* **70**, 200-214.
- Angulo P (2007). GI epidemiology: nonalcoholic fatty liver disease. *Aliment Pharmacol Ther* **25**, 883-889.
- Argaud L, Gomez L, Gateau-Roesch O, Couture-Lepetit E, Loufouat J, Robert D, & Ovize M (2005). Trimetazidine inhibits mitochondrial permeability transition pore opening and prevents lethal ischemia-reperfusion injury. *J Mol Cell Cardiol* **39**, 893-899.
- Armstrong DT, Steele R, Altszuler N, Dunn A, Bishop J, & De Bodo R (1961). Regulation of plasma free fatty acid turnover. *Am J Physiol* **201**, 9-15.
- Arner P & Bolinder J (1991). Microdialysis of adipose tissue. *J Intern Med* **230**, 381-386.
- Arner P & Bulow J (1993). Assessment of adipose tissue metabolism in man: comparison of Fick and microdialysis techniques. *Clin Sci (Lond)* **85**, 247-256.
- Atkinson LL, Kelly SE, Russell JC, Bar-Tana J, & Lopaschuk GD (2002). MEDICA 16 inhibits hepatic acetyl-CoA carboxylase and reduces plasma triacylglycerol levels in insulin-resistant JCR: LA-cp rats. *Diabetes* **51**, 1548-1555.
- Atkinson LL, Kozak R, Kelly SE, Onay BA, Russell JC, & Lopaschuk GD (2003). Potential mechanisms and consequences of cardiac triacylglycerol accumulation in insulin-resistant rats. *Am J Physiol Endocrinol Metab* **284**, E923-E930.
- Austen WG, Edwards JE, Frye RL, Gensini GG, Gott VL, Griffith LS, McGoon DC, Murphy ML, & Roe BB (1975). A reporting system on patients evaluated for coronary artery disease. Report of the Ad Hoc Committee for Grading of Coronary Artery Disease, Council on Cardiovascular Surgery, American Heart Association. *Circulation* **51**, 5-40.
- Badimon JJ, Fuster V, Chesebro JH, & Badimon L (1993). Coronary atherosclerosis. A multifactorial disease. *Circulation* **87**, I13-16.
- Bailey JE & Ollis DF (1986). *Biochemical engineering fundamentals*, 2nd ed., pp. 247. McGraw-Hill, New York.
- Baker AR, Silva NF, Quinn DW, Harte AL, Pagano D, Bonser RS, Kumar S, & McTernan PG (2006). Human epicardial adipose tissue expresses a pathogenic profile of adipocytokines in patients with cardiovascular disease. *Cardiovasc Diabetol* **5**, 1.
- Barandier C, Montani JP, & Yang Z (2005). Mature adipocytes and perivascular adipose tissue stimulate vascular smooth muscle cell proliferation: effects of aging and obesity. *Am J Physiol Heart Circ Physiol* **289**, H1807-H1813.
- Barr RL & Lopaschuk GD (2000). Methodology for measuring in vitro/ex vivo cardiac energy metabolism. *J Pharmacol Toxicol Methods* **43**, 141-152.
- Bartelt A, Bruns OT, Reimer R, Hohenberg H, Itrich H, Peldschus K, Kaul MG, Tromsdorf UI, Weller H, Waurisch C, Eychmuller A, Gortds PL, Rinninger F, Bruegelmann K, Freund B, Nielsen P, Merkel M, & Heeren J (2011). Brown adipose tissue activity controls triglyceride clearance. *Nat Med* **17**, 200-205.
- Bergmann SR, Weinheimer CJ, Markham J, & Herrero P (1996). Quantitation of myocardial fatty acid metabolism using PET. *J Nucl Med* **37**, 1723-1730.
- Bickerton AS, Roberts R, Fielding BA, Hodson L, Blaak EE, Wagenmakers AJ, Gilbert M, Karpe F, & Frayn KN (2007). Preferential uptake of dietary Fatty acids in

## REFERENCES

- adipose tissue and muscle in the postprandial period. *Diabetes* **56**, 168-176.
- Bickerton AS, Roberts R, Fielding BA, Tornqvist H, Blaak EE, Wagenmakers AJ, Gilbert M, Humphreys SM, Karpe F, & Frayn KN (2008). Adipose tissue fatty acid metabolism in insulin-resistant men. *Diabetologia* **51**, 1466-1474.
- Blaak EE (2004). Basic disturbances in skeletal muscle fatty acid metabolism in obesity and type 2 diabetes mellitus. *Proc Nutr Soc* **63**, 323-330.
- Boden G (1997). Role of fatty acids in the pathogenesis of insulin resistance and NIDDM. *Diabetes* **46**, 3-10.
- Boden G (1998). Free fatty acids (FFA), a link between obesity and insulin resistance. *Front Biosci* **3**, d169-d175.
- Boden G (2008). Obesity and free fatty acids. *Endocrinol Metab Clin North Am* **37**, 635-6ix.
- Boden G (2011). Obesity, insulin resistance and free fatty acids. *Curr Opin Endocrinol Diabetes Obes* **18**, 139-143.
- Boden G & Chen X (1995). Effects of fat on glucose uptake and utilization in patients with non-insulin-dependent diabetes. *J Clin Invest* **96**, 1261-1268.
- Boden G, Chen X, Ruiz J, White JV, & Rossetti L (1994). Mechanisms of fatty acid-induced inhibition of glucose uptake. *J Clin Invest* **93**, 2438-2446.
- Boden G, Jadali F, White J, Liang Y, Mozzoli M, Chen X, Coleman E, & Smith C (1991). Effects of fat on insulin-stimulated carbohydrate metabolism in normal men. *J Clin Invest* **88**, 960-966.
- Boden WE (2010). Ranolazine and its anti-ischemic effects: revisiting an old mechanistic paradigm anew? *J Am Coll Cardiol* **56**, 943-945.
- Boesch C, Slotboom J, Hoppeler H, & Kreis R (1997). In vivo determination of intra-myocellular lipids in human muscle by means of localized <sup>1</sup>H-MR-spectroscopy. *Magn Reson Med* **37**, 484-493.
- Bonen A, Chabowski A, Luiken JJ, & Glatz JF (2007). Is membrane transport of FFA mediated by lipid, protein, or both? Mechanisms and regulation of protein-mediated cellular fatty acid uptake: molecular, biochemical, and physiological evidence. *Physiology (Bethesda)* **22**, 15-29.
- Borra RJH. Nonalcoholic fatty liver disease in obesity and type 2 diabetes: studies using <sup>1</sup>H MRS and PET. 2009. Turku : University of Turku. Annales Universitatis Turkuensis. Ref Type: Thesis/Dissertation
- Boucher FR, Hearse DJ, & Opie LH (1994). Effects of trimetazidine on ischemic contracture in isolated perfused rat hearts. *J Cardiovasc Pharmacol* **24**, 45-49.
- Boudina S & Abel ED (2006). Mitochondrial uncoupling: a key contributor to reduced cardiac efficiency in diabetes. *Physiology (Bethesda)* **21**, 250-258.
- Boudina S, Sena S, O'Neill BT, Tathireddy P, Young ME, & Abel ED (2005). Reduced mitochondrial oxidative capacity and increased mitochondrial uncoupling impair myocardial energetics in obesity. *Circulation* **112**, 2686-2695.
- Boudina S, Sena S, Theobald H, Sheng X, Wright JJ, Hu XX, Aziz S, Johnson JJ, Bugger H, Zaha VG, & Abel ED (2007). Mitochondrial energetics in the heart in obesity-related diabetes: direct evidence for increased uncoupled respiration and activation of uncoupling proteins. *Diabetes* **56**, 2457-2466.
- Boveris A, Oshino N, & Chance B (1972). The cellular production of hydrogen peroxide. *Biochem J* **128**, 617-630.
- Brady LJ, Brady PS, Romsos DR, & Hoppel CL (1985). Elevated hepatic mitochondrial and peroxisomal oxidative capacities in fed and starved adult obese (ob/ob) mice. *Biochem J* **231**, 439-444.
- Bray GA (2004). Medical consequences of obesity. *J Clin Endocrinol Metab* **89**, 2583-2589.
- Brindley DN, Kok BP, Kienesberger PC, Lehner R, & Dyck JR (2010). Shedding light on the enigma of myocardial lipotoxicity: the involvement of known and putative regulators of fatty acid storage and mobilization. *Am J Physiol Endocrinol Metab* **298**, E897-E908.
- Bruce CR, Anderson MJ, Carey AL, Newman DG, Bonen A, Kriketos AD, Cooney GJ, & Hawley JA (2003). Muscle oxidative capacity is a better predictor of insulin sensitivity than lipid status. *J Clin Endocrinol Metab* **88**, 5444-5451.
- Cabrero A, Merlos M, Laguna JC, & Carrera MV (2003). Down-regulation of acyl-CoA oxidase gene expression and increased NF-kappaB activity in etomoxir-induced cardiac hypertrophy. *J Lipid Res* **44**, 388-398.
- Calori G, Lattuada G, Piemonti L, Garancini MP, Ragona F, Villa M, Mannino S, Crosignani P, Bosi E, Luzi L, Ruotolo G, & Perseghin G (2011). Prevalence, metabolic features, and prognosis of metabolically healthy obese Italian individuals: the Cremona Study. *Diabetes Care* **34**, 210-215.
- Campbell PJ, Carlson MG, Hill JO, & Nurjhan N (1992). Regulation of free fatty acid metabolism by insulin in humans: role of lipolysis and reesterification. *Am J Physiol* **263**, E1063-E1069.
- Cannon B & Nedergaard J (2004). Brown adipose tissue: function and physiological significance. *Physiol Rev* **84**, 277-359.
- Capaldo B, Napoli R, Di ML, Picardi A, Riccardi G, & Sacca L (1988). Quantitation of forearm glucose and free fatty acid (FFA) disposal in normal subjects and

## REFERENCES

- type II diabetic patients: evidence against an essential role for FFA in the pathogenesis of insulin resistance. *J Clin Endocrinol Metab* **67**, 893-898.
- Chanseume E, Bielicki G, Tardy AL, Renou JP, Freyssenet D, Boirie Y, & Morio B (2008). Impaired resting muscle energetics studied by <sup>31</sup>P-NMR in diet-induced obese rats. *Obesity (Silver Spring)* **16**, 572-577.
- Chaowalit N, Somers VK, Pellikka PA, Rihal CS, & Lopez-Jimenez F (2006). Subepicardial adipose tissue and the presence and severity of coronary artery disease. *Atherosclerosis* **186**, 354-359.
- Chavez AO, Gastaldelli A, Guardado-Mendoza R, Lopez-Alvarenga JC, Leland MM, Tejero ME, Sorice G, Casiraghi F, Davalli A, Bastarrachea RA, Comuzzie AG, DeFronzo RA, & Folli F (2009). Predictive models of insulin resistance derived from simple morphometric and biochemical indices related to obesity and the metabolic syndrome in baboons. *Cardiovasc Diabetol* **8**, 22.
- Choi CS, Savage DB, bu-Elheiga L, Liu ZX, Kim S, Kulkarni A, Distefano A, Hwang YJ, Reznick RM, Codella R, Zhang D, Cline GW, Wakil SJ, & Shulman GI (2007). Continuous fat oxidation in acetyl-CoA carboxylase 2 knockout mice increases total energy expenditure, reduces fat mass, and improves insulin sensitivity. *Proc Natl Acad Sci U S A* **104**, 16480-16485.
- Choi SS & Diehl AM (2008). Hepatic triglyceride synthesis and nonalcoholic fatty liver disease. *Curr Opin Lipidol* **19**, 295-300.
- Chow L, From A, & Seaquist E (2010). Skeletal muscle insulin resistance: the interplay of local lipid excess and mitochondrial dysfunction. *Metabolism* **59**, 70-85.
- Clarke B, Wyatt KM, & McCormack JG (1996). Ranolazine increases active pyruvate dehydrogenase in perfused normoxic rat hearts: evidence for an indirect mechanism. *J Mol Cell Cardiol* **28**, 341-350.
- Clarke NE & Mosher RE (1952). The water and electrolyte content of the human heart in congestive heart failure with and without digitalization. *Circulation* **5**, 907-914.
- Colberg SR, Simoneau JA, Thaete FL, & Kelley DE (1995). Skeletal muscle utilization of free fatty acids in women with visceral obesity. *J Clin Invest* **95**, 1846-1853.
- Cole MA, Murray AJ, Cochlin LE, Heather LC, McAleese S, Knight NS, Sutton E, Jamil AA, Parassol N, & Clarke K (2011). A high fat diet increases mitochondrial fatty acid oxidation and uncoupling to decrease efficiency in rat heart. *Basic Res Cardiol* **106**, 447-457.
- Cook GA & Gamble MS (1987). Regulation of carnitine palmitoyltransferase by insulin results in decreased activity and decreased apparent Ki values for malonyl-CoA. *J Biol Chem* **262**, 2050-2055.
- Coppack SW, Frayn KN, Humphreys SM, Dhar H, & Hockaday TD (1989). Effects of insulin on human adipose tissue metabolism in vivo. *Clin Sci (Lond)* **77**, 663-670.
- Coppack SW, Jensen MD, & Miles JM (1994). In vivo regulation of lipolysis in humans. *J Lipid Res* **35**, 177-193.
- Cusi K (2010). The role of adipose tissue and lipotoxicity in the pathogenesis of type 2 diabetes. *Curr Diab Rep* **10**, 306-315.
- Cusi K (2009). The Epidemic of Type 2 Diabetes Mellitus: Its Links to Obesity, Insulin Resistance, and Lipotoxicity. In *Diabetes and Exercise* pp. 1-52. Humana Press.
- Davidson MH (2008). Niacin use and cutaneous flushing: mechanisms and strategies for prevention. *Am J Cardiol* **101**, 14B-19B.
- Day CP & James OF (1998). Steatohepatitis: a tale of two "hits"? *Gastroenterology* **114**, 842-845.
- de Ferranti S & Mozaffarian D (2008). The perfect storm: obesity, adipocyte dysfunction, and metabolic consequences. *Clin Chem* **54**, 945-955.
- de Jong HW, Rijzewijk LJ, Lubberink M, van der Meer RW, Lamb HJ, Smit JW, Diamant M, & Lammertsma AA (2009). Kinetic models for analysing myocardial [(11)C]palmitate data. *Eur J Nucl Med Mol Imaging* **36**, 966-978.
- de Vos AM, Prokop M, Roos CJ, Meijs MF, van der Schouw YT, Rutten A, Gorter PM, Cramer MJ, Doevendans PA, Rensing BJ, Bartelink ML, Velthuis BK, Mosterd A, & Bots ML (2008). Peri-coronary epicardial adipose tissue is related to cardiovascular risk factors and coronary artery calcification in postmenopausal women. *Eur Heart J* **29**, 777-783.
- DeFronzo RA (1987). Use of the splanchnic/hepatic balance technique in the study of glucose metabolism. *Baillieres Clin Endocrinol Metab* **1**, 837-862.
- DeFronzo RA (2010). Insulin resistance, lipotoxicity, type 2 diabetes and atherosclerosis: the missing links. The Claude Bernard Lecture 2009. *Diabetologia* **53**, 1270-1287.
- DeFronzo RA & Tripathy D (2009). Skeletal muscle insulin resistance is the primary defect in type 2 diabetes. *Diabetes Care* **32 Suppl 2**, S157-S163.
- DeFronzo RA, Tripathy D, Schwenke DC, Banerji M, Bray GA, Buchanan TA, Clement SC, Henry RR, Hodis HN, Kitabchi AE, Mack WJ, Mudaliar S, Ratner RE, Williams K, Stentz FB, Musi N, & Reaven PD (2011). Pioglitazone for diabetes prevention in impaired glucose tolerance. *N Engl J Med* **364**, 1104-1115.

## REFERENCES

- Despres JP (2007). Cardiovascular disease under the influence of excess visceral fat. *Crit Pathw Cardiol* **6**, 51-59.
- Di Napoli P, Di GP, Gaeta MA, Taccardi AA, & Barsotti A (2007). Trimetazidine and reduction in mortality and hospitalization in patients with ischemic dilated cardiomyopathy: a post hoc analysis of the Villa Pini d'Abruzzo Trimetazidine Trial. *J Cardiovasc Pharmacol* **50**, 585-589.
- Di Napoli P, Taccardi AA, & Barsotti A (2005). Long term cardioprotective action of trimetazidine and potential effect on the inflammatory process in patients with ischaemic dilated cardiomyopathy. *Heart* **91**, 161-165.
- Diamond GA & Forrester JS (1979). Analysis of Probability As An Aid in the Clinical-Diagnosis of Coronary-Artery Disease. *New England Journal of Medicine* **300**, 1350-1358.
- Diamond GA, Staniloff HM, Forrester JS, Pollock BH, & Swan HJC (1983). Computer-Assisted Diagnosis in the Non-Invasive Evaluation of Patients with Suspected Coronary-Artery Disease. *Journal of the American College of Cardiology* **1**, 444-445.
- Ding J, Hsu FC, Harris TB, Liu Y, Kritchevsky SB, Szklo M, Ouyang P, Espeland MA, Lohman KK, Criqui MH, Allison M, Bluemke DA, & Carr JJ (2009). The association of pericardial fat with incident coronary heart disease: the Multi-Ethnic Study of Atherosclerosis (MESA). *Am J Clin Nutr* **90**, 499-504.
- Diraison F & Beylot M (1998). Role of human liver lipogenesis and reesterification in triglycerides secretion and in FFA reesterification. *Am J Physiol* **274**, E321-E327.
- Djaberi R, Schuijf JD, van Werkhoven JM, Nucifora G, Jukema JW, & Bax JJ (2008). Relation of epicardial adipose tissue to coronary atherosclerosis. *Am J Cardiol* **102**, 1602-1607.
- Dreyer C, Keller H, Mahfoudi A, Laudet V, Krey G, & Wahli W (1993). Positive regulation of the peroxisomal beta-oxidation pathway by fatty acids through activation of peroxisome proliferator-activated receptors (PPAR). *Biol Cell* **77**, 67-76.
- Dube J & Goodpaster BH (2006). Assessment of intramuscular triglycerides: contribution to metabolic abnormalities. *Curr Opin Clin Nutr Metab Care* **9**, 553-559.
- Durrington PN, Newton RS, Weinstein DB, & Steinberg D (1982). Effects of insulin and glucose on very low density lipoprotein triglyceride secretion by cultured rat hepatocytes. *J Clin Invest* **70**, 63-73.
- Dyck DJ, Peters SJ, Glatz J, Gorski J, Keizer H, Kiens B, Liu S, Richter EA, Spriet LL, van d, V, & Bonen A (1997). Functional differences in lipid metabolism in resting skeletal muscle of various fiber types. *Am J Physiol* **272**, E340-E351.
- El BH, Bernard M, Baetz D, Cabanes E, Cozzone P, Lucien A, & Feuvray D (2000). Changes in intracellular sodium and pH during ischaemia-reperfusion are attenuated by trimetazidine. Comparison between low- and zero-flow ischaemia. *Cardiovasc Res* **47**, 688-696.
- Eroglu S, Sade LE, Yildirim A, Bal U, Ozbicer S, Ozgul AS, Bozbas H, Aydinalp A, & Muderrisoglu H (2009). Epicardial adipose tissue thickness by echocardiography is a marker for the presence and severity of coronary artery disease. *Nutr Metab Cardiovasc Dis* **19**, 211-217.
- Farvid MS, Ng TW, Chan DC, Barrett PH, & Watts GF (2005). Association of adiponectin and resistin with adipose tissue compartments, insulin resistance and dyslipidaemia. *Diabetes Obes Metab* **7**, 406-413.
- Ferrannini E (1988). The theoretical bases of indirect calorimetry: a review. *Metabolism* **37**, 287-301.
- Fragasso G, Pallosi A, Puccetti P, Silipigni C, Rossodivita A, Pala M, Calori G, Alfieri O, & Margonato A (2006a). A randomized clinical trial of trimetazidine, a partial free fatty acid oxidation inhibitor, in patients with heart failure. *J Am Coll Cardiol* **48**, 992-998.
- Fragasso G, Perseghin G, De CF, Esposito A, Pallosi A, Lattuada G, Scifo P, Calori G, Del MA, & Margonato A (2006b). Effects of metabolic modulation by trimetazidine on left ventricular function and phosphocreatine/adenosine triphosphate ratio in patients with heart failure. *Eur Heart J* **27**, 942-948.
- Fragasso G, Piatti Md PM, Monti L, Pallosi A, Setola E, Puccetti P, Calori G, Lopaschuk GD, & Margonato A (2003). Short- and long-term beneficial effects of trimetazidine in patients with diabetes and ischemic cardiomyopathy. *Am Heart J* **146**, E18.
- Fragasso G, Salerno A, Lattuada G, Cuko A, Calori G, Scollo A, Ragogna F, Arioli F, Bassanelli G, Spoladore R, Luzi L, Margonato A, & Perseghin G (2011). Effect of partial inhibition of fatty acid oxidation by trimetazidine on whole body energy metabolism in patients with chronic heart failure. *Heart*.
- Frayn KN (2002). Adipose tissue as a buffer for daily lipid flux. *Diabetologia* **45**, 1201-1210.
- Frayn KN (2003). The glucose-fatty acid cycle: a physiological perspective. *Biochem Soc Trans* **31**, 1115-1119.
- Frayn KN, Coppack SW, Humphreys SM, & Whyte PL (1989). Metabolic characteristics of human adipose tissue in vivo. *Clin Sci (Lond)* **76**, 509-516.
- Frayn KN, Fielding BA, & Summers LK (1997). Investigation of human adipose tissue metabolism in vivo. *J Endocrinol* **155**, 187-189.
- Frayn KN, Karpe F, Fielding BA, Macdonald IA, & Coppack SW (2003). Integrative physiology of human

## REFERENCES

- adipose tissue. *Int J Obes Relat Metab Disord* **27**, 875-888.
- Frayn KN, Langin D, & Karpe F (2008). Fatty acid-induced mitochondrial uncoupling in adipocytes is not a promising target for treatment of insulin resistance unless adipocyte oxidative capacity is increased. *Diabetologia* **51**, 394-397.
- Frederickson DS & Gordon RS (1958). The metabolism of albumin-bound C14-labeled unesterified fatty acids in normal human subjects. *J Clin Invest* **37**, 1504-1515.
- Friedewald WT, Levy RI, & Fredrickson DS (1972). Estimation of the concentration of low-density lipoprotein cholesterol in plasma, without use of the preparative ultracentrifuge. *Clin Chem* **18**, 499-502.
- Fromenty B, Robin MA, Igoudjil A, Mansouri A, & Pessayre D (2004). The ins and outs of mitochondrial dysfunction in NASH. *Diabetes Metab* **30**, 121-138.
- Fruhbeck G, Becerril S, Sainz N, Garrastachu P, & Garcia-Velloso MJ (2009). BAT: a new target for human obesity? *Trends Pharmacol Sci* **30**, 387-396.
- Galster AD, Clutter WE, Cryer PE, Collins JA, & Bier DM (1981). Epinephrine plasma thresholds for lipolytic effects in man: measurements of fatty acid transport with [1-13C]palmitic acid. *J Clin Invest* **67**, 1729-1738.
- Galvez B, de CJ, Herold D, Dubrovska G, Arribas S, Gonzalez MC, Aranguez I, Luft FC, Ramos MP, Gollasch M, & Fernandez Alfonso MS (2006). Perivascular adipose tissue and mesenteric vascular function in spontaneously hypertensive rats 1. *Arterioscler Thromb Vasc Biol* **26**, 1297-1302.
- Gao D, Ning N, Niu X, Hao G, & Meng Z (2011). Trimetazidine: a meta-analysis of randomised controlled trials in heart failure. *Heart* **97**, 278-286.
- Gastaldelli A & Basta G (2010). Ectopic fat and cardiovascular disease: what is the link? *Nutr Metab Cardiovasc Dis* **20**, 481-490.
- Gertz EW, Wisneski JA, Stanley WC, & Neese RA (1988). Myocardial substrate utilization during exercise in humans. Dual carbon-labeled carbohydrate isotope experiments. *J Clin Invest* **82**, 2017-2025.
- Goodpaster BH & Kelley DE (2002). Skeletal muscle triglyceride: marker or mediator of obesity-induced insulin resistance in type 2 diabetes mellitus? *Curr Diab Rep* **2**, 216-222.
- Gorter PM, de Vos AM, van der GY, Stella PR, Doevendans PA, Meijs MF, Prokop M, & Visseren FL (2008). Relation of epicardial and pericoronary fat to coronary atherosclerosis and coronary artery calcium in patients undergoing coronary angiography. *Am J Cardiol* **102**, 380-385.
- Gould KL (2009). Does coronary flow trump coronary anatomy? *JACC Cardiovasc Imaging* **2**, 1009-1023.
- Greif M, Becker A, von ZF, Lebherz C, Lehrke M, Broedl UC, Tittus J, Parhofer K, Becker C, Reiser M, Knez A, & Leber AW (2009). Pericardial adipose tissue determined by dual source CT is a risk factor for coronary atherosclerosis. *Arterioscler Thromb Vasc Biol* **29**, 781-786.
- Group LC, Bonadonna RC, DelPrato S, Ratheiser K, Zyck K, Ferrannini E, & DeFronzo RA (1989). Glucose and free fatty acid metabolism in non-insulin-dependent diabetes mellitus. Evidence for multiple sites of insulin resistance. *J Clin Invest* **84**, 205-213.
- Group LC, Bonadonna RC, Shank M, Petrides AS, & DeFronzo RA (1991). Role of free fatty acids and insulin in determining free fatty acid and lipid oxidation in man. *J Clin Invest* **87**, 83-89.
- Group LC, Bonadonna RC, Simonson DC, Petrides AS, Shank M, & DeFronzo RA (1992). Effect of insulin on oxidative and nonoxidative pathways of free fatty acid metabolism in human obesity. *Am J Physiol* **263**, E79-E84.
- Guiducci L, Jarvisalo M, Kiss J, Nagren K, Viljanen A, Naum AG, Gastaldelli A, Savunen T, Knuuti J, Salvadori PA, Ferrannini E, Nuutila P, & Iozzo P (2006). [11C]palmitate kinetics across the splanchnic bed in arterial, portal and hepatic venous plasma during fasting and euglycemic hyperinsulinemia. *Nucl Med Biol* **33**, 521-528.
- Guo Z, Burguera B, & Jensen MD (2000). Kinetics of intramuscular triglyceride fatty acids in exercising humans. *J Appl Physiol* **89**, 2057-2064.
- Guo ZK (2007). Intramyocellular lipid kinetics and insulin resistance. *Lipids Health Dis* **6**, 18.
- Haarbo J, Gotfredsen A, Hassager C, & Christiansen C (1991). Validation of body composition by dual energy X-ray absorptiometry (DEXA). *Clin Physiol* **11**, 331-341.
- Hagenfeldt L, Wahren J, Pernow B, & Raf L (1972). Uptake of individual free fatty acids by skeletal muscle and liver in man. *J Clin Invest* **51**, 2324-2330.
- Hamacher K, Coenen HH, & Stocklin G (1986). Efficient stereospecific synthesis of no-carrier-added 2-[18F]-fluoro-2-deoxy-D-glucose using aminopolyether supported nucleophilic substitution. *J Nucl Med* **27**, 235-238.
- Hammer S, Snel M, Lamb HJ, Jazet IM, van der Meer RW, Pijl H, Meinders EA, Romijn JA, de RA, & Smit JW (2008). Prolonged caloric restriction in obese patients with type 2 diabetes mellitus decreases myocardial triglyceride content and improves myocardial function. *J Am Coll Cardiol* **52**, 1006-1012.
- Hannukainen JC, Borra R, Linderborg K, Kallio H, Kiss J, Lepomaki V, Kallioikoski KK, Kujala UM, Kaprio J, Heinonen OJ, Komu M, Parkkola R, Ahotupa M, Lehtimäki T, Huupponen R, Iozzo P, & Nuutila P



## REFERENCES

- (2011). Liver and pancreatic fat content and metabolism in healthy monozygotic twins with discordant physical activity. *J Hepatol* **54**, 545-552.
- Hannukainen JC, Kalliokoski KK, Borra RJ, Viljanen AP, Janatuinen T, Kujala UM, Kaprio J, Heinonen OJ, Viljanen T, Haaparanta M, Iozzo P, Parkkola R, & Nuutila P (2010). Higher free fatty acid uptake in visceral than in abdominal subcutaneous fat tissue in men. *Obesity (Silver Spring)* **18**, 261-265.
- Havel R, Naimark A, & Borchgrevink CF (1963). Turnover rate and oxidation of free fatty acids of blood plasma in man during exercise: studies during continuous infusion of palmitate-1-C14. *J Clin Invest* **42**, 1054-1063.
- Havel RJ, Kane JP, Balasse EO, Segel N, & Basso LV (1970). Splanchnic metabolism of free fatty acids and production of triglycerides of very low density lipoproteins in normotriglyceridemic and hypertriglyceridemic humans. *J Clin Invest* **49**, 2017-2035.
- Hellerstein MK (1999). De novo lipogenesis in humans: metabolic and regulatory aspects. *Eur J Clin Nutr* **53 Suppl 1**, S53-S65.
- Henrichot E, Juge-Aubry CE, Pemin A, Pache JC, Velebit V, Dayer JM, Meda P, Chizzolini C, & Meier CA (2005). Production of chemokines by perivascular adipose tissue: a role in the pathogenesis of atherosclerosis? *Arterioscler Thromb Vasc Biol* **25**, 2594-2599.
- Henze E, Huang SC, Ratib O, Hoffman E, Phelps ME, & Schelbert HR (1983). Measurements of regional tissue and blood-pool radiotracer concentrations from serial tomographic images of the heart. *J Nucl Med* **24**, 987-996.
- Hirabara SM, de Oliveira Carvalho CR, Mendonca JR, Piltcher HE, Fernandes LC, & Curi R (2003). Palmitate acutely raises glycogen synthesis in rat soleus muscle by a mechanism that requires its metabolization (Randle cycle). *FEBS Lett* **541**, 109-114.
- Hirabara SM, Silveira LR, Abdulkader F, Carvalho CR, Procopio J, & Curi R (2007). Time-dependent effects of fatty acids on skeletal muscle metabolism. *J Cell Physiol* **210**, 7-15.
- Hodson L & Frayn KN (2011). Hepatic fatty acid partitioning. *Curr Opin Lipidol* **22**, 216-224.
- Hodson L, McQuaid SE, Humphreys SM, Milne R, Fielding BA, Frayn KN, & Karpe F (2010). Greater dietary fat oxidation in obese compared with lean men: an adaptive mechanism to prevent liver fat accumulation? *Am J Physiol Endocrinol Metab* **299**, E584-E592.
- Holubarsch CJ, Rohrbach M, Karrasch M, Boehm E, Polonski L, Ponikowski P, & Rhein S (2007). A double-blind randomized multicentre clinical trial to evaluate the efficacy and safety of two doses of etomoxir in comparison with placebo in patients with moderate congestive heart failure: the ERGO (etomoxir for the recovery of glucose oxidation) study. *Clin Sci (Lond)* **113**, 205-212.
- Houstis N, Rosen ED, & Lander ES (2006). Reactive oxygen species have a causal role in multiple forms of insulin resistance. *Nature* **440**, 944-948.
- Hue L & Taegtmeier H (2009). The Randle cycle revisited: a new head for an old hat. *Am J Physiol Endocrinol Metab* **297**, E578-E591.
- Hulver MW, Berggren JR, Carper MJ, Miyazaki M, Ntambi JM, Hoffman EP, Thyfault JP, Stevens R, Dohm GL, Houmard JA, & Muoio DM (2005). Elevated stearoyl-CoA desaturase-1 expression in skeletal muscle contributes to abnormal fatty acid partitioning in obese humans. *Cell Metab* **2**, 251-261.
- Hulver MW, Berggren JR, Cortright RN, Dudek RW, Thompson RP, Pories WJ, MacDonald KG, Cline GW, Shulman GI, Dohm GL, & Houmard JA (2003). Skeletal muscle lipid metabolism with obesity. *Am J Physiol Endocrinol Metab* **284**, E741-E747.
- Hume R (1966). Prediction of lean body mass from height and weight. *J Clin Pathol* **19**, 389-391.
- Iacobellis G, Gao YJ, & Sharma AM (2008). Do cardiac and perivascular adipose tissue play a role in atherosclerosis? *Curr Diab Rep* **8**, 20-24.
- Iacobellis G, Pistilli D, Gucciardo M, Leonetti F, Miraldi F, Brancaccio G, Gallo P, & di Gioia CR (2005). Adiponectin expression in human epicardial adipose tissue in vivo is lower in patients with coronary artery disease. *Cytokine* **29**, 251-255.
- Iacobellis G & Willens HJ (2009). Echocardiographic epicardial fat: a review of research and clinical applications. *J Am Soc Echocardiogr* **22**, 1311-1319.
- Iozzo P (2009). Viewpoints on the way to the consensus session: where does insulin resistance start? The adipose tissue. *Diabetes Care* **32 Suppl 2**, S168-S173.
- Iozzo P (2010). Metabolic toxicity of the heart: insights from molecular imaging. *Nutr Metab Cardiovasc Dis* **20**, 147-156.
- Iozzo P (2011). Myocardial, perivascular, and epicardial fat. *Diabetes Care* **34 Suppl 2**, S371-S379.
- Iozzo P, Chareonthaitawee P, Di TM, Betteridge DJ, Ferrannini E, & Camici PG (2002). Regional myocardial blood flow and glucose utilization during fasting and physiological hyperinsulinemia in humans. *Am J Physiol Endocrinol Metab* **282**, E1163-E1171.
- Iozzo P, Gastaldelli A, Jarvisalo MJ, Kiss J, Borra R, Buzzigoli E, Viljanen A, Naum G, Viljanen T, Oikonen V, Knutti J, Savunen T, Salvadori PA, Ferrannini E, & Nuutila P (2006). 18F-FDG assessment of glucose disposal and production rates

## REFERENCES

- during fasting and insulin stimulation: a validation study. *J Nucl Med* **47**, 1016-1022.
- Iozzo P, Jarvisalo MJ, Kiss J, Borra R, Naum GA, Viljanen A, Viljanen T, Gastaldelli A, Buzzigoli E, Guiducci L, Barsotti E, Savunen T, Knuuti J, Haaparanta-Solin M, Ferrannini E, & Nuutila P (2007). Quantification of liver glucose metabolism by positron emission tomography: validation study in pigs. *Gastroenterology* **132**, 531-542.
- Iozzo P, Turpeinen AK, Takala T, Oikonen V, Bergman J, Gronroos T, Ferrannini E, Nuutila P, & Knuuti J (2004). Defective liver disposal of free fatty acids in patients with impaired glucose tolerance. *J Clin Endocrinol Metab* **89**, 3496-3502.
- Iozzo P, Turpeinen AK, Takala T, Oikonen V, Solin O, Ferrannini E, Nuutila P, & Knuuti J (2003). Liver uptake of free fatty acids in vivo in humans as determined with 14( R, S)-[18F]fluoro-6-thiaheptadecanoic acid and PET. *Eur J Nucl Med Mol Imaging* **30**, 1160-1164.
- Jensen MD (1995). Gender differences in regional fatty acid metabolism before and after meal ingestion. *J Clin Invest* **96**, 2297-2303.
- Jensen MD (2003). Fate of fatty acids at rest and during exercise: regulatory mechanisms. *Acta Physiol Scand* **178**, 385-390.
- Jensen MD (2008). Role of body fat distribution and the metabolic complications of obesity. *J Clin Endocrinol Metab* **93**, S57-S63.
- Jensen MD, Ekberg K, & Landau BR (2001). Lipid metabolism during fasting. *Am J Physiol Endocrinol Metab* **281**, E789-E793.
- Jensen MD, Nguyen TT, Hernandez MA, Johnson CM, & Murray MJ (1998). Effects of gender on resting leg blood flow: implications for measurement of regional substrate oxidation. *J Appl Physiol* **84**, 141-145.
- Jeong JW, Jeong MH, Yun KH, Oh SK, Park EM, Kim YK, Rhee SJ, Lee EM, Lee J, Yoo NJ, Kim NH, & Park JC (2007). Echocardiographic epicardial fat thickness and coronary artery disease. *Circ J* **71**, 536-539.
- Jeukendrup A & Gleeson M (2010). *Sport nutrition: an introduction to energy production and performance*, 2nd ed., pp. 82. Human Kinetics.
- Jou J, Choi SS, & Diehl AM (2008). Mechanisms of disease progression in nonalcoholic fatty liver disease. *Semin Liver Dis* **28**, 370-379.
- Jun M, Foote C, Lv J, Neal B, Patel A, Nicholls SJ, Grobbee DE, Cass A, Chalmers J, & Perkovic V (2010). Effects of fibrates on cardiovascular outcomes: a systematic review and meta-analysis. *Lancet* **375**, 1875-1884.
- Kahn SE, Hull RL, & Utzschneider KM (2006). Mechanisms linking obesity to insulin resistance and type 2 diabetes. *Nature* **444**, 840-846.
- Kajander S, Ukkonen H, Sipila H, Teras M, & Knuuti J (2009). Low radiation dose imaging of myocardial perfusion and coronary angiography with a hybrid PET/CT scanner. *Clin Physiol Funct Imaging* **29**, 81-88.
- Kampf JP & Kleinfeld AM (2007). Is membrane transport of FFA mediated by lipid, protein, or both? An unknown protein mediates free fatty acid transport across the adipocyte plasma membrane. *Physiology (Bethesda)* **22**, 7-14.
- Kanaley JA, Shadid S, Sheehan MT, Guo Z, & Jensen MD (2009). Relationship between plasma free fatty acid, intramyocellular triglycerides and long-chain acylcarnitines in resting humans. *J Physiol* **587**, 5939-5950.
- Kankaanpaa M, Lehto HR, Parkka JP, Komu M, Viljanen A, Ferrannini E, Knuuti J, Nuutila P, Parkkola R, & Iozzo P (2006). Myocardial triglyceride content and epicardial fat mass in human obesity: relationship to left ventricular function and serum free fatty acid levels. *J Clin Endocrinol Metab* **91**, 4689-4695.
- Kantor PF, Lucien A, Kozak R, & Lopaschuk GD (2000). The antianginal drug trimetazidine shifts cardiac energy metabolism from fatty acid oxidation to glucose oxidation by inhibiting mitochondrial long-chain 3-ketoacyl coenzyme A thiolase. *Circ Res* **86**, 580-588.
- Karelis AD, St-Pierre DH, Conus F, Rabasa-Lhoret R, & Poehlman ET (2004). Metabolic and body composition factors in subgroups of obesity: what do we know? *J Clin Endocrinol Metab* **89**, 2569-2575.
- Karpe F & Chamas L (2010). Hyperlipidaemia and cardiovascular disease: nonantipolytic effects of nicotinic acid in adipose tissue. *Curr Opin Lipidol* **21**, 282-283.
- Karpe F, Dickmann JR, & Frayn KN (2011). Fatty acids, obesity, and insulin resistance: time for a reevaluation. *Diabetes* **60**, 2441-2449.
- Kaufmann PA & Camici PG (2005). Myocardial blood flow measurement by PET: technical aspects and clinical applications. *J Nucl Med* **46**, 75-88.
- Kaufmann PA & Di Carli MF (2009). Hybrid SPECT/CT and PET/CT imaging: the next step in noninvasive cardiac imaging. *Semin Nucl Med* **39**, 341-347.
- Kelley DE, Goodpaster B, Wing RR, & Simoneau JA (1999). Skeletal muscle fatty acid metabolism in association with insulin resistance, obesity, and weight loss. *Am J Physiol* **277**, E1130-E1141.
- Kelley DE & Mandarino LJ (2000). Fuel selection in human skeletal muscle in insulin resistance: a reexamination. *Diabetes* **49**, 677-683.

## REFERENCES

- Kelley DE & Simoneau JA (1994). Impaired free fatty acid utilization by skeletal muscle in non-insulin-dependent diabetes mellitus. *J Clin Invest* **94**, 2349-2356.
- Kenchaiah S, Evans JC, Levy D, Wilson PW, Benjamin EJ, Larson MG, Kannel WB, & Vasan RS (2002). Obesity and the risk of heart failure. *N Engl J Med* **347**, 305-313.
- Kern MJ, Lerman A, Bech JW, De Bruyne B, Eeckhout E, Fearon WF, Higano ST, Lim MJ, Meuwissen M, Piek JJ, Pijls NH, Siebes M, & Spaan JA (2006). Physiological assessment of coronary artery disease in the cardiac catheterization laboratory: a scientific statement from the American Heart Association Committee on Diagnostic and Interventional Cardiac Catheterization, Council on Clinical Cardiology. *Circulation* **114**, 1321-1341.
- Killalea SM & Krum H (2001). Systematic review of the efficacy and safety of perhexiline in the treatment of ischemic heart disease. *Am J Cardiovasc Drugs* **1**, 193-204.
- Kisrieva-Ware Z, Coggan AR, Sharp TL, Dence CS, Gropler RJ, & Herrero P (2009). Assessment of myocardial triglyceride oxidation with PET and <sup>11</sup>C-palmitate. *J Nucl Cardiol* **16**, 411-421.
- Kleiner DE, Brunt EM, Van NM, Behling C, Contos MJ, Cummings OW, Ferrell LD, Liu YC, Torbenson MS, Unalp-Arida A, Yeh M, McCullough AJ, & Sanyal AJ (2005). Design and validation of a histological scoring system for nonalcoholic fatty liver disease. *Hepatology* **41**, 1313-1321.
- Knuuti J & Bengel FM (2008). Positron emission tomography and molecular imaging. *Heart* **94**, 360-367.
- Koonen DP, Sung MM, Kao CK, Dolinsky VW, Koves TR, Ilkayeva O, Jacobs RL, Vance DE, Light PE, Muoio DM, Febbraio M, & Dyck JR (2010). Alterations in skeletal muscle fatty acid handling predisposes middle-aged mice to diet-induced insulin resistance. *Diabetes* **59**, 1366-1375.
- Kotronen A, Juurinen L, Tiikkainen M, Vehkavaara S, & Yki-Jarvinen H (2008a). Increased liver fat, impaired insulin clearance, and hepatic and adipose tissue insulin resistance in type 2 diabetes. *Gastroenterology* **135**, 122-130.
- Kotronen A, Seppala-Lindroos A, Bergholm R, & Yki-Jarvinen H (2008b). Tissue specificity of insulin resistance in humans: fat in the liver rather than muscle is associated with features of the metabolic syndrome. *Diabetologia* **51**, 130-138.
- Koves TR, Ussher JR, Noland RC, Slentz D, Mosedale M, Ilkayeva O, Bain J, Stevens R, Dyck JR, Newgard CB, Lopaschuk GD, & Muoio DM (2008). Mitochondrial overload and incomplete fatty acid oxidation contribute to skeletal muscle insulin resistance. *Cell Metab* **7**, 45-56.
- Lafontan M (2008). Advances in adipose tissue metabolism. *Int J Obes (Lond)* **32 Suppl 7**, S39-S51.
- Langin D (2006). Adipose tissue lipolysis as a metabolic pathway to define pharmacological strategies against obesity and the metabolic syndrome. *Pharmacol Res* **53**, 482-491.
- Lee Y, Hirose H, Ohneda M, Johnson JH, McGarry JD, & Unger RH (1994). Beta-cell lipotoxicity in the pathogenesis of non-insulin-dependent diabetes mellitus of obese rats: impairment in adipocyte-beta-cell relationships. *Proc Natl Acad Sci U S A* **91**, 10878-10882.
- Lelliott C & Vidal-Puig AJ (2004). Lipotoxicity, an imbalance between lipogenesis de novo and fatty acid oxidation  
1. *Int J Obes Relat Metab Disord* **28 Suppl 4**, S22-S28.
- Lewis GF, Uffelman KD, Szeto LW, Weller B, & Steiner G (1995). Interaction between free fatty acids and insulin in the acute control of very low density lipoprotein production in humans. *J Clin Invest* **95**, 158-166.
- Li YJ, Wang PH, Chen C, Zou MH, & Wang DW (2010). Improvement of mechanical heart function by trimetazidine in db/db mice. *Acta Pharmacol Sin* **31**, 560-569.
- Li Z, Berk M, McIntyre TM, Gores GJ, & Feldstein AE (2008). The lysosomal-mitochondrial axis in free fatty acid-induced hepatic lipotoxicity. *Hepatology* **47**, 1495-1503.
- Liu X, Gai Y, Liu F, Gao W, Zhang Y, Xu M, & Li Z (2010). Trimetazidine inhibits pressure overload-induced cardiac fibrosis through NADPH oxidase-ROS-CTGF pathway. *Cardiovasc Res* **88**, 150-158.
- Loke YK, Kwok CS, & Singh S (2011). Comparative cardiovascular effects of thiazolidinediones: systematic review and meta-analysis of observational studies. *BMJ* **342**, d1309.
- Lopaschuk GD, Barr R, Thomas PD, & Dyck JR (2003). Beneficial effects of trimetazidine in ex vivo working ischemic hearts are due to a stimulation of glucose oxidation secondary to inhibition of long-chain 3-ketoacyl coenzyme a thiolase. *Circ Res* **93**, e33-e37.
- Lopaschuk GD, Ussher JR, Folmes CD, Jaswal JS, & Stanley WC (2010). Myocardial fatty acid metabolism in health and disease. *Physiol Rev* **90**, 207-258.
- Luiken JJ, Niessen HE, Coort SL, Hoebers N, Coumans WA, Schwenk RW, Bonen A, & Glatz JF (2009). Etomoxir-induced partial carnitine palmitoyltransferase-I (CPT-I) inhibition in vivo does not alter cardiac long-chain fatty acid uptake and oxidation rates. *Biochem J* **419**, 447-455.
- Mahabadi AA, Massaro JM, Rosito GA, Levy D, Murabito JM, Wolf PA, O'Donnell CJ, Fox CS, &

## REFERENCES

- Hoffmann U (2009). Association of pericardial fat, intrathoracic fat, and visceral abdominal fat with cardiovascular disease burden: the Framingham Heart Study. *Eur Heart J* **30**, 850-856.
- Maki MT, Haaparanta M, Nuutila P, Oikonen V, Luotolahti M, Eskola O, & Knuuti JM (1998). Free fatty acid uptake in the myocardium and skeletal muscle using fluorine-18-fluoro-6-thia-heptadecanoic acid. *J Nucl Med* **39**, 1320-1327.
- Malmstrom R, Packard CJ, Caslake M, Bedford D, Stewart P, Yki-Jarvinen H, Shepherd J, & Taskinen MR (1998). Effects of insulin and acipimox on VLDL1 and VLDL2 apolipoprotein B production in normal subjects. *Diabetes* **47**, 779-787.
- Maridonneau-Parini I & Harpey C (1985). Effect of trimetazidine on membrane damage induced by oxygen free radicals in human red cells. *Br J Clin Pharmacol* **20**, 148-151.
- Matsuzawa-Nagata N, Takamura T, Ando H, Nakamura S, Kurita S, Misu H, Ota T, Yokoyama M, Honda M, Miyamoto K, & Kaneko S (2008). Increased oxidative stress precedes the onset of high-fat diet-induced insulin resistance and obesity. *Metabolism* **57**, 1071-1077.
- Mazurek T, Zhang L, Zalewski A, Mannion JD, Diehl JT, Arafat H, Sarov-Blat L, O'Brien S, Keiper EA, Johnson AG, Martin J, Goldstein BJ, & Shi Y (2003). Human epicardial adipose tissue is a source of inflammatory mediators. *Circulation* **108**, 2460-2466.
- McClain CJ, Barve S, & Deaciuc I (2007). Good fat/bad fat. *Hepatology* **45**, 1343-1346.
- McCormack JG, Barr RL, Wolff AA, & Lopaschuk GD (1996). Ranolazine stimulates glucose oxidation in normoxic, ischemic, and reperfused ischemic rat hearts. *Circulation* **93**, 135-142.
- McGarry JD (1992). What if Minkowski had been ageusic? An alternative angle on diabetes. *Science* **258**, 766-770.
- McGarry JD, Mannaerts GP, & Foster DW (1977). A possible role for malonyl-CoA in the regulation of hepatic fatty acid oxidation and ketogenesis. *J Clin Invest* **60**, 265-270.
- McGavock JM, Lingvay I, Zib I, Tillery T, Salas N, Unger R, Levine BD, Raskin P, Victor RG, & Szczepaniak LS (2007). Cardiac steatosis in diabetes mellitus: a 1H-magnetic resonance spectroscopy study. *Circulation* **116**, 1170-1175.
- McQuaid SE, Hodson L, Neville MJ, Dennis AL, Cheeseman J, Humphreys SM, Ruge T, Gilbert M, Fielding BA, Frayn KN, & Karpe F (2011). Downregulation of adipose tissue fatty acid trafficking in obesity: a driver for ectopic fat deposition? *Diabetes* **60**, 47-55.
- Meek SE, Nair KS, & Jensen MD (1999). Insulin regulation of regional free fatty acid metabolism. *Diabetes* **48**, 10-14.
- Meier C, Wahllaender A, Hess CW, & Preisig R (1986). Perhexiline-induced lipidosis in the dark Agouti (DA) rat. An animal model of genetically determined neurotoxicity. *Brain* **109** (Pt 4), 649-660.
- Merrill CL, Ni H, Yoon LW, Tirmenstein MA, Narayanan P, Benavides GR, Easton MJ, Creech DR, Hu CX, McFarland DC, Hahn LM, Thomas HC, & Morgan KT (2002). Etomoxir-induced oxidative stress in HepG2 cells detected by differential gene expression is confirmed biochemically. *Toxicol Sci* **68**, 93-101.
- Miles JM, Park YS, Walewicz D, Russell-Lopez C, Windsor S, Isley WL, Coppack SW, & Harris WS (2004). Systemic and forearm triglyceride metabolism: fate of lipoprotein lipase-generated glycerol and free fatty acids. *Diabetes* **53**, 521-527.
- Mittendorfer B (2011). Origins of metabolic complications in obesity: adipose tissue and free fatty acid trafficking. *Curr Opin Clin Nutr Metab Care*.
- Mittendorfer B, Liem O, Patterson BW, Miles JM, & Klein S (2003). What does the measurement of whole-body fatty acid rate of appearance in plasma by using a fatty acid tracer really mean? *Diabetes* **52**, 1641-1648.
- Mittendorfer B, Magkos F, Fabbrini E, Mohammed BS, & Klein S (2009). Relationship between body fat mass and free fatty acid kinetics in men and women. *Obesity (Silver Spring)* **17**, 1872-1877.
- Mittendorfer B & Peterson LR (2008). Cardiovascular Consequences of Obesity and Targets for Treatment. *Drug Discov Today Ther Strateg* **5**, 53-61.
- Miyazaki Y, De Filippis E, Bajaj M, Wajsborg E, Glass L, Triplitt C, Cersosimo E, Mandarino LJ, & DeFronzo RA (2005). Predictors of improved glycaemic control with rosiglitazone therapy in type 2 diabetic patients: a practical approach for the primary care physician. *The British Journal of Diabetes & Vascular Disease* **5**, 28-35.
- Mohrman DE & Heller LJ (2006). *Cardiovascular physiology*, 6 ed., pp. 239. Appleton & Lange, Stamford, Conn.
- Montague CT, Prins JB, Sanders L, Zhang J, Sewter CP, Digby J, Byrne CD, & O'Rahilly S (1998). Depot-related gene expression in human subcutaneous and omental adipocytes. *Diabetes* **47**, 1384-1391.
- Monti LD, Setola E, Fragasso G, Camisasca RP, Lucotti P, Galluccio E, Origgi A, Margonato A, & Piatti P (2006). Metabolic and endothelial effects of trimetazidine on forearm skeletal muscle in patients with type 2 diabetes and ischemic cardiomyopathy. *Am J Physiol Endocrinol Metab* **290**, E54-E59.
- Muller MJ (1998). Hepatic energy and substrate metabolism: a possible metabolic basis for early

## REFERENCES

- nutritional support in cirrhotic patients. *Nutrition* **14**, 30-38.
- Muniyappa R, Lee S, Chen H, & Quon MJ (2008). Current approaches for assessing insulin sensitivity and resistance in vivo: advantages, limitations, and appropriate usage. *Am J Physiol Endocrinol Metab* **294**, E15-E26.
- Muoio DM & Newgard CB (2006). Obesity-related derangements in metabolic regulation. *Annu Rev Biochem* **75**, 367-401.
- Nair KS, Bigelow ML, Asmann YW, Chow LS, Coenen-Schimke JM, Klaus KA, Guo ZK, Sreekumar R, & Irving BA (2008). Asian Indians have enhanced skeletal muscle mitochondrial capacity to produce ATP in association with severe insulin resistance. *Diabetes* **57**, 1166-1175.
- Nakamura S, Takamura T, Matsuzawa-Nagata N, Takayama H, Misu H, Noda H, Nabemoto S, Kurita S, Ota T, Ando H, Miyamoto K, & Kaneko S (2009). Palmitate induces insulin resistance in H4IIEC3 hepatocytes through reactive oxygen species produced by mitochondria. *J Biol Chem* **284**, 14809-14818.
- Nelson AJ, Worthley MI, Psaltis PJ, Carbone A, Dundon BK, Duncan RF, Piantadosi C, Lau DH, Sanders P, Wittert GA, & Worthley SG (2009). Validation of cardiovascular magnetic resonance assessment of pericardial adipose tissue volume. *J Cardiovasc Magn Reson* **11**, 15.
- Nestel PJ, Ishikawa T, & Goldrick RB (1978). Diminished plasma free fatty acid clearance in obese subjects. *Metabolism* **27**, 589-597.
- Nesterov SV, Han C, Maki M, Kajander S, Naum AG, Helenius H, Lisinen I, Ukkonen H, Pietila M, Joutsiniemi E, & Knuuti J (2009). Myocardial perfusion quantitation with (15)O-labelled water PET: high reproducibility of the new cardiac analysis software (Carimas). *Eur J Nucl Med Mol Imaging*.
- Ng CK, Holden JE, DeGrado TR, Raffel DM, Kornguth ML, & Gatley SJ (1991). Sensitivity of myocardial fluorodeoxyglucose lumped constant to glucose and insulin. *Am J Physiol* **260**, H593-H603.
- Nielsen S, Guo Z, Johnson CM, Hensrud DD, & Jensen MD (2004). Splanchnic lipolysis in human obesity. *J Clin Invest* **113**, 1582-1588.
- Nikolaidis MG, Petridou A, & Mougios V (2006). Comparison of the phospholipid and triacylglycerol fatty acid profile of rat serum, skeletal muscle and heart. *Physiol Res* **55**, 259-265.
- Nussey S & Whitehead SA (2001). *Endocrinology: an integrated approach* BIOS Scientific Publishers, Oxford, UK.
- Nuutila P, Koivisto VA, Knuuti J, Ruotsalainen U, Teras M, Haaparanta M, Bergman J, Solin O, Voipio-Pulkki LM, Wegelius U, & . (1992). Glucose-free fatty acid cycle operates in human heart and skeletal muscle in vivo. *J Clin Invest* **89**, 1767-1774.
- Opie LH & Knuuti J (2009). The adrenergic-fatty acid load in heart failure. *J Am Coll Cardiol* **54**, 1637-1646.
- Ostman J, Arner P, Engfeldt P, & Kager L (1979). Regional differences in the control of lipolysis in human adipose tissue. *Metabolism* **28**, 1198-1205.
- Padgett HC, Robinson GD, & Barrio JR (1982). [1-(11)C]palmitic acid: improved radiopharmaceutical preparation. *Int J Appl Radiat Isot* **33**, 1471-1472.
- Pagotto U (2009). Where does insulin resistance start? The brain. *Diabetes Care* **32 Suppl 2**, S174-S177.
- Patlak CS & Blasberg RG (1985). Graphical evaluation of blood-to-brain transfer constants from multiple-time uptake data. Generalizations. *J Cereb Blood Flow Metab* **5**, 584-590.
- Payne GA, Bohlen HG, Dincer UD, Borbouse L, & Tune JD (2009). Periadventitial adipose tissue impairs coronary endothelial function via PKC-beta-dependent phosphorylation of nitric oxide synthase. *Am J Physiol Heart Circ Physiol* **297**, H460-H465.
- Payne GA, Borbouse L, Bratz IN, Roell WC, Bohlen HG, Dick GM, & Tune JD (2008). Endogenous adipose-derived factors diminish coronary endothelial function via inhibition of nitric oxide synthase. *Microcirculation* **15**, 417-426.
- Peltoniemi P, Lonnroth P, Laine H, Oikonen V, Tolvanen T, Gronroos T, Strindberg L, Knuuti J, & Nuutila P (2000). Lumped constant for [(18)F]fluorodeoxyglucose in skeletal muscles of obese and nonobese humans. *Am J Physiol Endocrinol Metab* **279**, E1122-E1130.
- Perseghin G (2005). Muscle lipid metabolism in the metabolic syndrome. *Curr Opin Lipidol* **16**, 416-420.
- Perseghin G (2009). Viewpoints on the way to a consensus session: where does insulin resistance start? The liver. *Diabetes Care* **32 Suppl 2**, S164-S167.
- Perseghin G (2011). Lipids in the wrong place: visceral fat and nonalcoholic steatohepatitis. *Diabetes Care* **34 Suppl 2**, S367-S370.
- Perseghin G, Petersen K, & Shulman GI (2003). Cellular mechanism of insulin resistance: potential links with inflammation. *Int J Obes Relat Metab Disord* **27 Suppl 3**, S6-11.
- Perseghin G, Scifo P, Danna M, Battezzati A, Benedini S, Meneghini E, Del MA, & Luzi L (2002). Normal insulin sensitivity and IMCL content in overweight humans are associated with higher fasting lipid oxidation. *Am J Physiol Endocrinol Metab* **283**, E556-E564.
- Peterson LR, Herrero P, Schechtman KB, Racette SB, Waggoner AD, Kisrieva-Ware Z, Dence C, Klein S, Marsala J, Meyer T, & Gropler RJ (2004). Effect of

## REFERENCES

- obesity and insulin resistance on myocardial substrate metabolism and efficiency in young women. *Circulation* **109**, 2191-2196.
- Pijls NH, de Bruyne B, Peels K, Van Der Voort PH, Bonnier HJ, Bartunek JKJ, & Koolen JJ (1996). Measurement of fractional flow reserve to assess the functional severity of coronary-artery stenoses. *N Engl J Med* **334**, 1703-1708.
- Pilo A, Zucchelli GC, Malvano R, & Masini S (1982). Main features of computer algorithms for RIA data reduction; comparison of some different approaches for the interpolation of the dose-response curve. *J Nucl Med Allied Sci* **26**, 235-248.
- Price RA, Charles MA, Pettitt DJ, & Knowler WC (1993). Obesity in Pima Indians: large increases among post-World War II birth cohorts. *Am J Phys Anthropol* **92**, 473-479.
- Prout W (1827). On the ultimate composition of simple alimentary substances; with some preliminary remarks on the analysis of organized bodies in general. *Philos Trans R Soc London* **357**.
- Provencher SW (1993). Estimation of metabolite concentrations from localized in vivo proton NMR spectra. *Magn Reson Med* **30**, 672-679.
- Randle P, Garland P, Hales C, & Newsholme E (1963). The glucose fatty-acid cycle. Its role in insulin sensitivity and the metabolic disturbances of diabetes mellitus. *Lancet* **1**, 785-789.
- Rigazio S, Lehto HR, Tuunanen H, Nagren K, Kankaanpaa M, Simi C, Borra R, Naum AG, Parkkola R, Knuuti J, Nuutila P, & Iozzo P (2008). The lowering of hepatic fatty acid uptake improves liver function and insulin sensitivity without affecting hepatic fat content in humans. *Am J Physiol Endocrinol Metab* **295**, E413-E419.
- Rijzewijk LJ, van der Meer RW, Smit JW, Diamant M, Bax JJ, Hammer S, Romijn JA, de RA, & Lamb HJ (2008). Myocardial steatosis is an independent predictor of diastolic dysfunction in type 2 diabetes mellitus. *J Am Coll Cardiol* **52**, 1793-1799.
- Roden M (2004). How free fatty acids inhibit glucose utilization in human skeletal muscle. *News Physiol Sci* **19**, 92-96.
- Roden M, Price TB, Perseghin G, Petersen KF, Rothman DL, Cline GW, & Shulman GI (1996). Mechanism of free fatty acid-induced insulin resistance in humans. *J Clin Invest* **97**, 2859-2865.
- Rosito GA, Massaro JM, Hoffmann U, Ruberg FL, Mahabadi AA, Vasan RS, O'Donnell CJ, & Fox CS (2008). Pericardial fat, visceral abdominal fat, cardiovascular disease risk factors, and vascular calcification in a community-based sample: the Framingham Heart Study. *Circulation* **117**, 605-613.
- Ross R (1999). Atherosclerosis--an inflammatory disease. *N Engl J Med* **340**, 115-126.
- Ruge T, Hodson L, Cheeseman J, Dennis AL, Fielding BA, Humphreys SM, Frayn KN, & Karpe F (2009). Fasted to fed trafficking of Fatty acids in human adipose tissue reveals a novel regulatory step for enhanced fat storage. *J Clin Endocrinol Metab* **94**, 1781-1788.
- Russell AP, Gastaldi G, Bobbioni-Harsch E, Arboit P, Gobelet C, Deriaz O, Golay A, Witztum JL, & Giacobino JP (2003). Lipid peroxidation in skeletal muscle of obese as compared to endurance-trained humans: a case of good vs. bad lipids? *FEBS Lett* **551**, 104-106.
- Sacchetti M, Saltin B, Olsen DB, & van HG (2004). High triacylglycerol turnover rate in human skeletal muscle. *J Physiol* **561**, 883-891.
- Sade LE, Eroglu S, Bozbas H, Ozbicer S, Hayran M, Haberal A, & Muderrisoglu H (2009). Relation between epicardial fat thickness and coronary flow reserve in women with chest pain and angiographically normal coronary arteries. *Atherosclerosis* **204**, 580-585.
- Santomauro AT, Boden G, Silva ME, Rocha DM, Santos RF, Ursich MJ, Strassmann PG, & Wajchenberg BL (1999). Overnight lowering of free fatty acids with Acipimox improves insulin resistance and glucose tolerance in obese diabetic and nondiabetic subjects. *Diabetes* **48**, 1836-1841.
- Sanyal AJ, Campbell-Sargent C, Mirshahi F, Rizzo WB, Contos MJ, Sterling RK, Luketic VA, Shiffman ML, & Clore JN (2001). Nonalcoholic steatohepatitis: association of insulin resistance and mitochondrial abnormalities. *Gastroenterology* **120**, 1183-1192.
- Sarin S, Wenger C, Marwaha A, Qureshi A, Go BD, Woomert CA, Clark K, Nassef LA, & Shirani J (2008). Clinical significance of epicardial fat measured using cardiac multislice computed tomography. *Am J Cardiol* **102**, 767-771.
- Schelbert HR, Henze E, Sochor H, Grossman RG, Huang SC, Barrio JR, Schwaiger M, & Phelps ME (1986). Effects of substrate availability on myocardial C-11 palmitate kinetics by positron emission tomography in normal subjects and patients with ventricular dysfunction. *Am Heart J* **111**, 1055-1064.
- Schenker MP, Dorbala S, Hong EC, Rybicki FJ, Hachamovitch R, Kwong RY, & Di Carli MF (2008). Interrelation of coronary calcification, myocardial ischemia, and outcomes in patients with intermediate likelihood of coronary artery disease: a combined positron emission tomography/computed tomography study. *Circulation* **117**, 1693-1700.
- Schepis T, Gaemperli O, Koepfli P, Ruegg C, Burger C, Leschka S, Desbiolles L, Husmann L, Alkadhi H, & Kaufmann PA (2007). Use of coronary calcium score scans from stand-alone multislice computed

## REFERENCES

- tomography for attenuation correction of myocardial perfusion SPECT 1. *Eur J Nucl Med Mol Imaging* **34**, 11-19.
- Schick F, Eismann B, Jung WI, Bongers H, Bunse M, & Lutz O (1993). Comparison of localized proton NMR signals of skeletal muscle and fat tissue in vivo: two lipid compartments in muscle tissue. *Magn Reson Med* **29**, 158-167.
- Schmitz FJ, Rosen P, & Reinauer H (1995). Improvement of myocardial function and metabolism in diabetic rats by the carnitine palmitoyl transferase inhibitor Etomoxir. *Horm Metab Res* **27**, 515-522.
- Schon HR, Schelbert HR, Najafi A, Hansen H, Huang H, Barrio J, & Phelps ME (1982). C- 11 labeled palmitic acid for the noninvasive evaluation of regional myocardial fatty acid metabolism with positron-computed tomography. II. Kinetics of C- 11 palmitic acid in acutely ischemic myocardium. *Am Heart J* **103**, 548-561.
- Schwarzer M, Faerber G, Rueckauer T, Blum D, Pytel G, Mohr FW, & Doenst T (2009). The metabolic modulators, Etomoxir and NVP-LAB121, fail to reverse pressure overload induced heart failure in vivo. *Basic Res Cardiol* **104**, 547-557.
- Sederholm K. Globaali optimointi positroniemissio-tomografia-kvantantamiseen liittyvässä mallintamisessa. Pro Gradu. Turun yliopisto. 2003. Ref Type: Thesis/Dissertation
- Sentex E, Helies-Toussaint C, Rousseau D, Lucien A, Ferrary E, & Grynberg A (2001). Influence of trimetazidine on the synthesis of complex lipids in the heart and other target organs. *Fundam Clin Pharmacol* **15**, 255-264.
- Sentex E, Sergiel JP, Lucien A, & Grynberg A (1997). Trimetazidine increases phospholipid turnover in ventricular myocyte. *Mol Cell Biochem* **175**, 153-162.
- Shah P & Mudaliar S (2010). Pioglitazone: side effect and safety profile. *Expert Opin Drug Saf* **9**, 347-354.
- Sidossis LS, Mittendorfer B, Chinkes D, Walser E, & Wolfe RR (1999). Effect of hyperglycemia-hyperinsulinemia on whole body and regional fatty acid metabolism. *Am J Physiol* **276**, E427-E434.
- Sipilä H, Clark JC, Peltola O, & Teräs M (2001). An automatic [<sup>15</sup>O]H<sub>2</sub>O production system for heart and brain studies. *J Labelled Comp Rad* **44**, S1066-S1068.
- Smith SC, Jr., Greenland P, & Grundy SM (2000). AHA Conference Proceedings. Prevention conference V: Beyond secondary prevention: Identifying the high-risk patient for primary prevention: executive summary. American Heart Association. *Circulation* **101**, 111-116.
- Sokoloff L, Reivich M, Kennedy C, Des Rosiers MH, Patlak CS, Pettigrew KD, Sakurada O, & Shinohara M (1977). The [<sup>14</sup>C]deoxyglucose method for the measurement of local cerebral glucose utilization: theory, procedure, and normal values in the conscious and anesthetized albino rat. *J Neurochem* **28**, 897-916.
- Spector AA (1975). Fatty acid binding to plasma albumin. *J Lipid Res* **16**, 165-179.
- Staels B, Dallongeville J, Auwerx J, Schoonjans K, Leitersdorf E, & Fruchart JC (1998). Mechanism of action of fibrates on lipid and lipoprotein metabolism. *Circulation* **98**, 2088-2093.
- Stanley WC, Lopaschuk GD, Hall JL, & McCormack JG (1997). Regulation of myocardial carbohydrate metabolism under normal and ischaemic conditions. Potential for pharmacological interventions. *Cardiovasc Res* **33**, 243-257.
- Stern D & Maickel R (1963). Studies on starvation-induced hypermobilization of free fatty acids (FFA). *Life Sci* **11**, 872-877.
- Stipanuk MH (2006). *Biochemical, physiological, & molecular aspects of human nutrition* 16, 2 ed., pp. 471. Elsevier Saunders, Philadelphia, Pa.
- Swinburn BA, Nyomba BL, Saad MF, Zurlo F, Raz I, Knowler WC, Lillioja S, Bogardus C, & Ravussin E (1991). Insulin resistance associated with lower rates of weight gain in Pima Indians. *J Clin Invest* **88**, 168-173.
- Szczepaniak LS, Babcock EE, Schick F, Dobbins RL, Garg A, Burns DK, McGarry JD, & Stein DT (1999). Measurement of intracellular triglyceride stores by H spectroscopy: validation in vivo. *Am J Physiol* **276**, E977-E989.
- Szczepaniak LS, Dobbins RL, Metzger GJ, Sartoni-D'Ambrosia G, Arbique D, Vongpatanasin W, Unger R, & Victor RG (2003). Myocardial triglycerides and systolic function in humans: in vivo evaluation by localized proton spectroscopy and cardiac imaging. *Magn Reson Med* **49**, 417-423.
- Tabbi-Anneni I, Helies-Toussaint C, Morin D, Bescond-Jacquet A, Lucien A, & Grynberg A (2003). Prevention of heart failure in rats by trimetazidine treatment: a consequence of accelerated phospholipid turnover? *J Pharmacol Exp Ther* **304**, 1003-1009.
- Taegtmeyer H & Harmancey R (2008). Virchow's metamorphosis revealed triglycerides in the heart. *J Am Coll Cardiol* **52**, 1013-1014.
- Taguchi R, Takasu J, Itani Y, Yamamoto R, Yokoyama K, Watanabe S, & Masuda Y (2001). Pericardial fat accumulation in men as a risk factor for coronary artery disease. *Atherosclerosis* **157**, 203-209.
- Takala TO, Nuutila P, Pulkki K, Oikonen V, Gronroos T, Savunen T, Vahasilta T, Luotolahti M, Kallajoki M, Bergman J, Forsback S, & Knuuti J (2002). 14(R,S)-[18F]Fluoro-6-thia-heptadecanoic acid as a tracer of free fatty acid uptake and oxidation in myocardium and

## REFERENCES

- skeletal muscle. *Eur J Nucl Med Mol Imaging* **29**, 1617-1622.
- Takamura T, Misu H, Matsuzawa-Nagata N, Sakurai M, Ota T, Shimizu A, Kurita S, Takeshita Y, Ando H, Honda M, & Kaneko S (2008). Obesity upregulates genes involved in oxidative phosphorylation in livers of diabetic patients. *Obesity (Silver Spring)* **16**, 2601-2609.
- Taskinen MR, Bogardus C, Kennedy A, & Howard BV (1985). Multiple disturbances of free fatty acid metabolism in noninsulin-dependent diabetes. Effect of oral hypoglycemic therapy. *J Clin Invest* **76**, 637-644.
- Tataranni PA & Ortega E (2005). A burning question: does an adipokine-induced activation of the immune system mediate the effect of overnutrition on type 2 diabetes? *Diabetes* **54**, 917-927.
- Thaler H (1975). Relation of steatosis to cirrhosis. *Clin Gastroenterol* **4**, 273-280.
- Thomsen C, Becker U, Winkler K, Christoffersen P, Jensen M, & Henriksen O (1994). Quantification of liver fat using magnetic resonance spectroscopy. *Magn Reson Imaging* **12**, 487-495.
- Thyfault JP, Kraus RM, Hickner RC, Howell AW, Wolfe RR, & Dohm GL (2004). Impaired plasma fatty acid oxidation in extremely obese women. *Am J Physiol Endocrinol Metab* **287**, E1076-E1081.
- Tonino PA, Fearon WF, De BB, Oldroyd KG, Leeser MA, Ver Lee PN, Maccarthy PA, Van't VM, & Pijls NH (2010). Angiographic versus functional severity of coronary artery stenoses in the FAME study fractional flow reserve versus angiography in multivessel evaluation. *J Am Coll Cardiol* **55**, 2816-2821.
- Törn A & Viitanen A (1994). Topographical global optimization using pre-sampled points. *Journal of Global Optimization* **5**, 267-276.
- Torriani M, Thomas BJ, Halpern EF, Jensen ME, Rosenthal DI, & Palmer WE (2005). Intramyocellular lipid quantification: repeatability with 1H MR spectroscopy. *Radiology* **236**, 609-614.
- Trayhurn P & Wood IS (2004). Adipokines: inflammation and the pleiotropic role of white adipose tissue. *Br J Nutr* **92**, 347-355.
- Turner N, Bruce CR, Beale SM, Hoehn KL, So T, Rolph MS, & Cooney GJ (2007). Excess lipid availability increases mitochondrial fatty acid oxidative capacity in muscle: evidence against a role for reduced fatty acid oxidation in lipid-induced insulin resistance in rodents. *Diabetes* **56**, 2085-2092.
- Turpeinen AK, Takala TO, Nuutila P, Axelin T, Luotolahti M, Haaparanta M, Bergman J, Hamalainen H, Iida H, Maki M, Uusitupa MI, & Knuuti J (1999). Impaired free fatty acid uptake in skeletal muscle but not in myocardium in patients with impaired glucose tolerance: studies with PET and 14(R,S)-[18F]fluoro-6-thia-heptadecanoic acid. *Diabetes* **48**, 1245-1250.
- Turrens JF (1997). Superoxide production by the mitochondrial respiratory chain. *Biosci Rep* **17**, 3-8.
- Tuunanen H, Engblom E, Naum A, Nagren K, Scheinin M, Hesse B, Juhani Airaksinen KE, Nuutila P, Iozzo P, Ukkonen H, Opie LH, & Knuuti J (2008). Trimetazidine, a metabolic modulator, has cardiac and extracardiac benefits in idiopathic dilated cardiomyopathy. *Circulation* **118**, 1250-1258.
- Ueno K, Anzai T, Jinzaki M, Yamada M, Jo Y, Maekawa Y, Kawamura A, Yoshikawa T, Tanami Y, Sato K, Kuribayashi S, & Ogawa S (2009). Increased epicardial fat volume quantified by 64-multidetector computed tomography is associated with coronary atherosclerosis and totally occlusive lesions. *Circ J* **73**, 1927-1933.
- Unger RH, Clark GO, Scherer PE, & Orci L (2010). Lipid homeostasis, lipotoxicity and the metabolic syndrome. *Biochim Biophys Acta* **1801**, 209-214.
- van der Meer RW, Hammer S, Smit JW, Frolich M, Bax JJ, Diamant M, Rijzewijk LJ, de RA, Romijn JA, & Lamb HJ (2007). Short-term caloric restriction induces accumulation of myocardial triglycerides and decreases left ventricular diastolic function in healthy subjects. *Diabetes* **56**, 2849-2853.
- van Loon LJ (2004). Use of intramuscular triacylglycerol as a substrate source during exercise in humans. *J Appl Physiol* **97**, 1170-1187.
- Van H, V, Reynisdottir S, Eriksson P, Thorne A, Hoffstedt J, Lonnqvist F, & Arner P (1998). Leptin secretion from subcutaneous and visceral adipose tissue in women. *Diabetes* **47**, 913-917.
- Virtanen KA, Lidell ME, Orava J, Heglind M, Westergren R, Niemi T, Taittonen M, Laine J, Savisto NJ, Enerback S, & Nuutila P (2009). Functional brown adipose tissue in healthy adults. *N Engl J Med* **360**, 1518-1525.
- Virtanen KA, Peltoniemi P, Marjamaki P, Asola M, Strindberg L, Parkkola R, Huupponen R, Knuuti J, Lonnroth P, & Nuutila P (2001). Human adipose tissue glucose uptake determined using [(18F)]-fluoro-deoxyglucose ([18F]FDG) and PET in combination with microdialysis. *Diabetologia* **44**, 2171-2179.
- Vogelberg KH, Gries FA, & Moschinski D (1980). Hepatic production of VLDL-triglycerides. Dependence of portal substrate and insulin concentration. *Horm Metab Res* **12**, 688-694.
- Wang P, Fraser H, Lloyd SG, McVeigh JJ, Belardinelli L, & Chatham JC (2007). A comparison between ranolazine and CVT-4325, a novel inhibitor of fatty acid oxidation, on cardiac metabolism and left ventricular function in rat isolated perfused heart during ischemia and reperfusion. *J Pharmacol Exp Ther* **321**, 213-220.



## REFERENCES

- Waterhouse C, Baker N, & Rostami H (1969). Effect of glucose ingestion on the metabolism of free fatty acids in human subjects. *J Lipid Res* **10**, 487-494.
- Watts GF & Karpe F (2011). Triglycerides and atherogenic dyslipidaemia: extending treatment beyond statins in the high-risk cardiovascular patient. *Heart* **97**, 350-356.
- Wende AR & Abel ED (2010). Lipotoxicity in the heart. *Biochim Biophys Acta* **1801**, 311-319.
- Whitlock G, Lewington S, Sherliker P, Clarke R, Emberson J, Halsey J, Qizilbash N, Collins R, & Peto R (2009). Body-mass index and cause-specific mortality in 900 000 adults: collaborative analyses of 57 prospective studies. *Lancet* **373**, 1083-1096.
- WHO Consultation. Obesity: preventing and managing the global epidemic. [http://whqlibdoc.who.int/trs/WHO TRS 894.pdf](http://whqlibdoc.who.int/trs/WHO_TRS_894.pdf). 1998. Ref Type: Electronic Citation
- Wieckowska A, McCullough AJ, & Feldstein AE (2007). Noninvasive diagnosis and monitoring of nonalcoholic steatohepatitis: present and future. *Hepatology* **46**, 582-589.
- Williams FM, Tanda K, Kus M, & Williams TJ (1993). Trimetazidine inhibits neutrophil accumulation after myocardial ischaemia and reperfusion in rabbits. *J Cardiovasc Pharmacol* **22**, 828-833.
- Wilson PW, D'Agostino RB, Levy D, Belanger AM, Silbershatz H, & Kannel WB (1998). Prediction of coronary heart disease using risk factor categories. *Circulation* **97**, 1837-1847.
- Wilson RF, Wyche K, Christensen BV, Zimmer S, & Laxson DD (1990). Effects of adenosine on human coronary arterial circulation. *Circulation* **82**, 1595-1606.
- Wu B, Fukuo K, Suzuki K, Yoshino G, & Kazumi T (2009). Relationships of systemic oxidative stress to body fat distribution, adipokines and inflammatory markers in healthy middle-aged women. *Endocr J* **56**, 773-782.
- Yamaguchi K, Yang L, McCall S, Huang J, Yu XX, Pandey SK, Bhanot S, Monia BP, Li YX, & Diehl AM (2007). Inhibiting triglyceride synthesis improves hepatic steatosis but exacerbates liver damage and fibrosis in obese mice with nonalcoholic steatohepatitis. *Hepatology* **45**, 1366-1374.
- Yang S, Zhu H, Li Y, Lin H, Gabrielson K, Trush MA, & Diehl AM (2000). Mitochondrial adaptations to obesity-related oxidant stress. *Arch Biochem Biophys* **378**, 259-268.
- Young ME, Guthrie PH, Razeghi P, Leighton B, Abbasi S, Patil S, Youker KA, & Taegtmeier H (2002). Impaired long-chain fatty acid oxidation and contractile dysfunction in the obese Zucker rat heart. *Diabetes* **51**, 2587-2595.
- Yusuf S, Hawken S, Ounpuu S, Dans T, Avezum A, Lanas F, McQueen M, Budaj A, Pais P, Varigos J, & Lisheng L (2004). Effect of potentially modifiable risk factors associated with myocardial infarction in 52 countries (the INTERHEART study): case-control study. *Lancet* **364**, 937-952.
- Zhang H & Zhang C (2009). Regulation of Microvascular Function by Adipose Tissue in Obesity and Type 2 Diabetes: Evidence of an Adipose-Vascular Loop. *Am J Biomed Sci* **1**, 133-142.
- Zhang L, Keung W, Samokhvalov V, Wang W, & Lopaschuk GD (2010). Role of fatty acid uptake and fatty acid beta-oxidation in mediating insulin resistance in heart and skeletal muscle. *Biochim Biophys Acta* **1801**, 1-22.
- Zhang Y & Ren J (2011). Role of cardiac steatosis and lipotoxicity in obesity cardiomyopathy. *Hypertension* **57**, 148-150.
- Zhou Y, Wei Y, Wang L, Wang X, Du X, Sun Z, Dong N, & Chen X (2011). Decreased adiponectin and increased inflammation expression in epicardial adipose tissue in coronary artery disease. *Cardiovasc Diabetol* **10**, 2.
- Zhou YT, Grayburn P, Karim A, Shimabukuro M, Higa M, Baetens D, Orci L, & Unger RH (2000). Lipotoxic heart disease in obese rats: implications for human obesity. *Proc Natl Acad Sci U S A* **97**, 1784-1789.
- Zimmermann R, Strauss JG, Haemmerle G, Schoiswohl G, Birner-Gruenberger R, Riederer M, Lass A, Neuberger G, Eisenhaber F, Hermetter A, & Zechner R (2004). Fat mobilization in adipose tissue is promoted by adipose triglyceride lipase. *Science* **306**, 1383-1386.
- Zurlo F, Larson K, Bogardus C, & Ravussin E (1990). Skeletal muscle metabolism is a major determinant of resting energy expenditure. *J Clin Invest* **86**, 1423-1427.